

4-5-2016

Nonreplicative DNA Helicases Involved in Maintaining Genome Stability

Salahuddin Syed

University of South Florida, ssyed2@mail.usf.edu

Follow this and additional works at: <http://scholarcommons.usf.edu/etd>

 Part of the [Cell Biology Commons](#), [Genetics Commons](#), and the [Molecular Biology Commons](#)

Scholar Commons Citation

Syed, Salahuddin, "Nonreplicative DNA Helicases Involved in Maintaining Genome Stability" (2016). *Graduate Theses and Dissertations*.

<http://scholarcommons.usf.edu/etd/6408>

This Thesis is brought to you for free and open access by the Graduate School at Scholar Commons. It has been accepted for inclusion in Graduate Theses and Dissertations by an authorized administrator of Scholar Commons. For more information, please contact scholarcommons@usf.edu.

Nonreplicative DNA Helicases Involved in Maintaining Genome Stability

by

Salahuddin Syed

A dissertation submitted in partial fulfillment
of the requirements for the degree of
Doctor of Philosophy
Department of Cell Biology, Molecular Biology, and Microbiology
College of Arts and Sciences
University of South Florida

Major Professor: Kristina H. Schmidt, Ph.D.
Patrick Bradshaw, Ph.D.
Meera Nanjundan, Ph.D.
Stanley Stevens, Ph.D.

Date of Approval:
April 6, 2016

Keywords: RecQ Helicases, DNA repair, Sgs1, RECQL5, Rrm3

Copyright © 2016, Salahuddin Syed

DEDICATION

I would like to dedicate this work to my Mother, Father, and Brother. I would like to thank my Mother for feeding me during those stressful nights when I would be preparing for lab meetings, my Father for continued encouragement when things got tough, and most importantly my Brother for always putting things into perspective and seeing the best in me. Without them I could not have come close to finishing my Ph.D.

ACKNOWLEDGMENTS

I would like to acknowledge my advisor, Dr. Kristina Schmidt, for accepting me into her lab and molding me into the scientist that I am today. Without her patience and support I could not have completed this program, and for that I am eternally grateful. I would also like to thank my committee members, Dr. Patrick Bradshaw, Dr. Meera Nanjundan, and Dr. Stanley Stevens for their encouragement and continual support throughout my time at USF.

I definitely could not have made it through my time in graduate school without my family and friends who preserved my sanity and laughed at my corny jokes.

Lastly, I would like to thank the Department of Cell Biology, Molecular Biology, and Microbiology and the College of Arts and Sciences for their support and help with my time here.

TABLE OF CONTENTS

| | |
|--|------|
| List of Tables | vi |
| List of Figures | viii |
| List of Acronyms | xii |
| Abstract | xv |
| Chapter One: Introduction | 1 |
| Superfamily 1 Helicases | 2 |
| Superfamily 2 Helicases | 2 |
| The RecQ protein family | 3 |
| <i>Saccharomyces cerevisiae</i> RecQ-like helicase, Sgs1 | 5 |
| Repair of double strand breaks by homologous recombination..... | 8 |
| Restart of damaged replication forks by Sgs1 | 8 |
| Role of Sgs1 in maintaining genome stability during meiosis..... | 11 |
| Sgs1 facilitates repair at telomeres..... | 11 |
| Sgs1 interacting proteins | 13 |
| Human RecQ-like helicases | 15 |
| Bloom Syndrome is an autosomal recessive disorder caused by a mutation in <i>BLM</i> | 16 |
| Werner syndrome is an autosomal recessive disorder characterized by premature aging | 18 |
| Rothmund-Thomson syndrome is caused by a mutation to <i>RECQL4</i> | 22 |
| <i>RECQL1</i> and <i>RECQL5</i> | 24 |
| Non-RecQ like DNA helicases and their role in the maintenance of genome integrity..... | 26 |
| Chl1 has a role in sister chromatid cohesion | 27 |
| Irc20 functions during DSB repair | 27 |
| Mph1 is involved in preventing crossovers and has a role in error- free bypass of DNA lesions | 28 |
| Pif1 has a role at telomeres, double-strand breaks and promoting progression through aberrant DNA structures..... | 28 |
| Rad5 is involved in error-free PRR | 29 |
| Rrm3 has a role in replication fork progression | 31 |
| Srs2 functions in multiple DNA metabolic processes | 34 |
| Hypothesis and Aims | 34 |
| Significance | 35 |
| References | 36 |

| | |
|--|-----|
| Chapter Two: Sgs1 Truncations Induce Genome Rearrangements but Suppresses Detrimental Effects of BLM Overexpression in <i>Saccharomyces cerevisiae</i> | 57 |
| Abstract..... | 57 |
| Introduction | 58 |
| Results..... | 62 |
| Requirement of the RQC domain of Sgs1, but not the HRDC domain, for GCR suppression | 62 |
| BS-associated RQC domain mutations cause loss of Sgs1 function <i>in vivo</i> | 64 |
| Expression of human <i>BLM</i> cDNA from the endogenous <i>SGS1</i> promoter does not complement <i>sgs1Δ</i> defects | 66 |
| Overexpression of BLM leads to increased sensitivity to DNA-damaging agents and rapid accumulation of GCRs | 67 |
| N-terminus of Sgs1 suppresses detrimental effects of BLM overexpression | 67 |
| Design of a functional Sgs1-BLM chimera..... | 69 |
| Discussion | 72 |
| Materials and Methods | 77 |
| Yeast strains and media | 77 |
| Western blot analysis..... | 79 |
| Sensitivity to DNA-damaging agents HU and MMS..... | 79 |
| GCR rate measurements..... | 80 |
| Random spore analysis | 81 |
| Figures and Tables | 82 |
| References | 101 |
| Chapter Three: Genetic characterization of <i>RECQL5</i> in <i>Saccharomyces cerevisiae</i> and identification of binding partners using a yeast 2-hybrid screen | 109 |
| Introduction..... | 109 |
| Materials and Methods | 111 |
| Yeast transformation and targeted gene disruption..... | 111 |
| Cloning of plasmid DNA using homologous recombination in yeast | 112 |
| Colony PCR | 112 |
| Fluctuation assay | 113 |
| Plasmid construction..... | 113 |
| Yeast strain construction | 115 |
| Analyzing protein expression by western blot..... | 118 |
| Yeast two-hybrid screen | 118 |
| Results..... | 120 |
| Expression of human <i>RECQL5</i> cDNA in <i>Saccharomyces cerevisiae</i> does not complement <i>sgs1Δ</i> defects..... | 120 |
| <i>SGS1-RECQL5</i> chimera is unable to suppress defects observed in the absence of Sgs1 | 121 |
| Yeast two-hybrid screen using human testis cDNA library to determine novel <i>RecQL5</i> interacting partners | 121 |

| | |
|---|-----|
| Discussion | 123 |
| Figures and Tables | 127 |
| References | 140 |
| | |
| Chapter Four: Novel role of RRM3 in controlling DNA synthesis is separable from its helicase-dependent role in avoidance of replication fork pausing | 145 |
| Abstract..... | 145 |
| Introduction | 146 |
| Results..... | 149 |
| SILAC-based proteomics to identify the cellular response to replication fork pausing..... | 149 |
| Rad5 and Rdh54 independently act on DNA lesions that arise in the absence of Rrm3 | 150 |
| A novel function of Rrm3 in controlling DNA replication maps the N- terminal tail and is independent of Rrm3 catalytic activity | 154 |
| Residues of Rrm3 required for control of DNA replication are critical for Orc5 binding | 157 |
| Differential requirements of Rrm3 function in controlling DNA replication and ATPase/helicase activity in cells lacking Rad5, Rdh54, Mph1 or replication checkpoint factors Mrc1 and Tof1 | 158 |
| Requirement of the Orc5-binding domain of Rrm3 for suppression of HU-induced mutations, but no MMS-induced mutations and gross chromosomal rearrangements..... | 160 |
| Discussion | 161 |
| Materials and Methods | 169 |
| Stable isotope labeling by amino acids in cell culture (SILAC) and isolation of chromatin fraction..... | 169 |
| Sample preparation and LC-MS/MS | 170 |
| Yeast strains and plasmids | 172 |
| Fluctuation assays | 172 |
| DNA damage sensitivity assay | 173 |
| DNA content analysis | 173 |
| Protein expression by western blot..... | 174 |
| Determination of dNTP levels | 174 |
| Yeast two-hybrid assay..... | 175 |
| Analysis of meiotic products | 175 |
| Figures and Tables | 177 |
| References | 197 |
| | |
| Chapter Five: Implications and Future Directions | 204 |
| Implications..... | 204 |
| Future Directions | 205 |
| Humanized yeast model for BLM characterization | 205 |
| RQC domain of Sgs1 is critical in maintaining genome stability whereas the HRDC domain is dispensable | 206 |
| Novel RecQL5 interactions with Ube2I and Hlp2..... | 207 |

| | |
|---|-----|
| New role for Rrm3 in controlling replication | 210 |
| References | 212 |
| Appendix A: Defects in DNA Lesion Bypass Lead to Spontaneous Chromosomal Rearrangements and Increased Cell Death..... | |
| Abstract..... | 215 |
| Introduction..... | 216 |
| Results..... | 219 |
| Translesion DNA synthesis suppresses GCR accumulation in <i>mph1</i> Δ cells | 219 |
| Suppression of genome rearrangements by <i>srs2</i> Δ depends on functional DNA damage checkpoint | 222 |
| Lack of Rev3 and Mph1 causes synergistic GCR rate increase in new GCR strain susceptible to duplication-mediated rearrangements | 223 |
| Genetic interactions between <i>MPH1</i> and other DNA helicases..... | 224 |
| Rad52/Rad51, but not Rad59, are essential for DNA damage tolerance and normal growth in the absence of translesion DNA synthesis..... | 226 |
| Discussion | 227 |
| Materials and Methods | 232 |
| Yeast strains and media | 232 |
| GCR analysis | 233 |
| Tetrad analysis..... | 234 |
| Doubling time measurement..... | 234 |
| DNA content analysis | 235 |
| MMS sensitivity..... | 235 |
| Figures and Tables | 236 |
| References | 248 |
| Appendix B: Structural motifs critical for <i>in vivo</i> function and stability of the RecQ- mediated genome instability protein Rmi1 | |
| Abstract..... | 253 |
| Introduction..... | 254 |
| Materials and Methods | 258 |
| Bioinformatics analysis | 258 |
| Plasmids | 258 |
| Hydroxyurea hypersensitivity assay | 259 |
| Viability assay | 259 |
| Protein extraction and western blotting..... | 260 |
| Results..... | 260 |
| Computational analysis of yeast Rmi1 structure..... | 260 |
| Mutational analysis of predicted structural elements of yeast Rmi1 | 261 |
| Structure predictions and <i>in vivo</i> mutagenesis suggest differences in the N-termini of yeast and human Rmi1 | 263 |

| | |
|--|-----|
| A conserved alpha helix in the C-terminus contributions to yeast Rmi1 stability | 265 |
| Discussion | 266 |
| Figures | 271 |
| Supporting Information | 279 |
| References | 280 |
| Appendix C: Yeast Strains | 284 |
| Appendix D: Plasmids | 304 |
| Appendix E: Permissions | 308 |

LIST OF TABLES

| | | |
|-------------|---|-----|
| Table 1.1: | Comparison of helicase activities of <i>E. coli</i> RecQ with human and <i>S. cerevisiae</i> RecQ helicases | 15 |
| Table 1.2: | DNA helicases involved in maintaining genome integrity | 25 |
| Table 2.1: | Accumulation of GCRs in cells expressing mutant alleles of <i>SGS1</i> | 88 |
| Table 2.2: | Effect of BLM expression on GCR accumulation in the <i>sgs1Δ</i> mutant..... | 89 |
| Table 2.S1: | Yeast Strains used in this study..... | 90 |
| Table 3.1: | Primers used in this study..... | 127 |
| Table 3.2: | Rate of accumulating gross-chromosomal rearrangements (GCRs)..... | 129 |
| Table 4.1: | Effect of deletions of <i>RRM3</i> , <i>RAD5</i> , <i>RDH54</i> on accumulation of gross-chromosomal rearrangements in the presence or absence of genotoxic agents | 188 |
| Table 4.2: | Accumulation of forward mutations at <i>CAN1</i> and gross-chromosomal rearrangements in untreated <i>rrm3</i> mutants and after treatment with genotoxic agents | 189 |
| Table 4.S1: | Proteins that undergo significant changes in cells lacking Rrm3 in the presence and absence of HU | 190 |
| Table 4.S2: | Yeast strains used in this study | 192 |
| Table 4.S3: | Plasmids used in this study | 195 |
| Table A.1: | <i>Saccharomyces cerevisiae</i> strains used in this study..... | 242 |
| Table A.2: | Effect of defects in DNA lesion bypass, homologous recombination, DNA helicases, and the DNA damage checkpoint on accumulation of gross chromosomal rearrangements in the standard GCR strain background RDKY3615 | 246 |

Table B.S1: Plasmids used in this study279

LIST OF FIGURES

| | | |
|--------------|---|-----|
| Figure 1.1: | RecQ-like helicases from various species | 3 |
| Figure 1.2: | Requirement for the RecQ helicase, Sgs1, during end resection | 6 |
| Figure 1.3: | Double strand break repair | 7 |
| Figure 1.4: | Checkpoint response | 10 |
| Figure 1.5: | Regulation of dNTP levels | 10 |
| Figure 1.6: | Conserved protein-protein interactions with Sgs1 and BLM..... | 13 |
| Figure 1.7: | Individuals with Bloom syndrome | 18 |
| Figure 1.8: | Patients with Werner syndrome at various ages | 22 |
| Figure 1.9: | Patients showing clinical features of Rothmund-Thomson syndrome | 24 |
| Figure 1.10: | Mechanisms for DNA lesion bypass | 31 |
| Figure 2.1: | C-terminal truncations of Sgs1 used in this study..... | 82 |
| Figure 2.2: | Sensitivity of cells expressing Sgs1 truncation alleles to the DNA damaging agents HU and MMS..... | 83 |
| Figure 2.3: | Effect of zinc-binding domain mutations on Sgs1 function <i>in vivo</i> | 84 |
| Figure 2.4: | BLM expression does not suppress <i>sgs1</i> Δ defects and BLM overexpression is detrimental to yeast cells | 85 |
| Figure 2.5: | HU sensitivity of diploid cells expressing <i>BLM</i> and mutant alleles of <i>SGS1</i> | 86 |
| Figure 2.6: | Construction of a functional chimerical protein composed of the N- terminus of Sgs1 and the C-terminus of BLM..... | 87 |
| Figure 3.1: | RecQ-like helicases | 130 |

| | | |
|--------------|---|-----|
| Figure 3.2: | Construction of a chimeric protein containing the N terminal region of Sgs1 and full length RecQL5 β | 131 |
| Figure 3.3: | Expression of RECQL5 at the endogenous <i>SGS1</i> locus | 132 |
| Figure 3.4: | RECQL5 does not suppress the defects seen in a <i>sgs1</i> Δ strain | 133 |
| Figure 3.5: | Expression of RECQL5 from bait plasmid containing a DNA binding domain | 134 |
| Figure 3.6: | Schematic of yeast two-hybrid using a testis cDNA library to find RECQL5 interacting proteins | 135 |
| Figure 3.7: | Strain AH109 (Clontech) with the four reporter constructs | 136 |
| Figure 3.8: | Positive candidates identified in the yeast two-hybrid system using human testis cDNA library against RECQL5 | 137 |
| Figure 3.9: | Western blot analysis of candidates identified in yeast two-hybrid using a human testis cDNA library for RECQL5 interacting proteins..... | 138 |
| Figure 3.10: | Manual verification of RECQL5 interacting proteins | 139 |
| Figure 4.1: | SILAC-based quantification of changes in chromatin association in cells lacking Rrm3..... | 177 |
| Figure 4.2: | Rad5 and Rdh54 contribute independently to DNA lesion bypass/repair in cells lacking Rrm3 | 178 |
| Figure 4.3: | A 26-residue region in the N-terminal tail of Rrm3 is required for the control of DNA replication under replication stress independently of ATPase/helicase activity | 180 |
| Figure 4.4: | The N-terminal Rrm3 region that controls DNA replication is an Orc5-binding site that is required for cell viability and DNA lesion avoidance in the absence of Mrc1/Tof1 but not in the absence of Rad5, Rdh54 or Mph1 | 182 |
| Figure 4.5: | Rrm3 performs two genetically and physically separable functions during DNA replication | 183 |
| Figure 4.S1: | Rad5 and Rdh54 are not required for S phase progression of <i>rrm3</i> Δ cells after release from 2 hour exposure to 100 mM HU | 184 |
| Figure 4.S2: | Deletion of the nonessential <i>HDA1</i> , <i>SET3</i> , or <i>MGM101</i> genes does not affect the DNA damage sensitivity of the <i>rrm3</i> Δ mutant | 185 |

| | |
|--|-----|
| Figure 4.S3: Requirement of Mph1 for DNA repair and DNA replication in the absence of Rrm3 | 186 |
| Figure 4.S4: The Rrm3 N-terminal tail controls DNA replication | 187 |
| Figure A.1: Genetic interactions between <i>rev3Δ</i> , <i>mph1Δ</i> , <i>srs2Δ</i> , and HR mutations were assessed by testing the fitness of mutants..... | 236 |
| Figure A.2: Effect of <i>rev3Δ</i> and <i>srs2Δ</i> mutations on cell cycle progression of cells lacking Mph1 | 237 |
| Figure A.3: The G2/M arrest of <i>mph1Δ srs2Δ</i> cells is suppressed by disrupting homologous recombination or the DNA damage checkpoint..... | 238 |
| Figure A.4: Effect of mutations affecting translesion DNA synthesis and homologous recombination on sensitivity to MMS..... | 239 |
| Figure A.5: Effect of an <i>mph1Δ</i> mutation on MMS sensitivity of mutants lacking various other confirmed (<i>Sgs1</i> , <i>Rrm3</i> , and <i>Srs2</i>) or putative (<i>Chl1</i>) DNA helicases | 240 |
| Figure A.6: Model for the role of Mph1 in the maintenance of genome stability | 241 |
| Figure B.1: Structure-prediction-guided mutagenesis of <i>S.c.</i> Rmi1 | 271 |
| Figure B.2: Effect on expression levels of mutations designed to disrupt structural motifs of yeast Rmi1 | 273 |
| Figure B.3: Structural prediction and <i>in vivo</i> functional analysis suggest differences between the N-termini of yeast and human Rmi1 | 274 |
| Figure B.4: Mutational analysis of the C-terminal region of increased helical propensity | 275 |
| Figure B.5: Proposed structure-prediction-based alignment of yeast and human Rmi1..... | 276 |
| Figure B.6: Conserved domains, and putative differences between yeast Rmi1 and the N-terminus of human Rmi1 | 277 |
| Figure E.1: Permissions for content in Chapter Two provided by the Journal of Molecular Biology and Elsevier..... | 308 |
| Figure E.2: Permissions for content in Appendix A provided by Eukaryotic Cell and the American Society for Microbiology | 309 |

Figure E.3: Permissions for content in Appendix B provided by PLOS ONE310

LIST OF ACRONYMS

| | |
|---------|---|
| 3-AT | 3 Amino 1,2,4 triazole |
| 4-NQO | 4-nitroquinoline 1-oxide |
| AD | Activation domain |
| ADE | Adenine |
| ALT | Alternative Lengthening of Telomeres |
| AMP | Ampicillin |
| AR loop | Aromatic rich loop |
| ATM | Ataxia telangiectasia mutated |
| ATP | Adenosine triphosphate |
| BER | Base excision repair |
| BGS | Baller-Gerold syndrome |
| BLAST | Basic Local Alignment Search Tool |
| BLM | Bloom syndrome protein |
| BRCA1 | Breast cancer type 1 susceptibility protein |
| BRCA2 | Breast cancer type 2 susceptibility protein |
| BS | Bloom's syndrome |
| CAN1 | Canavanine resistance gene 1 |
| CMP | Chloramphenicol |
| CPT | Camptothecin |
| DBD | DNA binding domain |
| dHJ | Double Holliday junction |
| D.m. | Drosophila melanogaster |
| DNA | Deoxyribonucleic acid |
| DNA2 | DNA synthesis defective protein 2 |
| DSB | Double strand break |
| dsDNA | Double-stranded DNA |
| DTT | Dithiothreitol |
| EDTA | Ethylenediaminetetraacetic acid |
| EXO1 | Exonuclease 1 |
| FEN1 | Flap endonuclease 1 |
| GCR | Gross chromosomal rearrangement |
| HIS | Histidine |
| HR | Homologous recombination |
| HRDC | Helicase/RNase D C-terminal |
| HU | Hydroxyurea |
| LB | Luria Broth |
| LEU | Leucine |
| LiAc | Lithium acetate |
| LIG4 | Ligase 4 |

| | |
|--------|---|
| LOH | Loss of heterozygosity |
| MCM10 | Mini chromosome maintenance 10 |
| MCM2-7 | Mini chromosome maintenance complex 2-7 |
| MDC1 | Mediator of DNA damage checkpoint protein 1 |
| MLH1 | MutL homolog 1 |
| MMS | Methyl methanesulfonate |
| MRC1 | Mediator of the replication checkpoint |
| MRE11 | Meiotic recombination |
| MRN | Mre11-Rad50-Nbs1 protein complex |
| MSH2 | MutS homolog 2 |
| MSH6 | MutS homolog 6 |
| mtDNA | Mitochondrial DNA |
| NER | Nucleotide excision repair |
| NHEJ | Non-homologous end joining |
| NMR | Nuclear magnetic resonance |
| OB | Oligonucleotide-binding |
| ORF | Open reading frame |
| PCNA | Proliferating cell nuclear antigen |
| PCR | Polymerase chain reaction |
| PEG | Polyethylene glycol |
| PVDF | Polyvinylidene fluoride |
| RAD51 | Radiation 51 |
| RECQL1 | Human RecQ-like helicase 1 |
| RECQL4 | Human RecQ-like helicase 4, Rothmund-Thomson syndrome protein |
| RECQL5 | Human RecQ-like helicase 5 |
| RNA | Ribonucleic acid |
| RPA | Replication protein A |
| RQC | RecQ-helicase conserved |
| RRM3 | rDNA recombination mutation |
| RTR | RecQ-Top3-Rmi1 complex |
| RTS | Rothmund-Thomson syndrome |
| S.c. | Saccharomyces cerevisiae |
| SC- | Synthetic complete media minus |
| SCE | Sister chromatid exchange |
| SE | Strand exchange |
| SF1 | Super family 1 |
| SF2 | Super family 2 |
| SGD | Saccharomyces genome database |
| SGS1 | Slow growth suppressor 1 |
| SRS2 | Suppressor of Rad6 |
| SSB | Single stranded binding protein |
| ssDNA | Single stranded DNA |
| TBST | Tris-buffered saline w/ Triton |
| TCA | Trichloroacetic acid |
| TOP1 | Topoisomerase 1 |

| | |
|-----------------|----------------------------------|
| TOP2 | Topoisomerase 2 |
| TOP3 | Topoisomerase 3 |
| TOPIII α | Topoisomerase III α |
| TRP | Tryptophan |
| URA | Uracil |
| UV | Ultraviolet |
| WB | Western blot |
| WH | Winged helix subdomain |
| WRN | Werner syndrome protein |
| YP | Yeast extract, peptone |
| YPD | Yeast extract, peptone, dextrose |

ABSTRACT

Double-strand breaks and stalled forks arise when the replication machinery encounters damage from exogenous sources like DNA damaging agents or ionizing radiation, and require specific DNA helicases to resolve these structures. Sgs1 of *Saccharomyces cerevisiae* is a member of the RecQ family of DNA helicases and has a role in DNA repair and recombination. The RecQ family includes human genes *BLM*, *WRN*, *RECQL4*, *RECQL1*, and *RECQL5*. Mutations in *BLM*, *WRN*, and *RECQL4* result in genetic disorders characterized by developmental abnormalities and a predisposition to cancer. All RecQ helicases have common features including a helicase domain, an RQC domain, and a HRDC domain. In order to elucidate the role of these domains and to identify additional regions in Sgs1 that are required for the maintenance of genome integrity, a series of systematic truncations to the C terminus of Sgs1 were created. We found that ablating the HRDC domain does not cause an increase in accumulating gross chromosomal rearrangements (GCRs). But deleting the RQC domain and leaving the helicase domain intact resulted in a rate similar to that of a helicase-defective mutant. Additionally, we exposed these truncation mutants to HU and MMS and demonstrated that losing up to 200 amino acids from the C terminus did not increase sensitivity to HU or MMS, whereas losing 300 amino acids or more led to sensitivity similar to that of an *sgs1* Δ cell. These results suggest that the RQC domain, believed to mediate protein-protein interactions and required for DNA recognition, is important for

Sgs1's role in suppressing GCRs and sensitivity to HU and MMS, whereas the HRDC domain that is important for DNA binding is not necessary. RecQL5 is a RecQ-like helicase that is distinct from the other members through its three different isoforms, RecQL5 α , RecQL5 β , and RecQL5 γ . It has a helicase domain and an RQC domain, but lacks the HRDC domain that other RecQ-like helicases possess. In contrast to Blm, Wrn, and RecQL4, no human disorder has been associated with defects in RecQL5. For this reason the role of RecQL5 in the cell has remained largely unknown. To try to elucidate the pathways RecQL5 may be involved in we performed a yeast two hybrid to identify RecQL5-interacting proteins. We found that RecQL5 interacts with Hlp2, an ATP-dependent RNA helicase, and Ube2I, a SUMO-conjugating enzyme. These novel interactions shed light on a potential role of RecQL5 in the cell as a transcriptional regulator.

Saccharomyces cerevisiae, Rrm3, is a 5'-3' DNA helicase that is part of the Pif1 family of DNA helicases and is conserved from yeast to humans. It was initially discovered as a suppressor of recombination between tandem arrays and ribosomal DNA (rDNA) repeats. In its absence there are increased rates of extra-chromosomal rDNA circles, and cells accumulate X-shaped intermediates at stalled forks. Rrm3 may be involved in displacing DNA-protein blocks and unwinding DNA to facilitate fork progression. We used stable isotope labeling by amino acids in cell culture (SILAC)-based quantitative mass spectrometry in order to determine proteins that deal with the stalled fork in the absence of Rrm3. We found that in the absence of Rrm3 and increased replication fork pausing, there is a requirement for the error-free DNA damage bypass factor Rad5 and the homologous recombination factor Rdh54 for fork

recovery. We also report a novel role for Rrm3 in controlling DNA synthesis upon exposure to replication stress and that this requirement is due to interaction with Orc5, a subunit of the origin recognition complex. Interaction of Orc5 was found to be located within a 26-residue region in the unstructured N-terminal tail of Rrm3 and loss of this interaction resulted in lethality with cells devoid of the replication checkpoint mediator Mrc1, and DNA damage sensitivity with cells lacking Tof1. In this study we describe two independent roles of Rrm3, a helicase-dependent role that requires Rad5 and Rdh54 for fork recovery, and a helicase-independent role that requires Orc5 interaction to control DNA synthesis.

Our data provides novel insight into the role of DNA helicases and their role in protecting the genome. Through yeast genetics it was possible to determine the importance of the C terminus of Sgs1 and elucidate new RecQL5 interacting partners that shed light onto roles for RecQL5 distinct from other RecQ like helicases. Quantitative mass spectrometry allowed us to take on a more global view of the cell and determine how it responds to replication fork pausing in the absence of Rrm3. Using both proteomics and yeast genetics we were able to better understand how these DNA helicases contribute to maintaining genome stability.

CHAPTER ONE: INTRODUCTION

Helicases have a role in numerous processes in the cell from DNA replication and repair, transcription, to translation. Defects in their function have been linked to several diseases, including neurodegenerative diseases, cancers, and developmental defects [1-4]. They were first discovered through multiple alignment and sequence conservation of three related sequence motifs within the ATPase domain [5]. Helicases were initially characterized by these conserved motifs, but it has become clear that these motifs characterize proteins, specifically translocases, which possess the ability to move along DNA [2, 6]. Helicases and translocases are characterized by their processivity, likely due to their interaction with other proteins, and polarity. Since DNA is double stranded and asymmetric within the duplex, it is important that the ATP-dependent helicases move along the nucleic acid with some direction or polarity [2, 7-9].

Helicases can be classified within six superfamilies with the largest groups being Superfamily 1 (SF1) and Superfamily 2 (SF2), which contain seven signature motifs [5]. They can also be distinguished based on their affinity for DNA, RNA, or DNA-RNA hybrids and ability to move on DNA with either 3'-5' or 5'-3' polarity [7]. The activity of these helicases is often altered by accessory domains, which may direct the helicase to a specific substrate or enhance its catalytic activity [10].

SUPERFAMILY 1 HELICASES

Superfamily 1 helicases are the best characterized, with roles in DNA or RNA metabolism, and can be subdivided into Superfamily 1A (SF1A) and Superfamily 1B (SF1B) helicases. The first crystal structure determined for a helicase was of PcrA, a UvrD-like enzyme from *Geobacillus stearothermophilus* [11]. SF1 helicases possess a four-subdomain structure with 1A/2A subdomains forming the helicase core and 1B/2B interacting with the duplex DNA substrate [11, 12]. After ssDNA binds to a helicase a conformational change allows the 1B/2B subdomains to interact with DNA. With the addition of ATP, an additional conformational change occurs and allows subdomains 1A/2A to encircle the nucleotide [13]. These core domains constantly open and close as ATP is bound, hydrolyzed, and released, resulting in translocation along DNA [14]. SF1 family of helicases are divided into three families (Rep/UrvD, Pif1/RecD, and Upf1-like) based on their polarity on ssDNA with SF1A moving 3'-5' and SF1B moving 5'-3' [2].

SUPERFAMILY 2 HELICASES

Superfamily 2 helicases contain a more diverse group of helicases than the SF1 family and are involved in DNA or RNA unwinding and have a role in DNA repair, transcription, RNA metabolism, and chromatin organization [9, 15-18]. They include the following families: RecG-like, Swi/Snf, Ski2-like, RIG-I-like, NS3/NPH-II, DEAH/RHA, DEAD-box, Rad3/XPD, type I restriction enzyme, and RecQ-like [10, 18, 19].

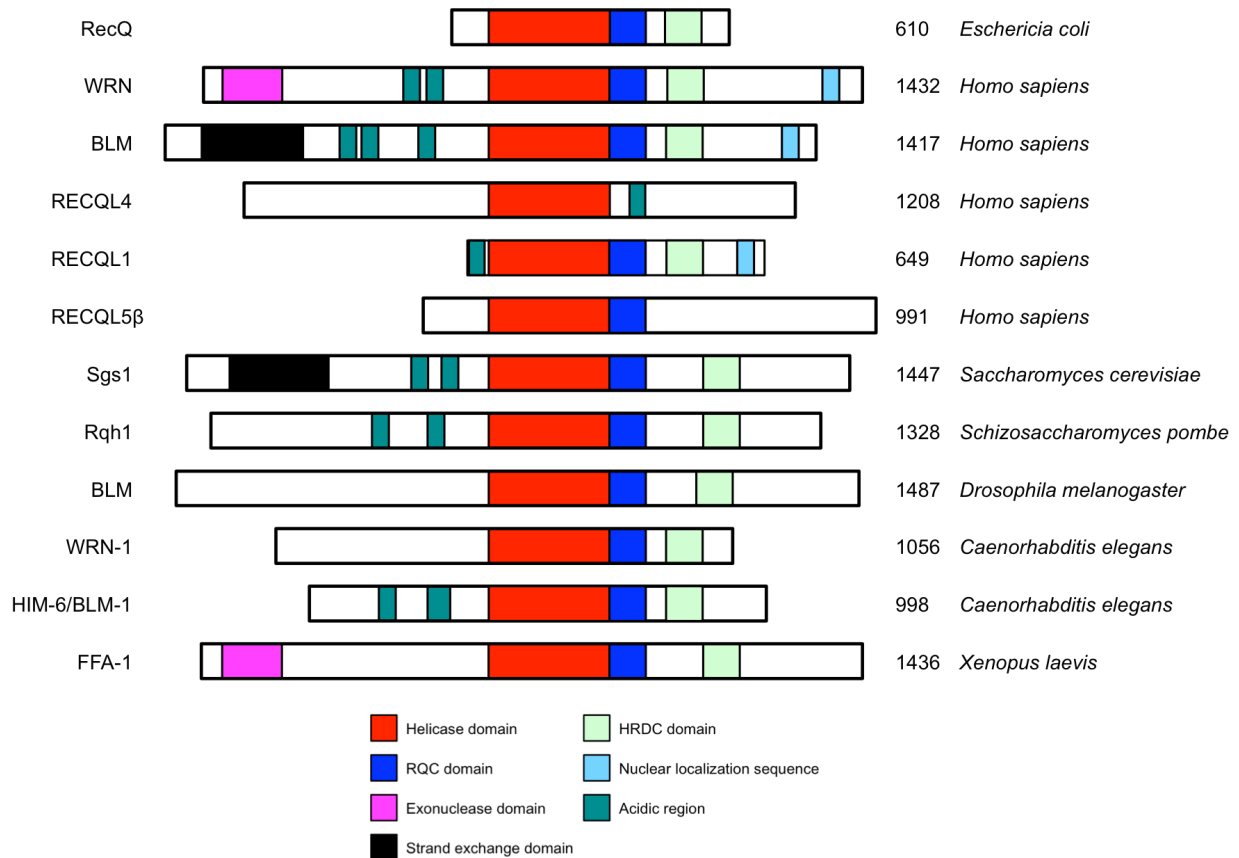


Figure 1.1. RecQ-like helicases from various species

RecQ helicases have several domains in common. The most conserved domain amongst RecQ-like helicases is the helicase core. Most RecQ helicases also share a conserved helicase and RNase D C-terminal (HRDC) and RecQ C-terminal (RQC) domain. WRN, BLM and RECQL1 contain a nuclear localization sequence and interestingly WRN and FFA-1 in *Xenopus* has an exonuclease domain.

THE RECQ PROTEIN FAMILY

RecQ-like helicases have 3'-5' polarity and have been implicated in recombination, telomere maintenance, and DNA repair [20]. They bind to specific DNA substrates and prevent unscheduled recombination. In their absence there is a higher level of recombination, chromosome missegregation, and meiotic defects [21, 22]. The first RecQ helicase was discovered in *Escherichia coli* as a mutant that was resistant to thymine starvation in the RecF pathway and in its absence there was increased

sensitivity to UV damage and genome instability [23]. *Saccharomyces cerevisiae* and *Schizosaccharomyces pombe* contain one RecQ helicase. Others contain multiple, like humans who possess five homologs; WRN, BLM, RecQL4, RecQL1, and RecQL5. RecQ helicases from different organisms are defined by their sequence similarity to the *E. coli* RecQ helicase. They possess highly conserved protein domains, the helicase domain, the RecQ C-terminal (RQC) domain, and the helicase and RNase D-like C-terminal (HRDC) domain (Figure 1.1) [5, 24].

RecQ helicases belong to the SF2 family of helicases and contain seven sequence motifs [25]. Functions of these motifs have been studied based on their structural similarity between motifs of other helicases. The function of Motif 0 was determined by looking at the crystal structure of *E. coli* RecQ and was found to facilitate ATP binding [2]. Motif 1 and Motif II are conserved amongst many helicases and have a role in binding and hydrolysis of ATP [10]. The crystal structure of the helicase domain of RecQ has revealed that there are two lobes that are separated by a cleft, which is thought to play a role in ATP and ssDNA binding [26-28]. Mutations to these motifs result in deleterious effects in the cell as seen in BLM, where mutations adjacent to the cleft of the helicase domain have resulted in reduced catalytic activity of this protein [2, 27-31].

The RQC domain is not a common feature of all RecQ helicases like the core helicase domain, but it is a unique characteristic of the RecQ family and has been implicated in DNA binding [32]. The structure of the RQC domain was initially resolved using X-ray crystallography [26, 27, 33]. This domain possesses a zinc-binding motif, a helix-hairpin-helix, winged-helix, and a β -hairpin motif [26, 27, 33]. The winged-helix

domain of both WRN and BLM shows affinity for DNA and the crystal structure for WRN shows that the winged-helix domain interacts with the phosphate backbone of a 5' single-stranded DNA overhang [28, 32]. Mutating the residues in WRN that interact with the phosphate backbone results in loss of DNA-binding and helicase activity [33, 34].

RecQL1, which is a much shorter protein than other RecQ like helicases, possesses a conserved RQC domain that has been shown to bind dsDNA through its winged helix [35]. Additionally, the β -hairpin motif in the RQC domain of RecQL1 coordinates its ATPase activity and ability to unwind DNA through dimer formation [31].

The helicase and RNase D-Like C-Terminal domain (HRDC) of RecQ-like helicases is seen in WRN, BLM, *E. coli* RecQ, and *S. cerevisiae* Sgs1 and its crystal structure has been resolved [24, 28, 36]. RecQ and Sgs1 have been shown to bind to the HRDC domain but interaction is not needed for their catalytic activity [37]. In human WRN and BLM, the HRDC domain is important for recruiting the protein to methyl methanesulfonate (MMS), mitomycin C damage as well as dsDNA breaks [38]. Although this domain is not needed for catalytic activity of these RecQ-like helicases, it is important for recruitment to damaged DNA [39].

SACCHAROMYCES CEREVISIAE RECQ-LIKE HELICASE, SGS1

RecQ helicases are highly conserved from bacteria to humans but, only one RecQ helicase is present in bacteria and yeast. Sgs1 was initially discovered as a suppressor to the slow-growth phenotype of a yeast strain lacking Topoisomerase 3 (Top3), a type IA topoisomerase capable of relaxing negatively supercoiled DNA [40]. Sgs1 is 1447 residues long and has a helicase domain, RQC domain, and a HRDC

domain (Figure 1.1) [41]. It is involved in repair of double strand breaks by homologous recombination (HR), restart of stalled replication forks, resolving aberrant intermediates during meiosis, and telomere maintenance [37, 42-46]. Cells lacking Sgs1 show increased sensitivity to DNA-damaging agents hydroxyurea (HU) and methyl methanesulfonate (MMS), accumulate gross-chromosomal rearrangements (GCRs), and have defects in chromosome segregation during mitosis and meiosis [21, 46-50].

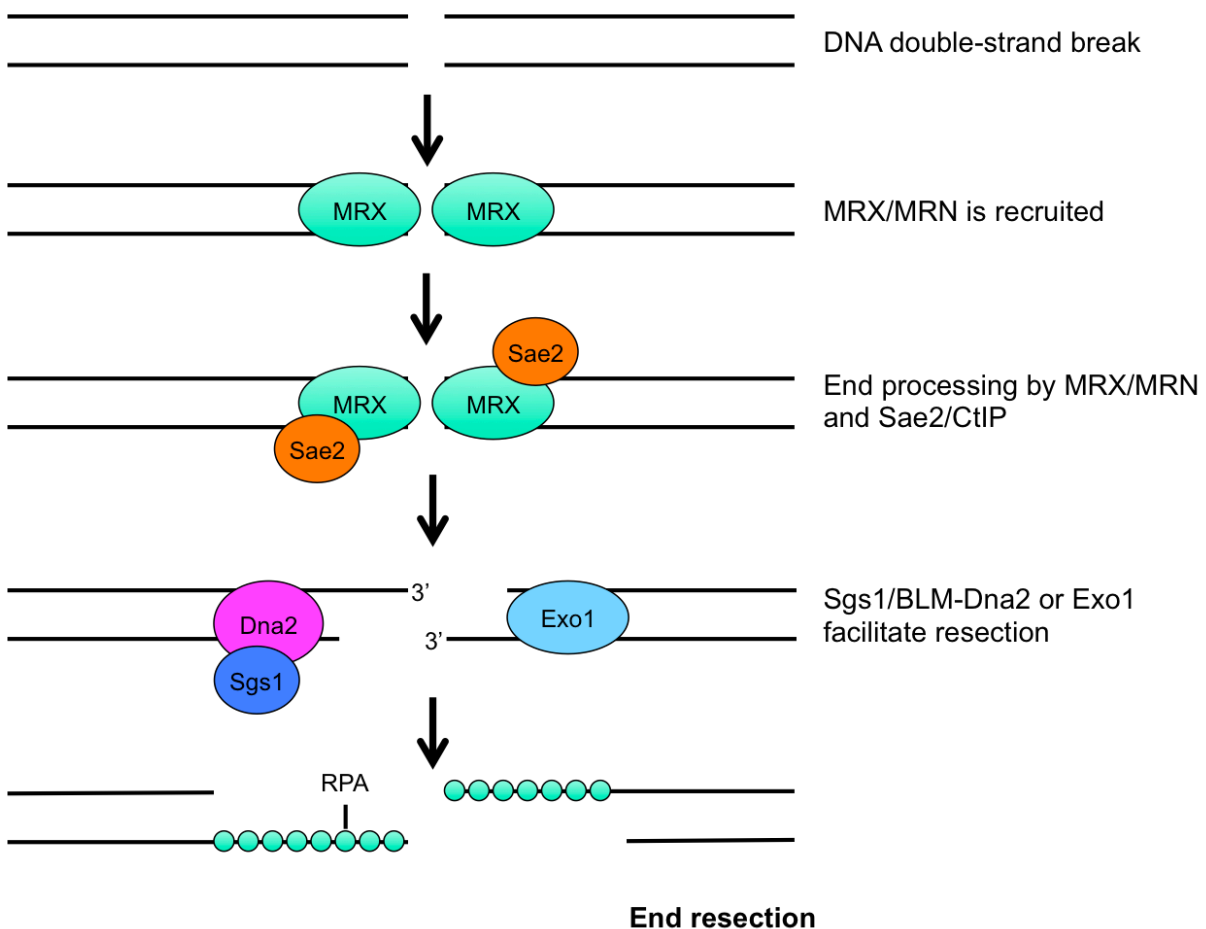


Figure 1.2. Requirement for the RecQ helicase, Sgs1, during end resection

Double-strand breaks are recognized by the Mre11-Rad50-Xrs2 (MRX) complex and the ends are partially resected by the Mre11 nuclease with help from Sae2 leaving a 3' ssDNA overhang. The ends are further resected by Sgs1 and Dna2 (left) or by the Exo1 nuclease (right) resulting in ssDNA that is coated by RPA. This image has been adapted and modified from Gobbin, Cesena et al. (2013).

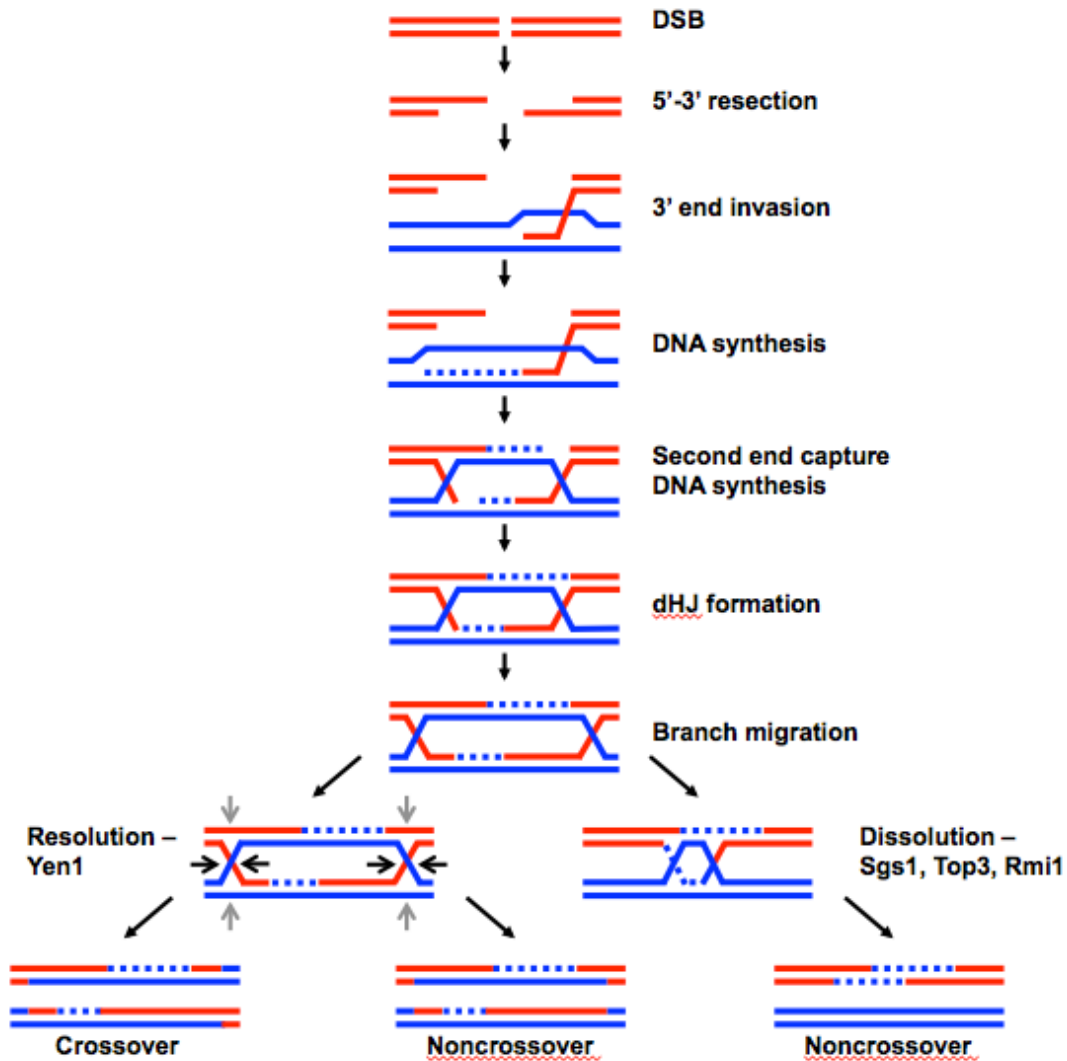


Figure 1.3. Double strand break repair

The RecQ helicase, Sgs1, of *S. cerevisiae* is required during double strand break repair by HR. After a double strand break has occurred the MRX complex and Sae resect the 5' ends. Sgs1, Exo1, and Dna2 then further resect resulting in a 3' ssDNA strand. This strand can invade the sister chromatid and be extended by DNA synthesis and aberrant structures can be prevented by the activity of Sgs1. A double Holliday junction (dHJ) is then formed and can undergo dissolution by Sgs1/Top3/Rmi1 resulting in non-crossover products. The dHJ can also be processed by other resolvases to create either a non-crossover product or crossover product. This image has been adapted and modified from Ashton and Hickson (2010), Brosh (2013).

Repair of double strand breaks by homologous recombination

HR is important to repair double strand breaks (DSBs) and DNA crosslinks by utilizing two homologous DNA sequences [51]. In the presence of a double strand break, the MRX complex (Mre11-Rad50-Xrs2) is recruited to each end of the break and initiates resection of the 5' ends (Figure 1.2) [51]. Sae2 interacts with Mre11 and its absence has shown reduced nuclease activity similar to a Mre11 deficient strain suggesting that these two proteins work in coordination with each other to produce a substrate for Sgs1 or Exo1 [52-56]. Sgs1, Exo1, and Dna2 are then needed to further resect the DNA in order to create a substrate for HR (Figure 1.2) [42].

After extensive resection, ssDNA is coated with Rad51, which searches for a homologous sequence to use for error-free repair [57]. Efficient resection during DSB repair requires not only Sgs1 but also its interacting partners Top3 and Rmi1 (STR complex) [58]. Rmi1 may have a role in recruiting Sgs1 and Top3 to ssDNA so that Top3 can remove any torsional strain caused by the helicase activity of Sgs1 during resection [45]. Cells deficient for any member of the STR complex results in increased rates of recombination [59].

Restart of damaged replication forks by Sgs1

In *S. cerevisiae* the intra-S phase checkpoint is activated in the presence of HU, which depletes dNTP pools, or MMS, which alkylates DNA, and results in slowing of DNA replication (Figure 1.5) [60]. Upon activation of the intra-S phase checkpoint, proteins involved in DNA repair are activated [61, 62]. When cells defective in intra-S phase checkpoint proteins, Mec1, Mrc1, Rad9, and Rad53 are exposed to DNA

damaging agents HU or MMS, the replication forks are unable to proceed and stall [63]. Therefore, it is thought that the intra-S phase checkpoint serves to stabilize the forks in order to resume replication after repair has occurred (Figure 1.4) [64].

DNA checkpoints are complex signal transduction pathways that require sensors, transducers, and effectors [65, 66]. The sensor, ATR-like Mec1 kinase and its binding partner, Ddc2, are required to sense and detect lesions [66]. The transducers Mrc1 which functions in the intra-S phase checkpoint, and Rad9, which functions in the DNA damage checkpoint receives, and transmits the signal [67]. Lastly, the effector kinase Rad53, functions in both the intra-S phase and DNA damage checkpoint, and is required to start downstream events [63]. Sgs1 interacts with Rad53 *in vitro* and *in vivo* and activates this kinase in the presence of HU [68, 69]. This activation is independent of Sgs1's helicase activity and suggests that the physical interaction between these two proteins is what is required [68]. In MMS, *sgs1* Δ cells accumulate HR intermediates that are not observed in the presence of HU, suggesting Sgs1 has several roles at forks upon MMS treatment [70-72]. Top3 and Rmi1 also activate Rad53 in a MMS dependent manner, which is independent of Top3 catalytic activity but dependent on protein-protein interaction with Sgs1 [72-74]. Sgs1 seems to have a HU dependent role in activating Rad53 through protein-protein interaction and a MMS dependent role, which requires Top3 and Rmi1.

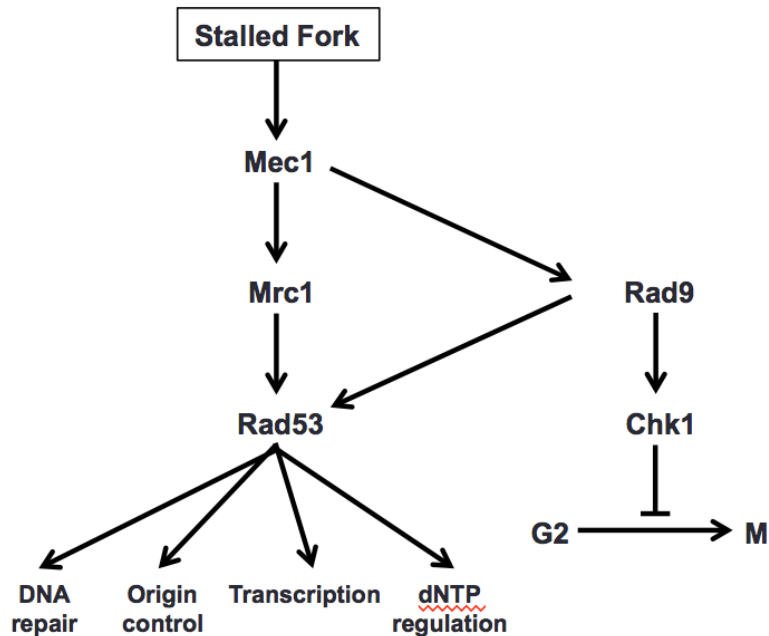


Figure 1.4. Checkpoint response

The sensor kinase, Mec1, detects lesions and helps to activate Mrc1 or Rad9, which are mediators of the checkpoint response. Mrc1, the replication stress checkpoint and Rad9, the DNA damage checkpoint can both activate Rad53 under replication stress. Activation of Rad53 leads to numerous downstream events that stabilize the fork and allow for repair to take place. Rad53 has roles in DNA repair, preventing late origins from firing, regulation of transcription and maintaining dNTP levels. In addition to Rad53, Rad9 can also activate the effector kinase Chk1, which functions during G2/M. This image is adapted from Fu et al. (2008).

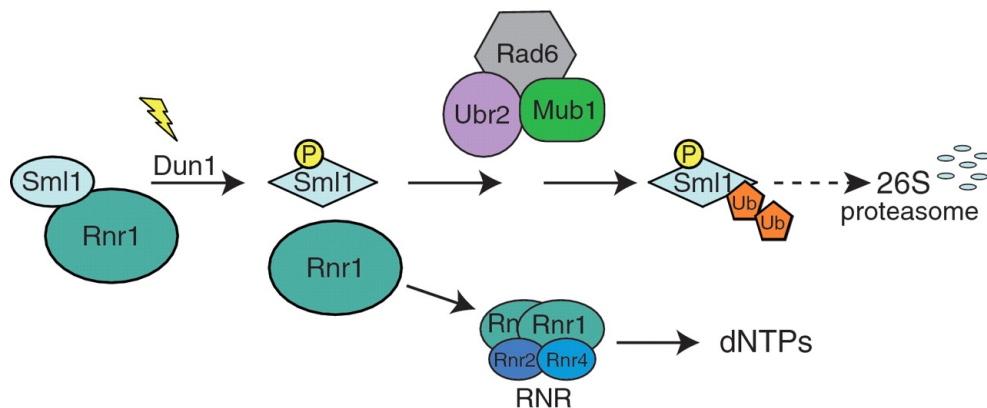


Figure 1.5. Regulation of dNTP levels

Sml1 inhibits Rnr1 from associating with the RNR complex and prevents production of dNTPs. Upon exposure to replication stress, Dun1 is activated and phosphorylates Sml1, targeting it for degradation by the 26S proteasome, allowing production of dNTPs. This image is adapted from Andreson et al. (2010).

Role of Sgs1 in maintaining genome stability during meiosis

Cells lacking Sgs1 show reduced spore viability and tetrad formation [75, 76]. The meiotic defect in *sgs1* Δ mutants can be attributed to missegregation of chromosomes during meiosis and unscheduled separation of sister chromatids [76]. Disrupting meiotic checkpoint genes, *RAD17* and *RED1*, results in rescue of the poor sporulation phenotype seen in an *sgs1* Δ mutant suggesting that this defect may be a result of accumulation of aberrant recombination intermediates that require Sgs1 to be resolved [77]. A *sgs1* Δ C795 allele sporulates just as well as a wildtype suggesting that the instability seen in *sgs1* Δ is due to loss of interaction with Top2 or Top3 which both interact with the N terminus of Sgs1 that is present in a *sgs1* Δ C795 mutant allele [78]. Additional work has revealed that Sgs1 is also able to disrupt D-loop structures and promotes formation of a Holliday junction intermediate that is dissolved by Top3/Rmi1 activity further supporting its role in meiosis considering similar substrates are present [37, 72, 79-82].

Sgs1 facilitates repair at telomeres

Telomeres are composed of protein-DNA complexes at the ends of chromosomes that help to maintain genome stability. In humans, telomeres contain a 10 kb TTAGGG repeat, the shelterin complex, and a 3' ssDNA overhang [83, 84]. In the absence of telomerase, the DNA ends shorten after each cell division and if left unchecked the cell will eventually die [85]. To avoid this, the cell can use telomerase or it can go through alternative lengthening of telomeres (ALT), which is a process that utilizes recombination [86-89]. The ALT pathway uses recombination to elongate

telomeres and is used in 5-15% of human cancers, including osteosarcoma and glioblastoma [88, 89]. RecQ helicases have been shown to co-localize with other components in this pathway, but their role remains unclear [90].

The G-rich regions of telomeric DNA may lead to the formation of G-quadruplexes, which if left unresolved can be toxic to the cell [91]. Sgs1 has been suggested to resolve these secondary structures and has been shown to resect telomeric regions that have a higher incidence of G-quadruplex formation [92, 93]. By inducing a site specific DSB in an *sgs1* Δ *exo1* Δ mutant, the presence of telomeric sequences in non-telomeric regions was observed suggesting Sgs1 and Exo1 work together to prevent these events from occurring [94, 95]. It was recently reported that Sgs1 is sumoylated at K621 and that this modification is important for its function in telomere-telomere recombination and is dispensable in its role in DNA repair [96]. If components at telomeres are dysregulated, unwanted intermediates may arise, which require the function of Sgs1 to be resolved and if they persist, can lead to cell death [97].

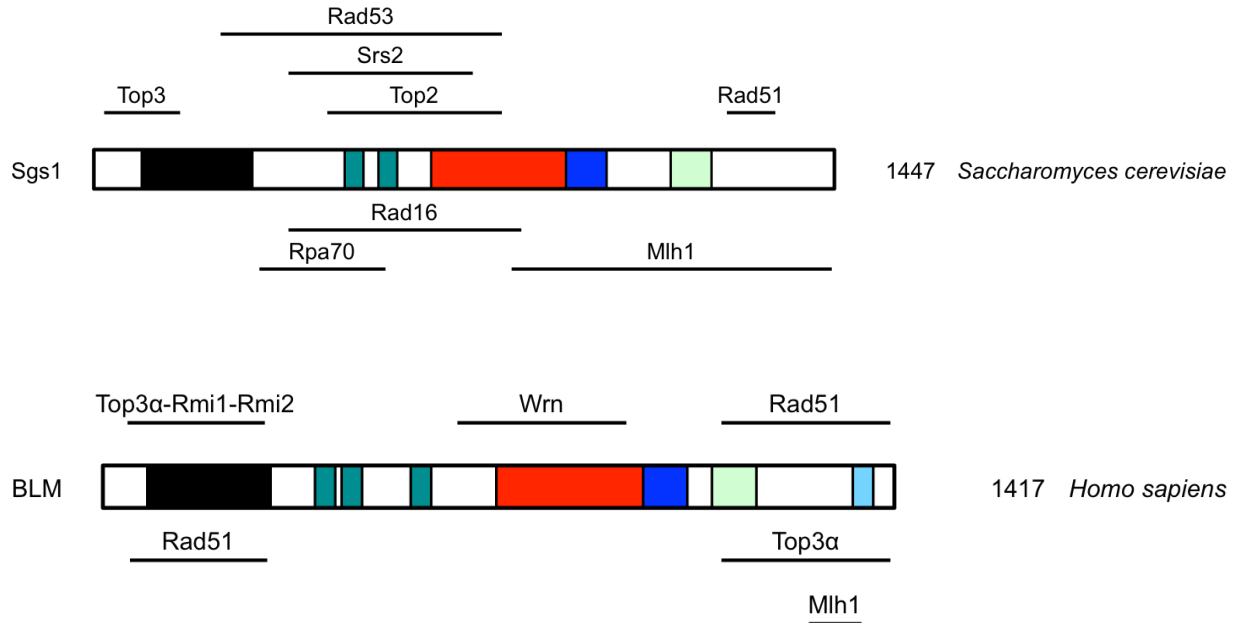


Figure 1.6. Conserved protein-protein interactions with Sgs1 and BLM

Sgs1 and BLM have several protein-protein interactions with proteins involved in DNA repair and recombination. Sgs1 interacts with Top3, Srs2, Top2, Rad16, Rpa70, Rad53, Mlh1, and Rad51. Many of the protein-protein interactions in Sgs1 are conserved in BLM with some additional interactions like WRN specific to BLM helicase. The colors for Sgs1 and BLM are the same as those in Figure 1.1.









Sgs1 interacting proteins

Sgs1 physically interacts with Top2 and Top3 through its N terminus (Figure 1.6) [76, 98]. In yeast, Top2 has a function in decatination of DNA molecules that form as a result of DNA replication [99, 100]. Without this function chromosomes run the risk of fragmenting and may not separate properly during mitosis [99, 100]. Top3 also interacts with Sgs1 and forms a complex that is required to resolve aberrant structures that result from Sgs1 activity [40, 101, 102]. Sgs1 has also been shown to interact genetically with Srs2, a DNA helicase involved in displacing Rad51 filaments. *sgs1Δ srs2Δ* double mutants show a growth defect suggesting the inability to displace Rad51 filaments may

be causing toxic intermediates, which, if left unresolved are deleterious to the cell [46, 103]. Rad51 of *S. cerevisiae* has a role in HR and repair of DSBs by recombination [104]. *rad51* Δ mutants have mitotic and meiotic defects and are sensitive to ionizing radiation (IR) [104]. Interaction between Sgs1 and its human counterpart, BLM, with Rad51 has been shown through yeast two-hybrid [104].

Apart from its role in DSB repair, Sgs1 also has a role in mismatch repair and nucleotide excision repair. Sgs1 interacts with Mlh1, a member of the MutL α complex that works with Pms1, required for ATP binding, during mismatch repair [105]. Through yeast two-hybrid analysis interaction with Rad16 has been observed. Rad16 belongs to the Swi2/Snf2 superfamily of DNA-dependent ATPase and functions during nucleotide excision repair [106]. Interaction between Sgs1 and Rad16 was confirmed by co-immunoprecipitation and the interaction was found to be between amino acids 421-792 [107]. *sgs1* Δ *rad16* Δ cells show slow growth in the presence of DNA damaging agents suggesting a role for Sgs1 during nucleotide excision repair [107].

Table 1.1. Comparison of helicase activities of *E. coli* RecQ with human and *S. cerevisiae* RecQ helicases^a

| | <i>E. coli</i> | Human RecQ helicases | | | | | <i>S. cerevisiae</i> |
|--|-------------------|----------------------|-----|-----|---------------------|----------------|----------------------|
| Substrate ^b | RecQ ^c | RECQL1 | BLM | WRN | RECQL4 ^d | RECQL5 β | Sgs1 |
|  | + | - | - | - | +/- | ND | +++ |
|  | + | ++ | + | + | + | + | +++ |
|  | + | ++ | ~/- | ~/- | ND | ND | +++ |
|  | ND | + | + | + | - | - | +++ |
|  | ND | ~/- | + | +++ | - | - | + |
|  | + | - | +++ | +++ | - | - | + |
|  | + | + | +++ | +++ | - | ~ | + |
|  | ND | - | + | + | ND | ND | ND |

This table has been adapted and modified from a review by Croteau, Popuri et al. (2014).

^a The data presented here is from the following studies: [44, 108-118]

^b DNA is represented as red and blue; RNA is represented as green.

^c Helicase activity: +, weak; ++, moderate; +++, strong; -, no activity; ~/-, partial activity; ND, not determined.

^d Activity of RECQL4 is shown in the absence of ssDNA

HUMAN RECQ-LIKE HELICASES

Humans possess five RecQ-like homologs BLM, WRN, RecQL1, RecQL4, and RecQL5. Defects in three of these five RecQ-like proteins (BLM, WRN, RECQL4) result in genetic disorders for which there is no cure as of yet.

Bloom Syndrome is an autosomal recessive disorder caused by a mutation in *BLM*

Mutations to *BLM* (15q26.1) result in Bloom syndrome (BS), also known as Bloom-Torre-Machacek syndrome, and patients have a predisposition to cancer, diabetes, and pulmonary disease [119-122]. Bloom syndrome is extremely rare and most patients are of Central and Eastern European (Ashkenazi) background [123]. Patients are characterized by having short stature and rarely exceed five feet in height during adulthood [123]. They are sensitive to sun exposure and suffer from telangiectases and hyper- or hypopigmentation of the skin (Figure 1.7) [124]. Other distinctive physical features include high vocal inflection and a long narrow face with prominent nose and ears [125]. Men usually do not produce sperm and are infertile and women have reduced fertility with early onset menopause [112]. *BLM* is expressed in the spleen, thymus, testis, and ovaries during embryogenesis [126]. Mouse models containing mutations in *BLM* found in the general population have been generated. *BLM*^{-/-} mice are smaller than *BLM*^{+/-} or wildtype mice, show developmental defects, have increased incidence of SCEs, and have a higher incidence of cancer upon inactivation of the helicase domain [120]. Additionally, inactivating the helicase domain of *BLM* in a cell with a mutation in the tumor suppressor gene *APC* results in higher levels of tumor formation [125]. Cells deficient for *BLM* are characterized by high levels of SCEs, increased mutation rates, inability to resolve DNA intermediates leading to slowed replication, and presence of quadriradials [20].

In mammalian cells, the central kinases ATM and ATR regulate the intra-S phase checkpoint, which responds to replication stress and inhibits cell cycle progression,

induces genes involved in the DNA damage response, restricts HR, and inhibits late origin firing [127]. Both ATM and ATR phosphorylate BLM at threonine 99 and 122 in the presence of UV irradiation, and phospho-defective mutants cannot recover [128]. Although phosphorylation of these residues inhibits recovery of BLM from replication stress, BLM is still able to suppress SCEs and localize to DNA damage foci [128]. In addition to being phosphorylated by ATM and ATR, BLM is also modified by Chk1 and Chk2, which are downstream of the checkpoint response and lead to localization of BLM to sites of DNA damage [129]. Cells depleted for BLM have checkpoint defects, cannot activate CHK1, and are more sensitive to the DNA damaging agent camptothecin [125, 130].

As it is a member of the RecQ family of helicases, BLM has a core helicase domain with ATP-binding and DEAH motifs, a RecQ helicase C-terminal domain (RQC) adjacent to the helicase domain that promotes protein-protein interactions, and a helicase and RNase D C-terminal domain (HRDC) that is on its C terminus [2, 10, 24, 32]. The disordered N terminal tail of BLM contains several sites of post-translational modifications (PTM) that mediate interaction with RMI1/2, TOP3 α , and RAD51 [40, 73, 104, 131-134]. BLM has a role in resolving recombination intermediates similar to that of Sgs1 in yeast and is able to dissociate D-loops *in vitro* with specificity for invaded 5' ends by preventing the formation of RAD51 filaments [135, 136]. It has been further shown that BLM and TOP3 α in combination with RMI1 and RMI2 are required for dHJ dissolution [125]. RMI1 and RMI2 are thought to help recruit TOP3 α to the dHJ [137].



Figure 1.7. Individuals with Bloom syndrome

Patient on the left and center have facial telangiectasias, a hallmark of the syndrome. The patients on the right are siblings with the brother to the left positive for Bloom syndrome. Images are from the Bloom syndrome registry, Weill Cornell Medical College.

Werner syndrome is an autosomal recessive disorder characterized by premature aging

Werner syndrome protein, WRN, like BLM is a RecQ-like DNA helicase and defects in this protein are associated with a predisposition to cancer with a majority of patients with this syndrome linked to a founder mutation in Japan [138]. Cells from individuals suffering from Werner syndrome have increased sister chromatid exchange, shortened telomeres, and genomic instability, specifically chromosome rearrangements like translocations, inversions, and deletions [139-141]. In addition to these cellular defects, patients with Werner syndrome show distinct clinical features such as type II diabetes, cataracts, atherosclerosis, arteriosclerosis, osteoporosis, and accelerated aging [142, 143]. Patients develop normally until adolescence, then symptoms manifest in early adulthood and death occurs around 46-54 years of age (Figure 1.8) [138]. BLM manifests different clinical symptoms and these differences in physical features of

patients with this syndrome compared to BLM show that WRN and BLM cannot compensate for each other, suggesting they have independent roles in the cell.

WRN is 1432 amino acids in length and contains an exonuclease domain on its N terminus, the RQC domain, and an HRDC domain (Figure 1.1) [144]. Both WRN and BLM possess the helicase core and HRDC domain, but the ATPase domain of WRN and BLM is only 30% similar while the RQC domain and HRDC domains are 10% and 20% similar [145]. The RQC domain of WRN is critical for DNA strand separation and is linked to the Zn binding domain by a short linker sequence resulting in a winged-helix motif [33, 146].

The function of the HRDC domain, unlike the RQC domain, is not well understood. In human RecQ helicases only WRN and BLM possess the HRDC domain. The HRDC domain was initially discovered from studies of bacterial DNA helicase PcrA and Rep [11, 12, 147]. Studies of *S. cerevisiae* Sgs1 have shown that the HRDC domain weakly binds DNA via its attraction to its positive surface [24]. Notably, the surface of WRN does not share the same characteristics as that of Sgs1. The HRDC domain of WRN is linked to the RQC domain by residues 1065-1141 which is unstructured and contributes to the distance of the HRDC domain from the RQC domain [142]. This flexibility might allow for protein-protein interactions that may help recruit WRN to sites of damage.

WRN has several roles during DNA repair. During base excision repair (BER), WRN, through its exonuclease activity is thought to have a role in post replication repair [148]. WRN interacts with poly (ADP-ribose) polymerase I (PARP1), which adds substrates into chromatin-binding proteins allowing for modification of chromatin

structure [149, 150]. Cells depleted for WRN are unable to activate PARP1, which results in an inability to resolve oxidized and alkylated DNA demonstrating an important role for WRN in BER [148]. During double strand break repair, DNA can be resolved by non-homologous end joining (NHEJ) or HR. NHEJ requires 53BP1, DNA-PKcs, XLF/XRCC4/LIG4, and Ku70/Ku80 (Ku) [151, 152]. WRN is a substrate for DNA-PKcs and physically interacts with Ku [153-156]. Cells depleted for WRN show increased chromosomal deletions and are sensitive to IR [155]. Even though WRN possesses exonuclease activity it has been observed that this activity hinders proper resection during HR and that BLM has a more important role with its interaction with EXO1 and DNA2 [157]. WRN lacks anti-recombinogenic activities like BLM but has been thought to suppress recombination [104, 158]. This may be mediated through its interaction with several HR proteins: BRCA1, MRN, RAD51, RAD54, and RAD52 [159-162]. WRN depleted cells are defective in telomere replication and these cells have increased sister telomere loss (STL) which suggest that WRN may prevent deletions during telomeric replication and that it may resolve secondary structures that may lead to telomere defects [163]. If the damage cannot be resolved then there is a risk of cell cycle arrest and chromosomal instability.

WRN also undergoes post-translational modifications, which are critical for regulating its catalytic activities, protein-protein interactions, and cellular localization. WRN undergoes phosphorylation by DNA-PKcs, ATR, ATM, and c-Abl tyrosine kinase [164-167]. Phosphorylation of WRN occurs when the replication machinery encounters a block, and both ATM and ATR kinases have been shown to activate WRN in the presence of HU [164]. Experiments have shown that inhibiting ATR mediated

phosphorylation prevents WRN from localizing to nuclear foci and can result in collapsed forks [164]. Acetylation of WRN by p300 allows WRN to move from nucleolar foci to nuclear foci and may enhance its helicase and exonuclease activity shedding light on its role during BER [168].

Mouse models, constitutively expressing *Wrn*, have been generated to study the phenotype seen in Werner patients. One specific model has the helicase domain disrupted resulting in a truncated protein [169]. Although this particular model did not exhibit the premature aging phenotype of Werner patients, it is sensitive to camptothecin, an inhibitor of topoisomerase I [170]. WRN has an important role in maintaining telomeres and mouse models with telomerase RNA, *Terc*, depleted in combination with a *Wrn*^{-/-} mutation showed premature aging phenotypes and early development of type II diabetes and osteoporosis [41, 171].

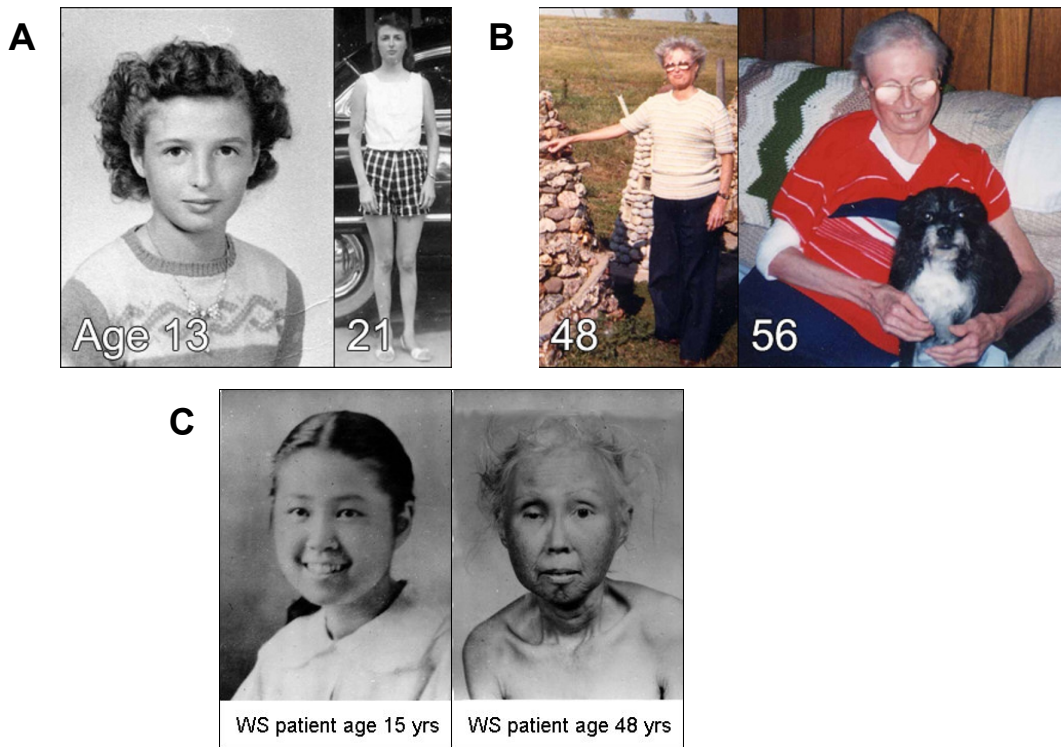


Figure 1.8. Patients with Werner syndrome at various ages

These images show patients who suffer from Werner syndrome and specifically premature ageing that is associated with this syndrome. **A and B)** Patients from America that suffer from Werner syndrome. **C)** A patient of Japanese descent that has Werner syndrome and premature ageing is most evident in this patient. Images are from University of Washington and a review by Bohr et al. (2008).

Rothmund-Thomson syndrome is caused by a mutation to *RECQL4*

Mutations in *RecQL4* result in Rothmund-Thomson Syndrome (RTS), RAPADALINO syndrome, or Baller-Gerold Syndrome (BGS). Patients suffering from these syndromes display growth retardation and radial defects [111]. RAPADALINO patients are most commonly found in Finland and are distinct from those suffering from the other syndromes in that they do not show clinical features such as poikiloderma. RTS is the most common of the three syndromes, and patients age rapidly, are

sensitive to light, have skin and skeletal abnormalities and, at the cellular level, cells depleted for RecQL4 have increased chromosomal instability (Figure 1.9) [172-174].

RecQL4 can be found in the cytosol, mitochondria and nucleus, has peak expression during S phase and highest expression is found in the testis and thymus [175]. RecQL4 has a role during replication, particularly in its initiation, and work has been carried out in *Drosophila*, *Xenopus*, and Chicken DT40 cells to explore this function. In *Drosophila* and Chicken DT40 cells, RecQL4 binds to origins of replication during G1/S phase of the cell cycle and physically interacts with MCM2-7 helicase, MCM10, GINS, and CDC45 [35, 176-179]. Additionally, RecQL4 in *Xenopus* shares sequence similarity to *S. cerevisiae* Sld2, which is responsible for initiating replication and DNA Pol α loading onto origins. RecQL4 interacts with TRF1, TRF2, and POT1 (shelterin proteins), which help unwind telomeric D-loops by stimulating RecQL4 activity [180-182]. Cells depleted for RecQL4 have telomere defects, specifically in telomere replication, and it has been shown that RecQL4 localizes to telomeres during S phase [157, 180, 181, 183-185]. RecQL4 may also play a role in the intra-S phase checkpoint response as cells depleted for RecQL4 are unable to arrest in S phase following treatment with HU, UV light, or IR [186, 187].

Mouse models have been generated to study RTS and most mutations in patients who have RTS syndrome map to the helicase domain [188]. One such mutation has exon 13 (motif III) deleted and mice have reduced lifespan and those that do survive are smaller and have skin abnormalities [188]. Another mouse model to study RTS was created by mutating the helicase domain in exons 9-13 of RecQL4, which results in a truncated protein. These mice die rapidly, within 24 hours of birth, and have

skin and skeletal abnormalities. Additionally, in these mice if the mutated tumor suppressor gene *APC* is combined with the *RecQL4* mutation, the mice have a higher incidence of cancer and increased chromosomal instability [189, 190].



Figure 1.9. Patients showing clinical features of Rothmund-Thomson syndrome

A) This patient is a 4 year-old girl who shows chronic poikiloderma on the cheek. **B)** This is another patient who shows poikiloderma on the cheek more visibly. **C)** X-Ray of a patient showing bone defects. Images are from Bartyik et al. (2013) and Wang et al. (2001).

RECQL1* and *RECQL5

RECQL1 has no associated human disease and is the smallest of the RecQ like proteins with a molecular mass of approximately 71 kD [173]. Several studies have implicated *RECQL1* as being an important component in regulating genome stability [35, 191]. Studies have revealed that *RECQL1* possess ATPase activity and is capable of unwinding short lengths of duplex DNA *in vitro* [192]. *RECQL1* has been shown to interact with RPA and mismatch repair factors Msh2/Msh6, Exo1, Mlh1/Pms2, Topoisomerase III, importin homologs, and Rad51 [191, 193-195]. The functional significance of these protein-protein interactions, however, remains unknown.

RecQL5 consists of 19 exons and encodes three alternatively spliced isoforms, *RecQL5 α* , *RecQL5 β* and *RecQL5 γ* [196]. In human tissues *RecQL5* isoforms are

expressed with high abundance in the testis [196]. *RECQL5* possess DNA dependent ATPase activity and contains a DExH and Zn binding domains at its N terminus [197]. The helicase possesses 3'-5' polarity and has a unique C terminal half that has been implicated in DNA strand annealing activity [197]. RecQL5 has also been found to interact with RNAPII, which may implicate RecQL5 in transcription [197].

Table 1.2. DNA helicases involved in maintaining genome integrity

| Gene | Disease | Metabolic Pathway | Biochemical properties | Type of Cancer |
|---------------|--|--|--|--|
| <i>BLM</i> | Bloom syndrome | DSB repair and repair of damage during replication | 3'-5' helicase, HJ branch migration, G4 structure resolution, fork regression and strand annealing | Leukemia, lymphomas, adult epithelial tumors |
| <i>WRN</i> | Werner syndrome | DSB repair and response to replication stress | 3'-5' helicase and exonuclease, HJ branch migration, G4 structure resolution, fork regression and strand annealing | Melanomas, sarcomas, meningiomas, osteosarcomas, thyroid neoplasms, lymphoid neoplasms |
| <i>RECQL4</i> | Rothmund-Thomson syndrome, Baller Gerald syndrome, and RAPADILINO syndrome | BER, mitochondrial genome stability, DNA replication | 3'-5' helicase and strand annealing | Lymphomas and osteogenic sarcomas |
| <i>RECQL1</i> | ND | DNA replication and oxidative DNA damage response | 3'-5' helicase, HJ branch migration and strand annealing | Pancreatic cancer |

Table 1.2 (continued)

| | | | | |
|--------------|---|--|--|--|
| <i>PIF1</i> | ND | Fork progression, telomere maintenance, and mitochondrial DNA metabolism | 5'-3' helicase and G4 resolvase | Breast cancer predisposition |
| <i>FANCI</i> | Fanconi Anemia (FA) | DSB repair and intercross link repair | 5'-3' helicase and G4 resolvase | Acute myeloid leukemia and breast cancer |
| <i>XPD</i> | Xeroderma pigmentosum, xeroderma pigmentosum with Cockayne syndrome, TTD and COFS | Nucleotide excision repair and transcription | 5'-3' helicase | Skin cancer |
| <i>XPB</i> | Xeroderma pigmentosum, xeroderma pigmentosum with Cockayne syndrome, and TTD | Nucleotide excision repair and transcription | 3'-5' helicase | Skin cancer |
| <i>RTEL1</i> | Dyskeratosis congenita | Maintenance of telomeres and HR | 5'-3' helicase, and disassembly of D-loops and T-loops | Adult glioma |

This table was adapted and modified from a review by Brosh (2013).

NON-RECQ LIKE DNA HELICASES AND THEIR ROLE IN THE MAINTENANCE OF GENOME INTEGRITY

Among nuclear proteins in *S. cerevisiae*, there are 23 with helicase activity and evidence for functions in DNA repair. Of the 23 proteins with helicase activity, non-RecQ DNA helicases with a role in DNA repair were selected and will be discussed here.

Chl1 has a role in sister chromatid cohesion

S. cerevisiae Chl1 is a DNA helicase that is important for sister chromatid cohesion. Mutations in the human cohesion subunits (SMC1A/Smc1, RAD21/Mcd1/Sccl, SMC3, HDAC8/Hos1, APRIN/Pds5, NPBL/Sccl, BACH1/BRIP/FANCI/Chl1, ESCO2/Eco1/Ctf7, and ChIR1/DDX11/Chl1) result in Cornelia de Lange Syndrome, Roberts Syndrome, Warsaw Breakage Syndrome and Fanconi Anemia [198-210]. Chl1 has recently been shown to play a role in recruiting and regulating the cohesion subunit Sccl to chromatin during S-phase [211]. It has been proposed that Chl1 may be removing DNA secondary structures to allow for recruitment of Sccl during S phase and thereby promoting sister chromatid cohesion [211].

Irc20 functions during DSB repair

IRC20 was found in a screen for gene deletions that increase the formation of Rad52 foci [212]. Irc20 is part of the Snf2/Swi2 family of helicases and has a C3HC4 domain that is part of the RING subset of E3 ligases [213]. Cells lacking Irc20 have reduced SDSA events, shows decreased crossover events, and inhibit activity of Srs2 and Mre11 [214]. It was found through crossover assays that Irc20 may function prior to the formation of a D-loop, followed by disassembly by Srs2 to promote SDSA over dHJ intermediate formation [214]. It was found that *irc20* Δ suppressed the defects of *mre11* Δ cells (inhibition of SDSA, NHEJ, and crossover events) and that this suppression was partially dependent on Exo1 [214]. This suggests that Irc20 is important in shuttling

DSBs to be processed by Mre11 to initiate end resection and that the absence of Irc20 results in formation of more 3' ssDNA at DSBs [215].

Mph1 is involved in preventing crossovers and has a role in error-free bypass of DNA lesions

Mph1, a 3'-5' DNA helicase, is related to human FANCM, and has been shown to disrupt Rad51 D-loops, suggesting that it has anti-recombination functions [216, 217]. The absence of Mph1 results in increased crossover frequency, and this role is independent of Sgs1 and Srs2 [218]. Mph1 has been proposed to play a role in error-free lesion bypass repair by template switching and cells lacking Mph1 have a mutator phenotype and impairment of sister chromatid cohesion [219, 220]. Mph1 can form and unwind D-loop structures during SDSA repair of DSBs, and may be involved in reversing these D-loop structures at stalled replication forks [218].

Pif1 has a role at telomeres, double-strand breaks and promoting fork progression through aberrant DNA structures

Pif1 is a 5'-3' DNA helicase that is found in the nucleus and mitochondria, and has roles in telomere maintenance, resolving G-quadruplex DNA, Okazaki fragment processing, and unwinding duplex DNA [221-226]. Pif1 was initially discovered from a screen for mutations that affect recombination between *rho*⁺ and *rho*⁻ mitochondrial genomes and it was found that Pif1 deficient cells had reduced mitochondrial DNA recombination resulting in a greater loss of mtDNA compared to wildtype [221, 227, 228].

In the absence of Pif1, the length of telomeres increased by ~75 base pairs and this was not only at chromosomal ends but also at intrachromosomal DSBs [229]. Pif1 directly disassembles telomerase from telomeric ends in a helicase dependent manner, thereby reducing the processivity of telomerase [226]. Pif1's role at telomeres is further evidenced by the fact that it binds RNA-DNA hybrids with greater affinity than DNA-DNA, supporting the notion that Pif1 disassembles *TLC1*, the RNA portion of telomerase [230-232].

Using ChIP analysis it was found that Pif1 has a strong affinity for G4 structures *in vivo* during late S/G2 phase of the cell cycle and fork progression is hindered in its absence [233]. Pif1 also has a role at the replication fork and is thought to pause the fork at the rDNA region. During HR, Pif1 works with Pol δ to displace the newly synthesized DNA strand and promote D-loop migration [225]. Although mutations in mice show no visible phenotype, defects in human PIF1 results in breast cancer predisposition, suggesting a possible role for PIF1 as a tumor suppressor [234].

Rad5 is involved in error-free PRR

DNA lesions can be resolved by post replication repair (PRR). PRR is dependent upon Rad6 and Rad18, which form a ubiquitin ligase and conjugating enzyme complex [235]. In *S. cerevisiae*, the Rad6-Rad18 complex promotes replication through DNA lesions through several pathways. DNA polymerase pol η and pol ξ allow for progression through DNA lesions in an error-prone manner [236]. Alternatively, an error-free mode of repair using Rad5-Mms2-Ubc13 can be used. Rad5 belongs to the SWI/SNF2 superfamily of proteins and contains seven conserved helicase-like motifs [237, 238].

Mms2 and Ubc13 interact and promote the assembly of polyubiquitin chains linked through lysine 63 [239, 240]. Pol30 encodes PCNA which is the proliferating cell nuclear antigen, a sliding clamp on DNA, which is important for modulating different lesion bypass pathways and possibly providing support for TLS polymerases to bind [240]. In the presence of DNA damage, PCNA is monoubiquitinated at lysine 164 by Rad6-Rad18 [241]. The lysine is then polyubiquitinated by a lysine 63-linked ubiquitin chain in an Mms2-Ubc13-Rad5 dependent manner [241]. Monoubiquitination of PCNA results in activation of TLS (Pol η and Pol ξ) whereas polyubiquitination of PCNA results in PRR [239, 242]. In PRR, it is thought that the lesion is bypassed by template switching and fork regression where the newly synthesized strand encountering an obstacle uses the sister duplex as a template to ensure error-free repair (Figure 1.10) [236].

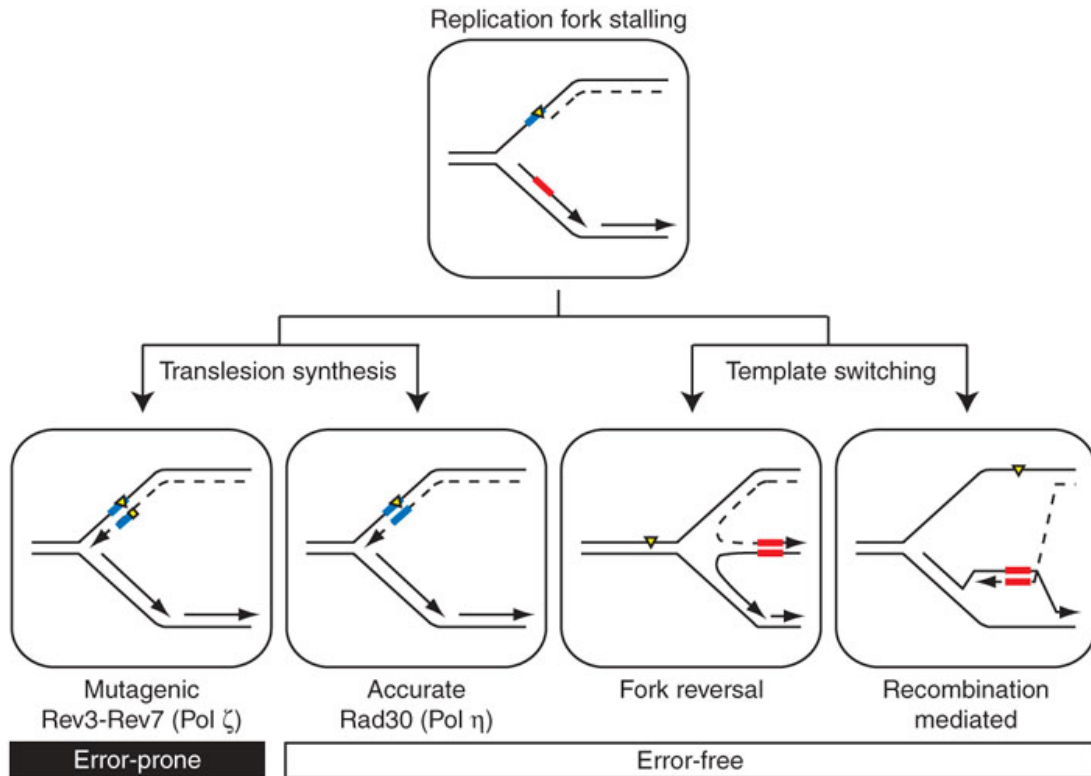


Figure 1.10. Mechanisms for DNA lesion bypass.

Lesions at the replication fork can lead to fork stalling and genome instability. The cell can bypass these lesions using translesion synthesis or template switching. In the presence of such lesions, Rad6-Rad18 have a key role in shuttling the damage to a particular pathway. Rad6-Rad18 monoubiquitinates PCNA, promoting error prone translesion synthesis. Rad5-Mms2-Ubc13 can promote polyubiquitination of PCNA which leads to an error-free mode of repair using template switching. The lesion can be bypassed using the nascent lagging strand as a template for synthesis past this lesion. Image adapted from Cimprich and Chang (2009).

Rrm3 has a role in replication fork progression

Rrm3 is a 5'-3' DNA helicase that is a member of the Pif1 family of DNA helicases and is highly conserved from yeast to humans [61]. *S. cerevisiae* RRM3 was first discovered as a suppressor of recombination between tandem arrays and ribosomal DNA (rDNA) repeats [243]. In the absence of Rrm3 there are elevated levels of extrachromosomal rDNA circles, suggesting a role in maintaining rDNA stability. The

cells accumulate X-shaped intermediates at stalled replication forks, which are detected by 2D gel electrophoresis. This has led to the possibility that Rrm3 facilitates in displacing the DNA-protein block and in unwinding of DNA to help fork convergence during replication termination [244]. Additionally, in the absence of Rrm3 there is an increase in replication fork pausing at the ribosomal DNA, centromeres, telomeres, tRNA, HML/HMR loci, inactive origins, and RNA polymerase II (Pol II) – transcribed genes [243, 245, 246].

Rrm3 has an important role in fork progression and maintaining genome integrity, because in its absence there are broken replication forks within rDNA, tRNA, and subtelomeric DNA [61, 245]. The mechanism by which Rrm3 aids in fork progression is poorly understood, but it is thought that Rrm3 removes aberrant structures during replication [61]. *S. cerevisiae* rDNA is composed of 200 tandem copies of ~9.1-kb repeating unit on chromosome XII [247, 248]. Within the coding regions of these RNAs there are two intergenic spacers, IGS1 and IGS2, that contain two tandem Ter sites [249]. The two Ter sites are bound by the replication terminator protein, Fob1, to promote fork arrest in order to prevent unscheduled transcription [250, 251]. The Ter sites also require the intra-S phase checkpoint proteins Tof1 and Csm3, which form a complex at the replication fork and antagonize Rrm3 function [252, 253]. It is thought that Rrm3 removes Fob1 and X-shaped intermediates from Ter sites during fork movement and other non-histone proteins on DNA ahead of the replication fork [244]. Type IA (Top3) and type II (Top2) topoisomerases have a role in replication termination, but Top2 resolves the strain created at TERs as evidenced by the fact that in the absence of Top2, there are increased levels of breaks and rearrangements [244, 254-

258]. Direct evidence for Rrm3 in facilitating fork merging has not been shown, but recent evidence shows that fission yeast Pfh1 has similar functions to Rrm3 and promotes fork merging at replication termination sites [259]. Rrm3 also has a role in replicating telomeric and subtelomeric DNA and in the absence of Rrm3 there is increased pausing within telomeric repeats [246]. It has been shown that the ability of Rrm3 to promote replication through these regions is dependent on its catalytic function [260]. Taken together this data suggests that Rrm3 helps to prevent aberrant chromosome segregation and helps to maintain genome stability.

Further evidence indicating Rrm3 has a role in fork progression is shown by the fact that *rrm3Δ* shows growth defects with *rad53Δ*, *srs2Δ*, *sgs1Δ*, *mrc1Δ*, and *rtt101Δ*, components involved in maintaining the stalled fork [261-263]. Srs2 is also a 3'-5' DNA helicase that has been implicated in resolving lethal recombination intermediates at sites of DNA damage and this function becomes crucial in the absence of Rrm3 or Sgs1 [261, 262]. Cells lacking Rrm3 and Sgs1 or Srs2 have increased doubling times and *rrm3Δ srs2Δ* cells accumulate in G₂/M [261]. In the absence of Mrc1 there is a slower rate of replication and it has been shown that Rrm3 is important in repairing the damage [264]. The sensor and effector kinases Mec1 and Rad53 are important in the absence of Rrm3, as there is a severe growth defect in their absence [245, 262]. Upon activation of the checkpoint response in the presence of DNA damage in *rrm3Δ* cells, Rad53 is constitutively phosphorylated [245, 265]. Rrm3 is hyper-phosphorylated by Rad53 under replication stress, and it has been proposed that this inhibits its activity in response to DNA damage to allow for repair [265].

Srs2 functions in multiple DNA metabolic processes

Srs2 is a DNA helicase that shares homology with the bacterial Rep, PcrA, and UvrD [266]. It was first discovered as a suppressor of sensitivity of *rad6Δ* and *rad18Δ* mutants (Suppressor of RAD Six mutant 2) [267, 268]. Srs2 has 3'-5' polarity, strong ssDNA dependent ATPase activity, and can resolve D-loops and forks [269]. RPA enhances Srs2's ability to resolve long substrates and in its absence cells have higher recombination events, cannot accurately complete post replication repair, and have problems with the DNA damage checkpoint [270-272].

Srs2 is thought to function early in HR and displaces Rad51 presynaptic filament [273]. This is supported by experiments in *S. cerevisiae* where *SRS2* deletion resulted in a hyper-recombination phenotype [272]. A *srs2Δ sgs1Δ* cell was found to be slow growing, suggesting that improper regulation of HR can be deleterious to the cell. Srs2 may also have a role in PRR as shown by increased sensitivity of *srs2Δ* cells to UV light [274]. Srs2 may be deciding whether a lesion should be repaired by HR or PRR [235].

HYPOTHESIS AND AIMS

Helicases have important roles in DNA metabolism and maintaining genome integrity. Defects in many helicases are associated with cancers and genetic disorders. Studying helicases involved in maintaining genome stability in *S. cerevisiae* has helped elucidate their functions in humans, but the complexity of the DNA damage response leaves us with many unanswered questions. Here, we functionally characterize RecQ-like (Sgs1 and RecQL5) and non-RecQ like (Rrm3) helicases and hypothesize that

defects in these helicases, with roles in DNA replication and repair, will result in genome instability. This hypothesis will be addressed through the following aims:

Aim 1 (Chapter Two) – We seek to identify the role of the conserved functional domains of Sgs1 of *S. cerevisiae* in the maintenance of genome integrity.

Aim 2 (Chapter Three) – We seek to identify human RecQL5 interacting proteins and to test the ability of RecQL5 to complement Sgs1 functions in yeast to shed light on cellular pathways that RecQL5 functions in.

Aim 3 (Chapter Four) – We seek to identify DNA metabolic pathways that respond to stalled forks in the absence of Rrm3 using stable isotope labeling by amino acids in cell culture (SILAC)-based quantitative mass spectrometry.

SIGNIFICANCE

This work will allow for a better understanding of nonreplicative helicases involved in DNA repair and may reveal additional components involved in the DNA damage response. Elucidating such factors may lead to a greater understanding of how these proteins are involved in the development of hereditary cancer syndromes, with implications that may lead to a greater quality of life among affected individuals.

REFERENCES

1. Khan, I., J.A. Sommers, and R.M. Brosh, Jr., *Close encounters for the first time: Helicase interactions with DNA damage*. DNA Repair (Amst), 2015. **33**: p. 43-59.
2. Singleton, M.R., M.S. Dillingham, and D.B. Wigley, *Structure and mechanism of helicases and nucleic acid translocases*. Annu Rev Biochem, 2007. **76**: p. 23-50.
3. Abdelhaleem, M., *Do human RNA helicases have a role in cancer?* Biochim Biophys Acta, 2004. **1704**(1): p. 37-46.
4. Hanada, K. and I.D. Hickson, *Molecular genetics of RecQ helicase disorders*. Cell Mol Life Sci, 2007. **64**(17): p. 2306-22.
5. Koonin, E.V., *A common set of conserved motifs in a vast variety of putative nucleic acid-dependent ATPases including MCM proteins involved in the initiation of eukaryotic DNA replication*. Nucleic Acids Res, 1993. **21**(11): p. 2541-7.
6. Guo, P., et al., *Common mechanisms of DNA translocation motors in bacteria and viruses using one-way revolution mechanism without rotation*. Biotechnol Adv, 2014. **32**(4): p. 853-72.
7. Abdel-Monem, M., H. Durwald, and H. Hoffmann-Berling, *Enzymic unwinding of DNA. 2. Chain separation by an ATP-dependent DNA unwinding enzyme*. Eur J Biochem, 1976. **65**(2): p. 441-9.
8. Lohman, T.M., E.J. Tomko, and C.G. Wu, *Non-hexameric DNA helicases and translocases: mechanisms and regulation*. Nat Rev Mol Cell Biol, 2008. **9**(5): p. 391-401.
9. Pyle, A.M., *Translocation and unwinding mechanisms of RNA and DNA helicases*. Annu Rev Biophys, 2008. **37**: p. 317-36.
10. Fairman-Williams, M.E., U.P. Guenther, and E. Jankowsky, *SF1 and SF2 helicases: family matters*. Curr Opin Struct Biol, 2010. **20**(3): p. 313-24.
11. Subramanya, H.S., et al., *Crystal structure of a DExx box DNA helicase*. Nature, 1996. **384**(6607): p. 379-83.
12. Korolev, S., et al., *Major domain swiveling revealed by the crystal structures of complexes of E. coli Rep helicase bound to single-stranded DNA and ADP*. Cell, 1997. **90**(4): p. 635-47.
13. Gu, M. and C.M. Rice, *Three conformational snapshots of the hepatitis C virus NS3 helicase reveal a ratchet translocation mechanism*. Proc Natl Acad Sci U S A, 2010. **107**(2): p. 521-8.

14. Yarranton, G.T. and M.L. Gefter, *Enzyme-catalyzed DNA unwinding: studies on Escherichia coli rep protein*. Proc Natl Acad Sci U S A, 1979. **76**(4): p. 1658-62.
15. Bennett, R.J. and J.L. Keck, *Structure and function of RecQ DNA helicases*. Crit Rev Biochem Mol Biol, 2004. **39**(2): p. 79-97.
16. Fuller-Pace, F.V., *DExD/H box RNA helicases: multifunctional proteins with important roles in transcriptional regulation*. Nucleic Acids Res, 2006. **34**(15): p. 4206-15.
17. Lusser, A. and J.T. Kadonaga, *Chromatin remodeling by ATP-dependent molecular machines*. Bioessays, 2003. **25**(12): p. 1192-200.
18. Jankowsky, E. and M.E. Fairman, *RNA helicases--one fold for many functions*. Curr Opin Struct Biol, 2007. **17**(3): p. 316-24.
19. Jankowsky, E. and H. Bowers, *Remodeling of ribonucleoprotein complexes with DExH/D RNA helicases*. Nucleic Acids Res, 2006. **34**(15): p. 4181-8.
20. Croteau, D.L., et al., *Human RecQ helicases in DNA repair, recombination, and replication*. Annu Rev Biochem, 2014. **83**: p. 519-52.
21. Schmidt, K.H. and R.D. Kolodner, *Suppression of spontaneous genome rearrangements in yeast DNA helicase mutants*. Proc Natl Acad Sci U S A, 2006. **103**(48): p. 18196-201.
22. Oh, S.D., et al., *RecQ helicase, Sgs1, and XPF family endonuclease, Mus81-Mms4, resolve aberrant joint molecules during meiotic recombination*. Mol Cell, 2008. **31**(3): p. 324-36.
23. Nakayama, H., et al., *Isolation and genetic characterization of a thymineless death-resistant mutant of Escherichia coli K12: identification of a new mutation (recQ1) that blocks the RecF recombination pathway*. Mol Gen Genet, 1984. **195**(3): p. 474-80.
24. Liu, Z., et al., *The three-dimensional structure of the HRDC domain and implications for the Werner and Bloom syndrome proteins*. Structure, 1999. **7**(12): p. 1557-66.
25. Gabaldon, T. and E.V. Koonin, *Functional and evolutionary implications of gene orthology*. Nat Rev Genet, 2013. **14**(5): p. 360-6.
26. Bernstein, D.A., M.C. Zittel, and J.L. Keck, *High-resolution structure of the E.coli RecQ helicase catalytic core*. EMBO J, 2003. **22**(19): p. 4910-21.
27. Pike, A.C., et al., *Structure of the human RECQ1 helicase reveals a putative strand-separation pin*. Proc Natl Acad Sci U S A, 2009. **106**(4): p. 1039-44.

28. Kitano, K., N. Yoshihara, and T. Hakoshima, *Crystal structure of the HRDC domain of human Werner syndrome protein, WRN*. J Biol Chem, 2007. **282**(4): p. 2717-28.
29. Mirzaei, H. and K.H. Schmidt, *Non-Bloom syndrome-associated partial and total loss-of-function variants of BLM helicase*. Proc Natl Acad Sci U S A, 2012. **109**(47): p. 19357-62.
30. Rong, S.B., J. Valiaho, and M. Vihinen, *Structural basis of Bloom syndrome (BS) causing mutations in the BLM helicase domain*. Mol Med, 2000. **6**(3): p. 155-64.
31. Lucic, B., et al., *A prominent beta-hairpin structure in the winged-helix domain of RECQ1 is required for DNA unwinding and oligomer formation*. Nucleic Acids Res, 2011. **39**(5): p. 1703-17.
32. Huber, M.D., et al., *A conserved G4 DNA binding domain in RecQ family helicases*. J Mol Biol, 2006. **358**(4): p. 1071-80.
33. Kitano, K., S.Y. Kim, and T. Hakoshima, *Structural basis for DNA strand separation by the unconventional winged-helix domain of RecQ helicase WRN*. Structure, 2010. **18**(2): p. 177-87.
34. Tadokoro, T., et al., *Human RECQL5 participates in the removal of endogenous DNA damage*. Mol Biol Cell, 2012. **23**(21): p. 4273-85.
35. Thangavel, S., et al., *Human RECQ1 and RECQ4 helicases play distinct roles in DNA replication initiation*. Mol Cell Biol, 2010. **30**(6): p. 1382-96.
36. Sato, A., et al., *Solution structure of the HRDC domain of human Bloom syndrome protein BLM*. J Biochem, 2010. **148**(4): p. 517-25.
37. Bennett, R.J., J.A. Sharp, and J.C. Wang, *Purification and characterization of the Sgs1 DNA helicase activity of Saccharomyces cerevisiae*. J Biol Chem, 1998. **273**(16): p. 9644-50.
38. Samanta, S. and P. Karmakar, *Recruitment of HRDC domain of WRN and BLM to the sites of DNA damage induced by mitomycin C and methyl methanesulfonate*. Cell Biol Int, 2012. **36**(10): p. 873-81.
39. Wu, L., et al., *The HRDC domain of BLM is required for the dissolution of double Holliday junctions*. EMBO J, 2005. **24**(14): p. 2679-87.
40. Gangloff, S., et al., *The yeast type I topoisomerase Top3 interacts with Sgs1, a DNA helicase homolog: a potential eukaryotic reverse gyrase*. Mol Cell Biol, 1994. **14**(12): p. 8391-8.

41. Bernstein, K.A., et al., *Sgs1 function in the repair of DNA replication intermediates is separable from its role in homologous recombinational repair*. EMBO J, 2009. **28**(7): p. 915-25.
42. Balogun, F.O., A.W. Truman, and S.J. Kron, *DNA resection proteins Sgs1 and Exo1 are required for G1 checkpoint activation in budding yeast*. DNA Repair (Amst), 2013. **12**(9): p. 751-60.
43. De Muyt, A., et al., *BLM helicase ortholog Sgs1 is a central regulator of meiotic recombination intermediate metabolism*. Mol Cell, 2012. **46**(1): p. 43-53.
44. Cejka, P. and S.C. Kowalczykowski, *The full-length Saccharomyces cerevisiae Sgs1 protein is a vigorous DNA helicase that preferentially unwinds holliday junctions*. J Biol Chem, 2010. **285**(11): p. 8290-301.
45. Cejka, P., et al., *DNA end resection by Dna2-Sgs1-RPA and its stimulation by Top3-Rmi1 and Mre11-Rad50-Xrs2*. Nature, 2010. **467**(7311): p. 112-6.
46. Mullen, J.R., et al., *Requirement for three novel protein complexes in the absence of the Sgs1 DNA helicase in Saccharomyces cerevisiae*. Genetics, 2001. **157**(1): p. 103-18.
47. Watt, P.M., et al., *SGS1, a homologue of the Bloom's and Werner's syndrome genes, is required for maintenance of genome stability in Saccharomyces cerevisiae*. Genetics, 1996. **144**(3): p. 935-45.
48. Mirzaei, H., et al., *Sgs1 truncations induce genome rearrangements but suppress detrimental effects of BLM overexpression in Saccharomyces cerevisiae*. J Mol Biol, 2011. **405**(4): p. 877-91.
49. Mullen, J.R., V. Kaliraman, and S.J. Brill, *Bipartite structure of the SGS1 DNA helicase in Saccharomyces cerevisiae*. Genetics, 2000. **154**(3): p. 1101-14.
50. Rockmill, B., et al., *The Sgs1 helicase regulates chromosome synapsis and meiotic crossing over*. Curr Biol, 2003. **13**(22): p. 1954-62.
51. Shibata, A., et al., *DNA double-strand break repair pathway choice is directed by distinct MRE11 nuclease activities*. Mol Cell, 2014. **53**(1): p. 7-18.
52. Lobachev, K.S., D.A. Gordenin, and M.A. Resnick, *The Mre11 complex is required for repair of hairpin-capped double-strand breaks and prevention of chromosome rearrangements*. Cell, 2002. **108**(2): p. 183-93.
53. Rattray, A.J., et al., *Fidelity of mitotic double-strand-break repair in Saccharomyces cerevisiae: a role for SAE2/COM1*. Genetics, 2001. **158**(1): p. 109-22.

54. Clerici, M., et al., *The Saccharomyces cerevisiae Sae2 protein promotes resection and bridging of double strand break ends*. J Biol Chem, 2005. **280**(46): p. 38631-8.
55. Limbo, O., et al., *Ctp1 is a cell-cycle-regulated protein that functions with Mre11 complex to control double-strand break repair by homologous recombination*. Mol Cell, 2007. **28**(1): p. 134-46.
56. Sartori, A.A., et al., *Human CtIP promotes DNA end resection*. Nature, 2007. **450**(7169): p. 509-14.
57. Symington, L.S. and J. Gautier, *Double-strand break end resection and repair pathway choice*. Annu Rev Genet, 2011. **45**: p. 247-71.
58. Mimitou, E.P. and L.S. Symington, *DNA end resection--unraveling the tail*. DNA Repair (Amst), 2011. **10**(3): p. 344-8.
59. Cannavo, E., P. Cejka, and S.C. Kowalczykowski, *Relationship of DNA degradation by Saccharomyces cerevisiae exonuclease 1 and its stimulation by RPA and Mre11-Rad50-Xrs2 to DNA end resection*. Proc Natl Acad Sci U S A, 2013. **110**(18): p. E1661-8.
60. Puddu, F., et al., *Sensing of replication stress and Mec1 activation act through two independent pathways involving the 9-1-1 complex and DNA polymerase epsilon*. PLoS Genet, 2011. **7**(3): p. e1002022.
61. Azvolinsky, A., et al., *The S. cerevisiae Rrm3p DNA helicase moves with the replication fork and affects replication of all yeast chromosomes*. Genes Dev, 2006. **20**(22): p. 3104-16.
62. Haber, J.E., *Chromosome breakage and repair*. Genetics, 2006. **173**(3): p. 1181-5.
63. Segurado, M. and J.A. Tercero, *The S-phase checkpoint: targeting the replication fork*. Biol Cell, 2009. **101**(11): p. 617-27.
64. Kondratova, A., et al., *Replication fork integrity and intra-S phase checkpoint suppress gene amplification*. Nucleic Acids Res, 2015. **43**(5): p. 2678-90.
65. Ohouo, P.Y. and M.B. Smolka, *The many roads to checkpoint activation*. Cell Cycle, 2012. **11**(24): p. 4495.
66. Majka, J., A. Niedziela-Majka, and P.M. Burgers, *The checkpoint clamp activates Mec1 kinase during initiation of the DNA damage checkpoint*. Mol Cell, 2006. **24**(6): p. 891-901.
67. Alcasabas, A.A., et al., *Mrc1 transduces signals of DNA replication stress to activate Rad53*. Nat Cell Biol, 2001. **3**(11): p. 958-65.

68. Bjergbaek, L., et al., *Mechanistically distinct roles for Sgs1p in checkpoint activation and replication fork maintenance*. *Embo J*, 2005. **24**(2): p. 405-17.
69. Frei, C. and S.M. Gasser, *RecQ-like helicases: the DNA replication checkpoint connection*. *J Cell Sci*, 2000. **113 (Pt 15)**: p. 2641-6.
70. Liberi, G., et al., *Rad51-dependent DNA structures accumulate at damaged replication forks in sgs1 mutants defective in the yeast ortholog of BLM RecQ helicase*. *Genes Dev*, 2005. **19**(3): p. 339-50.
71. Mankouri, H.W., H.P. Ngo, and I.D. Hickson, *Shu proteins promote the formation of homologous recombination intermediates that are processed by Sgs1-Rmi1-Top3*. *Mol Biol Cell*, 2007. **18**(10): p. 4062-73.
72. Mankouri, H.W. and I.D. Hickson, *Top3 processes recombination intermediates and modulates checkpoint activity after DNA damage*. *Mol Biol Cell*, 2006. **17**(10): p. 4473-83.
73. Chang, M., et al., *RMI1/NCE4, a suppressor of genome instability, encodes a member of the RecQ helicase/Topo III complex*. *EMBO J*, 2005. **24**(11): p. 2024-33.
74. Chakraverty, R.K. and I.D. Hickson, *Defending genome integrity during DNA replication: a proposed role for RecQ family helicases*. *Bioessays*, 1999. **21**(4): p. 286-94.
75. Gangloff, S., et al., *The essential role of yeast topoisomerase III in meiosis depends on recombination*. *EMBO J*, 1999. **18**(6): p. 1701-11.
76. Watt, P.M., et al., *Sgs1: a eukaryotic homolog of E. coli RecQ that interacts with topoisomerase II in vivo and is required for faithful chromosome segregation*. *Cell*, 1995. **81**(2): p. 253-60.
77. Miyajima, A., et al., *Sgs1 helicase activity is required for mitotic but apparently not for meiotic functions*. *Mol Cell Biol*, 2000. **20**(17): p. 6399-409.
78. Miyajima, A., et al., *Different domains of Sgs1 are required for mitotic and meiotic functions*. *Genes Genet Syst*, 2000. **75**(6): p. 319-26.
79. Ira, G., et al., *Srs2 and Sgs1-Top3 suppress crossovers during double-strand break repair in yeast*. *Cell*, 2003. **115**(4): p. 401-11.
80. Karow, J.K., et al., *The Bloom's syndrome gene product promotes branch migration of holliday junctions*. *Proc Natl Acad Sci U S A*, 2000. **97**(12): p. 6504-8.
81. Seki, M., et al., *Bloom helicase and DNA topoisomerase IIIalpha are involved in the dissolution of sister chromatids*. *Mol Cell Biol*, 2006. **26**(16): p. 6299-307.

82. Wu, L. and I.D. Hickson, *The Bloom's syndrome helicase suppresses crossing over during homologous recombination*. Nature, 2003. **426**(6968): p. 870-4.
83. Liu, D., et al., *Telosome, a mammalian telomere-associated complex formed by multiple telomeric proteins*. J Biol Chem, 2004. **279**(49): p. 51338-42.
84. Palm, W. and T. de Lange, *How shelterin protects mammalian telomeres*. Annu Rev Genet, 2008. **42**: p. 301-34.
85. Cong, Y.S., W.E. Wright, and J.W. Shay, *Human telomerase and its regulation*. Microbiol Mol Biol Rev, 2002. **66**(3): p. 407-25, table of contents.
86. Shay, J.W., *Meeting report: the role of telomeres and telomerase in cancer*. Cancer Res, 2005. **65**(9): p. 3513-7.
87. Artandi, S.E. and R.A. DePinho, *Telomeres and telomerase in cancer*. Carcinogenesis, 2010. **31**(1): p. 9-18.
88. Cesare, A.J. and R.R. Reddel, *Alternative lengthening of telomeres: models, mechanisms and implications*. Nat Rev Genet, 2010. **11**(5): p. 319-30.
89. Heaphy, C.M., et al., *Prevalence of the alternative lengthening of telomeres telomere maintenance mechanism in human cancer subtypes*. Am J Pathol, 2011. **179**(4): p. 1608-15.
90. Johnson, F.B., et al., *The Saccharomyces cerevisiae WRN homolog Sgs1p participates in telomere maintenance in cells lacking telomerase*. EMBO J, 2001. **20**(4): p. 905-13.
91. Smith, J.S., et al., *Rudimentary G-quadruplex-based telomere capping in Saccharomyces cerevisiae*. Nat Struct Mol Biol, 2011. **18**(4): p. 478-85.
92. Sun, H., R.J. Bennett, and N. Maizels, *The Saccharomyces cerevisiae Sgs1 helicase efficiently unwinds G-G paired DNAs*. Nucleic Acids Res, 1999. **27**(9): p. 1978-84.
93. Bonetti, D., et al., *Multiple pathways regulate 3' overhang generation at S. cerevisiae telomeres*. Mol Cell, 2009. **35**(1): p. 70-81.
94. Chung, W.H., et al., *Defective resection at DNA double-strand breaks leads to de novo telomere formation and enhances gene targeting*. PLoS Genet, 2010. **6**(5): p. e1000948.
95. Lydeard, J.R., et al., *Sgs1 and exo1 redundantly inhibit break-induced replication and de novo telomere addition at broken chromosome ends*. PLoS Genet, 2010. **6**(5): p. e1000973.

96. Rog, O., et al., *Sumoylation of RecQ helicase controls the fate of dysfunctional telomeres*. Mol Cell, 2009. **33**(5): p. 559-69.
97. Flynn, R.L., et al., *Alternative lengthening of telomeres renders cancer cells hypersensitive to ATR inhibitors*. Science, 2015. **347**(6219): p. 273-7.
98. Lu, J., et al., *Human homologues of yeast helicase*. Nature, 1996. **383**(6602): p. 678-9.
99. Adams, D.E., et al., *The role of topoisomerase IV in partitioning bacterial replicons and the structure of catenated intermediates in DNA replication*. Cell, 1992. **71**(2): p. 277-88.
100. Sundin, O. and A. Varshavsky, *Arrest of segregation leads to accumulation of highly intertwined catenated dimers: dissection of the final stages of SV40 DNA replication*. Cell, 1981. **25**(3): p. 659-69.
101. Bennett, R.J. and J.C. Wang, *Association of yeast DNA topoisomerase III and Sgs1 DNA helicase: studies of fusion proteins*. Proc Natl Acad Sci U S A, 2001. **98**(20): p. 11108-13.
102. Kennedy, J.A., G.W. Daughdrill, and K.H. Schmidt, *A transient alpha-helical molecular recognition element in the disordered N-terminus of the Sgs1 helicase is critical for chromosome stability and binding of Top3/Rmi1*. Nucleic Acids Res, 2013. **41**(22): p. 10215-27.
103. McVey, M., et al., *The short life span of Saccharomyces cerevisiae sgs1 and srs2 mutants is a composite of normal aging processes and mitotic arrest due to defective recombination*. Genetics, 2001. **157**(4): p. 1531-42.
104. Wu, L., et al., *Potential role for the BLM helicase in recombinational repair via a conserved interaction with RAD51*. J Biol Chem, 2001. **276**(22): p. 19375-81.
105. Dherin, C., et al., *Characterization of a highly conserved binding site of Mlh1 required for exonuclease I-dependent mismatch repair*. Mol Cell Biol, 2009. **29**(3): p. 907-18.
106. Paesi-Toresan, S.O., et al., *Gene PSO5 of Saccharomyces cerevisiae, involved in repair of oxidative DNA damage, is allelic to RAD16*. Curr Genet, 1995. **27**(6): p. 493-5.
107. Saffi, J., et al., *Interaction of the yeast Pso5/Rad16 and Sgs1 proteins: influences on DNA repair and aging*. Mutat Res, 2001. **486**(3): p. 195-206.
108. Garcia, P.L., et al., *Human RECQ5beta, a protein with DNA helicase and strand-annealing activities in a single polypeptide*. EMBO J, 2004. **23**(14): p. 2882-91.

109. Cui, S., et al., *Characterization of the DNA-unwinding activity of human RECQ1, a helicase specifically stimulated by human replication protein A*. J Biol Chem, 2003. **278**(3): p. 1424-32.
110. Rossi, M.L., et al., *Conserved helicase domain of human RecQ4 is required for strand annealing-independent DNA unwinding*. DNA Repair (Amst), 2010. **9**(7): p. 796-804.
111. Ferrarelli, L.K., et al., *The RECQL4 protein, deficient in Rothmund-Thomson syndrome is active on telomeric D-loops containing DNA metabolism blocking lesions*. DNA Repair (Amst), 2013. **12**(7): p. 518-28.
112. Bachrati, C.Z. and I.D. Hickson, *RecQ helicases: suppressors of tumorigenesis and premature aging*. Biochem J, 2003. **374**(Pt 3): p. 577-606.
113. Sharma, S., et al., *Biochemical analysis of the DNA unwinding and strand annealing activities catalyzed by human RECQ1*. J Biol Chem, 2005. **280**(30): p. 28072-84.
114. Popuri, V., et al., *The Human RecQ helicases, BLM and RECQ1, display distinct DNA substrate specificities*. J Biol Chem, 2008. **283**(26): p. 17766-76.
115. Ghosh, A., et al., *Telomeric D-loops containing 8-oxo-2'-deoxyguanosine are preferred substrates for Werner and Bloom syndrome helicases and are bound by POT1*. J Biol Chem, 2009. **284**(45): p. 31074-84.
116. Xu, X. and Y. Liu, *Dual DNA unwinding activities of the Rothmund-Thomson syndrome protein, RECQ4*. EMBO J, 2009. **28**(5): p. 568-77.
117. Cejka, P., et al., *Decatenation of DNA by the S. cerevisiae Sgs1-Top3-Rmi1 and RPA complex: a mechanism for disentangling chromosomes*. Mol Cell, 2012. **47**(6): p. 886-96.
118. Han, H., R.J. Bennett, and L.H. Hurley, *Inhibition of unwinding of G-quadruplex structures by Sgs1 helicase in the presence of N,N'-bis[2-(1-piperidino)ethyl]-3,4,9,10-perylenetetracarboxylic diimide, a G-quadruplex-interactive ligand*. Biochemistry, 2000. **39**(31): p. 9311-6.
119. Chester, N., et al., *Stage-specific apoptosis, developmental delay, and embryonic lethality in mice homozygous for a targeted disruption in the murine Bloom's syndrome gene*. Genes Dev, 1998. **12**(21): p. 3382-93.
120. Luo, G., et al., *Cancer predisposition caused by elevated mitotic recombination in Bloom mice*. Nat Genet, 2000. **26**(4): p. 424-9.
121. McDaniel, L.D. and R.A. Schultz, *Elevated sister chromatid exchange phenotype of Bloom syndrome cells is complemented by human chromosome 15*. Proc Natl Acad Sci U S A, 1992. **89**(17): p. 7968-72.

122. Chester, N., et al., *Mutation of the murine Bloom's syndrome gene produces global genome destabilization*. Mol Cell Biol, 2006. **26**(17): p. 6713-26.
123. German, J., et al., *Syndrome-causing mutations of the BLM gene in persons in the Bloom's Syndrome Registry*. Hum Mutat, 2007. **28**(8): p. 743-53.
124. Veith, S. and A. Mangerich, *RecQ helicases and PARP1 team up in maintaining genome integrity*. Ageing Res Rev, 2015. **23**(Pt A): p. 12-28.
125. Manthei, K.A. and J.L. Keck, *The BLM dissolvasome in DNA replication and repair*. Cell Mol Life Sci, 2013. **70**(21): p. 4067-84.
126. Moens, P.B., et al., *Expression and nuclear localization of BLM, a chromosome stability protein mutated in Bloom's syndrome, suggest a role in recombination during meiotic prophase*. J Cell Sci, 2000. **113** (Pt 4): p. 663-72.
127. Smith, J., et al., *The ATM-Chk2 and ATR-Chk1 pathways in DNA damage signaling and cancer*. Adv Cancer Res, 2010. **108**: p. 73-112.
128. Rao, V.A., et al., *Phosphorylation of BLM, dissociation from topoisomerase IIIalpha, and colocalization with gamma-H2AX after topoisomerase I-induced replication damage*. Mol Cell Biol, 2005. **25**(20): p. 8925-37.
129. Kaur, S., et al., *Chk1-dependent constitutive phosphorylation of BLM helicase at serine 646 decreases after DNA damage*. Mol Cancer Res, 2010. **8**(9): p. 1234-47.
130. Ashton, T.M. and I.D. Hickson, *Yeast as a model system to study RecQ helicase function*. DNA Repair (Amst), 2010. **9**(3): p. 303-14.
131. Chen, C.F. and S.J. Brill, *An essential DNA strand-exchange activity is conserved in the divergent N-termini of BLM orthologs*. EMBO J, 2010.
132. Wu, L., et al., *The Bloom's syndrome gene product interacts with topoisomerase III*. J Biol Chem, 2000. **275**(13): p. 9636-44.
133. Wu, L., et al., *BLAP75/RMI1 promotes the BLM-dependent dissolution of homologous recombination intermediates*. Proc Natl Acad Sci U S A, 2006. **103**(11): p. 4068-73.
134. Raynard, S., W. Bussen, and P. Sung, *A double Holliday junction dissolvasome comprising BLM, topoisomerase IIIalpha, and BLAP75*. J Biol Chem, 2006. **281**(20): p. 13861-4.
135. Bachrati, C.Z., R.H. Borts, and I.D. Hickson, *Mobile D-loops are a preferred substrate for the Bloom's syndrome helicase*. Nucleic Acids Res, 2006. **34**(8): p. 2269-79.

136. van Brabant, A.J., et al., *Binding and melting of D-loops by the Bloom syndrome helicase*. *Biochemistry*, 2000. **39**(47): p. 14617-25.
137. Singh, T.R., et al., *BLAP18/RMI2, a novel OB-fold-containing protein, is an essential component of the Bloom helicase-double Holliday junction dissolvosome*. *Genes Dev*, 2008. **22**(20): p. 2856-68.
138. Goto, M., *Hierarchical deterioration of body systems in Werner's syndrome: implications for normal ageing*. *Mech Ageing Dev*, 1997. **98**(3): p. 239-54.
139. Fukuchi, K., G.M. Martin, and R.J. Monnat, Jr., *Mutator phenotype of Werner syndrome is characterized by extensive deletions*. *Proc Natl Acad Sci U S A*, 1989. **86**(15): p. 5893-7.
140. Fukuchi, K., et al., *Elevated spontaneous mutation rate in SV40-transformed Werner syndrome fibroblast cell lines*. *Somat Cell Mol Genet*, 1985. **11**(4): p. 303-8.
141. Salk, D., et al., *Systematic growth studies, cocultivation, and cell hybridization studies of Werner syndrome cultured skin fibroblasts*. *Hum Genet*, 1981. **58**(3): p. 310-6.
142. Goto, M., et al., *Werner syndrome: a changing pattern of clinical manifestations in Japan (1917~2008)*. *Biosci Trends*, 2013. **7**(1): p. 13-22.
143. Goto, M., *Werner's syndrome: from clinics to genetics*. *Clin Exp Rheumatol*, 2000. **18**(6): p. 760-6.
144. Aggarwal, M. and R.M. Brosh, *WRN helicase defective in the premature aging disorder Werner syndrome genetically interacts with topoisomerase 3 and restores the top3 slow growth phenotype of sgs1 top3*. *Aging (Albany NY)*, 2009. **1**(2): p. 219-33.
145. Hoadley, K.A. and J.L. Keck, *Werner helicase wings DNA binding*. *Structure*, 2010. **18**(2): p. 149-51.
146. Hu, Y., et al., *Recq15 and Blm RecQ DNA helicases have nonredundant roles in suppressing crossovers*. *Mol Cell Biol*, 2005. **25**(9): p. 3431-42.
147. Velankar, S.S., et al., *Crystal structures of complexes of PcrA DNA helicase with a DNA substrate indicate an inchworm mechanism*. *Cell*, 1999. **97**(1): p. 75-84.
148. Harrigan, J.A., et al., *The Werner syndrome protein operates in base excision repair and cooperates with DNA polymerase beta*. *Nucleic Acids Res*, 2006. **34**(2): p. 745-54.
149. Sousa, F.G., et al., *PARPs and the DNA damage response*. *Carcinogenesis*, 2012. **33**(8): p. 1433-40.

150. Thomas, C. and A.V. Tulin, *Poly-ADP-ribose polymerase: machinery for nuclear processes*. Mol Aspects Med, 2013. **34**(6): p. 1124-37.
151. Rooney, S., J. Chaudhuri, and F.W. Alt, *The role of the non-homologous end-joining pathway in lymphocyte development*. Immunol Rev, 2004. **200**: p. 115-31.
152. Fattah, F., et al., *Ku regulates the non-homologous end joining pathway choice of DNA double-strand break repair in human somatic cells*. PLoS Genet, 2010. **6**(2): p. e1000855.
153. Cooper, M.P., et al., *Ku complex interacts with and stimulates the Werner protein*. Genes Dev, 2000. **14**(8): p. 907-12.
154. Li, B. and L. Comai, *Functional interaction between Ku and the werner syndrome protein in DNA end processing*. J Biol Chem, 2000. **275**(37): p. 28349-52.
155. Yannone, S.M., et al., *Werner syndrome protein is regulated and phosphorylated by DNA-dependent protein kinase*. J Biol Chem, 2001. **276**(41): p. 38242-8.
156. Karmakar, P., et al., *Ku heterodimer binds to both ends of the Werner protein and functional interaction occurs at the Werner N-terminus*. Nucleic Acids Res, 2002. **30**(16): p. 3583-91.
157. Perry, J.J., et al., *WRN exonuclease structure and molecular mechanism imply an editing role in DNA end processing*. Nat Struct Mol Biol, 2006. **13**(5): p. 414-22.
158. Franchitto, A., et al., *Replication fork stalling in WRN-deficient cells is overcome by prompt activation of a MUS81-dependent pathway*. J Cell Biol, 2008. **183**(2): p. 241-52.
159. Cheng, W.H., et al., *Linkage between Werner syndrome protein and the Mre11 complex via Nbs1*. J Biol Chem, 2004. **279**(20): p. 21169-76.
160. Cheng, W.H., et al., *Collaboration of Werner syndrome protein and BRCA1 in cellular responses to DNA interstrand cross-links*. Nucleic Acids Res, 2006. **34**(9): p. 2751-60.
161. Singh, D.K., et al., *The involvement of human RECQL4 in DNA double-strand break repair*. Aging Cell, 2010.
162. Otterlei, M., et al., *Werner syndrome protein participates in a complex with RAD51, RAD54, RAD54B and ATR in response to ICL-induced replication arrest*. J Cell Sci, 2006. **119**(Pt 24): p. 5137-46.
163. Crabbe, L., et al., *Telomere dysfunction as a cause of genomic instability in Werner syndrome*. Proc Natl Acad Sci U S A, 2007. **104**(7): p. 2205-10.

164. Cheng, W.H., et al., *WRN is required for ATM activation and the S-phase checkpoint in response to interstrand cross-link-induced DNA double-strand breaks*. Mol Biol Cell, 2008. **19**(9): p. 3923-33.
165. Patro, B.S., et al., *WRN helicase regulates the ATR-CHK1-induced S-phase checkpoint pathway in response to topoisomerase-I-DNA covalent complexes*. J Cell Sci, 2011. **124**(Pt 23): p. 3967-79.
166. Ammazalorso, F., et al., *ATR and ATM differently regulate WRN to prevent DSBs at stalled replication forks and promote replication fork recovery*. EMBO J, 2010. **29**(18): p. 3156-69.
167. Cheng, W.H., et al., *Werner syndrome protein phosphorylation by abl tyrosine kinase regulates its activity and distribution*. Mol Cell Biol, 2003. **23**(18): p. 6385-95.
168. Muftuoglu, M., et al., *Acetylation regulates WRN catalytic activities and affects base excision DNA repair*. PLoS One, 2008. **3**(4): p. e1918.
169. Lebel, M. and P. Leder, *A deletion within the murine Werner syndrome helicase induces sensitivity to inhibitors of topoisomerase and loss of cellular proliferative capacity*. Proc Natl Acad Sci U S A, 1998. **95**(22): p. 13097-102.
170. Kawabe, T., et al., *Differential regulation of human RecQ family helicases in cell transformation and cell cycle*. Oncogene, 2000. **19**(41): p. 4764-72.
171. Rossi, M.L., A.K. Ghosh, and V.A. Bohr, *Roles of Werner syndrome protein in protection of genome integrity*. DNA Repair (Amst), 2010. **9**(3): p. 331-44.
172. Kitao, S., et al., *Mutations in RECQL4 cause a subset of cases of Rothmund-Thomson syndrome*. Nat Genet, 1999. **22**(1): p. 82-4.
173. Seki, M., et al., *RecQ family helicases in genome stability: lessons from gene disruption studies in DT40 cells*. Cell Cycle, 2008. **7**(16): p. 2472-8.
174. Siitonen, H.A., et al., *The mutation spectrum in RECQL4 diseases*. Eur J Hum Genet, 2009. **17**(2): p. 151-8.
175. Kitao, S., et al., *Cloning of two new human helicase genes of the RecQ family: biological significance of multiple species in higher eukaryotes*. Genomics, 1998. **54**(3): p. 443-52.
176. Xu, X., et al., *MCM10 mediates RECQ4 association with MCM2-7 helicase complex during DNA replication*. EMBO J, 2009. **28**(19): p. 3005-14.
177. Im, J.S., et al., *Assembly of the Cdc45-Mcm2-7-GINS complex in human cells requires the Ctf4/And-1, RecQL4, and Mcm10 proteins*. Proc Natl Acad Sci U S A, 2009. **106**(37): p. 15628-32.

178. Abe, T., et al., *The N-terminal region of RECQL4 lacking the helicase domain is both essential and sufficient for the viability of vertebrate cells. Role of the N-terminal region of RECQL4 in cells.* Biochim Biophys Acta, 2011. **1813**(3): p. 473-9.
179. Capp, C., J. Wu, and T.S. Hsieh, *Drosophila RecQ4 has a 3'-5' DNA helicase activity that is essential for viability.* J Biol Chem, 2009. **284**(45): p. 30845-52.
180. Ghosh, A.K., et al., *RECQL4, the protein mutated in Rothmund-Thomson syndrome, functions in telomere maintenance.* J Biol Chem, 2012. **287**(1): p. 196-209.
181. Opresko, P.L., et al., *POT1 stimulates RecQ helicases WRN and BLM to unwind telomeric DNA substrates.* J Biol Chem, 2005. **280**(37): p. 32069-80.
182. Lee, O.H., et al., *Genome-wide YFP fluorescence complementation screen identifies new regulators for telomere signaling in human cells.* Mol Cell Proteomics, 2011. **10**(2): p. M110 001628.
183. Opresko, P.L., G. Sowd, and H. Wang, *The Werner syndrome helicase/exonuclease processes mobile D-loops through branch migration and degradation.* PLoS One, 2009. **4**(3): p. e4825.
184. Opresko, P.L., et al., *Telomere-binding protein TRF2 binds to and stimulates the Werner and Bloom syndrome helicases.* J Biol Chem, 2002. **277**(43): p. 41110-9.
185. Lillard-Wetherell, K., et al., *Association and regulation of the BLM helicase by the telomere proteins TRF1 and TRF2.* Hum Mol Genet, 2004. **13**(17): p. 1919-32.
186. Kohzaki, M., et al., *The helicase domain and C-terminus of human RecQL4 facilitate replication elongation on DNA templates damaged by ionizing radiation.* Carcinogenesis, 2012. **33**(6): p. 1203-10.
187. Park, S.J., et al., *A positive involvement of RecQL4 in UV-induced S-phase arrest.* DNA Cell Biol, 2006. **25**(12): p. 696-703.
188. Mann, M.B., et al., *Defective sister-chromatid cohesion, aneuploidy and cancer predisposition in a mouse model of type II Rothmund-Thomson syndrome.* Hum Mol Genet, 2005. **14**(6): p. 813-25.
189. Grocock, L.M., et al., *The RecQ4 orthologue Hrq1 is critical for DNA interstrand cross-link repair and genome stability in fission yeast.* Mol Cell Biol, 2012. **32**(2): p. 276-87.
190. Liu, Y., *Rothmund-Thomson syndrome helicase, RECQ4: on the crossroad between DNA replication and repair.* DNA Repair (Amst), 2010. **9**(3): p. 325-30.

191. Sharma, S. and R.M. Brosh, Jr., *Human RECQ1 is a DNA damage responsive protein required for genotoxic stress resistance and suppression of sister chromatid exchanges*. PLoS One, 2007. **2**(12): p. e1297.
192. Cui, S., et al., *Analysis of the unwinding activity of the dimeric RECQ1 helicase in the presence of human replication protein A*. Nucleic Acids Res, 2004. **32**(7): p. 2158-70.
193. Doherty, K.M., et al., *RECQ1 helicase interacts with human mismatch repair factors that regulate genetic recombination*. J Biol Chem, 2005. **280**(30): p. 28085-94.
194. Johnson, F.B., et al., *Association of the Bloom syndrome protein with topoisomerase IIIalpha in somatic and meiotic cells*. Cancer Res, 2000. **60**(5): p. 1162-7.
195. Seki, T., et al., *Cloning of a cDNA encoding a novel importin-alpha homologue, Qip1: discrimination of Qip1 and Rch1 from hSrp1 by their ability to interact with DNA helicase Q1/RecQL*. Biochem Biophys Res Commun, 1997. **234**(1): p. 48-53.
196. Chu, W.K. and I.D. Hickson, *RecQ helicases: multifunctional genome caretakers*. Nat Rev Cancer, 2009. **9**(9): p. 644-54.
197. Aygun, O. and J.Q. Svejstrup, *RECQL5 helicase: connections to DNA recombination and RNA polymerase II transcription*. DNA Repair (Amst), 2010. **9**(3): p. 345-53.
198. Krantz, I.D., et al., *Cornelia de Lange syndrome is caused by mutations in NIPBL, the human homolog of Drosophila melanogaster Nipped-B*. Nat Genet, 2004. **36**(6): p. 631-5.
199. Gillis, L.A., et al., *NIPBL mutational analysis in 120 individuals with Cornelia de Lange syndrome and evaluation of genotype-phenotype correlations*. Am J Hum Genet, 2004. **75**(4): p. 610-23.
200. Tonkin, E.T., et al., *NIPBL, encoding a homolog of fungal Scc2-type sister chromatid cohesion proteins and fly Nipped-B, is mutated in Cornelia de Lange syndrome*. Nat Genet, 2004. **36**(6): p. 636-41.
201. Vega, H., et al., *Roberts syndrome is caused by mutations in ESCO2, a human homolog of yeast ECO1 that is essential for the establishment of sister chromatid cohesion*. Nat Genet, 2005. **37**(5): p. 468-70.
202. Schule, B., et al., *Inactivating mutations in ESCO2 cause SC phocomelia and Roberts syndrome: no phenotype-genotype correlation*. Am J Hum Genet, 2005. **77**(6): p. 1117-28.

203. Musio, A., et al., *X-linked Cornelia de Lange syndrome owing to SMC1L1 mutations*. Nat Genet, 2006. **38**(5): p. 528-30.
204. Deardorff, M.A., et al., *Mutations in cohesin complex members SMC3 and SMC1A cause a mild variant of cornelia de Lange syndrome with predominant mental retardation*. Am J Hum Genet, 2007. **80**(3): p. 485-94.
205. Zhang, B., et al., *Dosage effects of cohesin regulatory factor PDS5 on mammalian development: implications for cohesinopathies*. PLoS One, 2009. **4**(5): p. e5232.
206. van der Lelij, P., et al., *Warsaw breakage syndrome, a cohesinopathy associated with mutations in the XPD helicase family member DDX11/ChIR1*. Am J Hum Genet, 2010. **86**(2): p. 262-6.
207. Levitus, M., et al., *The DNA helicase BRIP1 is defective in Fanconi anemia complementation group J*. Nat Genet, 2005. **37**(9): p. 934-5.
208. Litman, R., et al., *BACH1 is critical for homologous recombination and appears to be the Fanconi anemia gene product FANCI*. Cancer Cell, 2005. **8**(3): p. 255-65.
209. Deardorff, M.A., et al., *RAD21 mutations cause a human cohesinopathy*. Am J Hum Genet, 2012. **90**(6): p. 1014-27.
210. Deardorff, M.A., et al., *HDAC8 mutations in Cornelia de Lange syndrome affect the cohesin acetylation cycle*. Nature, 2012. **489**(7415): p. 313-7.
211. Rudra, S. and R.V. Skibbens, *Chl1 DNA helicase regulates Scc2 deposition specifically during DNA-replication in Saccharomyces cerevisiae*. PLoS One, 2013. **8**(9): p. e75435.
212. Alvaro, D., M. Lisby, and R. Rothstein, *Genome-wide analysis of Rad52 foci reveals diverse mechanisms impacting recombination*. PLoS Genet, 2007. **3**(12): p. e228.
213. Flaus, A. and T. Owen-Hughes, *Mechanisms for ATP-dependent chromatin remodelling: the means to the end*. FEBS J, 2011. **278**(19): p. 3579-95.
214. Miura, T., et al., *Homologous recombination via synthesis-dependent strand annealing in yeast requires the Irc20 and Srs2 DNA helicases*. Genetics, 2012. **191**(1): p. 65-78.
215. Richardson, A., R.G. Gardner, and G. Prelich, *Physical and genetic associations of the Irc20 ubiquitin ligase with Cdc48 and SUMO*. PLoS One, 2013. **8**(10): p. e76424.

216. Whitby, M.C., F. Osman, and J. Dixon, *Cleavage of model replication forks by fission yeast Mus81-Eme1 and budding yeast Mus81-Mms4*. J Biol Chem, 2003. **278**(9): p. 6928-35.
217. Bernstein, K.A., S. Gangloff, and R. Rothstein, *The RecQ DNA helicases in DNA repair*. Annu Rev Genet, 2010. **44**: p. 393-417.
218. Mitchel, K., K. Lehner, and S. Jinks-Robertson, *Heteroduplex DNA position defines the roles of the Sgs1, Srs2, and Mph1 helicases in promoting distinct recombination outcomes*. PLoS Genet, 2013. **9**(3): p. e1003340.
219. Panico, E.R., et al., *Genetic evidence for a role of Saccharomyces cerevisiae Mph1 in recombinational DNA repair under replicative stress*. Yeast, 2010. **27**(1): p. 11-27.
220. Ede, C., et al., *Budding yeast Mph1 promotes sister chromatid interactions by a mechanism involving strand invasion*. DNA Repair (Amst), 2011. **10**(1): p. 45-55.
221. Lahaye, A., et al., *PIF1: a DNA helicase in yeast mitochondria*. Embo J, 1991. **10**(4): p. 997-1007.
222. Lahaye, A., S. Leterme, and F. Foury, *PIF1 DNA helicase from Saccharomyces cerevisiae. Biochemical characterization of the enzyme*. J Biol Chem, 1993. **268**(35): p. 26155-61.
223. Zhou, J., et al., *Pif1p helicase, a catalytic inhibitor of telomerase in yeast*. Science, 2000. **289**(5480): p. 771-4.
224. Budd, M.E., et al., *Evidence suggesting that Pif1 helicase functions in DNA replication with the Dna2 helicase/nuclease and DNA polymerase delta*. Mol Cell Biol, 2006. **26**(7): p. 2490-500.
225. Bochman, M.L., N. Sabouri, and V.A. Zakian, *Unwinding the functions of the Pif1 family helicases*. DNA Repair (Amst), 2010. **9**(3): p. 237-49.
226. Ribeyre, C., et al., *The yeast Pif1 helicase prevents genomic instability caused by G-quadruplex-forming CEB1 sequences in vivo*. PLoS Genet, 2009. **5**(5): p. e1000475.
227. Van Dyck, E., et al., *A single-stranded DNA binding protein required for mitochondrial DNA replication in S. cerevisiae is homologous to E. coli SSB*. EMBO J, 1992. **11**(9): p. 3421-30.
228. Foury, F. and E.V. Dyck, *A PIF-dependent recombinogenic signal in the mitochondrial DNA of yeast*. EMBO J, 1985. **4**(13A): p. 3525-30.

229. Schulz, V.P. and V.A. Zakian, *The saccharomyces PIF1 DNA helicase inhibits telomere elongation and de novo telomere formation*. Cell, 1994. **76**(1): p. 145-55.
230. Boule, J.B., L.R. Vega, and V.A. Zakian, *The yeast Pif1p helicase removes telomerase from telomeric DNA*. Nature, 2005. **438**(7064): p. 57-61.
231. Boule, J.B. and V.A. Zakian, *The yeast Pif1p DNA helicase preferentially unwinds RNA DNA substrates*. Nucleic Acids Res, 2007. **35**(17): p. 5809-18.
232. Zhang, D.H., et al., *The human Pif1 helicase, a potential Escherichia coli RecD homologue, inhibits telomerase activity*. Nucleic Acids Res, 2006. **34**(5): p. 1393-404.
233. Paeschke, K., J.A. Capra, and V.A. Zakian, *DNA replication through G-quadruplex motifs is promoted by the Saccharomyces cerevisiae Pif1 DNA helicase*. Cell, 2011. **145**(5): p. 678-91.
234. Chisholm, K.M., et al., *A genomewide screen for suppressors of Alu-mediated rearrangements reveals a role for PIF1*. PLoS One, 2012. **7**(2): p. e30748.
235. Xu, X., et al., *Error-free DNA-damage tolerance in Saccharomyces cerevisiae*. Mutat Res Rev Mutat Res, 2015. **764**: p. 43-50.
236. Ball, L.G., et al., *The Rad5 helicase activity is dispensable for error-free DNA post-replication repair*. DNA Repair (Amst), 2014. **16**: p. 74-83.
237. Jain, D. and W. Siede, *Rad5 template switch pathway of DNA damage tolerance determines synergism between cisplatin and NSC109268 in Saccharomyces cerevisiae*. PLoS One, 2013. **8**(10): p. e77666.
238. Daele, D.L., et al., *Rad5-dependent DNA repair functions of the Saccharomyces cerevisiae FANCM protein homolog Mph1*. J Biol Chem, 2012. **287**(32): p. 26563-75.
239. Prakash, R., et al., *Yeast Mph1 helicase dissociates Rad51-made D-loops: implications for crossover control in mitotic recombination*. Genes Dev, 2009. **23**(1): p. 67-79.
240. Pages, V., et al., *Requirement of Rad5 for DNA polymerase zeta-dependent translesion synthesis in Saccharomyces cerevisiae*. Genetics, 2008. **180**(1): p. 73-82.
241. Boiteux, S. and S. Jinks-Robertson, *DNA repair mechanisms and the bypass of DNA damage in Saccharomyces cerevisiae*. Genetics, 2013. **193**(4): p. 1025-64.

242. Prakash, R., et al., *Saccharomyces cerevisiae MPH1 gene, required for homologous recombination-mediated mutation avoidance, encodes a 3' to 5' DNA helicase*. J Biol Chem, 2005. **280**(9): p. 7854-60.
243. Keil, R.L. and A.D. McWilliams, *A gene with specific and global effects on recombination of sequences from tandemly repeated genes in Saccharomyces cerevisiae*. Genetics, 1993. **135**(3): p. 711-718.
244. Fachinetti, D., et al., *Replication termination at eukaryotic chromosomes is mediated by Top2 and occurs at genomic loci containing pausing elements*. Mol Cell, 2010. **39**(4): p. 595-605.
245. Ivessa, A.S., et al., *The Saccharomyces cerevisiae helicase Rrm3p facilitates replication past nonhistone protein-DNA complexes*. Mol Cell, 2003. **12**(6): p. 1525-36.
246. Ivessa, A.S., et al., *Saccharomyces Rrm3p, a 5' to 3' DNA helicase that promotes replication fork progression through telomeric and subtelomeric DNA*. Genes Dev, 2002. **16**(11): p. 1383-1396.
247. Petes, T.D., *Yeast ribosomal DNA genes are located on chromosome XII*. Proc Natl Acad Sci U S A, 1979. **76**(1): p. 410-4.
248. Brewer, B.J., V.A. Zakian, and W.L. Fangman, *Replication and meiotic transmission of yeast ribosomal RNA genes*. Proc Natl Acad Sci U S A, 1980. **77**(11): p. 6739-43.
249. Kobayashi, T., M. Nomura, and T. Horiuchi, *Identification of DNA cis elements essential for expansion of ribosomal DNA repeats in Saccharomyces cerevisiae*. Mol Cell Biol, 2001. **21**(1): p. 136-47.
250. Mohanty, B.K. and D. Bastia, *Binding of the replication terminator protein Fob1p to the Ter sites of yeast causes polar fork arrest*. J Biol Chem, 2004. **279**(3): p. 1932-41.
251. Kobayashi, T., *The replication fork barrier site forms a unique structure with Fob1p and inhibits the replication fork*. Mol Cell Biol, 2003. **23**(24): p. 9178-88.
252. Mohanty, B.K., N.K. Bairwa, and D. Bastia, *The Tof1p-Csm3p protein complex counteracts the Rrm3p helicase to control replication termination of Saccharomyces cerevisiae*. Proc Natl Acad Sci U S A, 2006. **103**(4): p. 897-902.
253. Mohanty, B.K., N.K. Bairwa, and D. Bastia, *Contrasting roles of checkpoint proteins as recombination modulators at Fob1-Ter complexes with or without fork arrest*. Eukaryot Cell, 2009. **8**(4): p. 487-95.
254. Baxter, J. and J.F. Diffley, *Topoisomerase II inactivation prevents the completion of DNA replication in budding yeast*. Mol Cell, 2008. **30**(6): p. 790-802.

255. Cuvier, O., et al., *A topoisomerase II-dependent mechanism for resetting replicons at the S-M-phase transition*. *Genes Dev*, 2008. **22**(7): p. 860-5.
256. DiNardo, S., K. Voelkel, and R. Sternglanz, *DNA topoisomerase II mutant of Saccharomyces cerevisiae: topoisomerase II is required for segregation of daughter molecules at the termination of DNA replication*. *Proc Natl Acad Sci U S A*, 1984. **81**(9): p. 2616-20.
257. Suski, C. and K.J. Marians, *Resolution of converging replication forks by RecQ and topoisomerase III*. *Mol Cell*, 2008. **30**(6): p. 779-89.
258. Wang, J.C., *Cellular roles of DNA topoisomerases: a molecular perspective*. *Nat Rev Mol Cell Biol*, 2002. **3**(6): p. 430-40.
259. Steinacher, R., et al., *The DNA helicase Pfh1 promotes fork merging at replication termination sites to ensure genome stability*. *Genes Dev*, 2012. **26**(6): p. 594-602.
260. Ivessa, A.S., J.Q. Zhou, and V.A. Zakian, *The Saccharomyces Pif1p DNA helicase and the highly related Rrm3p have opposite effects on replication fork progression in ribosomal DNA*. *Cell*, 2000. **100**(4): p. 479-489.
261. Schmidt, K.H. and R.D. Kolodner, *Requirement of Rrm3 helicase for repair of spontaneous DNA lesions in cells lacking Srs2 or Sgs1 helicase*. *Mol Cell Biol*, 2004. **24**(8): p. 3213-26.
262. Torres, J.Z., S.L. Schnakenberg, and V.A. Zakian, *Saccharomyces cerevisiae Rrm3p DNA helicase promotes genome integrity by preventing replication fork stalling: viability of rrm3 cells requires the intra-S-phase checkpoint and fork restart activities*. *Mol Cell Biol*, 2004. **24**(8): p. 3198-212.
263. Luke, B., et al., *The cullin Rtt101p promotes replication fork progression through damaged DNA and natural pause sites*. *Curr Biol*, 2006. **16**(8): p. 786-92.
264. Szyjka, S.J., C.J. Viggiani, and O.M. Aparicio, *Mrc1 is required for normal progression of replication forks throughout chromatin in S. cerevisiae*. *Mol Cell*, 2005. **19**(5): p. 691-7.
265. Rossi, S.E., et al., *Rad53-Mediated Regulation of Rrm3 and Pif1 DNA Helicases Contributes to Prevention of Aberrant Fork Transitions under Replication Stress*. *Cell Rep*, 2015. **13**(1): p. 80-92.
266. Pfander, B., et al., *SUMO-modified PCNA recruits Srs2 to prevent recombination during S phase*. *Nature*, 2005. **436**(7049): p. 428-33.
267. Hall, M.C. and S.W. Matson, *Helicase motifs: the engine that powers DNA unwinding*. *Mol Microbiol*, 1999. **34**(5): p. 867-77.

268. Aboussekhra, A., et al., *RADH, a gene of Saccharomyces cerevisiae encoding a putative DNA helicase involved in DNA repair. Characteristics of radH mutants and sequence of the gene.* Nucleic Acids Res, 1989. **17**(18): p. 7211-9.
269. Kerrest, A., et al., *SRS2 and SGS1 prevent chromosomal breaks and stabilize triplet repeats by restraining recombination.* Nat Struct Mol Biol, 2009. **16**(2): p. 159-67.
270. Chiolo, I., et al., *Srs2 and Sgs1 DNA helicases associate with Mre11 in different subcomplexes following checkpoint activation and CDK1-mediated Srs2 phosphorylation.* Mol Cell Biol, 2005. **25**(13): p. 5738-51.
271. Schiestl, R.H., S. Prakash, and L. Prakash, *The SRS2 suppressor of rad6 mutations of Saccharomyces cerevisiae acts by channeling DNA lesions into the RAD52 DNA repair pathway.* Genetics, 1990. **124**(4): p. 817-31.
272. Robert, T., et al., *Mrc1 and Srs2 are major actors in the regulation of spontaneous crossover.* Embo J, 2006. **25**(12): p. 2837-46.
273. Sasanuma, H., et al., *Remodeling of the Rad51 DNA strand-exchange protein by the Srs2 helicase.* Genetics, 2013. **194**(4): p. 859-72.
274. Anand, R.P., et al., *Overcoming natural replication barriers: differential helicase requirements.* Nucleic Acids Res, 2012. **40**(3): p. 1091-105.

CHAPTER TWO:

SGS1 TRUNCATIONS INDUCE GENOME REARRANGEMENTS BUT SUPPRESSES DETRIMENTAL EFFECTS OF BLM OVEREXPRESSION IN SACCHAROMYCES CEREVISIAE

Note to the reader: This chapter has been previously published with permission from the publisher as Mirzaei, H, Syed, S, Kennedy, JA, and Schmidt, KH (2011). "Sgs1 Truncations Induce Genome Rearrangements but Suppress Detrimental Effects of BLM Overexpression in *Saccharomyces cerevisiae*." *J Mol Biol.*, 405(4); 877-891. Research was designed by K. Schmidt. Sgs1 Truncations and experiments were performed by S. Syed. BLM diploid experiments and chimera protein construction was done by H. Mirzaei. Point mutations and experiments in zinc-binding domain were done by H. Mirzaei and J. Kennedy. Corresponding author: Kristina Schmidt, Department of Cell Biology, Microbiology and Molecular Biology, University of South Florida, 4202 E. Fowler Avenue, ISA2015, Tampa, FL 33620. Phone: (813) 974-1592. Fax: (813) 974-1614.; E-mail: kschmidt@usf.edu

ABSTRACT

RecQ-like DNA helicases are conserved from bacteria to humans. They perform functions in the maintenance of genome stability, and their mutation is associated with cancer predisposition and premature aging syndromes in humans. Here, a series of C-terminal deletions and point mutations of Sgs1, the only RecQ-like helicase in yeast,

show that the HRDC and Rad51 interaction domain are dispensable for Sgs1's role in suppressing genome instability, whereas the zinc-binding domain and the helicase domain are required. BLM expression from the native *SGS1* promoter had no adverse effects on cell growth, but also was unable to complement any *sgs1Δ* defects. BLM overexpression, however, significantly increased the rate of accumulating GCRs in a dosage dependent manner and greatly exacerbated sensitivity to DNA-damaging agents. Co-expressing *sgs1* truncations of up to 900 residues, lacking all known functional domains of Sgs1, suppressed HU sensitivity of BLM overexpressing cells, suggesting a functional relationship between Sgs1 and BLM. Indeed, protein disorder prediction analysis of Sgs1 and BLM was used to produce a functional Sgs1-BLM chimera by replacing the N-terminus of BLM with the disordered N-terminus of Sgs1. The functionality of this chimera suggests that it is the disordered N-terminus, a site of protein binding and post-translational modification, that confers species-specificity to these two RecQ-like proteins.

INTRODUCTION

RecQ-like DNA helicases, named after the DNA repair protein RecQ of *Escherichia coli*, (Hegde, Qin et al. 1996, Morimatsu and Kowalczykowski 2003, Ivancic-Bace, Salaj-Smic et al. 2005) are evolutionarily highly conserved. These 3'- to 5'-helicases function at the interface between DNA replication and recombination to maintain genome integrity. Sgs1 is the only known member of this helicase family in *Saccharomyces cerevisiae* (Gangloff, McDonald et al. 1994). Sgs1-deficient cells show increased sensitivity to the DNA-damaging agents hydroxyurea (HU) and methyl

methanesulfonate (MMS), missegregate chromosomes, accumulate gross-chromosomal rearrangements (GCRs), and have a shortened life span (Sinclair, Mills et al. 1997, Mullen, Kaliraman et al. 2000, Fricke and Brill 2003, Schmidt, Wu et al. 2006). In contrast, five RecQ-like helicases (RecQL1, BLM, WRN, RecQL4, and RecQL5) are known in humans, and mutations in the *BLM*, *WRN*, and *RECQL4* genes are associated with the rare, cancer-prone Bloom's syndrome (BS), Werner syndrome, and Rothmund–Thompson syndrome, respectively (Ellis, Groden et al. 1995, Yu, Oshima et al. 1996, Kitao, Ohsugi et al. 1998, Kitao, Shimamoto et al. 1999, German, Sanz et al. 2007, Garcia-Rubio, Chavez et al. 2008). All RecQ-like helicases share a seven-motif helicase domain with Walker A and DEAH motifs. The RecQ-helicase-conserved (RQC) domain, located C-terminal to the helicase domain, is thought to be involved in DNA binding and conferring specificity of binding to DNA structures, such as G4 tetrads (von Kobbe, Thoma et al. 2003, Guo, Rigolet et al. 2005, Lee, Kusumoto et al. 2005, Huber, Duquette et al. 2006). The Helicase/RNase D C-terminal (HRDC) domain is the most C-terminal of the conserved domains and resembles domains in other proteins that are involved in nucleic acid metabolism, such as RNase D and UvrD; however, similar to the RQC domain, it is not found in all RecQ-like helicases (Morozov, Mushegian et al. 1997, Kitano, Yoshihara et al. 2007). The HRDC domain has been implicated in binding and resolving DNA structures, such as Holliday junctions, and in mediating protein–protein interactions (Liu, Macias et al. 1999, Bernstein and Keck 2005, Wu, Chan et al. 2005, Kitano, Yoshihara et al. 2007, Killoran and Keck 2008). Two acidic regions have also been identified N-terminal of the helicase domain and may be involved in mediating protein–protein interactions (Kitao, Ohsugi et al. 1998, Miyajima, Seki et al. 2000,

Bernstein, Shor et al. 2009). Sgs1 is found in a complex with Top3 and Rmi1, and there is also evidence of physical interactions of the N-terminal half of Sgs1 with Top2, Srs2, and Rad16 and interactions of the C-terminus with Mlh1 and Rad51 (Watt, Louis et al. 1995, Bennett, Noiro-Gros et al. 2000, Duno, Thomsen et al. 2000, Fricke, Kaliraman et al. 2001, Chang, Bellaoui et al. 2005, Chiolo, Carotenuto et al. 2005).

Defects in BLM, the human RecQ helicase considered to be most closely related to Sgs1, cause BS, an autosomal recessive disorder characterized by chromosome gaps and breaks, elevated sister chromatid exchange, mitotic hyper-recombination, and aberrant DNA replication events (Chaganti, Schonberg et al. 1974, Hojo, van Diemen et al. 1995, Bachrati and Hickson 2003). Affected individuals suffer from a high incidence and wide variety of cancers, infertility, and dwarfism (reviewed in Bachrati et al. 2003). BLM catalyzes ATP-dependent 3'- to 5'-DNA unwinding, with a preference for DNA structures that may arise spontaneously during DNA replication or as a result of homologous recombination (HR) (Mohaghegh, Karow et al. 2001). For example, by unwinding unusual secondary DNA structures, BLM may aid replication fork progression, prevent illegitimate recombination during replication, and assist in restarting stalled forks (Ralf, Hickson et al. 2006, Wu and Hickson 2006, Hanada and Hickson 2007, Bachrati and Hickson 2008). Evidence supporting a role of BLM in maintaining genome integrity has been accumulating. For example, BLM-defective cells exhibit a retarded rate of strand elongation during DNA replication (Hand and German 1975), accumulate abnormal replication intermediates (Lonn, Lonn et al. 1990), and are hypersensitive to agents that impair DNA replication (Davies, North et al. 2004). BLM physically interacts with several proteins that play important roles during DNA

replication and repair, such as replication protein A, flap endonuclease 1, chromatin assembly factor 1, the mismatch repair protein Mlh1, HR factor Rad51, and topoisomerase III α (Brosh, Li et al. 2000, Johnson, Lombard et al. 2000, Langland, Kordich et al. 2001, Wu, Davies et al. 2001, Jiao, Bachrati et al. 2004, Sharma, Sommers et al. 2004, Wu, Bachrati et al. 2006). BLM peaks in S phase and it localizes to replication foci, most likely through its physical interaction with a subunit of DNA polymerase δ (Dutertre, Ababou et al. 2000, Sanz, Proytcheva et al. 2000, Yankiwski, Marciniak et al. 2000, Bischof, Kim et al. 2001, Selak, Bachrati et al. 2008).

Here, we have determined the role of C-terminal domains and protein interaction sites of Sgs1 in suppressing GCR accumulation by expressing point mutants and truncations of Sgs1, lacking as few as 20 residues and as many as 1428 residues. Human *BLM* cDNA was expressed under control of the native *SGS1* promoter and overexpressed from a galactose-inducible promoter to investigate BLM's ability to complement *sgs1* Δ defects (such as increased genome instability and sensitivity to HU and MMS), revealing that BLM could suppress *sgs1* Δ defects neither in haploid nor in diploid cells. However, using computational protein disorder prediction tools, we have designed a yeast–human chimera that consists of two nonfunctional segments of BLM and Sgs1. The ability of this chimera to suppress all *sgs1* Δ defects that we tested suggests a functional relationship between BLM and Sgs1, which is also supported by our finding that short N-terminal fragments of Sgs1, which are devoid of all known functional domains for helicase activity and DNA binding, suppress severely detrimental effects of BLM overexpression in yeast.

RESULTS

Requirement of the RQC domain of Sgs1, but not the HRDC domain, for GCR suppression

Sgs1 contains a conserved DEAH helicase domain, a conserved HRDC domain, two acidic regions (AR1 and AR2), and an RQC domain composed of zinc-binding and winged-helix domains. Several protein interaction sites have also been located in the 1447-amino-acid-long protein (Fig. 1a). To determine the role of these domains in the maintenance of genome stability, we generated systematic deletions to the 3'-end of the chromosomal *SGS1* gene, such that truncations of the C-terminus of Sgs1, ranging from 20 to 1428 amino acids, were expressed as fusions to a myc epitope. Truncations of up to 80 amino acids were constructed to not affect any known functional domain of Sgs1, while $\Delta C100$ and $\Delta C200$ deletions partially and completely removed the HRDC domain and $\Delta C300$ and $\Delta C400$ deletions partially and completely removed the RQC domain, respectively. The largest deletions ($\Delta C700$, $\Delta C800$, $\Delta C900$, $\Delta C1000$, and $\Delta C1100$) eliminate the entire helicase domain, including the Walker A motif (residues 803-812), with the $\Delta C800$ – $\Delta C1100$ deletions also affecting the part of the N-terminal half of Sgs1 that contains protein interaction sites (e.g., Rad16, residues 421–792; Top2, residues 432–724; and Srs2, residues 422–722) and two acidic regions (AR1, residues 321–447; AR2, residues 502–648), whereas $\Delta C500$ and $\Delta C600$ deletions partially remove the helicase domain while leaving the Walker A motif intact (Fig. 1a). All truncation alleles were stably expressed from the chromosomal *SGS1* locus under control of the native *SGS1* promoter (Fig. 1b). C-terminal fusion to the myc epitope did not adversely affect Sgs1 function, as indicated by equal sensitivity to HU and MMS of

strains expressing tagged and untagged Sgs1 (wild type) (Fig. 2a). The largest deletion, leaving intact only the 19 N-terminal amino acids of Sgs1 (*sgs1ΔC1428*), was as sensitive to HU and MMS as a complete *SGS1* deletion (*sgs1Δ*), thus behaving similar to a null allele (Fig. 2a). Loss of up to 200 C-terminal amino acids did not increase sensitivity to HU or MMS, whereas loss of 300 or more amino acids led to sensitivity similar to that of the *sgs1ΔC1428* and *sgs1Δ* mutants (Fig. 2a). The construction of additional 20-amino-acid truncations extended the C-terminal region that is dispensable for HU/MMS resistance to 240 amino acids (Fig. 2b).

It was previously shown that cells lacking the DNA helicase Srs2 (*srs2Δ*) depend on functional Sgs1 for their viability (Lee, Johnson et al. 1999). To assess the ability of *sgs1* truncation alleles to support growth of the *srs2Δ* mutant, we constructed diploid strains heterozygous for the *srs2Δ* deletion and heterozygous for the *sgs1ΔC200*, *sgs1ΔC260*, or *sgs1ΔC300* allele. The meiotic products of the sporulated diploids were spread on nonselective, rich media [yeast–peptone–dextrose (YPD)], allowing all spores to grow (Fig. 2c). Diploids heterozygous for the *srs2Δ* deletion and for the *sgs1ΔC200* truncation yielded spores that grew into colonies of the same size, suggesting that the 200 C-terminal amino acid residues of Sgs1, which harbor the HRDC domain and an interaction site with the HR factor Rad51, are not required for the viability of the *srs2Δ* mutant. In contrast, sporulation of diploids heterozygous for the *srs2Δ* deletion and *sgs1ΔC260* or *sgs1ΔC300* allele yielded mixtures of normal-sized and small colonies. Genotyping revealed that the small colonies were *srs2Δ sgs1ΔC260* or *srs2Δ sgs1ΔC300* mutants, whereas the normal-sized colonies corresponded to wild-type spores or single mutants. Thus, Sgs1 that lacks 260 or more C-terminal residues and

therefore does not contain a complete RQC domain cannot support normal growth of cells lacking Srs2.

When we tested the effect of the C-terminal deletions on the accumulation of GCRs, we found that 240 C-terminal amino acids were dispensable for maintaining genome integrity, whereas deleting as little as an additional 20 amino acids (*sgs1ΔC260*) caused the GCR rate to increase to that exhibited by the null mutant without a discernable intermediate phenotype (Table 1). Combining the *sgs1ΔC300* truncation allele with a deletion of the DNA-damage checkpoint sensor *MEC3* led to a synergistic GCR rate increase, while, as expected, combining the *sgs1ΔC200* allele with a *mec3Δ* mutation did not. Thus, these findings show that the HRDC domain and the previously reported C-terminal interaction with Rad51 are not required for Sgs1's role in preventing the accumulation of GCRs and supporting normal growth of the *srs2Δ* mutant, whereas the integrity of the RQC domain, which has been suggested to span residues 1075–1207 based on the alignment of three-dimensional structures (Kitano, Kim et al. 2010), is essential.

BS-associated RQC domain mutations cause loss of Sgs1 function *in vivo*

Of the 32 exonic base substitutions that are causative of BS, 13 are missense mutations (Ellis, Groden et al. 1995, Foucault, Vaury et al. 1997, Barakat, Ababou et al. 2000, German, Sanz et al. 2007), with 6 of these mutations affecting conserved residues that have been shown *in vitro* to participate in zinc binding and G-tetrad DNA binding activity (Fig. 3a). Studies, however, have been limited to biochemical and biophysical analyses of mutant proteins and were hampered by the inability to purify

some mutant BLM proteins (Janscak, Garcia et al. 2003, Guo, Rigolet et al. 2005, Huber, Duquette et al. 2006). Since the cysteine residues are highly conserved between RecQ-like helicases, including Sgs1, we replaced the corresponding cysteine residue in Sgs1 with the BS-associated mutation (*sgs1-C1047F*). Unlike BLM with mutations in any of the three conserved cysteine residues C1036, C1063, or C1066, which degraded upon purification and could therefore not be characterized (Janscak, Garcia et al. 2003), the *sgs1-C1047F* mutant allele was stably expressed *in vivo* from the native *SGS1* locus (Fig. 3b). The *sgs1-C1047F* mutant showed an increased HU and MMS sensitivity, which, however, did not reach the level of the *sgs1Δ* allele, and exhibited levels of GCR accumulation comparable to the *sgs1Δ* mutant, demonstrating that the C1047F mutation severely impairs Sgs1 function (Fig. 3c; Table 1). In addition to conserved cysteine residues and immediately adjoining arginine (R1037) and aspartic acid (D1064) residues, ClustalW2 alignments showed F1056 to be the only other fully conserved amino acid residue in the zinc-binding domain of Sgs1 (Fig. 3a). Although the corresponding residue in BLM (F1045) is not associated with a BS mutation, the BLM-F1045A mutation has been shown to cause a severe helicase defect and a single-stranded DNA (ssDNA) binding deficiency *in vitro* (Janscak, Garcia et al. 2003). When we introduced the corresponding mutation into Sgs1 (F1056A), however, the mutant was no more sensitive to HU and MMS than wild-type cells (Fig. 3c) but instead appeared fully functional with a wild-type GCR rate (Table 1).

Expression of human BLM cDNA from the endogenous *SGS1* promoter does not complement *sgs1Δ* defects

RecQ-like DNA helicases are evolutionarily conserved from bacteria to humans. Since cells from BS patients share defects seen in *sgs1Δ* cells, including increased sensitivity to DNA-damaging agents, increased levels of aberrant genetic exchange, and reduced life span, it has been suggested that RecQ-like DNA helicases from different phyla or even kingdoms might complement each other, thus allowing the development of simple model organisms for the functional and mutational characterization of disease-associated human RecQ-like helicases, such as BLM and WRN (Yamagata, Kato et al. 1998). Thus, to assess the ability of BLM to suppress genome instability in the *sgs1Δ* mutant, BLM cDNA was inserted in-frame with the start codon of *SGS1* at its chromosomal locus (*P_{SGS1}BLM*). We reasoned that insertion at the wild-type *SGS1* locus would promote cell-cycle-dependent regulation of BLM expression and expression levels similar to those previously shown for Sgs1 (Frei and Gasser 2000). Stable expression of BLM was confirmed by Western blot analysis, using a yeast strain expressing myc-tagged BLM (Fig. 4a); however, all subsequent experiments were carried out with untagged BLM. Expression of a single copy of BLM (*P_{SGS1}BLM*) neither led to a statistically significant difference in the GCR rate compared to the *sgs1Δ* mutant (Table 1 and Table 2) nor alleviated HU sensitivity (Fig. 4b), demonstrating that *BLM* can be successfully expressed in yeast under control of the native *SGS1* promoter without detrimental effects on cell growth, but is unable to complement the tested *sgs1Δ* defects to any extent.

Overexpression of BLM leads to increased sensitivity to DNA-damaging agents and rapid accumulation of GCRs

Since a single copy of *BLM* ($P_{SGS1}BLM$) did not complement *sgs1Δ* defects, we examined the effect of increasing BLM expression levels on *sgs1Δ* mutant phenotypes. For this purpose, the native *SGS1* promoter was replaced with a *GAL1* promoter and galactose-dependent expression of BLM was verified by fusing *BLM* to a myc epitope tag (Fig. 4a). Overexpression of BLM did not compensate for the lack of Sgs1 when cells were exposed to HU but instead led to a further increase in sensitivity to HU compared to the *sgs1ΔC1428* cells or cells expressing BLM under the *SGS1* promoter (Fig. 4b). We found that maximum induction of *BLM* expression led to a 1665-fold increase in the GCR rate compared to wild type and a 34-fold increase compared to the *sgs1Δ* mutant assayed under the same conditions (Table 2). In contrast, overexpression of Sgs1 from the *GAL1* promoter did not lead to GCR accumulation (Table 2). The GCR rate increase upon BLM overexpression was dependent on induction levels, with the GCR rate gradually decreasing to that of the *sgs1Δ* mutant as the galactose concentration in the media decreased (Table 2). Thus, *sgs1Δ* defects cannot be complemented by any level of BLM expression; in fact, increasing BLM expression levels induce higher sensitivity to DNA-damaging agents and significantly higher genome instability compared to that of the *sgs1Δ* mutant.

N-terminus of Sgs1 suppresses detrimental effects of BLM overexpression

Since Sgs1 is important for the suppression of illegitimate recombination between identical sequences, such as those found in related genes, on homologous

chromosomes, and on sister chromatids, we tested the HU sensitivity of diploid strains expressing truncated *sgs1* alleles in the presence or in the absence of the *SGS1* wild-type allele (Fig. 5). HU sensitivity was fully suppressed for all alleles if a single copy of wild-type *SGS1* was expressed from the other allele (Fig. 5a), demonstrating that the *sgs1* truncation alleles did not have a dominant effect. As in haploid cells, only the *sgs1ΔC200* allele complemented HU sensitivity of the *sgs1Δ* diploid completely (Fig. 5b); however, cells expressing the *sgs1ΔC300* to *sgs1ΔC900* alleles were less sensitive than diploids that expressed larger truncations or the *sgs1ΔC1428* null allele (Fig. 5b). This ability of *sgs1Δ300–sgs1ΔC900* truncation alleles to at least partially suppress HU sensitivity indicates that there may be N-terminal segments in Sgs1 that contribute to HU resistance.

Diploids expressing *BLM* from native *SGS1* promoters on both alleles were as sensitive to HU as diploids not expressing Sgs1, whereas diploids overexpressing BLM from one allele or from both alleles were severely HU sensitive, with the highest expression level lacking any growth on 100 mM HU (Fig. 5c), reflecting the severe HU sensitivity of haploid cells expressing the *P_{GAL}BLM* allele (Fig. 4b). Diploids overexpressing BLM also appeared to grow more slowly than any other diploid tested here (Fig. 5c). Remarkably, expression of a single copy of *SGS1* from its endogenous promoter (*SGS1/P_{GAL}BLM*) completely eliminated the severe HU sensitivity conferred by overexpression of BLM. To determine if full-length Sgs1 was required for this suppression, we crossed the haploid strain overexpressing BLM with haploids expressing various Sgs1 truncations. We found that a single copy of the *sgs1ΔC200* allele was as sufficient as wild-type Sgs1 in suppressing HU sensitivity and slow growth

of the BLM-overexpressing strain, and as few as 547 N-terminal amino acids remaining in the *sgs1ΔC900* allele were sufficient for significant suppression of HU sensitivity and slow growth caused by BLM overexpression (Fig. 5c). These findings suggest that none of the known enzymatic activities or functional and conserved domains are required for suppressing the HU sensitivity of the BLM-overexpressing diploids but that 547 N-terminal amino acids are sufficient for suppressing the detrimental effects of BLM overexpression in a diploid. That the *sgs1ΔC1000* and *sgs1ΔC1100* alleles were clearly less effective at suppressing HU sensitivity shows that 447 N-terminal amino acids, which contain the Top3 interaction site, are necessary but not sufficient for complementation.

Design of a functional Sgs1–BLM chimera

Sgs1 and BLM share about 21% of their amino acid residues in a pairwise alignment of the full-length proteins (ClustalW2), with most of the identical residues in the helicase domain. In fact, the N-terminal segment of Sgs1 expressed by the *sgs1ΔC800* allele, which is able to suppress the HU sensitivity of BLM-overexpressing diploids, shares only 11% with the corresponding N-terminal segment of BLM. Devoid of conserved domains and known enzymatic activities, the N-terminus of Sgs1 has been shown to be required for physical interactions with Top3, Top2, Srs2, and Rad16 (Watt, Louis et al. 1995, Bennett, Noirot-Gros et al. 2000, Duno, Thomsen et al. 2000, Mullen, Kaliraman et al. 2000, Fricke, Kaliraman et al. 2001, Chiolo, Carotenuto et al. 2005). Using IUPred, an algorithm for the prediction of intrinsically disordered proteins, we found that the 650 N-terminal residues contain a similar distribution of ordered and

intrinsically disordered segments (Fig. 6a and b). In disorder prediction algorithms, such as IUPred (Dosztanyi, Csizmek et al. 2005, Dosztanyi, Csizmek et al. 2005) a score of > 0.5 predicts a disordered amino acid residue and a score of < 0.5 predicts an ordered residue, with 30 consecutive disordered amino acids commonly being used as a lower limit for detecting disorder in whole proteome searches (Ward, Sodhi et al. 2004, Dosztanyi, Csizmek et al. 2005, Dosztanyi, Csizmek et al. 2005, Peng, Vucetic et al. 2005). The helicase domains of Sgs1 and of BLM coincide with the predicted ordered regions in both proteins, starting at around residue 648, and are surrounded by a long N-terminal and a short C-terminal segment, which contain mostly disordered residues. In fact, based on the IUPred output scores, 83% of the 648 N-terminal residues of Sgs1 (538/648) are disordered, with 70% of all 648 residues being located in segments of more than 30 consecutive disordered residues, whereas only 16% of the 800 C-terminal residues of Sgs1 are predicted to be disordered, with only a single disordered segment that is longer than 30 residues (residues 1396–1447). Based on the IUPred prediction, BLM can also be divided into a disordered N-terminus and an ordered C-terminus (Fig. 6a and b). For BLM, 52% of 648 N-terminal residues are predicted to be disordered, but only 15% of these residues are found in stretches of more than 30 disordered residues. The difference in the pattern of disorder predicted for the N-terminal segments of Sgs1 and BLM led us to hypothesize that this region may be involved in conferring species specificity to BLM and Sgs1 function and, thus, prevent BLM from functioning in yeast. This hypothesis is supported by the fact that the N-terminus of Sgs1 is sufficient for the complementation of the HU sensitivity induced by overexpression of BLM. To test this hypothesis, we constructed a yeast–human chimera in which the 647 N-terminal

residues of BLM were replaced by the 647 N-terminal residues of Sgs1 (*sgs1ΔC800-blmΔN647*) (Fig. 6c). To express this chimera from the native *SGS1* promoter, we replaced nucleotides 1941 to 4344 of the endogenous *SGS1* gene with nucleotides 1941 to 4254 of *BLM* cDNA (Fig. 6e). Remarkably, the chimera was nearly as effective as wild-type *SGS1* in conferring resistance to HU, whereas the N-terminal segment of Sgs1 by itself was ineffective (Fig. 6d). Moreover, when we combined the chimeric allele with a *mec3Δ* mutation, GCRs accumulated at a significantly lower rate than in the *mec3Δ* mutant carrying the GCR-deficient *sgs1ΔC300* or *sgs1ΔC800* allele, albeit not at the low rate of the *mec3Δ* mutant carrying the GCR-proficient *sgs1ΔC200* allele, signifying partial functionality of the chimerical protein in the suppression of chromosomal rearrangements (Table 1). Finally, besides Srs2, the *sgs1Δ* mutant also requires the DNA helicase Rrm3 for viability. Synthetic lethality between *sgs1Δ* and *rrm3Δ* mutations is suppressed by disrupting HR factors such as Rad51 and Rad55, suggesting that the lethality is due to accumulation of aberrant HR intermediates (Ooi, Shoemaker et al. 2003, Schmidt and Kolodner 2004, Torres, Schnakenberg et al. 2004). To assess if the Sgs1–BLM chimera was capable of preventing the accumulation of lethal levels of aberrant recombination intermediates, we constructed a diploid heterozygous for the *rrm3Δ* mutation and heterozygous for the *sgs1ΔC800-blmΔN647* allele, expressing the Sgs1–BLM chimera. Spreading of spores from this diploid on YPD, which allows all spores to grow, showed that the *rrm3Δ* mutant expressing the chimera grows normally with the diameter of double-mutant colonies measuring approximately 90% of that of the single mutants (Fig. 6f). These findings indicate that the Sgs1–BLM chimera is functional and, while not capable of fully suppressing

chromosomal rearrangements, prevents the accumulation of lethal levels of aberrant recombination intermediates when Rrm3 helicase is absent.

DISCUSSION

Yeast cells that lack Sgs1 exhibit upregulated and aberrant recombination in mitosis, increased sensitivity to DNA-damaging agents, accumulation of GCRs, synthetic lethality with mutations in other DNA metabolic genes, such as the *SRS2* and *RRM3* helicase genes, and meiotic defects that lead to poor spore viability (Watt, Louis et al. 1995, Lee, Johnson et al. 1999, Frei and Gasser 2000, Miyajima, Seki et al. 2000, Myung, Datta et al. 2001, Cobb, Bjergbaek et al. 2002, Ira, Malkova et al. 2003, Versini, Comet et al. 2003, Schmidt and Kolodner 2004, Schmidt, Wu et al. 2006). Sgs1 contains several conserved domains (DEAD helicase, RQC, HRDC, AR1, and AR2), and protein interaction sites (Top2, Top3, Srs2, Rad16, Rad51, and Mlh1) have been identified by two-hybrid screens (Watt, Louis et al. 1995, Duno, Thomsen et al. 2000, Saffi, Feldmann et al. 2001, Wu, Davies et al. 2001, Chiolo, Carotenuto et al. 2005). How the integrity of these conserved motifs and protein–protein interaction sites affects the role of Sgs1 in suppression of aberrant genome rearrangements has not been determined. The requirement of some domains and/or protein interaction sites, but not others, may shed light on the poorly understood mechanism(s) by which Sgs1 contributes to the maintenance of genome integrity in yeast. Here, we find that the segment made up of 240 C-terminal amino acids, which contains Rad51 and Mlh1 interaction sites and the conserved HRDC domain thought to be involved in DNA binding and in recognition and processing of double Holliday junctions (Liu, Macias et

al. 1999, Wu, Chan et al. 2005), is dispensable for Sgs1's role in suppressing GCRs. The integrity of the RQC domain, however, is essential for GCR suppression. That zinc binding is crucial for Sgs1 activity, as well as the fact that loss of function of the C-terminal truncation allele was not due to disruption of protein structure/function because of such a large deletion, was further confirmed by the finding that the point mutation of a conserved zinc-coordinating cysteine, which has also been observed in BS patients (Foucault, Vaury et al. 1997), led to the loss of Sgs1's ability to suppress HU sensitivity and GCR accumulation. This loss of function was not due to degradation of the mutant protein as had been previously observed for some cysteine mutants of BLM during attempts at overexpression and purification from *E. coli*. However, we cannot exclude the possibility that the loss of function resulted from intracellular mislocalization of the mutant protein. Previously, modeling of the zinc-binding domain of BLM and instability of purified mutant proteins had indicated that hydrogen bonds between three conserved residues, Y1029 (Y1040 in Sgs1), R1037 (R1048 in Sgs1), and D1064 (D1070 in Sgs1), are required for the folding of the zinc-binding domain and overall protein stability (Guo, Rigolet et al. 2005). Although F1056 of Sgs1 does not appear to be involved in this zinc-domain stabilization and the Sgs1-F1056A mutant protein appears stable in this study, F1056 is the only other fully conserved residue in the zinc-binding domain of RecQ-like helicases, suggesting functional significance. However, introduction of the F1056A mutation had no effect on Sgs1 function *in vivo* when we assessed HU sensitivity, consistent with a previous study (Ui, Satoh et al. 2001), or GCR accumulation. That, in a previous *in vitro* study (Janscak, Garcia et al. 2003), the corresponding BLM mutation (F1045A) had severely impaired helicase and ssDNA binding activities could be either

due to differences in the importance of this residue for enzymatic activity of BLM and Sgs1 or, more likely, due to the fact that only the helicase-core segment of BLM, lacking 769 residues of N- and C-termini, was purified. The *in vitro* function of this isolated domain could be more strongly affected by a mutation than the *in vivo* function of the full-length Sgs1 mutant protein assessed here. Although nearly half of all BLM alleles that are associated with single-amino-acid changes (7 of 17 alleles) in BS patients are located in the RQC domain (Ellis, Groden et al. 1995, Foucault, Vaury et al. 1997, Barakat, Ababou et al. 2000, German, Sanz et al. 2007), none affect F1045, consistent with our finding that mutation of this conserved residue may not be associated with significant loss of function *in vivo*.

We find that Sgs1 retains partial functionality even when it lacks the HRDC, RQC, and DEAH helicase domains, as demonstrated by the greater HU resistance of diploids that only express 547 N-terminal amino acid residues compared to those alleles expressing fewer than 447 residues of Sgs1. One possible explanation for this finding is that protein–protein interactions conferred by the N-terminus could contribute to the structural stability of multi-protein complexes, such as the Sgs1–Top3–Rmi1 (Chang, Bellaoui et al. 2005) complex or, even more relevant to HU resistance, DNA-damage-specific complexes with Srs2 and Mre11 (Chiolo, Carotenuto et al. 2005). In these multi-protein complexes, enzymatic activity of Sgs1 may be dispensable. Indeed, *sgs1* alleles with point mutations in the helicase domain have been shown to be capable of performing some functions of the wild-type allele, including those carried out during meiosis and checkpoint activation (Miyajima, Seki et al. 2000, Bjergbaek, Cobb et al. 2005).

In contrast to two previous reports (Yamagata, Kato et al. 1998, Heo, Tatebayashi et al. 1999), which both used the same yeast strain that constitutively expressed *BLM* from a *GAPDH* promoter and showed partial suppression of some *sgs1Δ* defects, including HU sensitivity, we found that neither *BLM* expression under control of the natural *SGS1* promoter nor varying levels of *BLM* expression under control of a galactose-inducible promoter had any positive effect on the *sgs1Δ* mutant. That a single copy of BLM, when expressed under control of the native *SGS1* promoter, cannot alleviate *sgs1Δ* defects initially suggested to us that BLM had no functionality in yeast. In fact, the strong increase in genome instability, accompanied by severe HU sensitivity and some growth retardation upon overexpression of BLM, indicated that BLM expression is detrimental to yeast cells. The absence of any GCR accumulation upon Sgs1 overexpression suggests that increased accumulation of GCRs in BLM-overexpressing cells is not simply due to increased unwinding. Rather, we propose that BLM may possess helicase activity in yeast, leading to increased unwinding upon overexpression, but fails to elicit proper downstream responses, for example, due to lack of proper N-terminal protein–protein interactions, which ultimately leads to an overabundance of aberrantly repaired lesions. That endogenous levels of N-terminal segments of Sgs1 as short as 547 residues suppressed the slow growth phenotype and the severe HU sensitivity of BLM-overexpressing cells argues in favor of a functional relationship between Sgs1 and BLM. For example, co-expression of Sgs1 and BLM could alleviate HU sensitivity in BLM-overexpressing cells by acting as a bridge between BLM and Top3 (and/or other protein complexes interacting with the Sgs1 N-terminus), thereby linking enzymatic activity to appropriate upstream and downstream

events. Remarkably, even relatively short N-terminal fragments of Sgs1 are sufficient for the suppression of the increased HU sensitivity of BLM-overexpressing cells, further supporting the importance of the Sgs1 N-terminus with its role in mediating interaction with other DNA metabolic factors. HU resistance comparable to wild-type cells and significantly reduced GCR accumulation of cells expressing a chimeric fusion of the Sgs1 N-terminus, which is devoid of enzymatic function and dispensable for helicase activity and ssDNA binding *in vitro*, and the BLM C-terminus, which contains helicase/RQC and HRDC domains, are consistent with helicase activity of BLM in yeast and a biologically significant, functional interaction between BLM and Sgs1. That fusion of the Sgs1 and BLM segments provides HU resistance as well as co-expression of BLM and Sgs1 polypeptides from separate alleles in the same cell may indicate that the N-terminus of Sgs1 can physically interact with BLM. Our findings also suggest that it is the inability of the N-terminus of BLM to interact with or be modified by yeast proteins that leads to the inability of BLM to function in yeast. A previous report that BLM expression in yeast alleviates several *sgs1* Δ phenotypes, including partial suppression of HU sensitivity (Yamagata, Kato et al. 1998, Heo, Tatebayashi et al. 1999), could be explained by the fact that, in the earlier study, BLM was expressed from a *GAPDH* promoter, whereas here it was expressed either from the native *SGS1* promoter or from a galactose-inducible promoter. However, in light of the findings presented here, there could also be an alternative explanation. Since the *GAPDH* promoter–*BLM* construct appears to have been inserted into the middle of the wild-type *SGS1* gene, an N-terminal segment of Sgs1 could have been expressed from the native *SGS1* promoter in addition to BLM being expressed from the *GAPDH* promoter. As shown here for

haploids expressing the chimera and for diploids co-expressing the N-termini of Sgs1 and full-length BLM, such co-expression of an N-terminal Sgs1 segment from the native *SGS1* promoter and *BLM* from the *GAPDH* promoter could be an explanation for the reported increase in HU resistance of BLM-expressing cells compared to *sgs1Δ* cells.

Of the five human RecQ-like DNA helicases, BLM is considered to be most closely related to Sgs1. Even though we show here that BLM cannot suppress any defects of the *sgs1Δ* mutant, the functional chimera does provide evidence for a functional relationship between the two RecQ-like helicases and provides a model system for the further characterization of BLM functional domains in yeast. In fact, all BS-associated missense mutations and numerous polymorphisms are located within the 770-residue C-terminal fragment of BLM that is part of the chimera, so that they are now accessible to further functional and mutational characterization in yeast. The *in vivo* functionality of the Sgs1–BLM chimera also demonstrates the remarkable utility of protein disorder prediction as a tool for the construction of functional mutants. It will be interesting to see whether domains of any of the other human RecQ-like helicases, are capable of forming functional chimeras with the Sgs1 N-terminus.

MATERIALS AND METHODS

Yeast strains and media

All strains are derived from KHSY802, a derivative of S288C. Yeast strains expressing truncations of Sgs1 helicase were constructed by HR-mediated integration of PCR products, replacing the desired 3'-segment of *SGS1* on chromosome VIII with a myc epitope coding sequence (from pFA6a-13Myc.His3MX6 (Longtine, McKenzie et al.

1998), a gift from Mark Longtine, University of Washington) in-frame with the *SGS1* coding sequence. The expression of all truncation alleles and the myc-epitope-tagged wild-type allele of *SGS1* was confirmed by Western blot analysis. All gene replacements, insertions, and truncations were performed via the standard LiAc protocol (Gietz and Woods 2006), using PCR products with at least 50 nt on each end, which matched the chromosomal target locus. A PCR fragment containing *BLM* cDNA (Open Biosystems) and a *HIS3* cassette was amplified by PCR from plasmid pKHS293 using primers that include 50-nt homology to the chromosomal *SGS1* locus to express BLM from the native *SGS1* promoter (P_{SGS1}). This PCR product was fused to the native chromosomal *SGS1* promoter by HR-mediated integration (Gietz and Woods 2006). A PCR fragment coding for a 13Myc epitope tag was amplified from pFA6a-13Myc-kanMX6 (Longtine, McKenzie et al. 1998) and integrated in-frame at the 3'-end of cDNAs or *sgs1* alleles for detection of protein expression by Western blot analysis. In strains KHSY3350 and KHSY3218, galactose-inducible promoters amplified from plasmids pFA6a-kanMX6-PGAL1 and pFA6a-TRP1-PGAL1 (Longtine, McKenzie et al. 1998), respectively, were used to replace the native *SGS1* promoter. To construct KHSY3355, we amplified the 3'-terminal 2313 bp of BLM cDNA linked to a *HIS3* cassette by PCR from plasmid pKHS293 and used them to replace the 3'-terminal 2400 bp of *SGS1* in KHSY802. The accuracy of PCR-derived *SGS1* or *BLM* integrations was confirmed by sequencing. Amino acid changes C1047F and F1056A in Sgs1 were made by site-directed mutagenesis (QuikChange, Stratagene) of pKHS360 and integrated at the *sgs1::HIS3* locus in KHSY1338. All yeast strains used in this study are listed in Table S1. Cells were grown in YPD consisting of 10 g/l yeast extract (Fisher

Scientific), 20 g/l Bacto-peptone (BD Diagnostic Systems), and 2% glucose (Fisher Scientific), unless indicated otherwise. For plates, agar (BD Diagnostic Systems) was added at a concentration of 20 g/l.

Western blot analysis

Cells were grown to an $OD_{600} = 0.5$ in YPD, and whole-cell extracts were prepared from 5 ml of culture ($\sim 3.5 \times 10^7$ cells) by standard trichloroacetic acid (TCA, Fisher Scientific) extraction to confirm expression of myc-epitope-tagged *BLM* and *SGS1* alleles (Foiani, Liberi et al. 1999). Five microliters of TCA extract was separated on 10% polyacrylamide gels, transferred to a PVDF membrane (Bio-Rad), probed with anti-c-myc monoclonal antibody (9E10, Covance Research Products), and visualized by chemiluminescence (ECL Plus, GE Healthcare). To confirm expression of *SGS1* and *BLM* from the *GAL1* promoter, we used the same Western blot procedure, but cells were grown overnight in yeast-peptone (YP) [(10 g/l yeast extract (Fisher Scientific), 20 g/l Bacto-peptone (BD Diagnostic Systems)] supplemented with 2% sucrose (Fisher Scientific), diluted to an $OD_{600} = 0.2$ in YP supplemented with either 2% sucrose (uninduced sample) or 2% galactose (induced sample), and harvested for TCA extraction when cultures reached $OD_{600} = 0.5$. Molecular weight marker (Broad Range) was from Bio-Rad.

Sensitivity to DNA-damaging agents HU and MMS

Cell cultures were grown in YPD to an $OD_{600} = 0.5$, and 10-fold serial dilutions were spotted on YPD supplemented with 0.05% MMS (Sigma Aldrich) or with 50 mM or

100 mM HU (US Biological), as indicated. For experiments that included strains expressing BLM or Sgs1 from the *GAL1* promoter (Fig. 5), cultures were grown in YP-2% sucrose instead of YPD and spotted on YP-1% sucrose + 1% galactose (to induce gene expression) supplemented with 100 mM HU or without HU as the growth control.

GCR rate measurements

Rates of accumulating GCRs in YPD were determined as previously described (Schmidt, Pennaneach et al. 2006). For GCR rate measurements of yeast strains expressing BLM or Sgs1 from the *GAL1* promoter, the same procedure was followed, except that media were supplemented with 2% galactose to induce gene expression. Briefly, 10 ml of YP-2% galactose was inoculated with a single colony, which had been grown on YPD agar for 3 days. After 3 days of growth in liquid media at 30 °C with vigorous shaking, cells were plated on GCR plates (Schmidt, Pennaneach et al. 2006) supplemented with 2% galactose instead of 2% glucose, and 10^{-6} dilutions were plated on YPD to obtain the viable cell count. Colonies on GCR plates were counted after 5 days of incubation at 30 °C. For GCR rate measurements in the presence of varying BLM expression levels (Table 2), 0.1% or 0.5% galactose instead of 2% galactose was added to liquid YP media and to GCR plates, and sucrose was supplemented to reach a total of 2% sugar in the media. We calculated 95% confidence intervals according to Nair (Nair 1940).

Random spore analysis

Diploids heterozygous for the desired mutant alleles were grown overnight at 30 °C in YPD, washed, transferred to 0.1% potassium acetate (Fisher Scientific), and incubated for 5 days at 30 °C with vigorous shaking. Asci were incubated in the presence of 500 µg/ml zymolase (MP Biomedicals) in 1 M sorbitol (Fisher Scientific) for 20 min at 30 °C and enriched for haploid spores as previously described (Rockmill, Lambie et al. 1991). Spores were plated on YPD, incubated at 30 °C, and genotyped by spotting on synthetic drop-out media (US Biological) to detect the presence of *TRP1* and *HIS3* marker cassettes linked to the mutant alleles. The presence of mutant alleles linked to the kanMX6 cassette was detected by the ability of haploids to grow on YPD supplemented with 200 µg/ml G418 (Axxora LLC, San Diego, CA).

FIGURES AND TABLES

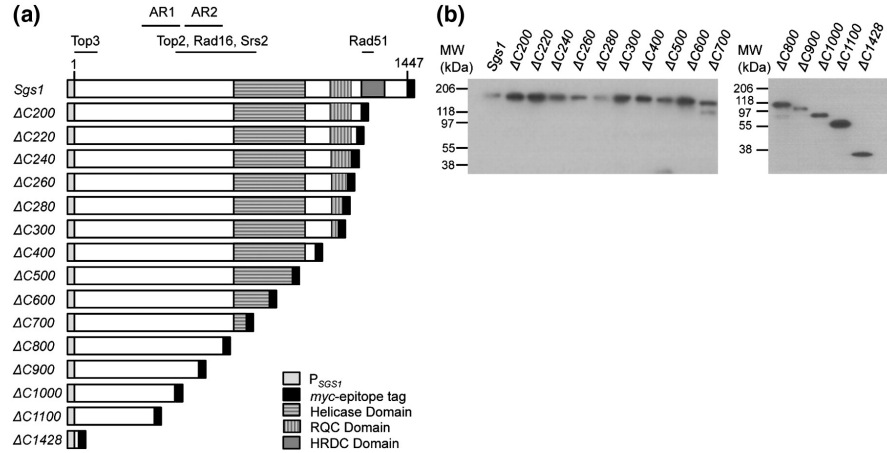


Figure 2.1. C-terminal truncations of Sgs1 used in this study.

(A) Full-length Sgs1 contains a DEAH-helicase domain, an RQC domain and an HRDC domain in its C-terminal half; interaction sites with Top3, Top2, Srs2, Rad51 and Rad16 are indicated. C-terminal truncations ranging in size from 200 residues to 1428 residues were constructed by fusion to a myc-epitope tag. All truncations were introduced to the endogenous *SGS1* locus on chromosome VIII. **(B)** Expression of wild-type Sgs1 and truncation alleles from the endogenous *SGS1* promoter (*P_{SGS1}*) was confirmed by Western blotting, using a myc-antibody. Molecular weights (MW) are indicated on the left.

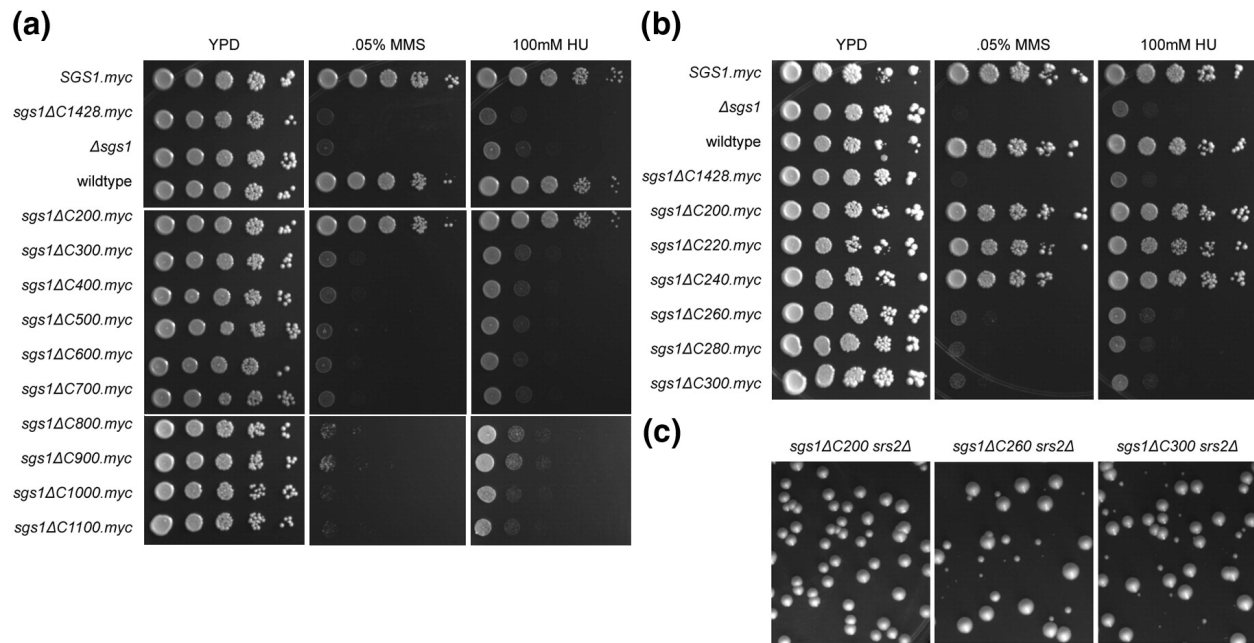


Figure 2.2. Sensitivity of cells expressing Sgs1 truncation alleles to the DNA damaging agents HU and MMS. Ten-fold dilutions of exponentially growing cultures (OD600 = 0.5) were spotted on YPD for viable cell count and on YPD containing 100mM HU or 0.05% MMS, followed by incubation at 30° C. **(A)** Haploid cells expressing *sgs1* alleles lacking 300 or more residues from the C-terminus are as sensitive to HU and MMS as the null allele. **(B)**. Additional incremental 20-amino-acid deletions reveal that cells expressing *sgs1* alleles lacking up to 240 residues are as resistant to HU and MMS as wildtype cells whereas those lacking 260 or more residues are as sensitive as the *sgs1Δ* mutant. **(C)** Spores from diploids heterozygous for an *srs2Δ* deletion and heterozygous either for the *sgs1-ΔC200*, *sgs1Δ-C260* or *sgs1-ΔC300* were spread on YPD to allow for growth of spores of all possible genotypes. Similar sized colonies obtained from the spores of the diploid heterozygous for *sgs1ΔC200* and *srs2Δ* mutations (left) indicate that the *sgs1ΔC200 srs2Δ* mutant grows as well as the single mutants, suggesting that deletion of the C-terminal 200 amino acid residues does not negatively affect growth of the *srs2Δ* mutant. In contrast, spores from diploids heterozygous for the *srs2Δ* mutation and the *sgs1ΔC260* allele (middle) or the *sgs1ΔC300* allele (right), grew into a mixture of normal-sized colonies (corresponding to single mutants and wildtype) and small-sized colonies (corresponding to *srs2Δ sgs1ΔC260* or *srs2Δ sgs1ΔC300* mutants as determined by genotyping), demonstrating that an intact RQC domain in Sgs1 is required for the viability of the *srs2Δ* mutant.

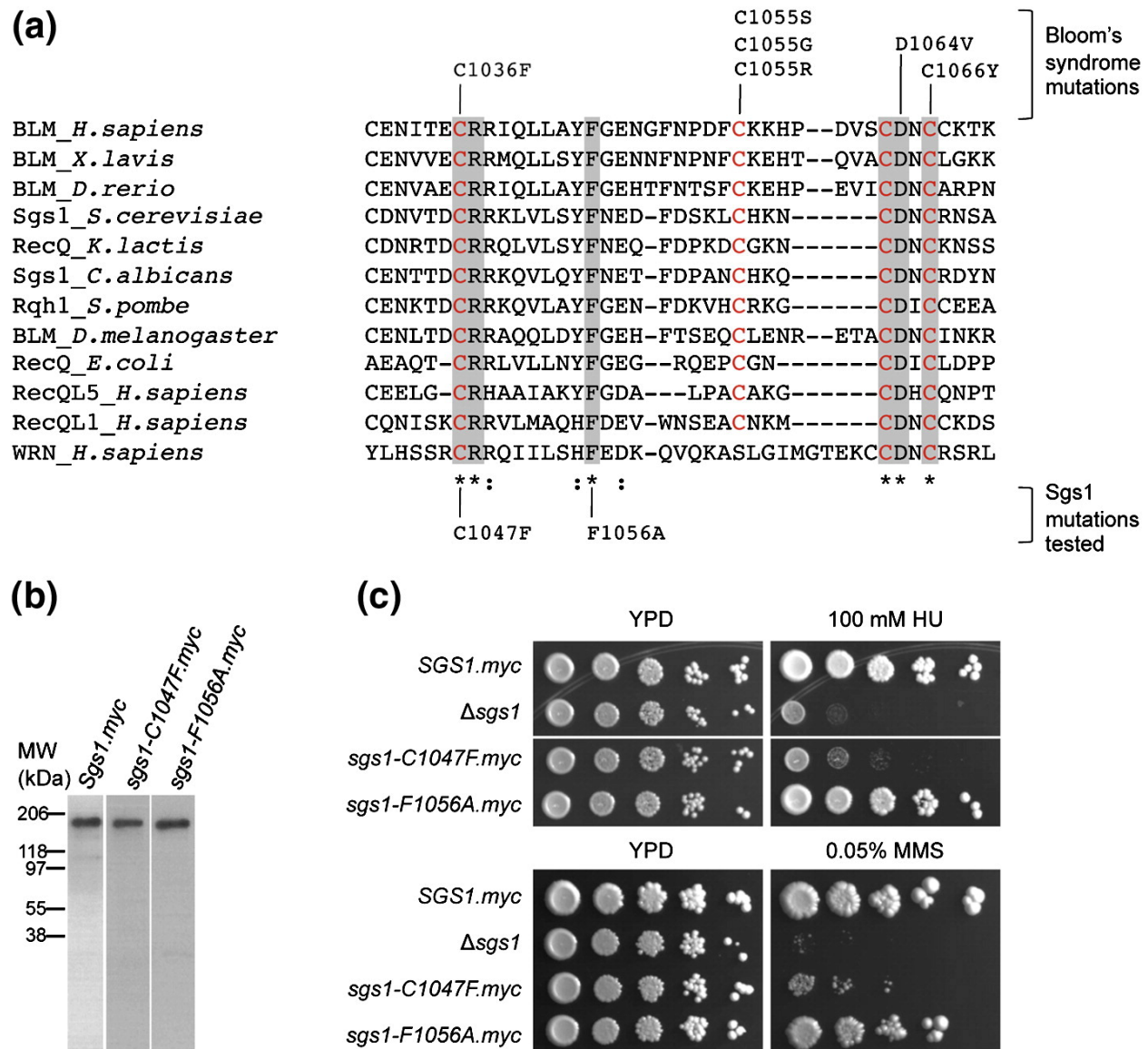


Figure 2.3. Effect of zinc-binding domain mutations on Sgs1 function *in vivo*. (A) Zinc-binding domain is conserved from bacterial to human RecQ-like DNA helicases. Protein sequences were aligned with ClustalW2 (Chenna, Sugawara et al. 2003). The alignment of RecQL1 was manually adjusted. Amino acid residues identical in all sequences are highlighted in gray and indicated by '*' below the alignment, conserved substitutions are indicated by ':' below the alignment, and cysteine residues thought to be involved in zinc-binding are shown in red. At least six different missense mutations in the zinc-binding domain are associated with Bloom's syndrome. (B) C1047F and F1056A mutations were introduced into Sgs1 and expression was confirmed by western blot using antibody against the C-terminal myc-epitope. Molecular weights (MW) are indicated in kDa to the left. (C) Mutation of the highly conserved F1056 does not impair Sgs1 function whereas the C1047F mutation leads to an increase in sensitivity to HU and MMS, but not to the level seen in the *sgs1* Δ mutant.

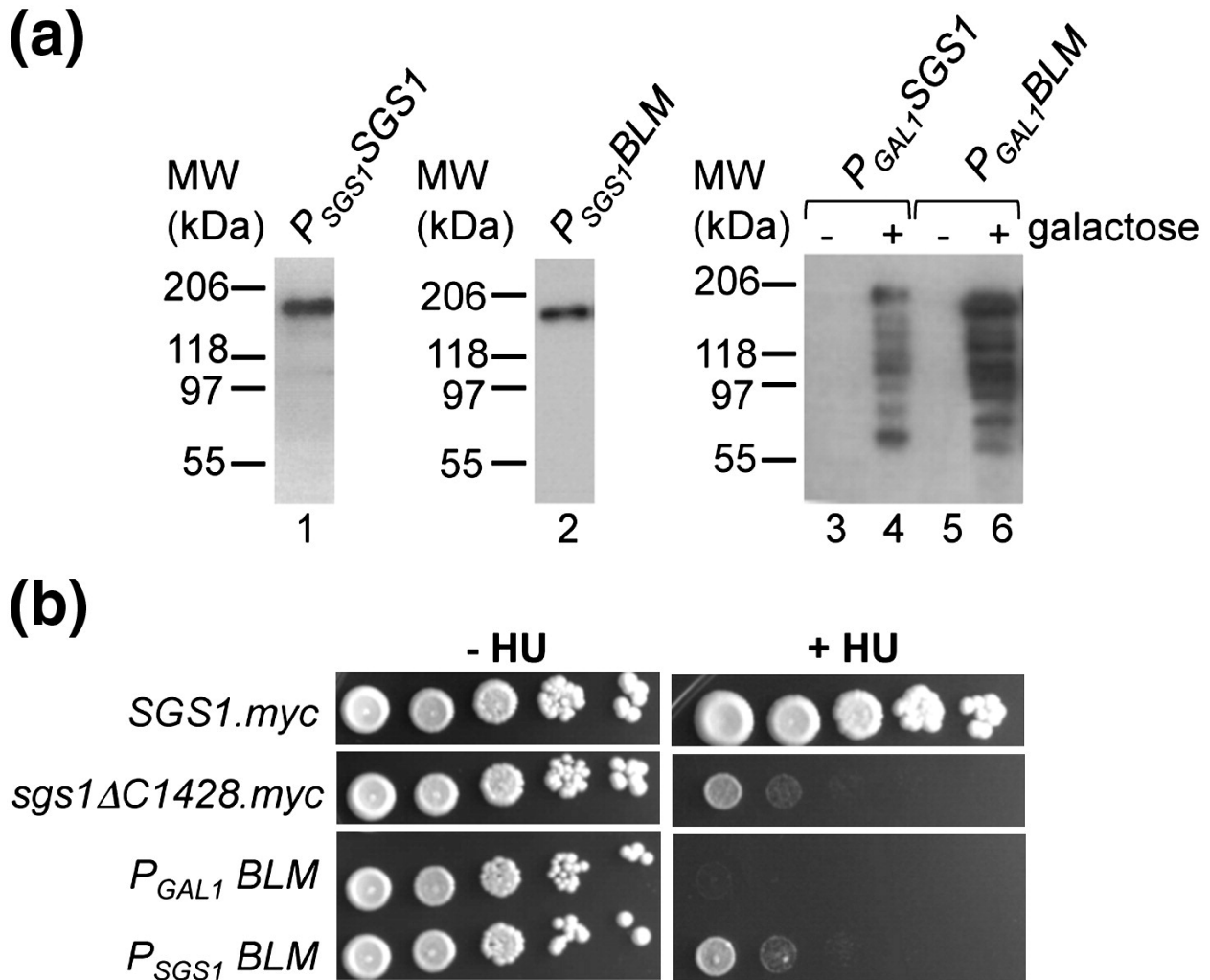


Figure 2.4. BLM expression does not suppress *sgs1Δ* defects and BLM overexpression is detrimental to yeast cells. (A) Expression of myc-epitope tagged Sgs1 (lane 1) and BLM (lane 2) from the native chromosomal *SGS1* locus or galactose-inducible overexpression of myc-epitope tagged Sgs1 (lane 4) and BLM (lane 6) in yeast cells grown in YP supplemented with 1% sucrose and 1% galactose (to induce expression, lanes 4 and 6) or without galactose (lanes 3 and 5). Both BLM and Sgs1 show signs of degradation upon overexpression (lanes 4 and 6) whereas expression from the native *SGS1* promoter is stable (lanes 1 and 2). Molecular weights (MW) are indicated in kDa on the left. **(B)** Cells expressing BLM from the *SGS1* promoter on chromosome VIII are as sensitive to HU as cells lacking Sgs1 ($\Delta sgs1$). Replacement of the natural *SGS1* promoter with a galactose-inducible *GAL1* promoter induces BLM overexpression and leads to increased HU sensitivity. Ten-fold dilutions of cells were spotted on media containing 1% sucrose and 1% galactose (to induce BLM overexpression) with and without 100 mM HU.

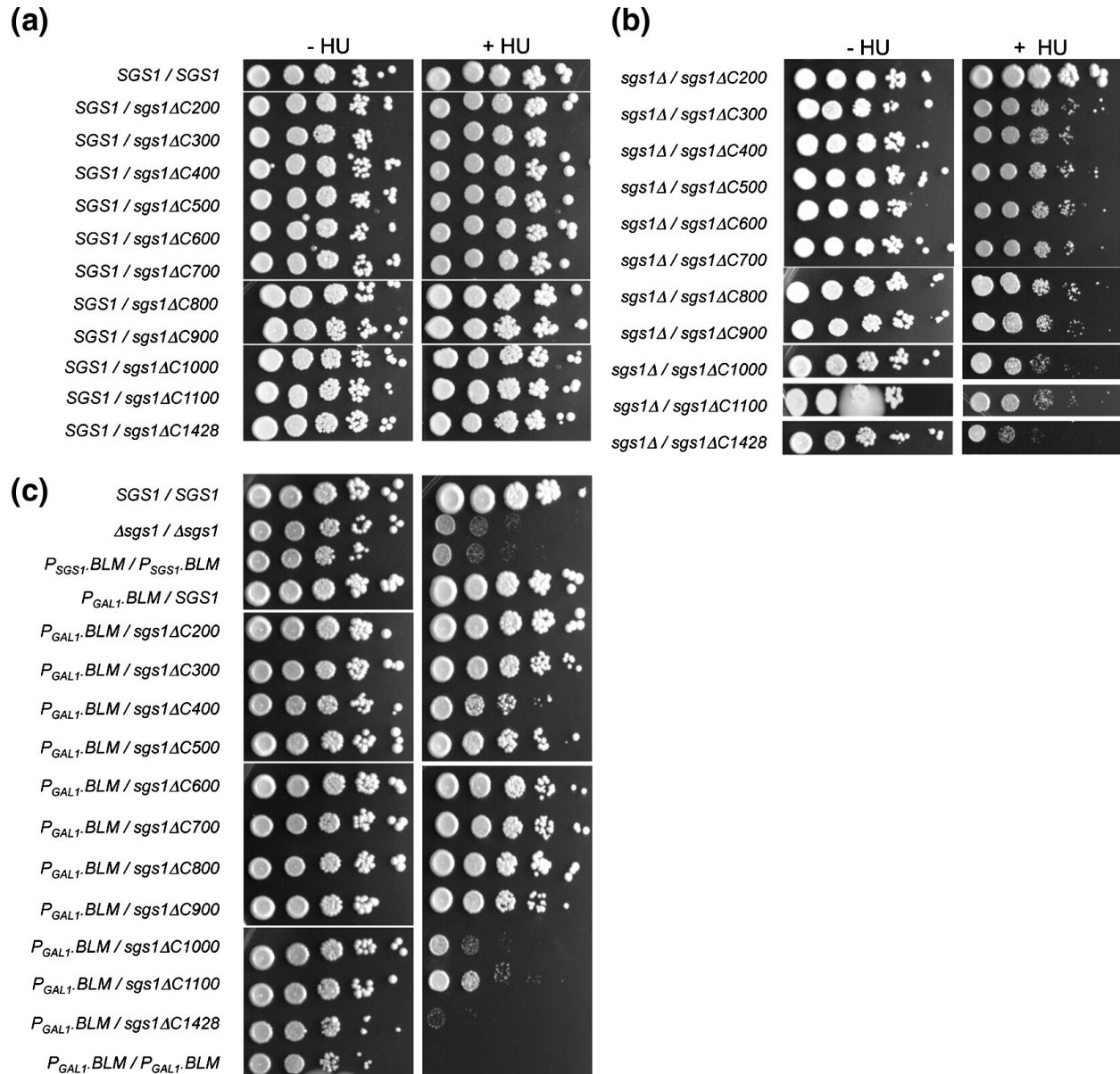


Figure 2.5. HU sensitivity of diploid cells expressing *BLM* and mutant alleles of *SGS1*. **(A)** Ten-fold dilutions of exponentially growing diploids expressing truncation alleles of *SGS1* in the presence of a wildtype allele were spotted on YPD media with and without 100 mM HU. **(B)** Ten-fold dilutions of exponentially growing diploids expressing truncation alleles of *SGS1* in the absence of a wildtype allele were spotted on YPD media with and without 100 mM HU. **(C)** Ten-fold dilutions of exponentially growing diploids overexpressing *BLM* from a *GAL1* promoter inserted at the native *SGS1* locus and expressing truncation alleles of *SGS1* under control of the native *SGS1* promoter on the other allele were spotted on media containing 1% galactose (to induce gene expression) and 1% sucrose with or without 100 mM HU.

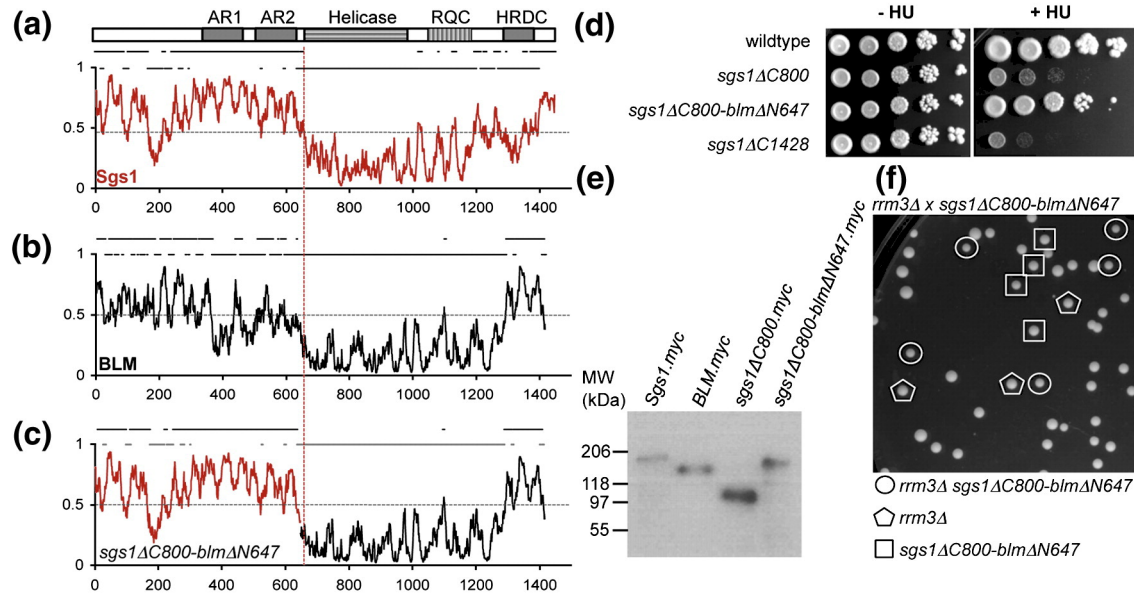


Figure 2.6. Construction of a functional chimerical protein composed of the N-terminus of Sgs1 and the C-terminus of BLM. (A – B) Protein disorder prediction of Sgs1 (red) and BLM (black) using the IUPred algorithm. Values above 0.5 indicate a disordered residue whereas values below 0.5 indicate ordered residues; amino acid residue numbers (1–1447) are indicated on the abscissa. Black lines above the graph show a simplified order and disorder distribution along the length of the protein with values above 0.5 being assigned a “1” and values below 0.5 being assigned a “0”. The vertical red line indicates the site in Sgs1, BLM and the chimera where the disordered N-terminal segment transitions into the ordered helicase domain at residue 647/648. This site was chosen as the fusion site for the chimera. The approximate location of Sgs1 domains is indicated above panel A. **(C)** Disorder prediction for the Sgs1-BLM chimera in which the N-terminal 647 residues of BLM (black) were replaced with the N-terminal 647 residues of Sgs1 (red). **(D)** Ten-fold dilutions of exponentially growing haploids were spotted on YPD with or without 100 mM HU. **(E)** The C-terminus of the Sgs1-BLM chimera was fused to a myc-epitope tag and expression was confirmed by western blotting. Molecular weight marker bands (kDa) are indicated on the left **(F)** A diploid heterozygous for the *rrm3Δ* mutation and the *sgs1ΔC800-blmΔN647* allele expressing the chimera was sporulated and random spores were plated on YPD to allow all spores to grow. An open circle indicates the haploid double mutant, and the open square and pentagon indicate haploid *sgs1ΔC800-blmΔN647* and *rrm3Δ* single mutants, respectively.

Table 2.1. Accumulation of GCRs in cells expressing mutant alleles of *SGS1*

| Relevant Genotype^a | GCR rate (Can^r 5-FOA^r × 10⁻¹⁰) | 95% CI^b (Can^r 5-FOA^r × 10⁻¹⁰) |
|--|--|--|
| Wild type | 1.1 | < 1–6.2 |
| <i>sgs1</i> Δ | 251 | 80–310 |
| <i>sgs1</i> ΔC200 | 7 | < 6–23 |
| <i>sgs1</i> ΔC220 | 31 | 5–41 |
| <i>sgs1</i> ΔC240 | 10 | < 6–27 |
| <i>sgs1</i> ΔC260 | 159 | 85–362 |
| <i>sgs1</i> ΔC280 | 244 | 166–387 |
| <i>sgs1</i> ΔC300 | 145 | 76–204 |
| <i>sgs1</i> ΔC400 | 106 | 60–180 |
| <i>sgs1</i> ΔC500 | 102 | 53–252 |
| <i>sgs1</i> ΔC600 | 152 | 26–283 |
| <i>sgs1</i> ΔC700 | 189 | 49–271 |
| <i>sgs1</i> ΔC800 | 133 | 71–225 |
| <i>sgs1</i> ΔC1428 | 206 | 97–273 |
| <i>sgs1</i> -C1047F | 64 | 35–131 |
| <i>sgs1</i> -F1056A | < 16 | < 10–26 |
| <i>mec3</i> Δ <i>sgs1</i> ΔC200 | 11 | < 7–22 |
| <i>mec3</i> Δ <i>sgs1</i> ΔC300 | 1003 | 691–1500 |
| <i>mec3</i> Δ <i>sgs1</i> ΔC800 | 758 | 645–895 |
| <i>mec3</i> Δ <i>sgs1</i> ΔC800- <i>blm</i> ΔN647 ^c | 361 | 330–419 |

a. All *sgs1* truncations (*sgs1*ΔC) are C-terminally fused to a myc epitope tag.

b. We calculated 95% confidence intervals (CIs) according to Nair (Nair 1940).

c. The *sgs1*ΔC800-*blm*ΔN647 allele expresses a chimeric protein that consists of the 647 N-terminal residues of *Sgs1* and the 770 C-terminal residues of human BLM.

Table 2.2. Effect of BLM expression on GCR accumulation in the *sgs1Δ* mutant

| Relevant genotype ^a | Galactose concentration in media (%) | GCR rate (Can ^r 5-FOA ^r × 10 ⁻¹⁰) | 95% CI ^b (Can ^r 5-FOA ^r × 10 ⁻¹⁰) |
|--------------------------------|--------------------------------------|---|--|
| Wild type | 0 | 1.1 | < 1–6.2 |
| <i>P_{SGS1}BLM</i> | 0 | 70 | 56–151 |
| <i>P_{GAL}BLM</i> | 0 | 61 | 30–153 |
| <i>P_{GAL}BLM</i> | 0.1 | 335 | 233–576 |
| <i>P_{GAL}BLM</i> | 0.5 | 382 | 170–777 |
| <i>P_{GAL}BLM</i> | 2 | 1832 | 1090–2910 |
| <i>P_{GAL}SGS1</i> | 2 | < 11 | < 9–12 |
| <i>sgs1Δ</i> | 2 | 54 | 23–104 |

a. Human *BLM* cDNA was inserted at the endogenous *SGS1* locus and fused to the native *SGS1* promoter (*P_{SGS1}*) or fused to a galactose-inducible promoter (*P_{GAL}*). In *P_{GAL}SGS1*, the native *SGS1* promoter region was disrupted by fusing the *SGS1* open reading frame to a galactose-inducible promoter. If strains expressing *BLM* or *SGS1* genes from the galactose-inducible GAL1 promoter were grown in less than 2% galactose (to lower protein expression levels), media were supplemented with sucrose to reach a total sugar concentration of 2%.

b. We calculated 95% confidence intervals (CIs)

TABLE 2.S1. Yeast Strains used in this study

| Strain | Genotype |
|----------|--|
| KHSY802 | <i>MATa ura3-52, leu2Δ1, trp1Δ63, his3Δ200, lys2ΔBgl, hom3-10, ade2Δ1, ade8, YEL069C::URA3</i> |
| KHSY1338 | <i>MATa ura3-52, leu2Δ1, trp1Δ63, his3Δ200, lys2ΔBgl, hom3-10, ade2Δ1, ade8, YEL069C::URA3, sgs1::HIS3</i> |
| KHSY1705 | <i>MATa ura3-52, leu2Δ1, trp1Δ63, his3Δ200, lys2ΔBgl, hom3-10, ade2Δ1, ade8, YEL069C::ura3::TRP1, sgs1::BLM.HIS3</i> |
| KHSY2341 | <i>MATa ura3-52, leu2Δ1, trp1Δ63, his3Δ200, lys2ΔBgl, hom3-10, ade2Δ1, ade8, YEL069C::URA3, mec3::kanMX6, sgs1ΔC200.MYC.HIS3</i> |
| KHSY2347 | <i>MATa ura3-52, leu2Δ1, trp1Δ63, his3Δ200, lys2ΔBgl, hom3-10, ade2Δ1, ade8, YEL069C::URA3, mec3::kanMX6, sgs1ΔC300.MYC.HIS3</i> |
| KHSY2599 | <i>ura3-52/ura3-52, leu2Δ1/ leu2Δ1, trp1Δ63/trp1Δ63, his3Δ200/his3Δ200, lys2ΔBgl/ lys2ΔBgl, hom3-10/ hom3-10, ade2Δ1/ade2Δ1, ade8/ade8, YEL069C::URA3/YEL069C::URA3</i> |
| KHSY2602 | <i>ura3-52/ura3-52, leu2Δ1/ leu2Δ1, trp1Δ63/trp1Δ63, his3Δ200/his3Δ200, lys2ΔBgl/ lys2ΔBgl, hom3-10/ hom3-10, ade2Δ1/ade2Δ1, ade8/ade8, YEL069C::ura3::TRP1/YEL069C::ura3::TRP1, sgs1::kanMX6/sgs1::kanMX6</i> |
| KHSY2726 | <i>ura3-52/ura3-52, leu2Δ1/ leu2Δ1, trp1Δ63/trp1Δ63, his3Δ200/his3Δ200, lys2ΔBgl/ lys2ΔBgl, hom3-10/ hom3-10, ade2Δ1/ade2Δ1, ade8/ade8, YEL069C::URA3/YEL069C::URA3, SGS1/sgs1C200.MYC.HIS3</i> |

TABLE 2.S1 (continued)

| | |
|----------|---|
| KHSY2828 | <i>ura3-52/ura3-52, leu2Δ1/ leu2Δ1, trp1Δ63/trp1Δ63, his3Δ200/his3Δ200, lys2ΔBgl/ lys2ΔBgl, hom3-10/ hom3-10, ade2Δ1/ade2Δ1, ade8/ade8, YEL069C::URA3/YEL069C::ura3::TRP1, sgs1::kanMX6/sgs1C200.MYC.HIS3</i> |
| KHSY2837 | <i>ura3-52/ura3-52, leu2Δ1/ leu2Δ1, trp1Δ63/trp1Δ63, his3Δ200/his3Δ200, lys2ΔBgl/ lys2ΔBgl, hom3-10/ hom3-10, ade2Δ1/ade2Δ1, ade8/ade8, YEL069C::URA3/YEL069C::ura3::TRP1, sgs1::kanMX6/sgs1C300.MYC.HIS3</i> |
| KHSY2880 | <i>ura3-52/ura3-52, leu2Δ1/ leu2Δ1, trp1Δ63/trp1Δ63, his3Δ200/his3Δ200, lys2ΔBgl/ lys2ΔBgl, hom3-10/ hom3-10, ade2Δ1/ade2Δ1, ade8/ade8, YEL069C::URA3/YEL069C::URA3, SGS1/sgs1ΔC300.MYC.HIS3</i> |
| KHSY2883 | <i>ura3-52/ura3-52, leu2Δ1/ leu2Δ1, trp1Δ63/trp1Δ63, his3Δ200/his3Δ200, lys2ΔBgl/ lys2ΔBgl, hom3-10/ hom3-10, ade2Δ1/ade2Δ1, ade8/ade8, YEL069C::URA3/YEL069C::URA3, SGS1/sgs1ΔC400.MYC.HIS3</i> |
| KHSY2886 | <i>ura3-52/ura3-52, leu2Δ1/ leu2Δ1, trp1Δ63/trp1Δ63, his3Δ200/his3Δ200, lys2ΔBgl/ lys2ΔBgl, hom3-10/ hom3-10, ade2Δ1/ade2Δ1, ade8/ade8, YEL069C::URA3/YEL069C::URA3, SGS1/sgs1ΔC500.MYC.HIS3</i> |
| KHSY2889 | <i>ura3-52/ura3-52, leu2Δ1/ leu2Δ1, trp1Δ63/trp1Δ63, his3Δ200/his3Δ200, lys2ΔBgl/ lys2ΔBgl, hom3-10/ hom3-10, ade2Δ1/ade2Δ1, ade8/ade8, YEL069C::URA3/YEL069C::URA3, SGS1/sgs1ΔC600.MYC.HIS3</i> |

TABLE 2.S1 (continued)

| | |
|----------|--|
| KHSY2892 | <i>ura3-52/ura3-52, leu2Δ1/ leu2Δ1, trp1Δ63/trp1Δ63, his3Δ200/his3Δ200, lys2ΔBgl/ lys2ΔBgl, hom3-10/ hom3-10, ade2Δ1/ade2Δ1, ade8/ade8, YEL069C::URA3/YEL069C::URA3, SGS1/sgs1ΔC700.MYC.HIS3</i> |
| KHSY2895 | <i>ura3-52/ura3-52, leu2Δ1/ leu2Δ1, trp1Δ63/trp1Δ63, his3Δ200/his3Δ200, lys2ΔBgl/ lys2ΔBgl, hom3-10/ hom3-10, ade2Δ1/ade2Δ1, ade8/ade8, YEL069C::URA3/YEL069C::URA3, SGS1/sgs1ΔC800.MYC.HIS3</i> |
| KHSY2898 | <i>ura3-52/ura3-52, leu2Δ1/ leu2Δ1, trp1Δ63/trp1Δ63, his3Δ200/his3Δ200, lys2ΔBgl/ lys2ΔBgl, hom3-10/ hom3-10, ade2Δ1/ade2Δ1, ade8/ade8, YEL069C::URA3/YEL069C::URA3, SGS1/sgs1ΔC1428.MYC.HIS3</i> |
| KHSY2928 | <i>ura3-52/ura3-52, leu2Δ1/ leu2Δ1, trp1Δ63/trp1Δ63, his3Δ200/his3Δ200, lys2ΔBgl/ lys2ΔBgl, hom3-10/ hom3-10, ade2Δ1/ade2Δ1, ade8/ade8, YEL069C::URA3/YEL069C::ura3::TRP1, sgs1::kanMX6/sgs1ΔC400.MYC.HIS3</i> |
| KHSY2931 | <i>ura3-52/ura3-52, leu2Δ1/ leu2Δ1, trp1Δ63/trp1Δ63, his3Δ200/his3Δ200, lys2ΔBgl/ lys2ΔBgl, hom3-10/ hom3-10, ade2Δ1/ade2Δ1, ade8/ade8, YEL069C::URA3/YEL069C::ura3::TRP1, sgs1::kanMX6/sgs1ΔC500.MYC.HIS3</i> |
| KHSY2934 | <i>ura3-52/ura3-52, leu2Δ1/ leu2Δ1, trp1Δ63/trp1Δ63, his3Δ200/his3Δ200, lys2ΔBgl/ lys2ΔBgl, hom3-10/ hom3-10, ade2Δ1/ade2Δ1, ade8/ade8, YEL069C::URA3/YEL069C::ura3::TRP1, sgs1::kanMX6/sgs1ΔC600.MYC.HIS3</i> |

TABLE 2.S1 (continued)

| | |
|----------|---|
| KHSY2937 | <i>ura3-52/ura3-52, leu2Δ1/ leu2Δ1, trp1Δ63/trp1Δ63, his3Δ200/his3Δ200, lys2ΔBgl/ lys2ΔBgl, hom3-10/ hom3-10, ade2Δ1/ade2Δ1, ade8/ade8, YEL069C::URA3/YEL069C::ura3::TRP1, sgs1::kanMX6/sgs1ΔC700.MYC.HIS3</i> |
| KHSY2940 | <i>ura3-52/ura3-52, leu2Δ1/ leu2Δ1, trp1Δ63/trp1Δ63, his3Δ200/his3Δ200, lys2ΔBgl/ lys2ΔBgl, hom3-10/ hom3-10, ade2Δ1/ade2Δ1, ade8/ade8, YEL069C::URA3/YEL069C::ura3::TRP1, sgs1::kanMX6/sgs1ΔC800.MYC.HIS3</i> |
| KHSY2943 | <i>ura3-52/ura3-52, leu2Δ1/ leu2Δ1, trp1Δ63/trp1Δ63, his3Δ200/his3Δ200, lys2ΔBgl/ lys2ΔBgl, hom3-10/ hom3-10, ade2Δ1/ade2Δ1, ade8/ade8, YEL069C::URA3/YEL069C::ura3::TRP1, sgs1::kanMX6/sgs1ΔC1428.MYC.HIS3</i> |
| KHSY2970 | <i>MATa ura3-52, leu2Δ1, trp1Δ63, his3Δ200, lys2ΔBgl, hom3-10, ade2Δ1, ade8, YEL069C::URA3, sgs1.MYC.HIS3</i> |
| KHSY2972 | <i>MATa ura3-52, leu2Δ1, trp1Δ63, his3Δ200, lys2ΔBgl, hom3-10, ade2Δ1, ade8, YEL069C::URA3, sgs1ΔC200.MYC.HIS3</i> |
| KHSY2973 | <i>MATa ura3-52, leu2Δ1, trp1Δ63, his3Δ200, lys2ΔBgl, hom3-10, ade2Δ1, ade8, YEL069C::URA3, sgs1ΔC300.MYC.HIS3</i> |
| KHSY2974 | <i>MATa ura3-52, leu2Δ1, trp1Δ63, his3Δ200, lys2ΔBgl, hom3-10, ade2Δ1, ade8, YEL069C::URA3, sgs1ΔC400.MYC.HIS3</i> |
| KHSY2975 | <i>MATa ura3-52, leu2Δ1, trp1Δ63, his3Δ200, lys2ΔBgl, hom3-10, ade2Δ1, ade8, YEL069C::URA3, sgs1ΔC500.MYC.HIS3</i> |

TABLE 2.S1 (continued)

| | |
|----------|---|
| KHSY2976 | <i>MATa ura3-52, leu2Δ1, trp1Δ63, his3Δ200, lys2ΔBgl, hom3-10, ade2Δ1, ade8, YEL069C::URA3, sgs1ΔC600.MYC.HIS3</i> |
| KHSY2977 | <i>MATa ura3-52, leu2Δ1, trp1Δ63, his3Δ200, lys2ΔBgl, hom3-10, ade2Δ1, ade8, YEL069C::URA3, sgs1ΔC700.MYC.HIS3</i> |
| KHSY2978 | <i>MATa ura3-52, leu2Δ1, trp1Δ63, his3Δ200, lys2ΔBgl, hom3-10, ade2Δ1, ade8, YEL069C::URA3, sgs1ΔC800.MYC.HIS3</i> |
| KHSY2979 | <i>MATa ura3-52, leu2Δ1, trp1Δ63, his3Δ200, lys2ΔBgl, hom3-10, ade2Δ1, ade8, YEL069C::URA3, sgs1ΔC1428.MYC.HIS3</i> |
| KHSY3181 | <i>ura3-52/ura3-52, leu2Δ1/ leu2Δ1, trp1Δ63/trp1Δ63, his3Δ200/his3Δ200, lys2ΔBgl/ lys2ΔBgl, hom3-10/ hom3-10, ade2Δ1/ade2Δ1, ade8/ade8, YEL069C::URA3/YEL069C::URA3, SGS1/sgs1ΔC1100.MYC.HIS3</i> |
| KHSY3218 | <i>MATa ura3-52, leu2Δ1, trp1Δ63, his3Δ200, lys2ΔBgl, hom3-10, ade2Δ1, ade8, YEL069C::URA3, TRP1.PGAL1.SGS1</i> |
| KHSY3332 | <i>MATa ura3-52, leu2Δ1, trp1Δ63, his3Δ200, lys2ΔBgl, hom3-10, ade2Δ1, ade8, YEL069C::URA3, sgs1::BLM.HIS3</i> |
| KHSY3346 | <i>MATa ura3-52, leu2Δ1, trp1Δ63, his3Δ200, lys2ΔBgl, hom3-10, ade2Δ1, ade8, YEL069C::ura3::TRP1, BLM.MYC.kanMX6.HIS3</i> |
| KHSY3350 | <i>MATa ura3-52, leu2Δ1, trp1Δ63, his3Δ200, lys2ΔBgl, hom3-10, ade2Δ1, ade8, YEL069C::URA3, kanMX6.PGAL1.BLM.HIS3</i> |
| KHSY3353 | <i>MATa ura3-52, leu2Δ1, trp1Δ63, his3Δ200, lys2ΔBgl, hom3-10, ade2Δ1, ade8, YEL069C::URA3, kanMX6.PGAL1.BLM.HIS3</i> |

TABLE 2.S1 (continued)

| | |
|----------|--|
| KHSY3355 | <i>MATa ura3-52, leu2Δ1, trp1Δ63, his3Δ200, lys2ΔBgl, hom3-10, ade2Δ1, ade8, YEL069C::URA3, sgs1ΔC800-blmΔN647.HIS3</i> |
| KHSY3363 | <i>MATa ura3-52, leu2Δ1, trp1Δ63, his3Δ200, lys2ΔBgl, hom3-10, ade2Δ1, ade8, YEL069C::URA3, sgs1ΔC800-blmΔN647.HIS3, Δmec3::kanMX6</i> |
| KHSY3372 | <i>ura3-52/ura3-52, leu2Δ1/ leu2Δ1, trp1Δ63/trp1Δ63, his3Δ200/his3Δ200, lys2ΔBgl/ lys2ΔBgl, hom3-10/ hom3-10, ade2Δ1/ade2Δ1, ade8/ade8, YEL069C::URA3/YEL069C::URA3, sgs1::BLM.HIS3/sgs1::BLM.HIS3</i> |
| KHSY3409 | <i>ura3-52/ura3-52, leu2Δ/leu2Δ , trp1Δ63/ trp1Δ63, his3Δ200/his3Δ200, lys2ΔBgl/lys2ΔBgl, hom3-10/hom3-10, ade2Δ1/ade2Δ1, ade8/ade8, YEL069C::URA3/YEL069C::URA3, kanMX6.PGAL1.BLM.HIS3/SGS1.MYC.HIS3</i> |
| KHSY3410 | <i>ura3-52/ura3-52, leu2Δ/leu2Δ , trp1Δ63/ trp1Δ63, his3Δ200/his3Δ200, lys2ΔBgl/lys2ΔBgl, hom3-10/hom3-10, ade2Δ1/ade2Δ1, ade8/ade8, YEL069C::URA3/YEL069C::URA3, kanMX6.PGAL1.BLM.HIS3/sgs1ΔC200.MYC.HIS3</i> |
| KHSY3412 | <i>ura3-52/ura3-52, leu2Δ/leu2Δ , trp1Δ63/ trp1Δ63, his3Δ200/his3Δ200, lys2ΔBgl/lys2ΔBgl, hom3-10/hom3-10, ade2Δ1/ade2Δ1, ade8/ade8, YEL069C::URA3/YEL069C::URA3, kanMX6.PGAL1.BLM.HIS3/sgs1ΔC300.MYC.HIS3</i> |

TABLE 2.S1 (continued)

- KHSY3414 *ura3-52/ura3-52, leu2Δ/leu2Δ , trp1Δ63/ trp1Δ63, his3Δ200/his3Δ200, lys2ΔBgl/lys2ΔBgl, hom3-10/hom3-10, ade2Δ1/ade2Δ1, ade8/ade8, YEL069C::URA3/YEL069C::URA3, kanMX6.PGAL1.BLM.HIS3/sgs1ΔC400.MYC.HIS3*
- KHSY3416 *ura3-52/ura3-52, leu2Δ/leu2Δ , trp1Δ63/ trp1Δ63, his3Δ200/his3Δ200, lys2ΔBgl/lys2ΔBgl, hom3-10/hom3-10, ade2Δ1/ade2Δ1, ade8/ade8, YEL069C::URA3/YEL069C::URA3, kanMX6.PGAL1.BLM.HIS3/sgs1ΔC500.MYC.HIS3*
- KHSY3417 *ura3-52/ura3-52, leu2Δ/leu2Δ , trp1Δ63/ trp1Δ63, his3Δ200/his3Δ200, lys2ΔBgl/lys2ΔBgl, hom3-10/hom3-10, ade2Δ1/ade2Δ1, ade8/ade8, YEL069C::URA3/YEL069C::URA3, kanMX6.PGAL1.BLM.HIS3/sgs1ΔC600.MYC.HIS3*
- KHSY3419 *ura3-52/ura3-52, leu2Δ/leu2Δ , trp1Δ63/ trp1Δ63, his3Δ200/his3Δ200, lys2ΔBgl/lys2ΔBgl, hom3-10/hom3-10, ade2Δ1/ade2Δ1, ade8/ade8, YEL069C::URA3/YEL069C::URA3, kanMX6.PGAL1.BLM.HIS3/sgs1ΔC700.MYC.HIS3*
- KHSY3420 *ura3-52/ura3-52, leu2Δ/leu2Δ , trp1Δ63/ trp1Δ63, his3Δ200/his3Δ200, lys2ΔBgl/lys2ΔBgl, hom3-10/hom3-10, ade2Δ1/ade2Δ1, ade8/ade8, YEL069C::URA3/YEL069C::URA3, kanMX6.PGAL1.BLM.HIS3/sgs1ΔC800.MYC.HIS3*

TABLE 2.S1 (continued)

- KHSY3422 *ura3-52/ura3-52, leu2Δ/leu2Δ , trp1Δ63/ trp1Δ63, his3Δ200/his3Δ200, lys2ΔBgl/lys2ΔBgl, hom3-10/hom3-10, ade2Δ1/ade2Δ1, ade8/ade8, YEL069C::URA3/YEL069C::URA3, kanMX6.PGAL1.BLM.HIS3/sgs1ΔC900.MYC.HIS3*
- KHSY3423 *ura3-52/ura3-52, leu2Δ/leu2Δ , trp1Δ63/ trp1Δ63, his3Δ200/his3Δ200, lys2ΔBgl/lys2ΔBgl, hom3-10/hom3-10, ade2Δ1/ade2Δ1, ade8/ade8, YEL069C::URA3/YEL069C::URA3, kanMX6.PGAL1.BLM.HIS3/sgs1ΔC1000.MYC.HIS3*
- KHSY3424 *ura3-52/ura3-52, leu2Δ/leu2Δ , trp1Δ63/ trp1Δ63, his3Δ200/his3Δ200, lys2ΔBgl/lys2ΔBgl, hom3-10/hom3-10, ade2Δ1/ade2Δ1, ade8/ade8, YEL069C::URA3/YEL069C::URA3, kanMX6.PGAL1.BLM.HIS3/sgs1ΔC1100.MYC.HIS3*
- KHSY3425 *ura3-52/ura3-52, leu2Δ/leu2Δ , trp1Δ63/ trp1Δ63, his3Δ200/his3Δ200, lys2ΔBgl/lys2ΔBgl, hom3-10/hom3-10, ade2Δ1/ade2Δ1, ade8/ade8, YEL069C::URA3/YEL069C::URA3, kanMX6.PGAL1.BLM.HIS3/sgs1ΔC1428.MYC.HIS3*
- KHSY3426 *ura3-52/ura3-52, leu2Δ/leu2Δ , trp1Δ63/ trp1Δ63, his3Δ200/his3Δ200, lys2ΔBgl/lys2ΔBgl, hom3-10/hom3-10, ade2Δ1/ade2Δ1, ade8/ade8, YEL069C::URA3/YEL069C::URA3, kanMX6.PGAL1.BLM.HIS3/kanMX6.PGAL1.BLM.HIS3*

TABLE 2.S1 (continued)

| | |
|----------|---|
| KHSY3429 | <i>ura3-52/ura3-52, leu2Δ1/ leu2Δ1, trp1Δ63/trp1Δ63, his3Δ200/his3Δ200, lys2ΔBgl/ lys2ΔBgl, hom3-10/ hom3-10, ade2Δ1/ade2Δ1, ade8/ade8, YEL069C::URA3/YEL069C::ura3::TRP1, sgs1::kanMX6/sgs1ΔC1100.MYC.HIS3</i> |
| KHSY3470 | <i>MATa ura3-52, leu2Δ1, trp1Δ63, his3Δ200, lys2ΔBgl, hom3-10, ade2Δ1, ade8, YEL069C::URA3, sgs1ΔC220.MYC.HIS3</i> |
| KHSY3473 | <i>MATa ura3-52, leu2Δ1, trp1Δ63, his3Δ200, lys2ΔBgl, hom3-10, ade2Δ1, ade8, YEL069C::URA3, sgs1ΔC240.MYC.HIS3</i> |
| KHSY3476 | <i>MATa ura3-52, leu2Δ1, trp1Δ63, his3Δ200, lys2ΔBgl, hom3-10, ade2Δ1, ade8, YEL069C::URA3, sgs1ΔC260.MYC.HIS3</i> |
| KHSY3479 | <i>MATa ura3-52, leu2Δ1, trp1Δ63, his3Δ200, lys2ΔBgl, hom3-10, ade2Δ1, ade8, YEL069C::URA3, sgs1ΔC280.MYC.HIS3</i> |
| KHSY3500 | <i>MATa ura3-52, leu2Δ1, trp1Δ63, his3Δ200, lys2ΔBgl, hom3-10, ade2Δ1, ade8, YEL069C::URA3, sgs1ΔC900.MYC.HIS3</i> |
| KHSY3502 | <i>MATa ura3-52, leu2Δ1, trp1Δ63, his3Δ200, lys2ΔBgl, hom3-10, ade2Δ1, ade8, YEL069C::URA3, sgs1ΔC1000.MYC.HIS3</i> |
| KHSY3504 | <i>MATa ura3-52, leu2Δ1, trp1Δ63, his3Δ200, lys2ΔBgl, hom3-10, ade2Δ1, ade8, YEL069C::URA3, sgs1ΔC1100.MYC.HIS3</i> |
| KHSY3510 | <i>MATa ura3-52, leu2Δ1, trp1Δ63, his3Δ200, lys2ΔBgl, hom3-10, ade2Δ1, ade8, YEL069C::URA3, TRP1.PGAL1. SGS1.MYC.HIS3</i> |
| KHSY3512 | <i>MATa ura3-52, leu2Δ1, trp1Δ63, his3Δ200, lys2ΔBgl, hom3-10, ade2Δ1, ade8, YEL069C::URA3, sgs1-C1047F.TRP1</i> |

TABLE 2.S1 (continued)

| | |
|----------|---|
| KHSY3516 | <i>MATa ura3-52, leu2Δ1, trp1Δ63, his3Δ200, lys2ΔBgl, hom3-10, ade2Δ1, ade8, YEL069C::URA3, sgs1-F1056A.TRP1</i> |
| KHSY3517 | <i>MATa ura3-52, leu2Δ1, trp1Δ63, his3Δ200, lys2ΔBgl, hom3-10, ade2Δ1, ade8, YEL069C::URA3, sgs1-C1047F.MYC.HIS3</i> |
| KHSY3520 | <i>MATa ura3-52, leu2Δ1, trp1Δ63, his3Δ200, lys2ΔBgl, hom3-10, ade2Δ1, ade8, YEL069C::URA3, sgs1-F1056A.MYC.HIS3</i> |
| KHSY3523 | <i>MATa ura3-52, leu2Δ1, trp1Δ63, his3Δ200, lys2ΔBgl, hom3-10, ade2Δ1, ade8, YEL069C::URA3, kanMX6.PGAL1.BLM.MYC.TRP1.HIS3</i> |
| KHSY3528 | <i>ura3-52/ura3-52, leu2Δ1/ leu2Δ1, trp1Δ63/trp1Δ63, his3Δ200/his3Δ200, lys2ΔBgl/ lys2ΔBgl, hom3-10/ hom3-10, ade2Δ1/ade2Δ1, ade8/ade8, YEL069C::URA3/YEL069C::ura3::TRP1, sgs1::kanMX6/sgs1ΔC1000.MYC.HIS3</i> |
| KHSY3534 | <i>ura3-52/ura3-52, leu2Δ1/ leu2Δ1, trp1Δ63/trp1Δ63, his3Δ200/his3Δ200, lys2ΔBgl/ lys2ΔBgl, hom3-10/ hom3-10, ade2Δ1/ade2Δ1, ade8/ade8, YEL069C::URA3/YEL069C::ura3::TRP1, sgs1::kanMX6/sgs1ΔC900.MYC.HIS3</i> |
| KHSY3536 | <i>ura3-52/ura3-52, leu2Δ1/ leu2Δ1, trp1Δ63/trp1Δ63, his3Δ200/his3Δ200, lys2ΔBgl/ lys2ΔBgl, hom3-10/ hom3-10, ade2Δ1/ade2Δ1, ade8/ade8, YEL069C::URA3/YEL069C::URA3, SGS1/sgs1ΔC1000.MYC.HIS3</i> |
| KHSY3539 | <i>ura3-52/ura3-52, leu2Δ1/ leu2Δ1, trp1Δ63/trp1Δ63, his3Δ200/his3Δ200, lys2ΔBgl/ lys2ΔBgl, hom3-10/ hom3-10, ade2Δ1/ade2Δ1, ade8/ade8, YEL069C::URA3/YEL069C::URA3, SGS1/sgs1ΔC900.MYC.HIS3</i> |

TABLE 2.S1 (continued)

KHSY3543 *MATa ura3-52, leu2Δ1, trp1Δ63, his3Δ200, lys2ΔBgl, hom3-10, ade2Δ1, ade8. YEL069C::URA3, sgs1ΔC800-blmΔN647.MYC.TRP1*

REFERENCES

- Bachrati, C. Z. and I. D. Hickson (2003). "RecQ helicases: suppressors of tumorigenesis and premature aging." Biochem J **374**(Pt 3): 577-606.
- Bachrati, C. Z. and I. D. Hickson (2008). "RecQ helicases: guardian angels of the DNA replication fork." Chromosoma **117**(3): 219-233.
- Barakat, A., M. Ababou, R. Onclercq, S. Dutertre, E. Chadli, N. Hda, A. Benslimane and M. Amor-Gueret (2000). "Identification of a novel BLM missense mutation (2706T>C) in a Moroccan patient with Bloom's syndrome." Hum Mutat **15**(6): 584-585.
- Bennett, R. J., M. F. Noiro-Gros and J. C. Wang (2000). "Interaction between yeast sgs1 helicase and DNA topoisomerase III." J Biol Chem **275**(35): 26898-26905.
- Bernstein, D. A. and J. L. Keck (2005). "Conferring substrate specificity to DNA helicases: role of the RecQ HRDC domain." Structure **13**(8): 1173-1182.
- Bernstein, K. A., E. Shor, I. Sunjevaric, M. Fumasoni, R. C. Burgess, M. Foiani, D. Brnzei and R. Rothstein (2009). "Sgs1 function in the repair of DNA replication intermediates is separable from its role in homologous recombinational repair." EMBO J **28**(7): 915-925.
- Bischof, O., S. H. Kim, J. Irving, S. Beresten, N. A. Ellis and J. Campisi (2001). "Regulation and localization of the Bloom syndrome protein in response to DNA damage." Journal of Cell Biology **153**(2): 367-380.
- Bjergbaek, L., J. A. Cobb, M. Tsai-Pflugfelder and S. M. Gasser (2005). "Mechanistically distinct roles for Sgs1p in checkpoint activation and replication fork maintenance." Embo J **24**(2): 405-417.
- Brosh, R. M., Jr., J. L. Li, M. K. Kenny, J. K. Karow, M. P. Cooper, R. P. Kureekattil, I. D. Hickson and V. A. Bohr (2000). "Replication protein A physically interacts with the Bloom's syndrome protein and stimulates its helicase activity." J Biol Chem **275**(31): 23500-23508.
- Chaganti, R. S., S. Schonberg and J. German (1974). "A manyfold increase in sister chromatid exchanges in Bloom's syndrome lymphocytes." Proc Natl Acad Sci U S A **71**(11): 4508-4512.
- Chang, M., M. Bellaoui, C. Zhang, R. Desai, P. Morozov, L. Delgado-Cruzata, R. Rothstein, G. A. Freyer, C. Boone and G. W. Brown (2005). "RMI1/NCE4, a suppressor of genome instability, encodes a member of the RecQ helicase/Topo III complex." EMBO J **24**(11): 2024-2033.
- Chenna, R., H. Sugawara, T. Koike, R. Lopez, T. J. Gibson, D. G. Higgins and J. D. Thompson (2003). "Multiple sequence alignment with the Clustal series of programs." Nucleic Acids Res **31**(13): 3497-3500.

Chiolo, I., W. Carotenuto, G. Maffioletti, J. H. Petrini, M. Foiani and G. Liberi (2005). "Srs2 and Sgs1 DNA helicases associate with Mre11 in different subcomplexes following checkpoint activation and CDK1-mediated Srs2 phosphorylation." Mol Cell Biol **25**(13): 5738-5751.

Cobb, J. A., L. Bjergbaek and S. M. Gasser (2002). "RecQ helicases: at the heart of genetic stability." FEBS Lett **529**(1): 43-48.

Davies, S. L., P. S. North, A. Dart, N. D. Lakin and I. D. Hickson (2004). "Phosphorylation of the Bloom's syndrome helicase and its role in recovery from S-phase arrest." Molecular and Cellular Biology **24**(3): 1279-1291.

Dosztanyi, Z., V. Csizmok, P. Tompa and I. Simon (2005). "IUPred: web server for the prediction of intrinsically unstructured regions of proteins based on estimated energy content." Bioinformatics **21**(16): 3433-3434.

Dosztanyi, Z., V. Csizmok, P. Tompa and I. Simon (2005). "The pairwise energy content estimated from amino acid composition discriminates between folded and intrinsically unstructured proteins." J Mol Biol **347**(4): 827-839.

Duno, M., B. Thomsen, O. Westergaard, L. Krejci and C. Bendixen (2000). "Genetic analysis of the *Saccharomyces cerevisiae* Sgs1 helicase defines an essential function for the Sgs1-Top3 complex in the absence of SRS2 or TOP1." Mol Gen Genet **264**(1-2): 89-97.

Dutertre, S., M. Ababou, R. Onclercq, J. Delic, B. Chatton, C. Jaulin and M. Amor-Gueret (2000). "Cell cycle regulation of the endogenous wild type Bloom's syndrome DNA helicase." Oncogene **19**(23): 2731-2738.

Ellis, N. A., J. Groden, T. Z. Ye, J. Straughen, D. J. Lennon, S. Ciocci, M. Proytcheva and J. German (1995). "The Bloom's syndrome gene product is homologous to RecQ helicases." Cell **83**(4): 655-666.

Foiani, M., G. Liberi, S. Piatti and P. Plevani (1999). *Saccharomyces cerevisiae* as a model system to study DNA replication. Eukaryotic DNA Replication. A Practical Approach. S. Cotterill. Oxford, UK, Oxford University Press: 185-200.

Foucault, F., C. Vaury, A. Barakat, D. Thibout, P. Planchon, C. Jaulin, F. Praz and M. Amor-Gueret (1997). "Characterization of a new BLM mutation associated with a topoisomerase II alpha defect in a patient with Bloom's syndrome." Hum Mol Genet **6**(9): 1427-1434.

Frei, C. and S. M. Gasser (2000). "The yeast Sgs1p helicase acts upstream of Rad53p in the DNA replication checkpoint and colocalizes with Rad53p in S-phase-specific foci." Genes Dev **14**(1): 81-96.

Fricke, W. M. and S. J. Brill (2003). "Slx1-Slx4 is a second structure-specific endonuclease functionally redundant with Sgs1-Top3." Genes Dev **17**(14): 1768-1778.

Fricke, W. M., V. Kaliraman and S. J. Brill (2001). "Mapping the DNA topoisomerase III binding domain of the Sgs1 DNA helicase." *J Biol Chem* **276**(12): 8848-8855.

Gangloff, S., J. P. McDonald, C. Bendixen, L. Arthur and R. Rothstein (1994). "The yeast type I topoisomerase Top3 interacts with Sgs1, a DNA helicase homolog: a potential eukaryotic reverse gyrase." *Mol Cell Biol* **14**(12): 8391-8398.

Garcia-Rubio, M., S. Chavez, P. Huertas, C. Tous, S. Jimeno, R. Luna and A. Aguilera (2008). "Different physiological relevance of yeast THO/TREX subunits in gene expression and genome integrity." *Mol Genet Genomics* **279**(2): 123-132.

German, J., M. M. Sanz, S. Ciocci, T. Z. Ye and N. A. Ellis (2007). "Syndrome-causing mutations of the BLM gene in persons in the Bloom's Syndrome Registry." *Hum Mutat* **28**(8): 743-753.

Gietz, R. D. and R. A. Woods (2006). "Yeast transformation by the LiAc/SS Carrier DNA/PEG method." *Methods Mol Biol* **313**: 107-120.

Guo, R. B., P. Rigolet, L. Zargarian, S. Femandjian and X. G. Xi (2005). "Structural and functional characterizations reveal the importance of a zinc binding domain in Bloom's syndrome helicase." *Nucleic Acids Res* **33**(10): 3109-3124.

Hanada, K. and I. D. Hickson (2007). "Molecular genetics of RecQ helicase disorders." *Cell Mol Life Sci* **64**(17): 2306-2322.

Hand, R. and J. German (1975). "A retarded rate of DNA chain growth in Bloom's syndrome." *Proc Natl Acad Sci U S A* **72**(2): 758-762.

Hegde, S. P., M. H. Qin, X. H. Li, M. A. Atkinson, A. J. Clark, M. Rajagopalan and M. V. Madiraju (1996). "Interactions of RecF protein with RecO, RecR, and single-stranded DNA binding proteins reveal roles for the RecF-RecO-RecR complex in DNA repair and recombination." *Proc Natl Acad Sci U S A* **93**(25): 14468-14473.

Heo, S. J., K. Tatebayashi, I. Ohsugi, A. Shimamoto, Y. Furuichi and H. Ikeda (1999). "Bloom's syndrome gene suppresses premature ageing caused by Sgs1 deficiency in yeast." *Genes Cells* **4**(11): 619-625.

Hojo, E. T., P. C. van Diemen, F. Darroudi and A. T. Natarajan (1995). "Spontaneous chromosomal aberrations in Fanconi anaemia, ataxia telangiectasia fibroblast and Bloom's syndrome lymphoblastoid cell lines as detected by conventional cytogenetic analysis and fluorescence in situ hybridisation (FISH) technique." *Mutat Res* **334**(1): 59-69.

Huber, M. D., M. L. Duquette, J. C. Shiels and N. Maizels (2006). "A conserved G4 DNA binding domain in RecQ family helicases." *J Mol Biol* **358**(4): 1071-1080.

Ira, G., A. Malkova, G. Liberi, M. Foiani and J. E. Haber (2003). "Srs2 and Sgs1-Top3 suppress crossovers during double-strand break repair in yeast." *Cell* **115**(4): 401-411.

Ivancic-Bace, I., E. Salaj-Smic and K. Brcic-Kostic (2005). "Effects of recJ, recQ, and recFOR mutations on recombination in nuclease-deficient recB recD double mutants of *Escherichia coli*." J Bacteriol **187**(4): 1350-1356.

Janscak, P., P. L. Garcia, F. Hamburger, Y. Makuta, K. Shiraishi, Y. Imai, H. Ikeda and T. A. Bickle (2003). "Characterization and mutational analysis of the RecQ core of the bloom syndrome protein." J Mol Biol **330**(1): 29-42.

Jiao, R. J., C. Z. Bachrati, G. Pedrazzi, P. Kuster, M. Petkovic, J. L. Li, D. Egli, I. D. Hickson and I. Stajlar (2004). "Physical and functional interaction between the Bloom's syndrome gene product and the largest subunit of chromatin assembly factor 1." Molecular and Cellular Biology **24**(11): 4710-4719.

Johnson, F. B., D. B. Lombard, N. F. Neff, M. A. Mastrangelo, W. Dewolf, N. A. Ellis, R. A. Marciniak, Y. Yin, R. Jaenisch and L. Guarente (2000). "Association of the Bloom syndrome protein with topoisomerase IIIalpha in somatic and meiotic cells." Cancer Res **60**(5): 1162-1167.

Killoran, M. P. and J. L. Keck (2008). "Structure and function of the regulatory C-terminal HRDC domain from *Deinococcus radiodurans* RecQ." Nucleic Acids Res **36**(9): 3139-3149.

Kitano, K., S. Y. Kim and T. Hakoshima (2010). "Structural basis for DNA strand separation by the unconventional winged-helix domain of RecQ helicase WRN." Structure **18**(2): 177-187.

Kitano, K., N. Yoshihara and T. Hakoshima (2007). "Crystal structure of the HRDC domain of human Werner syndrome protein, WRN." J Biol Chem **282**(4): 2717-2728.

Kitao, S., I. Ohsugi, K. Ichikawa, M. Goto, Y. Furuichi and A. Shimamoto (1998). "Cloning of two new human helicase genes of the RecQ family: biological significance of multiple species in higher eukaryotes." Genomics **54**(3): 443-452.

Kitao, S., A. Shimamoto, M. Goto, R. W. Miller, W. A. Smithson, N. M. Lindor and Y. Furuichi (1999). "Mutations in RECQL4 cause a subset of cases of Rothmund-Thomson syndrome." Nat Genet **22**(1): 82-84.

Langland, G., J. Kordich, J. Creaney, K. H. Goss, K. Lillard-Wetherell, K. Bebenek, T. A. Kunkel and J. Groden (2001). "The Bloom's syndrome protein (BLM) interacts with MLH1 but is not required for DNA mismatch repair." J Biol Chem **276**(32): 30031-30035.

Lee, J. W., R. Kusumoto, K. M. Doherty, G. X. Lin, W. Zeng, W. H. Cheng, C. von Kobbe, R. M. Brosh, Jr., J. S. Hu and V. A. Bohr (2005). "Modulation of Werner syndrome protein function by a single mutation in the conserved RecQ domain." J Biol Chem **280**(47): 39627-39636.

Lee, S. K., R. E. Johnson, S. L. Yu, L. Prakash and S. Prakash (1999). "Requirement of yeast SGS1 and SRS2 genes for replication and transcription." Science **286**(5448): 2339-2342.

Liu, Z., M. J. Macias, M. J. Bottomley, G. Stier, J. P. Linge, M. Nilges, P. Bork and M. Sattler (1999). "The three-dimensional structure of the HRDC domain and implications for the Werner and Bloom syndrome proteins." Structure **7**(12): 1557-1566.

Longtine, M. S., A. McKenzie, 3rd, D. J. Demarini, N. G. Shah, A. Wach, A. Brachat, P. Philippsen and J. R. Pringle (1998). "Additional modules for versatile and economical PCR-based gene deletion and modification in *Saccharomyces cerevisiae*." Yeast **14**(10): 953-961.

Lonn, U., S. Lonn, U. Nylen, G. Winblad and J. German (1990). "An abnormal profile of DNA replication intermediates in Bloom's syndrome." Cancer Res **50**(11): 3141-3145.

Miyajima, A., M. Seki, F. Onoda, M. Shiratori, N. Odagiri, K. Ohta, Y. Kikuchi, Y. Ohno and T. Enomoto (2000). "Sgs1 helicase activity is required for mitotic but apparently not for meiotic functions." Mol Cell Biol **20**(17): 6399-6409.

Miyajima, A., M. Seki, F. Onoda, A. Ui, Y. Satoh, Y. Ohno and T. Enomoto (2000). "Different domains of Sgs1 are required for mitotic and meiotic functions." Genes Genet Syst **75**(6): 319-326.

Mohaghegh, P., J. K. Karow, R. M. Brosh Jr, Jr., V. A. Bohr and I. D. Hickson (2001). "The Bloom's and Werner's syndrome proteins are DNA structure-specific helicases." Nucleic Acids Res **29**(13): 2843-2849.

Morimatsu, K. and S. C. Kowalczykowski (2003). "RecFOR proteins load RecA protein onto gapped DNA to accelerate DNA strand exchange: a universal step of recombinational repair." Mol Cell **11**(5): 1337-1347.

Morozov, V., A. R. Mushegian, E. V. Koonin and P. Bork (1997). "A putative nucleic acid-binding domain in Bloom's and Werner's syndrome helicases." Trends Biochem Sci **22**(11): 417-418.

Mullen, J. R., V. Kaliraman and S. J. Brill (2000). "Bipartite structure of the SGS1 DNA helicase in *Saccharomyces cerevisiae*." Genetics **154**(3): 1101-1114.

Myung, K., A. Datta, C. Chen and R. D. Kolodner (2001). "SGS1, the *Saccharomyces cerevisiae* homologue of BLM and WRN, suppresses genome instability and homeologous recombination." Nat Genet **27**(1): 113-116.

Nair, K. R. (1940). "Table of confidence intervals for the median in samples from any continuous population." Sankhya(4): 551-558.

- Ooi, S. L., D. D. Shoemaker and J. D. Boeke (2003). "DNA helicase gene interaction network defined using synthetic lethality analyzed by microarray." Nat Genet **35**(3): 277-286.
- Peng, K., S. Vucetic, P. Radivojac, C. J. Brown, A. K. Dunker and Z. Obradovic (2005). "Optimizing long intrinsic disorder predictors with protein evolutionary information." J Bioinform Comput Biol **3**(1): 35-60.
- Ralf, C., I. D. Hickson and L. Wu (2006). "The Bloom's syndrome helicase can promote the regression of a model replication fork." J Biol Chem **281**(32): 22839-22846.
- Rockmill, B., E. J. Lambie and G. S. Roeder (1991). "Spore enrichment." Methods Enzymol **194**: 146-149.
- Saffi, J., H. Feldmann, E. L. Winnacker and J. A. Henriques (2001). "Interaction of the yeast Pso5/Rad16 and Sgs1 proteins: influences on DNA repair and aging." Mutat Res **486**(3): 195-206.
- Sanz, M. M., M. Proytcheva, N. A. Ellis, W. K. Holloman and J. German (2000). "BLM, the Bloom's syndrome protein, varies during the cell cycle in its amount, distribution, and co-localization with other nuclear proteins." Cytogenetics and Cell Genetics **91**(1-4): 217-223.
- Schmidt, K. H. and R. D. Kolodner (2004). "Requirement of Rrm3 helicase for repair of spontaneous DNA lesions in cells lacking Srs2 or Sgs1 helicase." Mol Cell Biol **24**(8): 3213-3226.
- Schmidt, K. H., V. Pennaneach, C. D. Putnam and R. D. Kolodner (2006). "Analysis of gross-chromosomal rearrangements in *Saccharomyces cerevisiae*." Methods Enzymol **409**: 462-476.
- Schmidt, K. H., J. Wu and R. D. Kolodner (2006). "Control of translocations between highly diverged genes by Sgs1, the *Saccharomyces cerevisiae* homolog of the Bloom's syndrome protein." Mol Cell Biol **26**(14): 5406-5420.
- Selak, N., C. Z. Bachrati, I. Shevelev, T. Dietschy, B. van Loon, A. Jacob, U. Hubscher, J. D. Hoheisel, I. D. Hickson and I. Stagljar (2008). "The Bloom's syndrome helicase (BLM) interacts physically and functionally with p12, the smallest subunit of human DNA polymerase delta." Nucleic Acids Res **36**(16): 5166-5179.
- Sharma, S., J. A. Sommers, L. Wu, V. A. Bohr, I. D. Hickson and R. M. Brosh, Jr. (2004). "Stimulation of flap endonuclease-1 by the Bloom's syndrome protein." J Biol Chem **279**(11): 9847-9856.
- Sinclair, D. A., K. Mills and L. Guarente (1997). "Accelerated aging and nucleolar fragmentation in yeast *sgs1* mutants." Science **277**(5330): 1313-1316.

- Torres, J. Z., S. L. Schnakenberg and V. A. Zakian (2004). "Saccharomyces cerevisiae Rrm3p DNA helicase promotes genome integrity by preventing replication fork stalling: viability of rrm3 cells requires the intra-S-phase checkpoint and fork restart activities." Mol Cell Biol **24**(8): 3198-3212.
- Ui, A., Y. Satoh, F. Onoda, A. Miyajima, M. Seki and T. Enomoto (2001). "The N-terminal region of Sgs1, which interacts with Top3, is required for complementation of MMS sensitivity and suppression of hyper-recombination in sgs1 disruptants." Mol Genet Genomics **265**(5): 837-850.
- Versini, G., I. Comet, M. Wu, L. Hoopes, E. Schwob and P. Pasero (2003). "The yeast Sgs1 helicase is differentially required for genomic and ribosomal DNA replication." EMBO J **22**(8): 1939-1949.
- von Kobbe, C., N. H. Thoma, B. K. Czyzewski, N. P. Pavletich and V. A. Bohr (2003). "Werner syndrome protein contains three structure-specific DNA binding domains." J Biol Chem **278**(52): 52997-53006.
- Ward, J. J., J. S. Sodhi, L. J. McGuffin, B. F. Buxton and D. T. Jones (2004). "Prediction and functional analysis of native disorder in proteins from the three kingdoms of life." J Mol Biol **337**(3): 635-645.
- Watt, P. M., E. J. Louis, R. H. Borts and I. D. Hickson (1995). "Sgs1: a eukaryotic homolog of E. coli RecQ that interacts with topoisomerase II in vivo and is required for faithful chromosome segregation." Cell **81**(2): 253-260.
- Wu, L., C. Z. Bachrati, J. Ou, C. Xu, J. Yin, M. Chang, W. Wang, L. Li, G. W. Brown and I. D. Hickson (2006). "BLAP75/RMI1 promotes the BLM-dependent dissolution of homologous recombination intermediates." Proc Natl Acad Sci U S A **103**(11): 4068-4073.
- Wu, L., K. L. Chan, C. Ralf, D. A. Bernstein, P. L. Garcia, V. A. Bohr, A. Vindigni, P. Janscak, J. L. Keck and I. D. Hickson (2005). "The HRDC domain of BLM is required for the dissolution of double Holliday junctions." Embo J **24**(14): 2679-2687.
- Wu, L., S. L. Davies, N. C. Levitt and I. D. Hickson (2001). "Potential role for the BLM helicase in recombinational repair via a conserved interaction with RAD51." J Biol Chem **276**(22): 19375-19381.
- Wu, L. and I. D. Hickson (2006). "DNA helicases required for homologous recombination and repair of damaged replication forks." Annu Rev Genet **40**: 279-306.
- Yamagata, K., J. Kato, A. Shimamoto, M. Goto, Y. Furuichi and H. Ikeda (1998). "Bloom's and Werner's syndrome genes suppress hyperrecombination in yeast sgs1 mutant: implication for genomic instability in human diseases." Proc Natl Acad Sci U S A **95**(15): 8733-8738.

Yankiwski, V., R. A. Marciniak, L. Guarente and N. F. Neff (2000). "Nuclear structure in normal and Bloom syndrome cells." Proceedings of the National Academy of Sciences of the United States of America **97**(10): 5214-5219.

Yu, C. E., J. Oshima, Y. H. Fu, E. M. Wijsman, F. Hisama, R. Alisch, S. Matthews, J. Nakura, T. Miki, S. Ouais, G. M. Martin, J. Mulligan and G. D. Schellenberg (1996). "Positional cloning of the Werner's syndrome gene." Science **272**(5259): 258-262.

CHAPTER THREE:

GENETIC CHARACTERIZATION OF *RECQL5* IN *SACCHAROMYCES CEREVISIAE* AND IDENTIFICATION OF BINDING PARTNERS USING A YEAST TWO-HYBRID SCREEN

Note to reader: Unpublished data. Experiments were designed by Kristina H. Schmidt and Salahuddin Syed. Experiments were performed by Salahuddin Syed.

INTRODUCTION

RecQL5 is a RecQ like helicase found in humans, but has no known attributed genetic disease. It contains 19 exons and encodes three isoforms, RecQL5 α , RecQL5 β and RecQL5 γ [1]. In human tissues RecQL5 isoforms are expressed with high abundance in the testes [1]. Of the three isoforms RecQL5 α and RecQL5 γ are found in the cytoplasm whereas RecQL5 β is found in the nucleus [2]. RecQL5 α and RecQL5 γ lack a substantial amount of homology to the other RecQ homologs (Figure 1). Although all the isoforms of RecQL5 have a conserved helicase domain, only RecQL5 β contains ATPase activity [3, 4]. This activity is insufficient to unwind D-loops, G-quadruplexes, and Holliday junctions [3, 4]. However, in the presence of ssDNA binding protein and RPA, RecQL5 β can unwind forked duplexes [5]. The inability to efficiently unwind DNA may be due to the fact that RecQL5 β does not have a winged-helix motif, which is present in RecQL1 and WRN and has been shown to be important for DNA unwinding [6, 7]. We used RecQL5 β in this study because it is the only isoform that has been

observed to possess enzymatic activity and is abundantly found in humans and mice [8].

RecQL5 has several protein-protein interactions involved in DNA repair, such as Rad51, PCNA, Topo3 α , Topo3 β , the MRN complex, and Pol II [2, 9-14]. RecQL5 is found at DSBs, but for a shorter time compared to BLM and WRN, suggesting that the biochemical properties of RecQL5 are important for its activity [15]. In the presence of HU or UV light, Mre11 recruits RecQL5 to the site of damage and co-localizes with the MRN complex and has been implicated in regulating the exonuclease activity of MRN during end resection [12]. RecQL5 has a KIX domain on its C terminus distal to the RQC domain, which is required for resistance to DNA damaging agents and binding to DSBs [16]. In addition to having a role at DSBs, RecQL5 has a role during HR as an anti-recombinase and inhibits the formation of D-loops by removing Rad51 from ssDNA [17]. It has also been shown that RecQL5 interacts with phosphorylated RPBI, a subunit of Pol II, which indicates elongation of transcripts, implicating RecQL5 in transcription [16].

Mouse embryonic fibroblast cell lines deficient for RecQL5 show increased sister chromatid exchanges (SCEs), elevated number of broken chromosomes, and quadriradials [9]. Cells deficient for RecQL5 are sensitive to CPT and it has been suggested that this is due to an inability to restart stalled forks [18]. Although defects in RecQL5 have not been associated with a known human disease, mice lacking RecQL5 have a higher incidence of cancer, including lymphomas and lung adenocarcinoma [19]. To further characterize the function of RecQL5, human RecQL5 cDNA was expressed using the *SGS1* promoter and overexpressed to assess its ability to complement *sgs1* Δ

defects. Additionally, we performed a yeast two-hybrid screen using the human testis library to identify pathways, in DNA repair, which RecQL5 functions in, thus shedding light on its cellular role.

MATERIALS AND METHODS

Yeast transformation and targeted gene disruption

Modifications to the yeast genome are carried through a lithium acetate mediated transformation [20]. Cells are grown overnight in liquid YPD media until they reach saturation and then diluted into 25 ml of YPD media for an initial OD of 0.2. The cells are grown to an OD of 0.8 and then centrifuged for 2 minutes at 2000 rpm, washed with dH₂O, and centrifuged once more to remove any residual YPD. They are then re-suspended in 100mM LiAc and centrifuged for 30 seconds at 14000 rpm. The cells are re-suspended in 240µl of 100mM LiAc and spread equally amongst 4 eppendorf tubes. The tubes are centrifuged for 1 minute at 14000 rpm and the following reagents are added sequentially: 50% PEG, 36µl of 1M LiAc, 75µl of DNA, and 5µl of boiled and snap-cooled salmon sperm DNA. The pellet is loosely re-suspended using a toothpick and vortexed for 1 min at high speed. The cells are then incubated at 30°C for 30 min followed by heat shocking for 15 min at 42°C. Cells are then centrifuged at 7000 rpm for 1 min and the pellet re-suspended in 100 µl of dH₂O and plated on selective media corresponding to the type of mutation that is being introduced into the cell. Cells were grown for 2-3 days at 30°C and colonies were re-streaked onto new plates and grown for another 2 days at 30°C followed by freezing at -80°C. The transformations were verified by isolating genomic DNA from positives followed by PCR confirmation.

Cloning of plasmid DNA using homologous recombination in yeast

DNA of interest is amplified by PCR using primers that share 50-nt homology upstream and downstream of the plasmid of interest and 20-nt homology to the DNA. The plasmid of interest is linearized using two different restriction enzymes to reduce re-ligation events. Transformations were performed in strain KHSY2331 (Appendix C), which is deficient for non-homologous end joining (*lig4*Δ). Lig4, DNA Ligase 4, is important for resolution of NHEJ by ligating the ends of a double strand break. The purpose of using this strain is to minimize the possibility that the plasmid of interest will re-circularize by NHEJ and to force it to use HR to integrate the amplicon into the plasmid. During the transformation 50-100 ng of linearized plasmid DNA is combined with 10-75 μl of PCR product and the experiment is carried out using the same method as that found in the “yeast transformation and targeted gene disruption” section. Cells are plated on media that selects for the plasmid of interest and plasmid DNA is extracted using the QIAprep Miniprep Kit (QIAGEN).

Colony PCR

Colony PCR is a method that allows for verification of a large quantity of *E. coli* transformants for integration of a plasmid of interest. After the plasmid is transformed into *E. coli*, the colonies are re-streaked onto agar LB plates supplemented with the appropriate antibiotic for selection and incubated overnight at 37°C. A small quantity of cells are then inoculated into 100 μl of sterile water and boiled at 100°C for 10 min in an Applied Biosystems PCR GeneAmp 9700 Thermocycler. The samples are then

centrifuged at 14000 rpm for 2 minutes and 2 μ l of the top layer is used as a template for PCR.

Fluctuation assay

GCR rates were determined using a method previously described [21]. In order to assess overexpression of RecQL5 on accumulating GCRs we modified the assay such that strains containing a *GAL1* promoter were incubated on YPD agar plates for three days and a single colony was cultured in liquid YP-Galactose (yeast extract 10 g/L, peptone 20 g/L, 2% galactose) instead of YPD. The strains were allowed to reach saturation and the cultures were spread on synthetic complete agar plates containing 5-FOA (1 g/L), canavanine (60 mg/L), and galactose instead of dextrose.

Plasmid construction

RECQL5 β cDNA was obtained from Open Biosystems in vector pCMV-SPORT6. In order to integrate *RECQL5* in *S. cerevisiae*, a selectable marker was integrated downstream of the cDNA. A *HIS3MX6* cassette, in plasmid pRS303, was used [22]. Using PCR, *HIS3MX6*, was amplified and cloned into vector pCR2.1-TOPO (Invitrogen). The PCR primers anneal upstream and downstream to the *HIS3MX6* cassette and contain a 5' *XhoI* restriction site. The *RECQL5* cDNA in pCMV-SPORT6 (pKHS265) contains an *XhoI* restriction site at the 3' end. The plasmids containing *RECQL5* and *HIS3MX6* were digested using *XhoI* and *HIS3MX6* was ligated into the pCMV-SPORT6 plasmid using DNA Ligation Kit Ver. 2.1 (Takara) per manufacturer instructions. The resulting ligated products were introduced into electro-competent *E. coli* cells and

selected for on LB agar plates (Tryptone 10 g/L, Yeast extract 5 g/L, and NaCl 5 g/L) supplemented with 100 µg/ml of Chloramphenicol (CMP). Using colony PCR *E. coli* transformants were tested for the presence of *HIS3MX6* cassette using primers 1032R and 1676F that anneal to *RECQL5* and *HIS3MX6*. Plasmid DNA from positive transformants was isolated using QIAGEN's QIAprep Spin Miniprep Kit (per manufacturers directions). The plasmid DNA was further confirmed for integration of *RECQL5* with the *HIS3MX6* cassette using restriction digestion with *HindIII* to determine the relative orientation of *RECQL5* in respect to *HIS3MX6*. Three isolates were obtained containing *RECQL5* linked to *HIS3MX6* (pKHS671, pKHS672, pKHS673).

For yeast two-hybrid, a bait plasmid (pKHS392, Appendix D) containing a *GAL4* DNA binding domain (DBD) was linearized by double restriction enzyme digestion using *PvuII* and *NotI*. Using PCR, *RECQL5* cDNA was amplified with primers 1672F and 1673R that share 50-nt homology, upstream and downstream of the bait plasmid and 20-nt homology to *RECQL5*. Transformation was carried out in KHSY2331 in order to use homologous recombination to integrate the amplicon into the plasmid. Transformants were selected for on SC-Trp and genomic DNA was isolated from these positive transformants. Genomic DNA was introduced into electrocompetent *E. coli* cells using a MicroPulse device (BioLab). Plasmid DNA was isolated and *RECQL5* was sequenced completely to ensure mutations were not introduced in-frame with the DNA binding domain and the strain was saved as pKHS525.

Yeast strain construction

To integrate *RECQL5* at the *SGS1* locus, *RECQL5.HIS3MX6* (pKHS671) was used and PCR was performed using primers 1911F and 1912R that anneal upstream of *RECQL5* and downstream of *HIS3MX6* cassette. The primers also contain 50-nucleotide homology, upstream and downstream of the *SGS1* locus. The PCR product *RECQL5.HIS3MX6* was transformed into yeast strain KHSY1633 (*sgs1::kanMX6*) using a LiAc-mediated transformation method [23]. KHSY1633 has *SGS1* replaced with *kanMX6*, which confers resistance to G418-sulfate (Alexis Biochemicals). In order to isolate *RECQL5.HIS3MX6*, transformants were picked by plating on agar lacking histidine (SC-His). To determine if *kanMX6* was replaced by *RECQL5.HIS3MX6*, PCR was performed using primers 1143F and 1680R, which are specific to *RECQL5* and a sequence upstream of the *SGS1* locus. To ensure that this process was not mutagenic *RECQL5* cDNA was amplified by PCR from colonies that had *RECQL5.HIS3MX6* integrated into KHSY1633 and the amplicon was sent out for sequencing using primers 1674F, 1675F, 1676F, 1677F, 1678F, 1679F, and 1680R. Three independent isolates (KHSY3777, KHSY3778, KHSY3779) were obtained without any mutations and were used for further characterization.

In order to verify protein expression of RecQL5 a myc-epitope tag was fused to the 3' end of *RECQL5* in the strain containing *RECQL5.HIS3MX6* (KHSY3777). A *13MYC.TRP1* cassette was amplified by PCR from plasmid *pFA6a.13MYC.TRP1* (pKHS230, Appendix D) [24]. The myc-epitope was amplified using primers 1911F and 1912R that share 50-nt homology with the 3' end of *RECQL5* and downstream of *HIS3MX6*. The PCR amplicon was transformed into the strain containing

RECQL5.HIS3MX6 (KHSY3777) using standard LiAc-mediated transformation [23]. Transformants were selected for integration of *13MYC.TRP1* on synthetic complete agar minus tryptophan (SC-Trp). Integration of the myc-epitope was verified by PCR using primers 1678F and 2455R, which anneal to the myc epitope and *RECQL5*. Positive transformants were saved as KHSY5172, KHSY5173, and KHSY5174 (Appendix C).

To overexpress RecQL5 a galactose inducible promoter was added upstream of *RECQL5*. To achieve this, *TRP1.P_{GAL1}* was amplified by PCR using plasmid *pFA6a.TRP1.P_{GAL1}* (pKHS236, Appendix D). Primers 1850F and 1851R were used to amplify the plasmid and share 50-nt homology upstream of *RECQL5* and 5' of the cDNA so that the native *SGS1* promoter can be replaced. The amplicon was transformed into a strain containing *RECQL5.HIS3MX6* (KHSY3777) using LiAc-mediated transformation [23] and positive transformants were selected for on SC-Trp agar plates. To determine if the *GAL1* promoter was integrated, PCR was performed using primers 1045F and 1680R, which anneal upstream of the *GAL1* promoter and internal to *RECQL5* in order to obtain *TRP1.P_{GAL1}.RECQL5.HIS3MX6* and three isolates (KHSY3827, KHSY3828, KHSY3829) were confirmed and saved. To verify protein expression a myc epitope tag was added to the 3' end of *RECQL5* in KHSY3827. A *13MYC.kanMX6* cassette was amplified by PCR from plasmid *pFA6a.13MYC.kanMX6* (pKHS229, Appendix D) [24]. The myc-epitope was amplified using primers 1911F and 1912R that share 50-nt homology with the 3' end of *RECQL5* and downstream of *kanMX6*. The PCR amplicon was transformed into the strain containing *TRP1.P_{GAL1}.RECQL5.HIS3MX6* (KHSY3827) using standard LiAc-mediated transformation [23]. Transformants were selected for

integration of *13MYC.kanMX6* on SC-G418 plates and integration of the myc-epitope was verified by PCR using primers 1678F and 2455R that anneal to the myc epitope and *RECQL5*. Positive transformants were saved as KHSY5175, KHSY5176, and KHSY5177 (Appendix C).

To generate a Sgs1-RecQL5 chimeric protein the entire *RECQL5* cDNA was used. *RECQL5.HIS3MX6* (KHSY3777) was amplified by PCR and the amplicon was transformed into KHSY802 at the *SGS1* locus (wildtype, Appendix C). The primers for this PCR were designed so that 50-nt would anneal to *SGS1* in order to retain its N terminal 1-647 residues and its native promoter. Positive transformants were selected for on SC-His for the presence of *RECQL5.HIS3MX6*. These isolates were tested by PCR for further confirmation that a chimeric protein was generated using primers 1257F and 1680R that anneal to the 5' end of *SGS1* and internal to *RECQL5*. Primer combinations were used to ensure that the *SGS1* N terminal sequence and *RECQL5* would be amplified and the entire ORF was sent out for sequencing to ensure that mutations were not incorporated using the following primers: 1256F, 1257F, 1258F, 1259F, 1260F, 1261F, 1262F, 1674F, 1675F, 1676F, 1677F, 1678F, 1679F, 1680R. Positive candidates were saved as KHSY5178, KHSY5179, and KHSY5180 (Appendix C). To verify protein expression of the Sgs1-RecQL5 chimeric protein a myc epitope was added to the C terminus of Sgs1-RecQL5 using plasmid *pFA6a.13MYC.TRP1* (pKHS230, Appendix D) [24]. Positive transformants were saved as KHSY5181, KHSY5182, and KHSY5183 (Appendix C).

Analyzing protein expression by western blot

An overnight culture of cells was diluted to an $OD_{600} = 0.2$ in YPD and allowed to grow to an $OD_{600} = 0.5$. Protein was extracted using the trichloroacetic acid method using $\sim 3.5 \times 10^7$ cells to confirm expression of the myc epitope tagged strains. The TCA extract was analyzed on a 10% polyacrylamide gel, transferred to PVDF membrane (Bio-Rad), and then analyzed with anti-c-myc monoclonal antibody (9E10, Covance Research Products). Myc tagged proteins were visualized by chemoluminescence (ECL Plus, GE Healthcare). To induce *RECQL5* cDNA under the control of a *GAL1* promoter media was supplemented with 2% galactose or 1% sucrose/1% galactose instead of 2% dextrose.

Yeast two-hybrid screen

This screen utilized the Clontech Matchmaker Gold Yeast Two-Hybrid System and the Clontech Mate and Plate Human Testis cDNA library. For our yeast two-hybrid screen, we used yeast strain AH109 (KHSY3130, Appendix C), which we obtained from the Clontech Matchmaker Gold Yeast Two-Hybrid System. This strain possess four different reporter genes, which allow for varying degrees of stringency (Figure 3.7). pKHS525 containing *RECQL5* was transformed into AH109 (Appendix C) using standard LiAc-mediated transformation. Protein from yeast strain AH109 containing RecQL5 was isolated by TCA extraction and verified by Western blot analysis. The membrane was incubated with anti-DBD monoclonal antibody (Santa Cruz) and three isolates were found to express RecQL5 (KHSY5184, KHSY5185, KHSY5186).

The bait strain (KHSY5184) was inoculated and cultured overnight in 100 ml of SC-Trp liquid media until it reached an optical density of 0.6. The culture was centrifuged and divided into eight aliquots and 600 ng of plasmid DNA (Clontech Mate and Plate Human Testis cDNA Library) was transformed using standard LiAc-mediated transformation and plated on SC-Leu-Trp and SC-Leu-Trp-His_{+3AT}. SC-Leu-Trp plates were incubated for 2 days at 30°C and SC-Leu-Trp-His_{+3AT} plates were incubated for 14 days at 30°C. To exclude false positives, colonies that appeared on SC-Leu-Trp-His_{+3AT} were re-streaked on new SC-Leu-Trp-His_{+3AT} plates and incubated for two days. These colonies were re-suspended in 40% glycerol and saved at -80°C for further analysis. Western blot was performed on positive candidates using anti-AD monoclonal antibody (Santa Cruz). It is important to note that the molecular weight of the activation domain is 30 kDa and for this reason candidates that are larger than 30 kDa were excluded.

For manual verification of interactions between RecQL5 and candidates identified through yeast two-hybrid, colonies that were saved for further analysis were spotted onto SC-Leu-Trp, SC-Leu-Trp-His, and SC-Leu-Trp-His_{+3AT}. Using candidates that grow on all three plates, plasmids from these positives were rescued. The rescued AD plasmids were introduced into the bait strain (KHSY5184) containing RecQL5 using standard LiAc transformation. Positives were spotted onto SC-Leu-Trp, SC-Leu-Trp-His, and SC-Leu-Trp-His_{+3AT} to determine if interaction is reproducible.

RESULTS

Expression of human RecQL5 cDNA in *S. cerevisiae* does not complement *sgs1*Δ defects

Cells lacking Sgs1 are not resistant to DNA-damaging agents hydroxyurea (HU) and methyl methanesulfonate (MMS) and have increased gross-chromosomal rearrangements (GCRs) [25, 26]. RecQ-like helicases are conserved across species and share many of the functional domains so it is possible that RecQ-like helicases from different species may be able to complement each others functions. In order to assess RecQL5's ability to suppress *sgs1*Δ defects we placed *RECQL5* cDNA in-frame with the start codon of *SGS1* in order to regulate RecQL5 expression similar to that of Sgs1. Protein expression of RecQL5 was determined through Western blot analysis from yeast strain KHSY5172 (Figure 3.3). RecQL5 was unable to suppress the sensitivity on HU and MMS seen in an *sgs1*Δ cell and was unable to suppress the accumulation of GCRs (Figure 3.4 and Table 3.2).

Next, we explored the possibility that a single copy of *RECQL5* was insufficient to suppress *sgs1*Δ defects, and overexpressed RecQL5 in a *sgs1*Δ strain (KHSY5175). In order to do this, the *SGS1* promoter was replaced with a *GAL1* promoter and overexpression of RecQL5 was verified by probing for a myc epitope tag on the C terminus of RecQL5 (Figure 3.3). Overexpression of RecQL5 was unable to suppress the sensitivity on HU and MMS, nor was it able to suppress the accumulation of GCRs (Figure 3.4 and Table 3.2).

Sgs1-RecQL5 chimera is unable to suppress defects observed in the absence of Sgs1

The N terminus of Sgs1 does not possess any catalytic activity but interacts with Top3, Top2, Srs2, and Rad16 [27-33]. *RECQL5* is unable to complement *sgs1* Δ defects and this may be because it lacks a conserved N terminal region found in other RecQ-like helicases. We have previously shown that an N-terminal fragment of Sgs1 expressed by the *sgs1* Δ *C800* allele can suppress HU sensitivity seen in a BLM overexpressing cell suggesting Sgs1 and BLM have a functional relationship [34]. The Sgs1-BLM chimeric protein was able to suppress defects seen in a *sgs1* Δ cell [34]. To test if RecQL5 can suppress defects of a *sgs1* Δ cell with addition of the N terminal region of Sgs1 (Sgs1 1-647), we fused this region to RecQL5 to produce a Sgs1-RecQL5 chimera. Protein expression of Sgs1-RecQL5 was confirmed through Western blot (Figure 3.3), probing for a myc epitope. The Sgs1-RecQL5 chimera was unable to suppress sensitivity to HU and MMS, nor was it able to suppress the accumulation of GCRs seen in an *sgs1* Δ strain (Figure 3.4 and Table 3.2).

Yeast two-hybrid screen using human testis cDNA library to determine novel RecQL5 interacting partners

There are ten known RecQL5 interacting partners to date: Fen1, Topolla, TopoIII α/β , PCNA, WRN, Rad51, Mre11, Nbs1, Rad50, RnaP II, SWI/SNF, and PARP-1 [2, 7, 10-12, 15, 17, 35-41]. These interacting partners have all been discovered through either pull down assays or proteomic analysis. To date a comprehensive screen was not performed to identify RecQL5 interacting proteins. So we set out to perform a yeast two-

hybrid screen using the human testis cDNA library since RecQL5 is abundantly expressed in the testis [1]. Using the Clontech Matchmaker Gold Yeast Two-Hybrid system we were screened approximately 1.5 million transformants. Transformants that grew on SC-His, SC-Leu, and SC-Trp indicate a interaction with RecQL5 and these isolates were frozen for further analysis. The potential positive transformants were spotted once more on selective media for further stringency and validation. From this additional test we obtained 61 positive transformants that may be potential RecQL5 interacting partners. These transformants were then set up for TCA protein extraction and Western blot was performed using an antibody against the activating domain. We decided to exclude any protein bands less than 30kDa because that is indicative of the activating domain (Figure 3.9). Through this exclusion we pursued 36 candidates that have a high likelihood of interaction with RecQL5. Lastly, we performed a manual test and spotted the transformants on selective media to confirm interaction and determined isolates 1 and 10 to express interacting proteins of RecQL5 (Figure 3.10). This test was to ensure that there is a positive interaction between the bait and prey and not a result of auto-activation by the prey plasmid. For this purpose, the prey plasmid, expressing RecQL5 interacting protein, was isolated and transformed into strain KHSY3989 (reporter strain with empty bait plasmid) and a strain expressing RecQL5 (KHSY5184), and then spotted on the following selective media: SC-Leu-Trp, SC-Leu-Trp-His, SC-Leu-Trp-His_{+3AT}. Growth on SC-Leu-Trp suggests presence of both bait and prey plasmids. Growth on SC-Leu-Trp-His plates has lower stringency for selection of protein-protein interaction and growth on SC-Leu-Trp-His_{+3AT} has the highest stringency because of the presence of 3AT (3-Amino-1,2,3-triazole), which is a competitive

inhibitor of the *HIS3* gene and is utilized to isolate strong protein-protein interactions. Of the 36 transformants that were tested only two were able to activate the reporter genes (Figure 3.10). To determine the identity of these isolates, the cDNA insert in the prey plasmid was isolated from yeast and primer F1975, that binds upstream of the cDNA insert was used to sequence the prey plasmid. The sequences were analyzed using NCBI BLAST and isolate 1 and 10 (Figure 3.10) were found to be *UBE2I* and *HLP2* respectively.

DISCUSSION

BLM and WRN, human RecQ-like helicases, have been studied in depth in a yeast system, but RecQL5 had not been investigated in a similar fashion, so this study sets out to functionally characterize RecQL5 in order to better understand its cellular function. We hypothesized that RecQL5, being a RecQ-like helicase, could suppress defects seen in an *sgs1* Δ cell. We found that cells expressing RecQL5 under control of the native *SGS1* promoter were as sensitive as an *sgs1* Δ cell on both HU and MMS, were unable to suppress this sensitivity when overexpressed, and could not suppress the accumulation of GCRs. The inability of RecQL5 to suppress the defects of an *sgs1* Δ cell may be due to the fact that RecQL5 lacks a long N terminal region found in Sgs1, which is important for protein-protein interaction with Top2, Top3, Srs2, and Rad16 [26, 27, 33, 42-44]. The absence of this N terminus may prevent Top3 from localizing to sites of damage, resulting in toxic intermediates that cannot be resolved without the combined function of the RecQ helicase and topoisomerase. It has been shown that an Sgs1-BLM chimera can suppress defects seen in an *sgs1* Δ cell because it regains the

important N terminal functions of Sgs1 so we fused the long N terminal region of Sgs1 to RecQL5 to determine if retaining these functions could suppress defects similar to a Sgs1-BLM chimera [34]. We exposed cells expressing the chimeric protein to DNA damaging agents HU and MMS and also assessed its ability to suppress accumulation of GCRs and found that the Sgs1-RecQL5 chimeric protein was unable to suppress these defects suggesting a separation of function between this helicase and BLM. The inability to complement may be because the fusion protein lacks the HRDC domain. Removing the HRDC domain in BLM has been shown to reduce its ability to unwind double Holliday junctions, and both BLM and WRN are unable to recognize damage induced by MMS and mitomycin C in the absence of the HRDC domain [45, 46]. Considering RecQL5 lacks an HRDC domain, it is possible that it is unable to respond to DNA damage because it cannot recognize these structures. Additionally, looking at protein disorder, RecQL5 is distinct from BLM because its C terminus is disordered [34]. Disordered regions have been associated with protein-protein interactions so it is possible that the C terminus of RecQL5 mediates interactions with proteins involved in DNA repair, but inability to recognize DNA substrates may be inhibitory to its function.

A useful approach to understand the cellular mechanisms in which RecQL5 functions is to identify proteins it interacts with. Through yeast two-hybrid screen of a human testis cDNA library we identified strong interaction with Hlp2 and Ube2I (Figure 3.10). Human Hlp2 is an ATP-dependent RNA helicase that is part of the DEAD box family of helicases [47, 48]. The homolog in *S. cerevisiae*, Ded1, is an essential gene, which has ATP-dependent RNA helicase activity and plays a role in translation initiation [49]. Ded1 has been shown to displace protein complexes from RNA and is capable of

RNA duplex unwinding [49]. Proteomics studies have shown that RecQL5 can associate with Pol II through its KIX domain, providing a role for RecQL5 in transcription [16]. Further evidence has indicated that in the absence of RecQL5, DSBs accumulate during replication as a result of the transcription machinery converging with the replication fork [15]. The interaction between RecQL5 and Hlp2 may suggest a role for RecQL5 apart from DNA metabolism.

Ube2I is a SUMO-conjugating enzyme that is important in regulating DNA repair, the stress response, and cell cycle progression [50-54]. In *S. cerevisiae* *UBE2I* is essential and is required for cell viability and defects in this gene result in abnormal chromosome segregation [55]. Ube2I has also been shown to interact with transcription factor AP-2 [56]. AP-2 belongs to a transcription factor family that is involved in regulating genes that have a role in differentiation including *ERBB2*, a proto-oncogene, and has functions during embryonic development [57, 58]. Ube2I has been shown to associate with this transcription factor and down-regulate its activity by protein-protein interaction and post-translational modification [56]. Since Ube2I has such diverse roles in the cell, RecQL5 may target Ube2I to damage in the cell so that it can regulate proteins involved in repair [59].

It will be important to confirm the interaction with endogenous proteins in human cells by co-immunoprecipitation. It is possible that Hlp2 and Ube2I interact with the unstructured C terminal half of RecQL5. By creating systematic deletions to the C terminus of RecQL5, we can narrow the site of interaction and may be able to identify if the KIX domain and SRI domain have a role in this interaction. Better understanding the

role of novel interacting proteins, such as Ube2I and Hlp2 with RecQL5 will give us better insight into the molecular mechanism by which RecQL5 functions.

FIGURES AND TABLES

Table 3.1. Primers used in this study

| Primer ID | Name | Sequence |
|------------------|----------------|---|
| 1031F | HIS3-5'Chk | TCGAGTGCTCTATCGCTAGGGGACC |
| 1032R | HIS3-3'Chk | AGTGCGTTCAAGGCTCTTGCGGTTG |
| 1045F | SGS1Confirm | GGTTGATATAACCAGCCAGCA |
| 1143F | SGS1-5'Chk | CTGGGTGATCATTGGTGATA |
| 1144R | SGS1-3'Chk | GCACACCACAATATGTCGTG |
| 1256F | SGS1 SEQ1 | ATGGTGACGAAGCCGTCACA |
| 1257F | SGS1 SEQ2 | GTATAGGCAAACAGCTCGAA |
| 1258F | SGS1 SEQ3 | ACTGTGACCCTCCTGTAATA |
| 1259F | SGS1 SEQ4 | GTTCCCTCAAATGGCCAAAA |
| 1260F | SGS1 SEQ5 | GAGGAAGACGATTTTGATGA |
| 1261F | SGS1 SEQ6 | GAAGTCTTTAAACTGCCTGG |
| 1262F | SGS1 SEQ7 | CTGCAAGTGAACAAGTCAGA |
| 1263F | SGS1 SEQ8 | GCAGACAATGATCCAGAAGG |
| 1264F | SGS1 SEQ9 | GCTGACTGGAAAAATGGAGA |
| 1265F | SGS1 SEQ10 | GATCAAGCGAGGATCATGAA |
| 1266F | SGS1 SEQ11 | CCGAGGTCACTACAGAGGAA |
| 1267R | SGS1 SEQ12R | TAACCATTTGTGCTCCCTTC |
| 1268R | SGS1 SEQ13R | CTTGAAGGCGGATCACCTCT |
| 1672F | POBD2 RECQL5 F | AAGATACCCACCAAACCCAAAAAAGAGATCGAATTCC AGCTGACCACCATGAGCAGCCACCATAACCAC |
| 1673R | POBD2 RECQL5 R | CTACGATTTCATAGATCTCTGCAGGTGCACGGATCCCCGG GAATTGCCATGTCATCTCTGGGGGCCACACA |
| 1674F | RECQL5 SEQ F 1 | ATGAGCAGCCACCATAACCAC |
| 1675F | RECQL5 SEQ F 2 | AGCCACCCACAGGTCCAAG |
| 1676F | RECQL5 SEQ F 3 | TCTATTACTCCAGGAATGAC |
| 1677F | RECQL5 SEQ F 4 | CCAGATGAGAACTGTCCCCT |
| 1678F | RECQL5 SEQ F 5 | GAGCCGGCCCTGTGGCCTCC |
| 1679F | RECQL5 SEQ F 6 | AGAACCAGAGAGCCAGCCT |
| 1680R | RECQL5 SEQ R 1 | AATGAGCTTCATCCACCACC |
| 1697R | RECQL5 R | TCATCTCTGGGGGCCACACA |
| 1850F | R5 F | ATTATTGTTGTATATATTTAAAAAATCATACACGTACAC ACAAGGCGGTAATGAGCAGCCACCATAACCAC |
| 1851R | R5 R | TTGGCGAATGGTGTCGTAGTTATAAGTAACACTATTTAT TTTTCTACTCTTCATCTCTGGGGGCCACACA |
| 1911F | R5 HIS3 F | TTCCCAGTCACGACGTTGTAAAACGACGGCCAGTGCCAA GCTTGCATGCCATGAGCAGCCACCATAACCAC |
| 1912R | R5 HIS3 R | CCAAGCTCTTAAAACGATAACTTCGTATAAATGTATGCTA TACGAAGTTATTCATCTCTGGGGGCCACACA |
| 1913R | R5 HIS3 KI R | TTGGCGAATGGTGTCGTAGTTATAAGTAACACTATTTAT TTTTCTACTCTATTTCGAGCTCGGTACCCGGG |

Table 3.1 (continued)

| | | |
|-------|----------|----------------------|
| 1975F | pact2ADF | ACCACTACAATGGATGATGT |
| 2454F | MycChkF | CAGAAACTGATCTCTGAAGA |
| 2455R | MycChkR | TCTTCAGAGATCAGTTTCTG |

Table 3.2. Rate of accumulating Gross Chromosomal Rearrangements (GCRs)

| Strain | GCR Rate (Can^r 5-FOA r $\times 10^{-10}$) | 95% CI (Can^r 5-FOA r $\times 10^{-10}$) |
|--|---|---|
| Wildtype | 1.1 | <1-6.2 |
| $\Delta sgs1$ | 251 | 80-310 |
| <i>RECQL5</i> | 187 | 40-200 |
| <i>Pgal.RECQL5</i> | 96 | 71-264 |
| <i>sgs1</i> Δ C800. <i>RECQL5</i> | 110 | 47-250 |

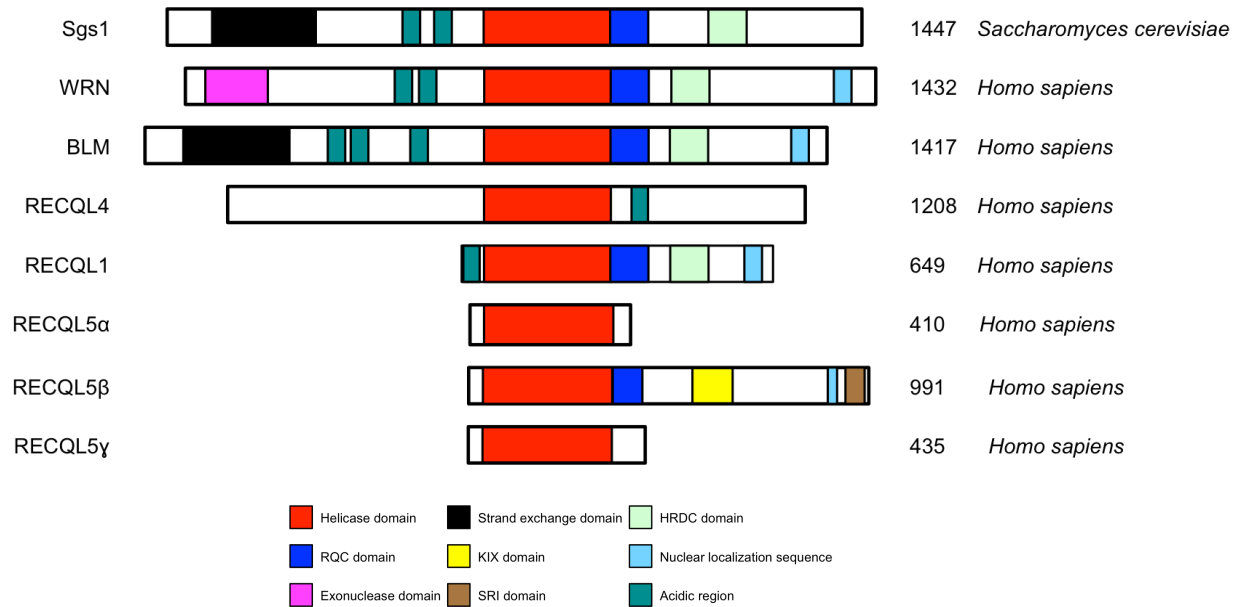


Figure 3.1. RecQ-like helicases

Domain structures of RecQ-like helicases from *Saccharomyces cerevisiae* and *Homo sapiens*. RecQL5β lacks the N terminal region present in Sgs1, WRN, BLM, and RecQL4, but still contains a conserved helicase domain and partial RQC domain. In addition to these domains RecQL5β possess a KIX domain and a SRI domain not present in any of the other RecQ-like helicases. For this study RecQL5β was used instead of RecQL5α and RecQL5γ because of its localization to the nucleus and implicated roles in DNA repair.

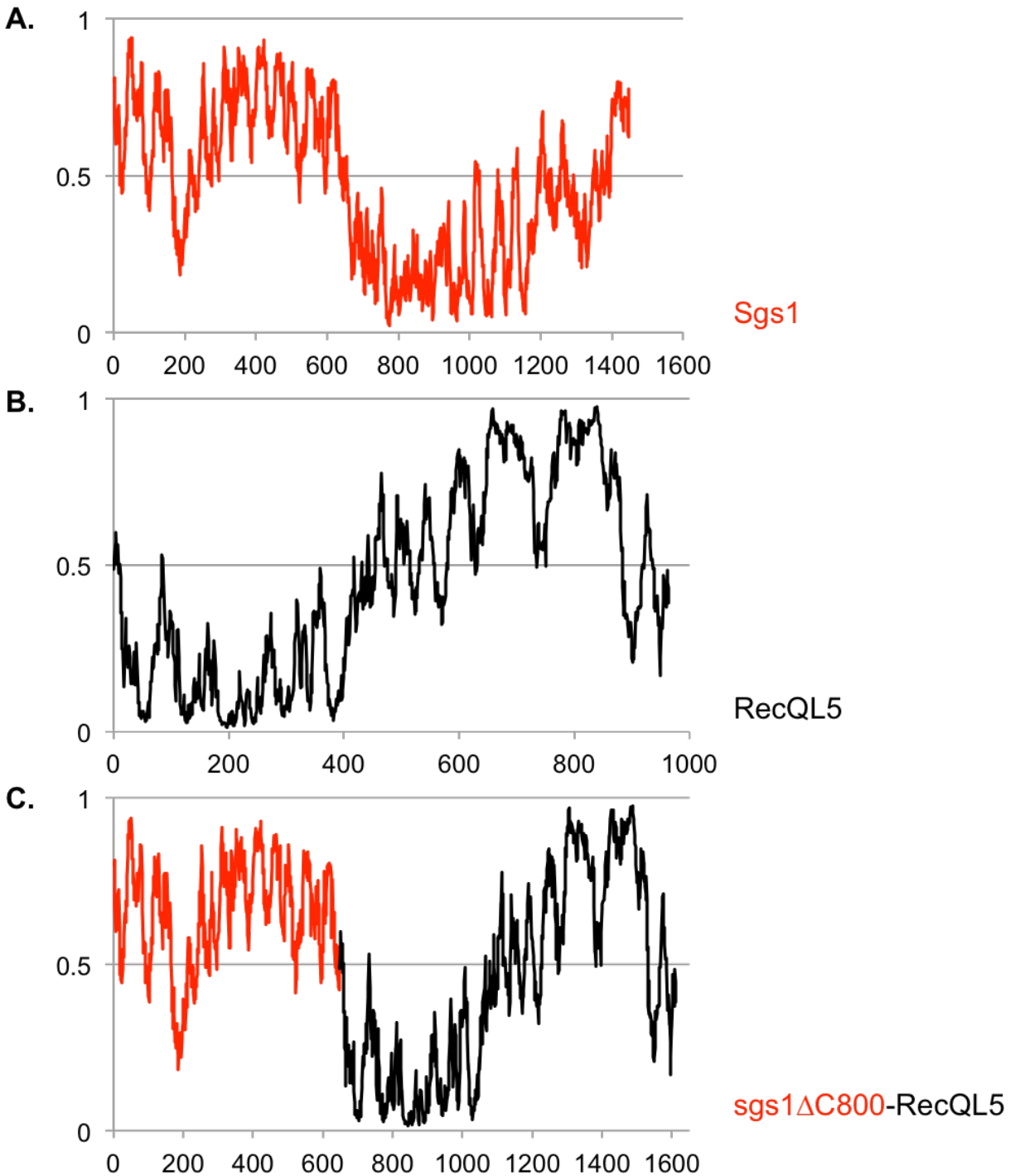


Figure 3.2. Construction of a chimeric protein containing the N terminal region of Sgs1 and full length RecQL5 β

Protein disorder was determined using IUPred algorithm. Data points above 0.5 indicate a disordered residue and data points below 0.5 indicate ordered residues. N terminal region of Sgs1, residues 1-647 were fused to RecQL5.

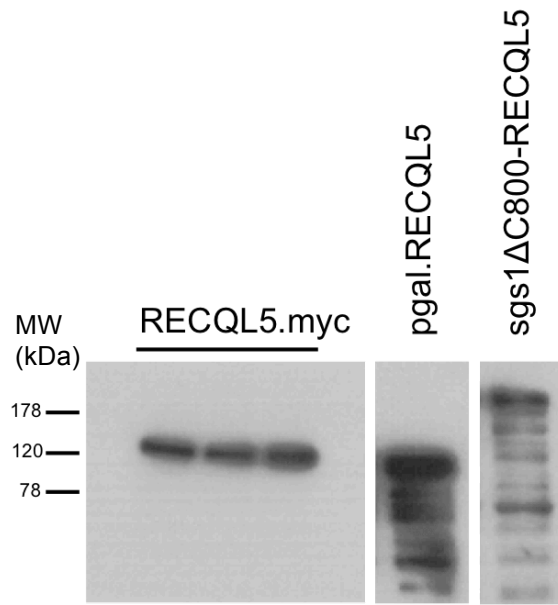


Figure 3.3. Expression of RecQL5 at the endogenous SGS1 locus

RECQL5 was integrated into a strain deficient for *SGS1* and a myc epitope tag was added to the C terminus. Protein was extracted using standard TCA extraction and run on a 10% SDS-PAGE gel and transferred to a PVDF membrane before visualization with ECL Plus (GE Healthcare). RecQL5 was probed by using anti-myc (COVANCE) antibody. In order to overexpress RecQL5, a GAL1 promoter was added to the N terminus of RecQL5 while maintaining the myc epitope tag at the C terminus and expression was verified using anti-myc antibody (COVANCE). The N terminus of *SGS1* was fused to RecQL5 and expression verified using anti-myc antibody (COVANCE).

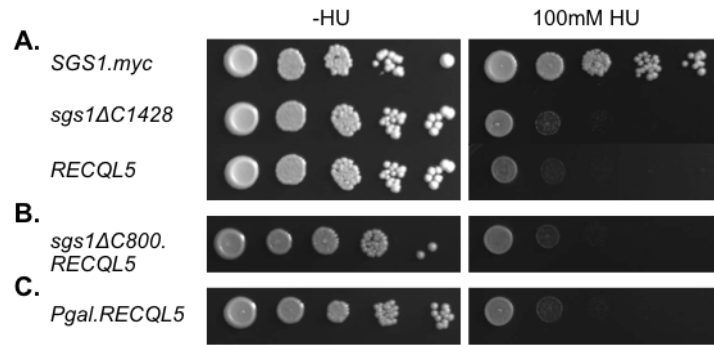


Figure 3.4. RecQL5 does not suppress the defects seen in a *sgs1Δ* strain

Exponentially growing haploid cells were spotted on YPD media in the presence and absence of DNA damaging agent hydroxyurea. Expressing RecQL5 from the native *SGS1* promoter, overexpressing, or generating a chimeric Sgs1-RecQL5 protein were as sensitive as the *sgs1Δ* strain.

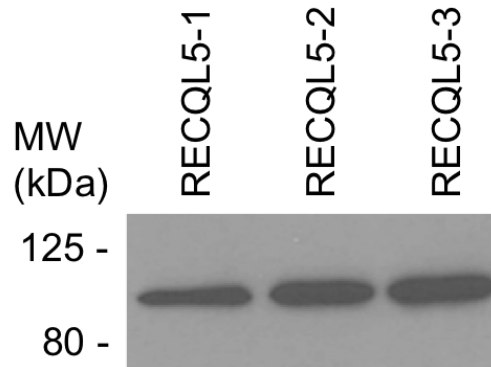


Figure 3.5. Expression of RecQL5 from bait plasmid containing a DNA binding domain

Cells were grown to an $OD_{600} = 0.5$ in SC-Trp media and protein was extracted using standard TCA extraction. Sample was loaded on a 10% SDS-PAGE gel and transferred to a PVDF membrane (Bio-Rad) then probed with anti-DBD monoclonal antibody (Santa Cruz). Protein was visualized using ECL Plus (GR Healthcare). RecQL5 β is approximately 109kDa and all three independent isolates produced similar expression and were therefore used for the yeast two-hybrid.

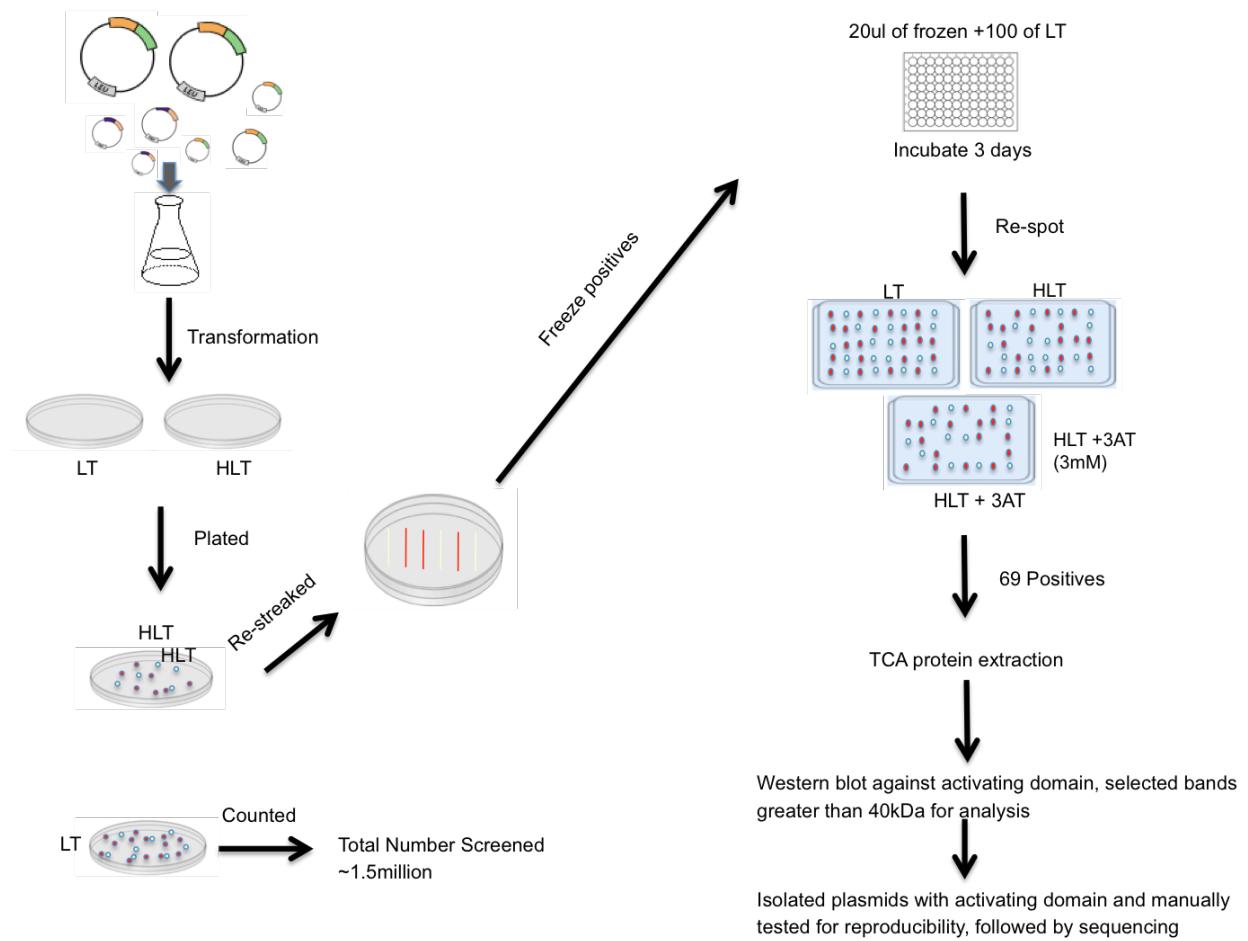


Figure 3.6. Schematic of yeast two-hybrid using a testis cDNA library to find RecQL5 interacting proteins

| | | |
|-----------------|------------------|-------------|
| <i>GAL1 UAS</i> | <i>GAL1 TATA</i> | <i>HIS3</i> |
| <i>GAL2 UAS</i> | <i>GAL2 TATA</i> | <i>ADE2</i> |
| <i>MEL1 UAS</i> | <i>MEL1 TATA</i> | <i>LacZ</i> |
| <i>MEL1 UAS</i> | <i>MEL1 TATA</i> | <i>MEL1</i> |

Figure 3.7. Strain AH109 (Clontech) with the four reporter constructs

Strain AH109 used in the Clontech Matchmaker Gold Yeast Two-Hybrid System containing the four reporter constructs. *HIS3* and *ADE2* contain *GAL1* and *GAL2* promoter elements and an upstream activating sequence. *LacZ* and *MEL1* contain a *MEL1 UAS* promoter element, which is a GAL4 response gene. The reporter genes in this strain allow for a high level of stringency to determine RecQL5 interacting proteins when using the human testis cDNA library.

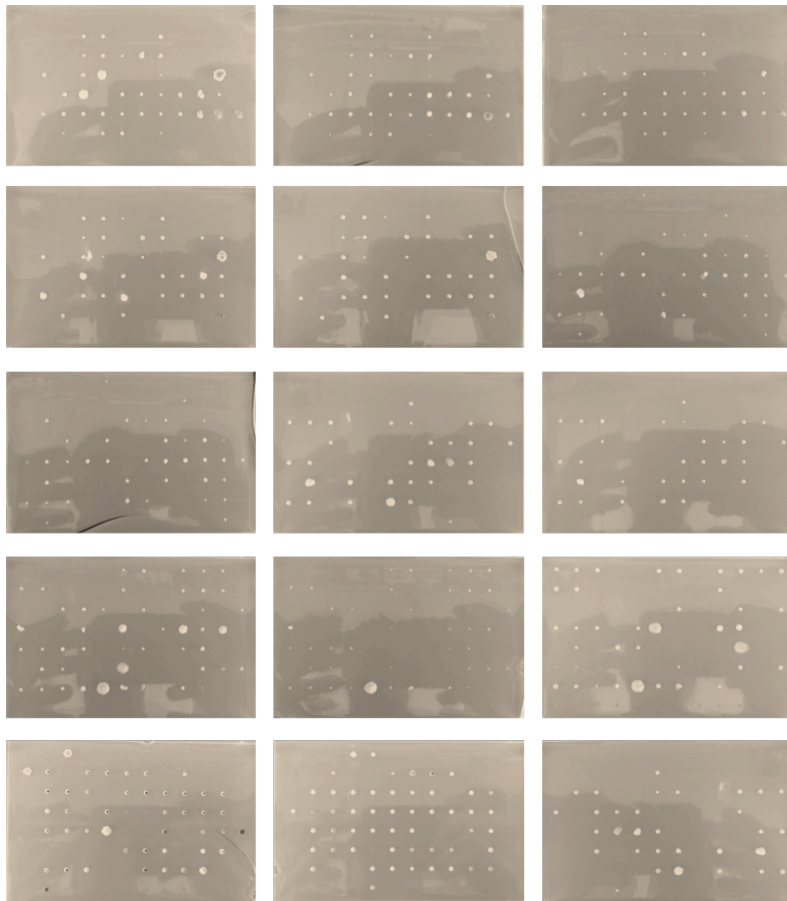


Figure 3.8. Positive candidates identified in the yeast two-hybrid system using human testis cDNA library against RecQL5

Colonies that show a noticeable growth on SC-Leu-Trp-His_{+3AT} were saved for protein extraction and further analysis.

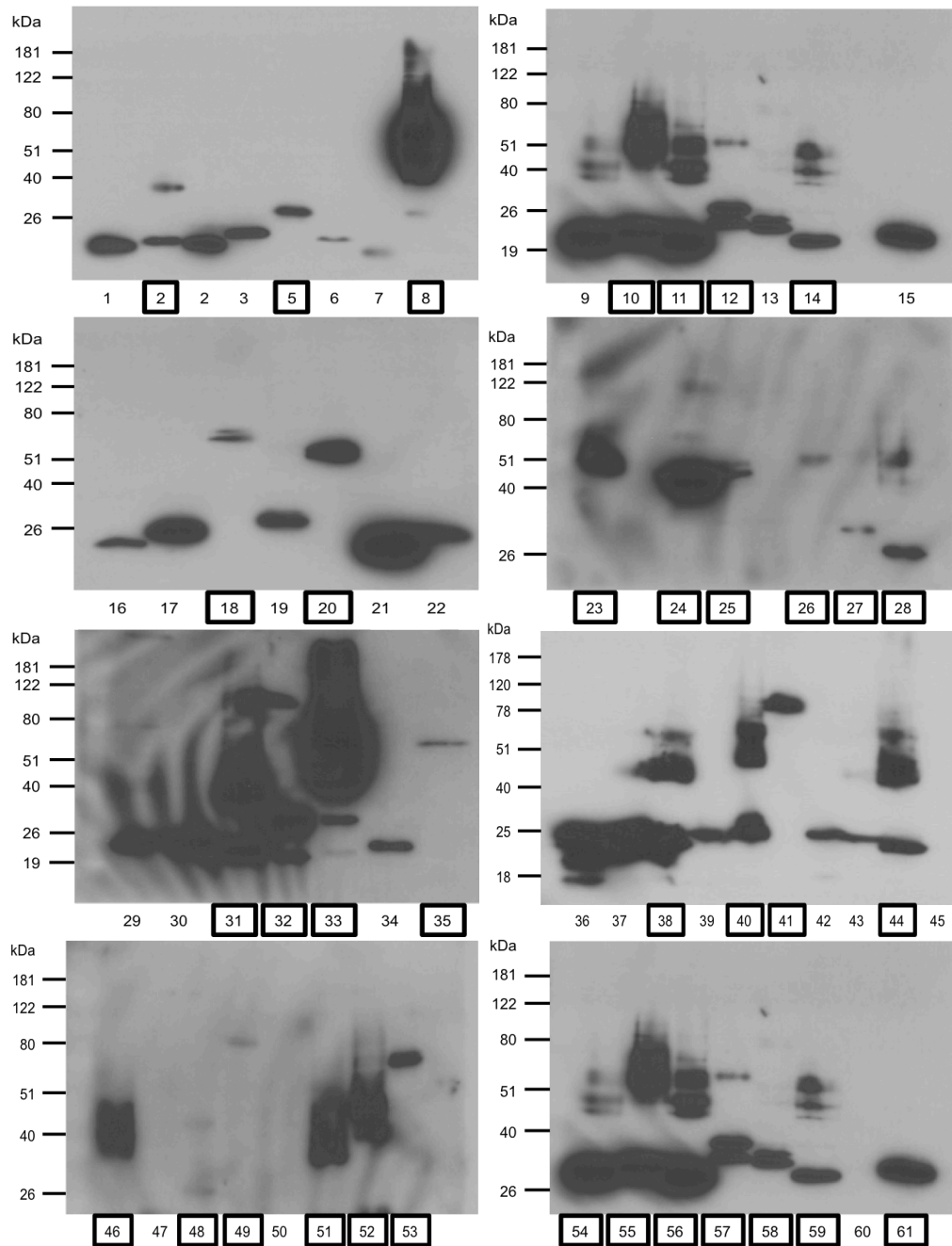


Figure 3.9. Western blot analysis of candidates identified in yeast two-hybrid using a human testis cDNA library for RecQL5 interacting proteins

Positive transformants from the yeast two-hybrid screen were grown to an $OD_{600} = 0.5$ in SC-Leu-Trp media and protein was extracted using standard TCA extraction to confirm the expression of the activating domain and cDNA ORF from the testis library. TCA extractions were run on 10% SDS-PAGE gels and transferred to a PVDF membrane (Bio-Rad) and probed with anti-AD monoclonal antibody (Santa Cruz). Protein was visualized using ECL Plus (GE Healthcare). The activating domain within the plasmid containing the cDNA is approximately 30kDa. For this study candidates that are greater than 30kDa are circled and were utilized for further analysis.

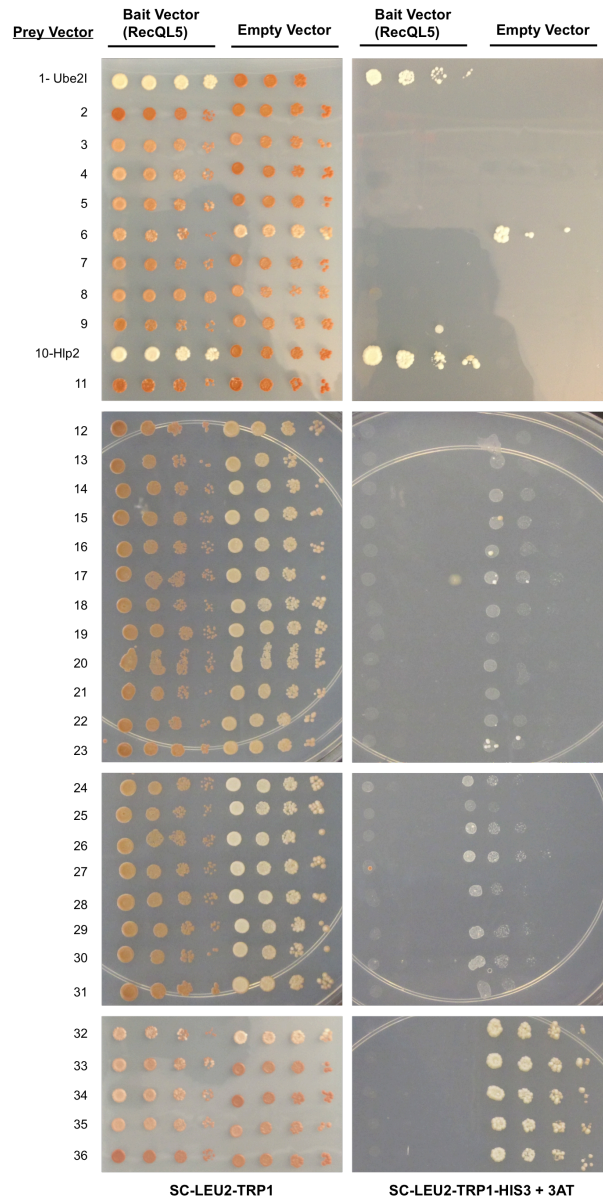


Figure 3.10. Manual verification of RecQL5 interacting proteins

Positive candidates from yeast two-hybrid were evaluated for expression using an activating antibody and candidates larger than 30kDa were used for further evaluation are shown above. Genomic DNA from candidates larger than 30kDa was isolated and transformed into *E. coli* in order to isolate the plasmid containing the cDNA. The isolated plasmid was transformed into a strain containing the bait plasmid with *RECQL5* (KHSY5184) and a strain with an empty bait vector (KHSY3989) in order to ensure that the interaction observed was not a byproduct of the prey plasmid self-activating. The candidates were spotted on SC-Leu-Trp, to select for presence of both plasmids and on SC-Leu-Trp-His_{+3AT}, to select for activation of the *HIS3* reporter gene with 3AT allowing for an extra level of stringency. The images on the left are of candidates grown on SC-Leu-Trp and the images on the right are of candidates grown on SC-Leu-Trp-His_{+3AT}. From 36 candidates tested only two reproduced as positives, Ube2l and Hlp2.

REFERENCES

1. Kitao, S., et al., *Cloning of two new human helicase genes of the RecQ family: biological significance of multiple species in higher eukaryotes*. Genomics, 1998. **54**(3): p. 443-52.
2. Shimamoto, A., et al., *Human RecQ5beta, a large isomer of RecQ5 DNA helicase, localizes in the nucleoplasm and interacts with topoisomerases 3alpha and 3beta*. Nucleic Acids Res, 2000. **28**(7): p. 1647-55.
3. Ren, H., et al., *The zinc-binding motif of human RECQ5beta suppresses the intrinsic strand-annealing activity of its DExH helicase domain and is essential for the helicase activity of the enzyme*. Biochem J, 2008. **412**(3): p. 425-33.
4. Croteau, D.L., et al., *Human RecQ helicases in DNA repair, recombination, and replication*. Annu Rev Biochem, 2014. **83**: p. 519-52.
5. Garcia, P.L., et al., *Human RECQ5beta, a protein with DNA helicase and strand-annealing activities in a single polypeptide*. EMBO J, 2004. **23**(14): p. 2882-91.
6. Pike, A.C., et al., *Structure of the human RECQ1 helicase reveals a putative strand-separation pin*. Proc Natl Acad Sci U S A, 2009. **106**(4): p. 1039-44.
7. Tadokoro, T., et al., *Human RECQL5 participates in the removal of endogenous DNA damage*. Mol Biol Cell, 2012. **23**(21): p. 4273-85.
8. Ohhata, T., et al., *Cloning, genomic structure and chromosomal localization of the gene encoding mouse DNA helicase RECQL5beta*. Gene, 2001. **280**(1-2): p. 59-66.
9. Hu, Y., et al., *RECQL5/Recql5 helicase regulates homologous recombination and suppresses tumor formation via disruption of Rad51 presynaptic filaments*. Genes Dev, 2007. **21**(23): p. 3073-84.
10. Kanagaraj, R., et al., *RECQ5 helicase associates with the C-terminal repeat domain of RNA polymerase II during productive elongation phase of transcription*. Nucleic Acids Res, 2010. **38**(22): p. 8131-40.
11. Kanagaraj, R., et al., *Human RECQ5beta helicase promotes strand exchange on synthetic DNA structures resembling a stalled replication fork*. Nucleic Acids Res, 2006. **34**(18): p. 5217-31.
12. Zheng, L., et al., *MRE11 complex links RECQ5 helicase to sites of DNA damage*. Nucleic Acids Res, 2009. **37**(8): p. 2645-57.
13. Aygun, O. and J.Q. Svejstrup, *RECQL5 helicase: connections to DNA recombination and RNA polymerase II transcription*. DNA Repair (Amst), 2010. **9**(3): p. 345-53.

14. Izumikawa, K., et al., *Association of human DNA helicase RecQ5beta with RNA polymerase II and its possible role in transcription*. *Biochem J*, 2008. **413**(3): p. 505-16.
15. Popuri, V., et al., *Recruitment and retention dynamics of RECQL5 at DNA double strand break sites*. *DNA Repair (Amst)*, 2012. **11**(7): p. 624-35.
16. Kassube, S.A., et al., *Structural mimicry in transcription regulation of human RNA polymerase II by the DNA helicase RECQL5*. *Nat Struct Mol Biol*, 2013. **20**(7): p. 892-9.
17. Schwendener, S., et al., *Physical interaction of RECQ5 helicase with RAD51 facilitates its anti-recombinase activity*. *J Biol Chem*, 2010. **285**(21): p. 15739-45.
18. Hu, Y., et al., *Recql5 plays an important role in DNA replication and cell survival after camptothecin treatment*. *Mol Biol Cell*, 2009. **20**(1): p. 114-23.
19. Hu, Y., et al., *Recql5 and Blm RecQ DNA helicases have nonredundant roles in suppressing crossovers*. *Mol Cell Biol*, 2005. **25**(9): p. 3431-42.
20. Gietz, R.D. and R.A. Woods, *Yeast transformation by the LiAc/SS Carrier DNA/PEG method*. *Methods Mol Biol*, 2006. **313**: p. 107-20.
21. Schmidt, K.H., et al., *Analysis of gross-chromosomal rearrangements in Saccharomyces cerevisiae*. *Methods Enzymol*, 2006. **409**: p. 462-76.
22. Sikorski, R.S. and P. Hieter, *A system of shuttle vectors and yeast host strains designed for efficient manipulation of DNA in Saccharomyces cerevisiae*. *Genetics*, 1989. **122**(1): p. 19-27.
23. Schiestl, R.H., S. Prakash, and L. Prakash, *The SRS2 suppressor of rad6 mutations of Saccharomyces cerevisiae acts by channeling DNA lesions into the RAD52 DNA repair pathway*. *Genetics*, 1990. **124**(4): p. 817-31.
24. Longtine, M.S., et al., *Additional modules for versatile and economical PCR-based gene deletion and modification in Saccharomyces cerevisiae*. *Yeast*, 1998. **14**(10): p. 953-61.
25. Schmidt, K.H. and R.D. Kolodner, *Suppression of spontaneous genome rearrangements in yeast DNA helicase mutants*. *Proc Natl Acad Sci U S A*, 2006. **103**(48): p. 18196-201.
26. Mullen, J.R., V. Kaliraman, and S.J. Brill, *Bipartite structure of the SGS1 DNA helicase in Saccharomyces cerevisiae*. *Genetics*, 2000. **154**(3): p. 1101-14.
27. Bennett, R.J., M.F. Noiro-Gros, and J.C. Wang, *Interaction between yeast sgs1 helicase and DNA topoisomerase III*. *J Biol Chem*, 2000. **275**(35): p. 26898-905.

28. Argueso, J.L., et al., *Systematic mutagenesis of the Saccharomyces cerevisiae MLH1 gene reveals distinct roles for Mlh1p in meiotic crossing over and in vegetative and meiotic mismatch repair*. Mol Cell Biol, 2003. **23**(3): p. 873-86.
29. Saffi, J., et al., *Interaction of the yeast Pso5/Rad16 and Sgs1 proteins: influences on DNA repair and aging*. Mutat Res, 2001. **486**(3): p. 195-206.
30. Wu, L., et al., *Potential role for the BLM helicase in recombinational repair via a conserved interaction with RAD51*. J Biol Chem, 2001. **276**(22): p. 19375-81.
31. Wang, T.F. and W.M. Kung, *Supercomplex formation between Mlh1-Mlh3 and Sgs1-Top3 heterocomplexes in meiotic yeast cells*. Biochem Biophys Res Commun, 2002. **296**(4): p. 949-53.
32. Dherin, C., et al., *Characterization of a highly conserved binding site of Mlh1 required for exonuclease I-dependent mismatch repair*. Mol Cell Biol, 2009. **29**(3): p. 907-18.
33. Chiolo, I., et al., *Srs2 and Sgs1 DNA helicases associate with Mre11 in different subcomplexes following checkpoint activation and CDK1-mediated Srs2 phosphorylation*. Mol Cell Biol, 2005. **25**(13): p. 5738-51.
34. Mirzaei, H., et al., *Sgs1 truncations induce genome rearrangements but suppress detrimental effects of BLM overexpression in Saccharomyces cerevisiae*. J Mol Biol, 2011. **405**(4): p. 877-91.
35. Speina, E., et al., *Human RECQL5beta stimulates flap endonuclease 1*. Nucleic Acids Res, 2010. **38**(9): p. 2904-16.
36. Ramamoorthy, M., et al., *RECQL5 cooperates with Topoisomerase II alpha in DNA decatenation and cell cycle progression*. Nucleic Acids Res, 2012. **40**(4): p. 1621-35.
37. Popuri, V., et al., *The Human RecQ helicases, BLM and RECQ1, display distinct DNA substrate specificities*. J Biol Chem, 2008. **283**(26): p. 17766-76.
38. Popuri, V., et al., *RECQL5 plays co-operative and complementary roles with WRN syndrome helicase*. Nucleic Acids Res, 2013. **41**(2): p. 881-99.
39. Aygun, O., J. Svejstrup, and Y. Liu, *A RECQ5-RNA polymerase II association identified by targeted proteomic analysis of human chromatin*. Proc Natl Acad Sci U S A, 2008. **105**(25): p. 8580-4.
40. Islam, M.N., et al., *RecQL5 promotes genome stabilization through two parallel mechanisms--interacting with RNA polymerase II and acting as a helicase*. Mol Cell Biol, 2010. **30**(10): p. 2460-72.

41. Zhou, G., et al., *Purification of a novel RECQL5-SWI/SNF-RNAPII super complex*. Int J Biochem Mol Biol, 2010. **1**(1): p. 101-111.
42. Watt, P.M., et al., *Sgs1: a eukaryotic homolog of E. coli RecQ that interacts with topoisomerase II in vivo and is required for faithful chromosome segregation*. Cell, 1995. **81**(2): p. 253-60.
43. Duno, M., et al., *Genetic analysis of the Saccharomyces cerevisiae Sgs1 helicase defines an essential function for the Sgs1-Top3 complex in the absence of SRS2 or TOP1*. Mol Gen Genet, 2000. **264**(1-2): p. 89-97.
44. Fricke, W.M., V. Kaliraman, and S.J. Brill, *Mapping the DNA topoisomerase III binding domain of the Sgs1 DNA helicase*. J Biol Chem, 2001. **276**(12): p. 8848-55.
45. Wu, L., et al., *The HRDC domain of BLM is required for the dissolution of double Holliday junctions*. Embo J, 2005. **24**(14): p. 2679-87.
46. Samanta, S. and P. Karmakar, *Recruitment of HRDC domain of WRN and BLM to the sites of DNA damage induced by mitomycin C and methyl methanesulfonate*. Cell Biol Int, 2012. **36**(10): p. 873-81.
47. Cordin, O., et al., *The DEAD-box protein family of RNA helicases*. Gene, 2006. **367**: p. 17-37.
48. Rocak, S. and P. Linder, *DEAD-box proteins: the driving forces behind RNA metabolism*. Nat Rev Mol Cell Biol, 2004. **5**(3): p. 232-41.
49. Banroques, J., et al., *Motif III in superfamily 2 "helicases" helps convert the binding energy of ATP into a high-affinity RNA binding site in the yeast DEAD-box protein Ded1*. J Mol Biol, 2010. **396**(4): p. 949-66.
50. Scheffner, M., J.M. Huibregtse, and P.M. Howley, *Identification of a human ubiquitin-conjugating enzyme that mediates the E6-AP-dependent ubiquitination of p53*. Proc Natl Acad Sci U S A, 1994. **91**(19): p. 8797-801.
51. Goebel, M.G., et al., *The yeast cell cycle gene CDC34 encodes a ubiquitin-conjugating enzyme*. Science, 1988. **241**(4871): p. 1331-5.
52. Jentsch, S., J.P. McGrath, and A. Varshavsky, *The yeast DNA repair gene RAD6 encodes a ubiquitin-conjugating enzyme*. Nature, 1987. **329**(6135): p. 131-4.
53. Jungmann, J., et al., *Resistance to cadmium mediated by ubiquitin-dependent proteolysis*. Nature, 1993. **361**(6410): p. 369-71.
54. Seufert, W. and S. Jentsch, *Ubiquitin-conjugating enzymes UBC4 and UBC5 mediate selective degradation of short-lived and abnormal proteins*. EMBO J, 1990. **9**(2): p. 543-50.

55. Dieckhoff, P., et al., *Smt3/SUMO and Ubc9 are required for efficient APC/C-mediated proteolysis in budding yeast*. Mol Microbiol, 2004. **51**(5): p. 1375-87.
56. Eloranta, J.J. and H.C. Hurst, *Transcription factor AP-2 interacts with the SUMO-conjugating enzyme UBC9 and is sumolated in vivo*. J Biol Chem, 2002. **277**(34): p. 30798-804.
57. Schorle, H., et al., *Transcription factor AP-2 essential for cranial closure and craniofacial development*. Nature, 1996. **381**(6579): p. 235-8.
58. Zhang, J., et al., *Neural tube, skeletal and body wall defects in mice lacking transcription factor AP-2*. Nature, 1996. **381**(6579): p. 238-41.
59. Tahmasebi, S., et al., *The SUMO conjugating enzyme Ubc9 is required for inducing and maintaining stem cell pluripotency*. Stem Cells, 2014. **32**(4): p. 1012-20.

CHAPTER FOUR:

NOVEL ROLE OF RRM3 IN CONTROLLING DNA SYNTHESIS IS SEPARABLE FROM ITS HELICASE-DEPENDENT ROLE IN AVOIDANCE OF REPLICATION FORK PAUSING

Note to reader: Unpublished data. Experiments were designed by Kristina H. Schmidt and Salahuddin Syed. Experiments were performed by Salahuddin Syed.

ABSTRACT

In response to replication stress cells activate the DNA Damage checkpoint, induce DNA repair pathways, increasing nucleotide levels, and inhibit late origin firing. Here, we report that Rrm3 controls DNA synthesis during replication stress and normal S phase. This novel Rrm3 function is independent of its established role as an ATPase/helicase in facilitating replication fork progression through polymerase blocking obstacles; instead the new functional domain maps to residues 186-212 that are also critical for binding Orc5 of the origin recognition complex. Deletion of this domain is lethal to cells lacking the replication checkpoint mediator Mrc1 and leads to mutations upon exposure to the replication stressor hydroxyurea, but not upon induction of alkylating DNA damage. Using quantitative mass spectrometry and genetic analysis, we find that the chromatin remodeler Rdh54 and Rad5-dependent error-free DNA damage bypass act as independent mechanisms on DNA lesions that arise when Rrm3 catalytic activity is disrupted whereas these mechanisms are dispensable for DNA damage

tolerance when the replication function is disrupted, indicating that the DNA lesions generated by the loss of each Rrm3 function are distinct. Although both lesion types activate the DNA-damage checkpoint, we find that the resultant increase in nucleotide levels is not sufficient for continues DNA synthesis under replication stress. Together, our findings suggest a role of Rrm3, via its Orc5-binding domain, in restricting DNA synthesis that is genetically and physical separable from its established catalytic role in facilitating fork progression through replication blocks.

INTRODUCTION

The replication machinery constantly at risk of encountering obstacles such as protein-DNA complexes, DNA secondary structures, transcribing RNA polymerases, and DNA damage, which can block fork progression. If these structures cannot immediately be resolved the paused fork may eventually collapse as replisome components become irretrievably inactivated.

The 5' to 3' DNA helicase Rrm3 is a member of the Pif1 family, which is conserved from yeast to humans (Azvolinsky, Dunaway et al. 2006). *Saccharomyces cerevisiae* *RRM3* was first discovered as a suppressor of recombination between tandem arrays and ribosomal DNA (rDNA) repeats (Keil and McWilliams 1993). Without Rrm3, extrachromosomal rDNA circles accumulate, suggesting a role in maintaining rDNA stability, and cells accumulate recombination intermediates at stalled replication forks, suggesting that Rrm3 facilitates DNA unwinding and the removal of protein blocks from DNA to help fork convergence during replication termination (Ivessa, Zhou et al. 2000, Ivessa, Zhou et al. 2002, Ivessa, Lenzmeier et al. 2003, Fachinetti, Bermejo et al.

2010). Additionally, replication fork pausing has been observed in the absence of Rrm3 at centromeres, telomeres, tRNA genes, the mating type loci, inactive origins of replication, and RNA polymerase II-transcribed genes (Keil and McWilliams 1993, Ivessa, Zhou et al. 2002, Ivessa, Lenzmeier et al. 2003).

The mechanism by which Rrm3 aids fork progression is poorly understood, but it is thought that Rrm3 facilitates replication through protein blocks and may also be able to remove RNA transcripts (Ivessa, Lenzmeier et al. 2003, Stamenova, Maxwell et al. 2009). Within each rRNA coding region are two intergenic spacers that contain termination (Ter) sites that are bound by the replication terminator protein Fob1 to promote fork arrest in order to prevent unscheduled transcription (Kobayashi, Nomura et al. 2001, Kobayashi 2003, Mohanty and Bastia 2004). Ter function also requires the intra-S phase checkpoint proteins Tof1 and Csm3, which form a complex with the replisome and antagonize Rrm3 function (Mohanty, Bairwa et al. 2006, Mohanty, Bairwa et al. 2009). It is thought that Rrm3 removes Fob1 and other non-histone proteins from DNA before the replication fork encounters them. This ability of Rrm3 to promote replication fork progression is dependent on its catalytic activity (Ivessa, Zhou et al. 2000). Further supporting a role of Rrm3 in fork progression are synthetic fitness defects or lethality between *rrm3Δ* and mutations that disrupt genes involved in maintaining the integrity of stalled forks, including *rad53Δ*, *mec1Δ*, *srs2Δ*, *sgs1Δ*, *mrc1Δ*, and *rtt101Δ* (Ivessa, Lenzmeier et al. 2003, Schmidt and Kolodner 2004, Torres, Schnakenberg et al. 2004, Luke, Versini et al. 2006).

Rrm3 possesses an N-terminal PCNA-interacting motif, associates with the replication fork *in vivo* and is hyperphosphorylated by Rad53 under replication stress

(Schmidt, Derry et al. 2002, Azvolinsky, Dunaway et al. 2006, Rossi, Ajazi et al. 2015). The replication damage that arises in the absence of Rrm3 causes constitutive, Mec3/Mec1/Rad9-dependent activation of the checkpoint kinase Rad53 (Ivessa, Lenzmeier et al. 2003, Schmidt and Kolodner 2006, Rossi, Ajazi et al. 2015). As a result, Dun1 kinase is activated, leading to degradation of the ribonucleotide reductase (RNR) inhibitor Sml1 and an increase in the dNTP pool (Zhao and Rothstein 2002, Poli, Tsaponina et al. 2012). This increased dNTP pool has been associated with enhanced DNA synthesis in hydroxyurea (HU) in chromosome instability mutants (Poli, Tsaponina et al. 2012).

Here we show that cells lacking Rrm3 fail to inhibit DNA replication in the presence of HU-induced replication stress and that this failure is not caused by the increased dNTP pool resulting from constitutive DNA-damage checkpoint activation. This novel function of Rrm3 is independent of its ATPase/helicase activity and, thus, distinct from Rrm3's established catalytic role in facilitating fork progression through replication blocks. Instead, we have identified dependency on a novel functional domain in the Rrm3 N-terminus that we find is critical for binding the Orc5 subunit of the origin recognition complex (ORC), suggesting that Rrm3 may control DNA synthesis by controlling origin activity. Quantitative mass spectrometry and genetic analyses further implicate Rad5-dependent error-free DNA damage bypass and Rdh54 translocase as novel repair mechanisms for DNA lesions that result from inactivating the catalytic activity of Rrm3, whereas the same DNA repair factors are dispensable when the Orc5-binding domain is disrupted, leading us to conclude that the types of DNA lesions that result from the inactivation of the two independent Rrm3 functions are distinct.

RESULTS

SILAC-based proteomics to identify the cellular response to replication fork pausing

In the absence of Rrm3 cells accumulate replication pause sites at the rDNA locus, in tRNA genes and at centromeric regions, as well as many other sites throughout the genome (Ivessa, Zhou et al. 2002, Ivessa, Lenzmeier et al. 2003, Torres, Schnakenberg et al. 2004). To identify DNA metabolic pathways that deal with stalled forks, we sought to identify proteins whose association with chromatin changed in the absence of Rrm3 using stable isotope labeling by amino acids in cell culture (SILAC)-based quantitative mass spectrometry (Ong, Blagoev et al. 2002, Ong and Mann 2006). We extracted the chromatin fraction from nuclei purified from a mixture of wildtype and *rrm3Δ* cells grown in the presence of heavy- or light-labeled arginine and lysine, respectively (Figures 1A and 1B). Across chromatin fractions from three biological replicates we identified 490 peptides from 137 different proteins, with the abundance of 11 proteins changing significantly in at least two out of the three replicates (Figure 1C). The largest change in chromatin association was a 5.1-fold increase ($p < 0.001$) of Rad5, which belongs to the SWI/SNF family of ATPases and defines an error-free pathway for bypassing replication-blocking DNA lesions (Torres-Ramos, Prakash et al. 2002, Gangavarapu, Haracska et al. 2006, Blastyak, Pinter et al. 2007, Ortiz-Bazan, Gallo-Fernandez et al. 2014). The increase in Rad5 was followed by smaller, but significant, increases for Top2 (1.9-fold, $p < 0.01$), a type II topoisomerase that is important for the decatenation of replication intermediates, and Rdh54 (1.8-fold, $p < 0.01$), a chromatin remodeler with a role in homologous recombination that is still largely unclear. Like

Rad5, Rdh54 is a member of the SWI/SNF family of ATPases; it possesses translocase activity on double-stranded (ds) DNA and has been shown to be capable of modifying DNA topology, especially in chromatinized DNA (Petukhova, Sung et al. 2000, Chi, Kwon et al. 2006, Shah, Zheng et al. 2010). We observed significant decreases in chromatin association for the Rsc1 subunit of the chromatin-structure-remodeling (RSC) complex (2-fold, $p < 0.01$), the Mcm4 subunit of the minichromosome maintenance (MCM) replicative DNA helicase (1.9-fold, $p < 0.01$), and the catalytic subunit Hda1 of the histone deacetylase (HDAC) complex (1.7-fold, $p < 0.01$).

Upon treatment with HU, which induces replication stress by reducing the nucleotide pool, Rdh54 abundance in the chromatin fraction of the *rrm3Δ* mutant increased the most (2.6-fold, $p < 0.01$) whereas the histone deacetylase Set3 and the Rsc9 subunit of the RSC chromatin remodelling complex saw the largest decreases (2.7-fold, $p < 0.05$) (Figures 1D and 1E). The complete list of proteins that underwent significant changes in the HU-treated or untreated *rrm3Δ* mutant, including the FANCM-related Mph1 helicase, the recombination factor Mgm101, and the cohesion components Smc1, Smc3 and Scc3, is provided in Supplemental Table S1.

Rad5 and Rdh54 independently act on DNA lesions that arise in the absence of Rrm3

Rrm3 helicase is required to prevent excessive replication fork pausing at protein-bound sites, possibly by acting as a protein displacement helicase (Ivessa, Zhou et al. 2002). The role of Rdh54 as a chromatin remodeler (Kwon, Seong et al. 2008, San Filippo, Sung et al. 2008) and the fork reversal activity of Rad5 suggest that they

are recruited to chromatin to recover forks that are blocked due to the lack of Rrm3 or to substitute for Rrm3 in preventing fork pausing. We therefore examined the effect of deleting *RAD5* and *RDH54* in the *rrm3Δ* mutant on genome stability and sensitivity to DNA damage and replication stress. We found synergistic increases in DNA damage sensitivity in the *rrm3Δ rad5Δ* and *rrm3Δ rdh54Δ* mutants (Figure 2A). The negative genetic interaction between *rrm3Δ* and *rad5Δ* was particularly strong; both single mutants were no more sensitive to HU than wildtype, but the double mutant failed to form colonies on 100 mM HU and grew very poorly even on 20 mM HU. In contrast to HU, the *rad5Δ* mutant was extremely sensitive to methyl methanesulfonate (MMS), and deleting *RRM3* led to a further, synergistic increase in MMS sensitivity. Inactivation of the ATPase activity of Rrm3 (*rrm3-K260A/D*) caused the same DNA-damage sensitivity in the *rad5Δ* mutant as an *RRM3* deletion (Figure 2B). We also identified a negative genetic interaction between *rrm3Δ* and *rdh54Δ*, which was especially strong on MMS. The increase in DNA-damage sensitivity of *rdh54Δ* cells upon deletion of *RRM3* extended to diploid cells (Figure 2G), suggesting that the lesions generated in the absence of Rrm3 are substrates for recombination between homologous chromosomes that is controlled by Rdh54. Even though the *rrm3Δ rad5Δ* mutant was hypersensitive to MMS and HU, deletion of *RDH54* caused further synergistic increases in sensitivity to both DNA damaging agents, suggesting that Rad5 and Rdh54 define important pathways for dealing with DNA lesions that arise in the absence of Rrm3, and that they perform (at least some) independent roles.

In addition to structure-specific helicase activity, Rad5 also possesses a RING motif associated with ubiquitin ligase activity that plays a role in polyubiquitination of

PCNA (Johnson, Henderson et al. 1992, Johnson, Prakash et al. 1994, Ulrich and Jentsch 2000, Hoege, Pfander et al. 2002). Disrupting the ubiquitin-ligase activity (*rad5-Ub*) or ubiquitin ligase and ATPase activity (*rad5-Ub-ATPase*), had the same effect on the MMS and HU sensitivity of wildtype cells (Figure 2B), consistent with a previous report (Gangavarapu, Haracska et al. 2006). In the *rrm3Δ* mutant, however, disrupting both activities caused significantly greater DNA damage sensitivity than disrupting either activity (*rrm3Δ rad5-Ub*, *rrm3Δ rad5-ATPase*), indicating that the ATPase/helicase and ubiquitin ligase activities of Rad5 contribute independently to repair of DNA lesions that arise in the absence of Rrm3.

Although Rad5 and Rdh54 chromatin association increased most in the absence of Rrm3 (Figure 1E), gross-chromosomal rearrangements (GCRs) did not accumulate at higher rates in the *rrm3Δ rad5Δ* or *rrm3Δ rdh54Δ* mutants compared to the single mutants, even after exposure to HU and MMS (Table 1). However, disruption of both, Rad5 and Rdh54, in the *rrm3Δ* mutant caused significantly higher chromosome instability than disruption of a single pathway, especially upon exposure to HU or MMS, underlining the independent contributions of Rdh54 and Rad5-mediated repair mechanisms to genome stability and DNA damage tolerance in the absence of Rrm3.

Whereas *rdh54Δ* and *rad5Δ* cells moved through an undisturbed cell cycle with similar kinetics as wildtype cells, *rrm3Δ* cells were delayed in progressing through S phase (Figure 2C), consistent with previous observations (Ivessa, Zhou et al. 2002, Schmidt and Kolodner 2004). We find that this accumulation of *rrm3Δ* cells in S phase was enhanced when *RDH54* or *RAD5* were deleted. To examine progression of *rrm3Δ rad5Δ* and *rrm3Δ rdh54Δ* cells through S phase under replication stress, we released α -

factor arrested cells from G1 in the presence of hydroxyurea and trapped them in G2/M with nocodazole. After 140 minutes, virtually all wildtype cells had reached 2C DNA content, whereas *rrm3Δ* and *rdh54Δ* entered S phase similarly to wildtype cells, but then slowed down significantly (Figure 2D, 100 minute time point). When we combined *rrm3Δ* and *rdh54Δ* mutations, this slowdown was so severe that most cells still had near 1C DNA content 100 minutes after release from G1 arrest. Similarly, *rad5Δ rrm3Δ* cells were delayed in reaching 2C DNA content in HU (Figure 2E). However, all mutants were able to recover from a 2-hour arrest in 100 mM HU and resume the cell cycle normally (Supplemental Figure S1). When we examined the ability of cells arrested in G2/M with nocodazole to complete mitosis and reach G1 phase we found that a significant number of wildtype cells had reached G1 after 20 minutes, whereas virtually all *rrm3Δ*, *rad5Δ* and *rrm3Δ rad5Δ* cells remained arrested in mitosis (Figure 2F). Together, these findings indicate that Rad5 and Rdh54 facilitate the progression of *rrm3Δ* cells through S phase, both in the presence and in the absence of HU, and that in the absence of Rrm3, cells accumulate DNA damage that impairs mitosis.

In addition to Rad5 and Rdh54, which exhibited the most significant increases in chromatin association in the absence of Rrm3 (Figure 1E), we tested DNA damage sensitivity of cells that lacked Rrm3 in combination with other nonessential factors revealed in the proteome screen (Figures 1C and 1D), including Mgm101, Hda1, Set3, and Mph1. Whereas deletions of *MGM101*, *HDA1* or *SET3* had no effect on DNA damage sensitivity of wildtype or *rrm3Δ* cells (Supplemental Figure S2), deletion of *MPH1* caused synergistic increases in HU and MMS sensitivity of the *rrm3Δ* mutant (Supplemental Figure S3), consistent with our previous finding (Schmidt, Viebranz et al.

2010). In the absence of Mph1, *rrm3Δ* cells progressed very slowly through an undisturbed cell cycle and accumulated in G2/M when they were released from a 2-hour incubation in 100 mM HU (Supplemental Figures 3B and 3C). When cells were released from HU arrest into media with 40 mM HU and α -factor, virtually all wildtype cells and the single mutants had been trapped in G1 after 60 minutes (with a slight S-phase delay in the *mph1Δ* mutant), whereas the majority of *rrm3Δ mph1Δ* cells accumulated in S phase, never forming a majority peak at 1C DNA content in the 120-minute time course (Supplemental Figure S3D). These findings implicate Mhp1 as another crucial factor for overcoming spontaneous and DNA-damage-induced replication-blocking lesions. Together these findings suggest error-free DNA lesion bypass, implicated by Rad5 and Mph1, and homologous recombination, implicated by Rdh54, as two mechanisms that can act independently on blocked replication forks.

A novel function of Rrm3 in controlling DNA replication maps to the N-terminal tail and is independent of Rrm3 catalytic activity

All functions of the Rrm3 helicase known to date are dependent on its ATPase/helicase activity. During our analysis of cell cycle progression, however, we observed that cells with a deletion of *RRM3* continue to replicate DNA in the presence of HU, similar to a *rad53Δ* checkpoint mutant, whereas the helicase-defective *rrm3-K260A* and *rrm3-K260D* mutants maintained near 1C DNA content after 2 hours in HU, similar to wildtype (Figures 3B and 3C). This observation suggested the presence of a previously unknown, ATPase/helicase-independent function of Rrm3 in DNA replication. Since this replication defect was independent of the ATPase/helicase activity located in

the ordered C-terminal domain of Rrm3 (residues 250-723), we explored a possible involvement of the 230-residue, disordered N-terminal tail (Figure 3A, Supplemental Figure S4A). The only motifs previously identified in this tail are a putative PCNA-interacting peptide (PIP) box between residues 35-42 (Schmidt, Derry et al. 2002) and a cluster of phosphorylated residues between S85 and S92 (Rossi, Ajazi et al. 2015). Deletion or mutation of the PIP-box (*rrm3-ΔN54*, *rrm3-FFAA*) had no effect on DNA replication in HU, whereas deletion of the entire N-terminal tail (*rrm3-ΔN230*) caused the same replication defect as deleting *RRM3* (*rrm3Δ*) (Figure 3D). By constructing a series of N-terminal truncations (Figure 3A and 3D) we determined that deletion of up to 186 residues, which include the PIP-box and the phosphorylation site, was able to maintain the wildtype replication phenotype in HU (Figures 3D and 3E), whereas deletion of 212 residues caused the same replication defect as *rrm3-ΔN230*, thus narrowing down the critical functional site for control of DNA replication to the 26 residues between residues 186-212. The importance of this region for controlling DNA replication was limited to HU, and not observed when cells were exposed to the alkylating agent methane methylsulfonate (Supplementary Figure S4B).

Deletion of *RRM3* or inactivation of its ATPase/helicase activity was recently reported to partially suppresses the HU hypersensitivity of the *rad53Δ* mutant (Rossi, Ajazi et al. 2015). We obtained the same findings, but also observed that the *rrm3-ΔN212* allele does not act as a suppressor (Figure 3J), indicating that this *rrm3-ΔN212* codes for a functional ATPase/helicase. This is also supported by the finding that a introduction of the K260A mutation in *rrm3-ΔN212* allele suppressed HU hypersensitivity of the *rad53Δ* mutant to the same extent as the *rrm3-K260A* allele (Figure 3J). Still, the

Rad53 checkpoint kinase was constitutively activated in the *rrm3-ΔN212* mutant just like in the ATPase/helicase-defective *rrm3-K260A/D* mutants, and Rad53 activation in both mutants was dependent on the mediator of the DNA damage checkpoint Rad9 (Figures 3G and 3I).

Through degradation of the ribonucleotide reductase (RNR) inhibitor Sml1, the nucleotide pool increases upon Rad53 activation, and this correlates with enhanced fork progression (Poli, Tsaponina et al. 2012). However, we found that the *rrm3* mutants that continued DNA replication in HU (*rrm3Δ*, *rrm3ΔN212*) and the *rrm3* mutant that maintained 1C DNA content (*rrm3-K260D*) had a constitutively increased nucleotide pool (Figure 3F), indicating that the continued DNA replication in HU seen in the *rrm3-ΔN212* mutant could not be explained by a larger nucleotide reservoir prior to its depletion by HU addition. In fact, we estimate that in the *rrm3Δ* and *rrm3Δ-N212* mutants the peak of cells with 1C DNA content had progressed nearly 40% toward 2C DNA content after 2 hours in HU (Figure 3H), and continued to progress (Supplemental Figure S4C), whereas wildtype cells, the helicase-dead *rrm3* mutants, and *rrm3Δ-N186* mutant had progressed less than 10%.

Together, these findings indicate a novel function of Rrm3 in the control of DNA replication and prevention of S phase damage, which maps to residues 186-212 of the N-terminal tail and does not require Rrm3's established activity as an ATPase/DNA helicase.

Residues of Rrm3 required for control of DNA replication are critical for Orc5 binding

Long disordered tails, such as the N-terminal 230 residues of Rrm3, which extend from its structured catalytic core, typically serve as sites for protein binding and posttranslational modification (Gsponer and Babu 2009). The phenotype of the *rrm3-ΔN212* allele in the *rad53Δ* mutant indicates that it encodes a proficient ATPase/helicase, raising the possibility that the replication defect of this allele is caused by loss of a protein-binding site. Because deletion of the putative PIP-box (Schmidt, Derry et al. 2002) and the recently identified phosphorylation site (Rossi, Ajazi et al. 2015) did not impair the ability of Rrm3 to control DNA replication, we explored the possibility that Orc5, an ATP-binding subunit of the origin recognition complex (ORC), binds to the N-terminal tail of Rrm3. An interaction between the two full-length proteins had previously been identified in a yeast-two-hybrid screen (Matsuda, Makise et al. 2007). When we combined *ORC5* with the various *rrm3* truncation alleles in a yeast two-hybrid assay, we found that deletion of 186 residues did not diminish Orc5 binding to Rrm3, in the presence or absence of MMS or HU, whereas deletion of 212 or 230 residues eliminated binding (Figure 4A). These findings show that the same site of Rrm3 that controls DNA replication is required for a physical interaction with Orc5 and raise the possibility that Rrm3 may control DNA replication by affecting origin activity.

Differential requirements of Rrm3 function in controlling DNA replication and ATPase/helicase activity in cells lacking Rad5, Rdh54, Mph1 or replication checkpoint factors Mrc1 and Tof1

To investigate the link between Rrm3 functions and DNA replication, we first examined the replication checkpoint. Replication mutants exhibit strong genetic interactions with Mrc1/Claspin, which acts as a mediator of the replication stress checkpoint – a Rad9-independent pathway of the intra-S-phase checkpoint (Alcasabas, Osborn et al. 2001, Katou, Kanoh et al. 2003, Osborn and Elledge 2003, Suter, Tong et al. 2004, Xu, Boone et al. 2004). Mrc1 is also a component of normal replication forks, which is loaded at origins of replication and stays associated with the replisome (Alcasabas, Osborn et al. 2001, Osborn and Elledge 2003, Szyjka, Viggiani et al. 2005, Tourriere, Versini et al. 2005). Mrc1, like Rrm3, is required for efficient replication (Naylor, Li et al. 2009). The function of Mrc1 in DNA replication is essential for the viability of cells lacking Rrm3 (Szyjka, Viggiani et al. 2005) whereas Mrc1 phosphorylation on SQ and TQ sites linked to its checkpoint function is dispensable (Schmidt and Kolodner 2006). However, the role of this functional interaction between Rrm3 and Mrc1 in DNA replication has remained unclear. We therefore tested if the ability of Rrm3 to control DNA replication was required for the viability of the *mrc1Δ* mutant. For this purpose, we transformed diploids heterozygous for the *mrc1Δ* and *rrm3Δ* mutations with plasmids expressing N-terminal truncations of Rrm3 and analyzed the viability of meiotic products. Figure 4B shows that the *rrm3-ΔN186* allele supported viability of the *rrm3Δ mrc1Δ* mutant as effectively as the wildtype *RRM3* allele, whereas the helicase-dead alleles and the *rrm3-ΔN212* allele were as ineffective as the null allele

(empty vector). Thus the helicase activity of Rrm3 is not sufficient for viability of the *mrc1Δ* mutant; Rrm3's new N-terminal domain for controlling DNA replication is also required.

In addition to Mrc1, Tof1 promotes normal progression of the replication fork; however, in contrast to Mrc1, its requirement for fork progression appears more limited, assisting primarily replication through non-histone protein complexes with DNA (Hodgson, Calzada et al. 2007). *TOF1* deletion was not lethal in the *rrm3Δ* mutant and neither single mutant was hypersensitive to HU or MMS. The combined loss of Rrm3 and Tof1, however, caused a synergistic increase in DNA-damage sensitivity (Figure 4C). Identical to the functional requirements in the absence of Mrc1 both, the ATPase/helicase activity of Rrm3 and the Orc5 binding domain, were required for growth in the presence of DNA damage and replication stress in the absence of Tof1.

In contrast to *mrc1Δ* and *tof1Δ* mutants, we found that only the ATPase/helicase activity of Rrm3 was required for the suppression of HU and MMS hypersensitivity of the *rad5Δ*, *rdh54Δ*, and *mph1Δ* mutants (Figures 4D – 4F, Figure 2B). The N-terminal tail, including its function in controlling DNA replication, was dispensable, with the *rrm3-ΔN212* allele exhibiting wildtype phenotypes in *rad5Δ*, *rdh54Δ*, and *mph1Δ* mutants (Figures 4D – 4F).

Together, these findings suggest two separable functions of Rrm3 in DNA replication. First, an ATPase/helicase-dependent function that promotes fork progression through protein-DNA complexes, which if disrupted (*rrm3-K260A/D*) causes aberrant replication intermediates that can be rescued by Rad5, Rdh54 or Mph1 mechanisms. Second, an N-terminal function that controls DNA replication, possibly

mediated by Rrm3's physical interaction with ORC, which if disrupted (*rrm3-ΔN212*) requires the replication checkpoint factors Mrc1 and Tof1 for viability and DNA damage survival. These differential requirements of factors involved in DNA repair and DNA damage tolerance pathways in the *rrm3-ΔN212* and *rrm3-K260A/D* mutants also suggests that the types of DNA lesions that accumulate upon inactivation of the two Rrm3 functions are different, but both lead to dependence on Mrc1 for survival and both are sufficient for constitutive activation of the DNA-damage checkpoint.

Requirement of the Orc5-binding domain of Rrm3 for suppression of HU-induced mutations, but not MMS-induced mutations and gross-chromosomal rearrangements

If Rrm3 is important for the response to replication stress, cells lacking the catalytic activity of Rrm3 or its Orc5-binding domain may be prone to accumulating mutations at higher rates than wildtype cells. To test this, we measured forward mutation rates at the *CAN1* locus and the accumulation of GCRs on chromosome V in the presence and absence of HU or MMS (Table 2). Two-fold (*ung1Δ*) to 50-fold (*rad27Δ*) increases in *CAN1* forward mutation rates compared to wildtype have previously been reported for numerous DNA metabolism mutants (Huang, Rio et al. 2003). Deletion of *RRM3* or disruption of its ATPase activity caused a significant increase in spontaneous *CAN1* mutations. Of the truncation alleles, which encode catalytically active *rrm3* mutants, *rrm3Δ-N186* was indistinguishable from wildtype whereas *rrm3Δ-N212* caused a small, but significant, increase in the *CAN1* mutation rate in untreated cells and upon exposure to HU (Table 2). In contrast, expression of the

rrm3Δ-N212 allele had no effect on the *CAN1* mutation rate if cells were treated with MMS, consistent with our observation that the *rrm3-ΔN212* mutant exhibits a defect in controlling replication in HU, but not MMS. GCRs accumulated at increased rates in the *rrm3Δ* and *rrm3-K260A/D* mutants in the absence and presence of DNA damaging agents, but accumulated at wildtype levels in cells expressing N-terminal truncations under all conditions. These mutator phenotypes, albeit mild, reveal that Rrm3's ATPase/helicase activity is required for the suppression of all tested mutation types induced by either HU or MMS, or in their absence, whereas the N-terminal site that controls DNA replication and binds Orc5 plays a role specifically in the suppression of spontaneous and HU-induced mutations, but not for the suppression of MMS-induced mutations, or GCRs under any conditions.

DISCUSSION

By quantifying changes in chromatin composition we have identified Rad5 and Rdh54 as novel factors that respond to increased replication fork stalling induced by the absence of Rrm3, and affirmed the importance of Mph1. These factors suggest that error-free post-replicative repair (PRR), implicated by Rad5 and Mph1, and HR, implicated by Rdh54, act on DNA polymerase blocking sites in the genome that arise in the absence of Rrm3. The N-terminal unstructured tail is entirely dispensable for this ATPase/helicase-dependent role of Rrm3 in facilitating fork progression. Instead, we have discovered that the N-terminal tail encodes a new function of Rrm3 – to control DNA replication. This function of Rrm3 is distinct from its established role as an ATPase/helicase, is not regulated by the previously identified phosphorylation cluster

(Rossi, Ajazi et al. 2015) or the PIP-box (Schmidt, Derry et al. 2002) and, in contrast to the ATPase/helicase activity, does not contribute to the HU hypersensitivity of the *rad53Δ* mutant.

Based on changes in DNA content as measure by flow cytometry, we observed that wildtype cells maintained near 1C DNA content for 180 minutes after release from G1 phase into HU, whereas *rad53Δ*, *rrm3Δ* and *rrm3-ΔN212* did so for only 60 minutes (Figure 3C, Supplemental Figure S4C). The extent of continuing DNA replication in the presence of HU, however, was not as pronounced in the *rrm3* mutants as in the intra-S checkpoint-deficient *rad53Δ* mutant. Although the Rad9-dependent DNA-damage checkpoint is chronically activated in the *rrm3-ΔN212* mutant and, as a consequence, nucleotide levels are increased compared to wildtype cells and the *rrm3-ΔN186* mutant, the increased nucleotide levels are not the cause for the ability of the *rrm3-ΔN212* mutant to continue DNA replication upon HU exposure because the *rrm3-K260A/D* mutants showed the same nucleotide level increase and DNA-damage checkpoint activation, but maintained a peak at 1C DNA content in HU.

Therefore, considering Rrm3's known function as an accessory ATPase/helicase that facilitates progression of the replication fork through obstacles, and its new function in controlling DNA synthesis reported here, we propose a model (Figure 5) where Rrm3 performs two genetically and physically separable functions to deal with challenges during genome duplication: the N-terminal tail of Rrm3 plays a structural role in preventing untimely replication in the presence of replication stress (HU) and in normal S phase, whereas the C-terminal ATPase/helicase domain plays a catalytic role in preventing fork pausing. The site between residues 186 to 212, which is in a segment of

the N-terminal tail not previously assigned a function, is not only critical for restricting DNA replication, but also for binding Orc5, raising the possibility that Rrm3 may exert control over DNA replication by affecting origin activity; such a link would be consistent with a previously identified role of ORC in suppressing late-origin firing under replication stress (Shirahige, Hori et al. 1998). For example, Rrm3 could be recruited to pre-replication complexes as they are assembled at origins during G1 by binding to the ATP-binding ORC subunit Orc5, which does not appear to play a role in the completion of S phase, or the remainder of the cell cycle (Bell and Dutta 2002, Labib 2010). There, Rrm3 could act as an inhibitor of ORC ATPase activity, which is required for loading of minichromosome maintenance (MCM) proteins and initiation of DNA replication (Bowers, Randell et al. 2004, Randell, Bowers et al. 2006).

Instead of a global role in controlling origin activity, however, the wildtype level of HU sensitivity of *rrm3Δ* cells and the importance of Rrm3 for replicating through certain nonhistone-protein-bound regions suggest that Rrm3 may play a role at origins in specific loci, such as those in highly transcribed regions and regions with converging transcription, which are often late-firing (Soriano, Morafraila et al. 2014), rRNA and tRNA coding loci, or highly transcribed metabolic genes, where ORC has been found to be bound to the open reading frames, possibly to coordinate the timing of replication with transcription (Shor, Warren et al. 2009). The absence of Rrm3 from these regions could cause more wide-spread (untimely) origin firing early in S-phase and, thus, an overabundance of replication intermediates and, eventually, DNA lesions, causing constitutive activation of the DNA-damage checkpoint (Figure 5B). It has been proposed that the temporal separation of origins into early and late firing might be required to

prevent excessive accumulation of replication intermediates, such as ssDNA, that could activate the intra-S checkpoint (Shimada, Pasero et al. 2002). In *rrm3Δ* and *rrm3-ΔN212* mutants, a subset of regions whose replication may be controlled by Rrm3 to fire late could convert to firing early, so that in HU, when firing of late origins is inhibited in cells with a proficient intra-S checkpoint (Santocanale and Diffley 1998, Shirahige, Hori et al. 1998), *rrm3Δ* and *rrm3-ΔN212* mutants exhibit a DNA replication profile that is similar to that of the *rad53Δ* mutant.

Inactivation of the ATPase/helicase activity does not affect Rrm3's novel role in controlling DNA replication. Instead, it impairs Rrm3's established function in facilitating fork progression through replication blocks, leading to the accumulation of DNA lesions that activate the DNA-damage checkpoint and increase formation of chromosome rearrangements and point mutations (Figure 5C). By identifying changes in chromatin composition combined with genetic assays we have identified Rad5 and Rdh54 as novel factors that contribute to the maintenance of genome stability in the absence of Rrm3's ATPase/helicase activity. Rad5 defines an error-free pathway for the bypass of DNA polymerase blocking lesions (Nelson, Lawrence et al. 1996, Johnson, Prakash et al. 1999, Torres-Ramos, Prakash et al. 2002, Prakash, Johnson et al. 2005, Gangavarapu, Haracska et al. 2006, Ortiz-Bazan, Gallo-Fernandez et al. 2014). As a structure-specific DNA helicase, Rad5 is capable of regressing replication forks *in vitro* (Blastyak, Pinter et al. 2007). Such a regressed fork is thought to provide an alternative template for DNA synthesis, generating enough nascent DNA to eventually bypass the replication block. The increased association of Rad5 with chromatin in *rrm3Δ* cells and the severe synergistic interaction between *rad5Δ* and *rrm3Δ* deletions in HU-treated

cells suggest that some type of nascent strand annealing by Rad5 is involved in replication fork progression in *rrm3Δ* cells. Notably, we found that the ATPase activity of Rad5 and the RING motif involved in polyubiquitination of PCNA (Johnson, Henderson et al. 1992, Johnson, Prakash et al. 1994, Hoegge, Pfander et al. 2002, Haracska, Torres-Ramos et al. 2004) make independent contributions to DNA damage tolerance in the absence of Rrm3. Evidence for a role of the ATPase activity of Rad5 in remodeling blocked replication forks has been obtained *in vitro* (Blastyak, Pinter et al. 2007) whereas a role of Rad5-dependent polyubiquitination of PCNA in activating HR-dependent template switching has more recently been suggested (Minca and Kowalski 2010). Evidence that these two Rad5 activities can function independently, albeit inefficiently, as we determined here in the *rrm3Δ* mutant, was also observed for bypass of MMS-induced lesions by sister-chromatid recombination (Minca and Kowalski 2010).

Besides fork regression, Rad5 has also been implicated in DNA damage bypass by HR-dependent template switching between sister-chromatids (Minca and Kowalski 2010) and the major HR factors Rad51, Rad52 and Rad54 as well as Sgs1 have been implicated in error-free DNA lesion bypass (Branzei, Sollier et al. 2006). It was therefore surprising that Rdh54, a chromatin remodeler that plays a major role in meiotic, but not mitotic, HR (Klein 1997, Shinohara, Shita-Yamaguchi et al. 1997, Holzen, Shah et al. 2006), is recruited to chromatin when Rrm3 is absent - both in the presence and absence of HU. Rdh54 was only required in the absence of the ATPase/helicase activity of Rrm3, but not in the absence of the Orc5-binding domain, implicating Rdh54 in repair of DNA lesions that arise when Rrm3 cannot facilitate fork progression through replication blocks. Even though Rdh54 does not affect gene conversion repair of a DSB,

a role specifically in repair that involves template switches was recently reported (Tsaponina and Haber 2014), and could be related to its increased chromatin association and the DNA-damage hypersensitivity of the *rrm3Δ rdh54Δ* and *rrm3-K260A rdh54Δ* mutants.

Although it is unknown how Rdh54 acts in template switching, its activities *in vitro* seem compatible with those that may be required to rescue a paused fork. Like Rad5 and the human Rad5 ortholog, HTLF, Rdh54 is a dsDNA translocase of the SWI/SNF family (Petukhova, Sung et al. 2000, Chi, Kwon et al. 2006, Blastyak, Hajdu et al. 2010). *In vitro*, it can dislodge the HR factor Rad51 from dsDNA and introduces negative supercoiling into dsDNA that can cause strand separation (Petukhova, Sung et al. 2000, Chi, Kwon et al. 2006, Shah, Zheng et al. 2010). These Rdh54 activities could help to regulate repair at fork pause sites within Rad5-mediated pathways, such as fork regression/reversal or template switching, and in HR-mediated template switching events outside of Rad5 mechanisms. Whereas Rdh54 can remove proteins from dsDNA and remodel chromatinized DNA, an ability to remove bound proteins from DNA has not yet been shown for Rad5, and RecQ-like helicases are only capable of acting on forked DNA structures that are protein-free (Kwon, Seong et al. 2008, San Filippo, Sung et al. 2008). The synergistic interactions between *rad5Δ* and *rdh54Δ* in the absence of *RRM3* clearly identify a role of Rdh54 outside of a Rad5 mechanism. In addition to facilitating template switching HR when error-free PRR is inactivated, Rdh54 could act in the avoidance of replication fork pausing in a manner similar to Rrm3 by removing certain proteins from dsDNA, such as shown for Rad51, which appears to have a tendency to

associate with nonrecombinogenic dsDNA (Chi, Kwon et al. 2006, Holzen, Shah et al. 2006, Shah, Zheng et al. 2010).

That the ATPase activity of Rrm3 is required in the absence of Rad5, Rdh54 and Mph1, whereas the role of Rrm3 in controlling DNA replication is dispensable strongly suggests that the types of DNA damage checkpoint activating DNA lesions in the *rrm3-K260A* and *rrm3-ΔN212* mutants are different, and that Rad5, Rdh54 and Mph1 act on DNA lesions that form when replication forks are unable to move through replication blocks, but not on DNA lesions that form during uncontrolled DNA replication. In contrast, Mrc1 and Tof1 were required for viability and DNA damage tolerance when either of the two Rrm3 activities was disrupted. Mrc1, the mediator of the replication stress checkpoint, mediates Rad53 phosphorylation specifically in response to replication fork pausing, leading to intra-S checkpoint activation and inhibition of late-origin firing (Osborn and Elledge 2003, Crabbe, Thomas et al. 2010). That synthetic lethality between *rrm3Δ* and *mrc1Δ* is limited to those *mrc1* alleles that cause DNA damage accumulation during S phase (Naylor, Li et al. 2009), whereas the checkpoint function of Mrc1 is dispensable (Schmidt and Kolodner 2006, Naylor, Li et al. 2009) suggests that the additive accumulation of S phase damage and slowing of S phase progression due to lack of both, Mrc1 and Rrm3, is lethal and suggests that uncontrolled replication in the *rrm3-ΔN212* mutant also leads to S phase damage, consistent with our observation of Rad9-dependent activation of Rad53 (Figure 5B).

Finally, the new N-terminal Rrm3 function in controlling DNA replication is separated from Rrm3's established C-terminal function as an ATPase/helicase in facilitating fork progression by the differential requirement of Rad5, Rdh54 and Mph1 for

DNA lesion repair and by the different spontaneous and DNA-damage induced mutation spectra. This suggests that the N-terminal tail is neither involved in the recruitment of Rrm3 to active replication forks nor in facilitating fork progression through protein-bound sites, and that a separate replisome binding site is likely to be located in the ATPase/helicase domain. The accumulation of GCRs and point mutations in the ATPase/helicase mutant, spontaneously or induced by HU or MMS, could be indicative of DNA break formation as a result of replication fork stalling. In contrast, the Orc5-binding domain mutant did not accumulate GCRs under any conditions, suggesting wildtype levels of DNA breaks, including in HU and MMS, but increasingly formed point mutations. That these point mutations formed specifically in response to HU, but not MMS, suggests that they arise during the unscheduled DNA synthesis that occurs in this mutant in HU.

In summary, this study has revealed a 26-residue region in Rrm3 that is critical for a novel, ATPase-independent function of Rrm3 in preventing untimely DNA replication and for binding Orc5, which might be mechanistically linked. Genome-wide quantification of DNA synthesis in cells expressing the new *rrm3* alleles will help to reveal any regions with increased origin activity and undergoing untimely DNA replication, and provide insight into the mechanism underlying continued DNA synthesis under replication stress and lethality with *mrc1* Δ . That Rrm3 does not appear to have a homolog in multicellular eukaryotes, although the Pif1 family to which it belongs is conserved, might be an indication that Rrm3's role in DNA replication is highly specialized to control replication and facilitate fork progression in genomic regions that are distinctively organized in yeast, such as its rDNA array, and to deal with the high

gene density imposed on its small genome that requires tight coordination between replication initiation and ongoing transcription.

MATERIALS AND METHODS

Stable isotope labeling by amino acids in cell culture (SILAC) and isolation of chromatin fraction

For double isotope labeling of lysine and arginine, yeast strain KHSY5144 (*lys2Δ arg4Δ*), was grown at 30°C with vigorous shaking for at least ten generations in “heavy” medium (6.9 g/l yeast nitrogen base without amino acids (Formedium), 1.85 g/l amino acid dropout mixture without arginine and lysine (Kaiser formulation, Formedium), 2% glucose, 15 mg/l [¹³C₆] L-arginine and 30 mg/l [¹³C₆] or [¹³C₆, ¹⁵N₂] L-lysine). KHSY5143 (*lys2Δ arg4Δ rrm3Δ*) was grown in “light” medium, containing 15 mg/l L-arginine and 30 mg/l L-lysine at 30°C with vigorous shaking.

Chromatin was isolated using a method adapted from (Kubota, Stead et al. 2012). Approximately 4 x 10⁹ cells were re-suspended in 10 ml of 100 mM PIPES/KOH, pH 9.4, 10 mM dithio-treitol (DTT), 0.1% sodium azide, then incubated for 10 min at room temperature, followed by incubation in 10 ml of 50 mM KH₂PO₄/K₂HPO₄, pH 7.4, 0.6 M Sorbitol, 10 mM DTT, containing 200 mg/ml Zymolyase-100T at 37°C for 30 min. Spheroplasts were washed with 5 ml of cold wash buffer (20 mM KH₂PO₄/K₂HPO₄, pH 6.5, 0.6 M Sorbitol, 1 mM MgCl₂, 1 mM DTT, 20 mM beta-glycerophosphate, 1 mM phenyl-methylsulfonyl fluoride (PMSF), protease inhibitor tablets (EDTA free, Roche) and re-suspended in 5 ml of cold wash buffer. The suspension was overlaid onto 5 ml of 7.5% Ficoll-Sorbitol cushion buffer (7.5% Ficoll, 20 mM KH₂PO₄/K₂HPO₄, pH 6.5, 0.6 M

sorbitol, 1 mM MgCl₂, 1 mM DTT, 20 mM beta-glycerophosphate, 1 mM PMSF, protease inhibitor tablets) and spheroplasts were centrifuged through the cushion buffer at 5000 rpm for 5 min to remove proteases derived from Zymolyase. Pelleted spheroplasts were re-suspended in 200 ml of cold wash buffer and dropped into 18% Ficoll, 20 mM KH₂PO₄/K₂HPO₄, pH 6.5, 1 mM MgCl₂, 1 mM DTT, 20 mM beta-glycerophosphate, 1 mM PMSF, protease inhibitor tablets, 0.01% Nonidet P-40, with stirring. Unbroken cells were removed by two spins (5000 x g for 5 min at 4°C). Nuclei were pelleted by centrifugation at 16,100 x g for 20 min and the cytoplasmic fraction removed. After washing in cold wash buffer, nuclei were re-suspended in 200 ml of EB buffer (50 mM HEPES/KOH, pH 7.5, 100 mM KCl, 2.5 mM MgCl₂, 0.1 mM ZnSO₄, 2 mM NaF, 0.5 mM spermidine, 1 mM DTT, 20 mM beta-glycerophosphate, 1 mM PMSF, protease inhibitor tablets) and lysed by addition of Triton X-100 to 0.25%, followed by incubation on ice for 10 min. Lysate was overlaid on 500 ml of EB buffer, 30% sucrose, 0.25% Triton X-100, and centrifuged at 12,000 rpm for 10 min at 4°C. The top layer was removed and the chromatin pellet was washed in 1 ml of EB buffer, 0.25% Triton X-100 and centrifuged at 10,000 rpm for 2 min at 4°C.

Sample preparation and LC-MS/MS

The chromatin pellet was re-suspended in 40 µl of 1.5x Tris-Glycine SDS Sample Buffer and incubated for 2 min at 85°C. DTT was added to a final concentration of 5 mM and incubated for 25 min at 56°C. Iodoacetamide was added to 14 mM final concentration and incubated for 30 min at room temperature in the dark. DTT was added to a final concentration of 5 mM and incubated for 15 minutes at room

temperature in the dark. The protein mixture was diluted 1:5 in 25 mM Tris-HCl, pH 8.2, CaCl₂ was added to a 1mM final concentration and trypsin was added to a concentration of 4-5 ng/μl, followed by incubation at 37°C overnight. Trifluoroacetic acid was added to 0.4% final concentration and centrifuged at 2,500 x *g* for 10 min at room temperature. Peptides in the supernatant were desalted using reverse-phase tC18 SepPak solid-phase extraction cartridges (Waters). The sample was eluted with 5 ml of 50% acetonitrile (ACN) and lyophilized. The lyophilized product was re-suspended in 0.1% formic acid prior to tandem mass spectrometric analysis on an LTQ Orbitrap XL (Thermo). Scans on the Orbitrap were obtained at a mass resolving power of 60000 at *m/z* 400 and top 10 abundant ions were selected for fragmentation in the LTQ ion trap. Further processing of the RAW files was done in MaxQuant version 1.5.3.30 (Cox and Mann 2008) against the *Saccharomyces* genome database (SGD). A database of known contaminants in MaxQuant was used as well as constant modification of cysteine by carbamidomethylation and variable modification of methionine oxidation. The first search tolerance was set at 20 ppm, then 8 ppm tolerance for the main search. Fragment ion mass tolerance was set to 0.5 Da and the minimum peptide length was 6 amino acids. Unique and razor peptides were used for identification and the false discovery rate was set to 1% for peptides and proteins (Hochberg and Benjamini 1990, Cox and Mann 2008). Statistical analysis of the data was carried out using Perseus software using an approach by Benjamini and Hochberg (Benjamini, Drai et al. 2001).

Yeast strains and plasmids

SILAC labeling and chromatin fractionation was performed using yeast strains from the same genetic background as KHSY5036 (*MAT a*, *ura3-52*, *trp1Δ63*, *his3Δ200*). To determine resistance to DNA damaging agents and mutation assays, yeast strains from the same genetic background as KHSY802 were used (*MAT a*, *ura3-52*, *trp1Δ63*, *his3Δ200*, *leu2Δ1*, *lys2Bgl*, *hom3-10*, *ade2Δ1*, *ade8*, *hxt13::URA3*). Genes were deleted through homologous recombination and integration of a selectable marker (Gietz and Woods 2006). To generate more than one gene deletion or point mutation, random spore isolation was performed using diploid yeast strains heterozygous for the mutations. Point mutations were introduced into plasmids by site-directed mutagenesis and confirmed by sequencing. RRM3 N-terminal truncations were created in plasmid pKHS137 and plasmid pJG4-5* using HR-mediated integration in KHSY2331 (*lig4Δ*) and verified by sequencing. Yeast strains and plasmids from this study are listed in Tables S2 and S3, respectively.

Fluctuation assays

GCR rates were determined as previously described (Schmidt, Pennaneach et al. 2006). To observe the effect of exposure of DNA damaging agents on GCR rates, cells were grown to $OD_{600} = 0.5$, placed into media containing the drug and cultured for 2 hours at 30°C. Cells were then inoculated in YPD and grown for 24 hours before being plated. Forward mutation rates were determined as described previously (Nair 1940, Lea and Coulson 1949, Reenan and Kolodner 1992). To obtain forward mutation rates and GCR rates after exposure to MMS and HU, cells were grown to $OD_{600} = 0.5$,

released into medium containing the drug and incubated for 2 hours at 30°C. Cells were then placed into YPD and grown for 24 hours before being subjected to fluctuation analysis.

DNA damage sensitivity assay

Cells were grown on either YPD or selective media to maintain plasmids (SC-Leu) to an $OD_{600} = 0.5$, serially diluted, and spotted on YPD or SC-Leu containing methyl methanesulfonate (Sigma Aldrich) or hydroxyurea (US Biological) at the indicated concentrations. Cell growth was recorded after 2 to 3 days of incubation at 30°C.

DNA content analysis

Cells were prepared for DNA content analysis as previously described (Nash, Tokiwa et al. 1988). Cells were washed and re-suspended in 70% ethanol for an hour at room temperature. The ethanol was removed and cells were re-suspended in 50 mM sodium citrate (pH 7), sonicated, washed in 50 mM sodium citrate (pH 7), and RNase A was added to a final concentration of 250µg/ml. The cells were incubated overnight at 37°C, washed in 50 mM sodium citrate and Sytox green (Molecular Probes) was added to reach a 1µM final concentration. These cells were incubated in the dark for an hour and then subjected to FACS analysis using a BLD LSR II analyzer. Cell distribution was analyzed using FlowJo v8.3.3.

Protein expression by western blot

Cells were cultured in YPD to a final OD₆₀₀ = 0.5 in YPD at 30°C, arrested in G₁ with α -factor (15 μ g/ml), and then released into pre-warmed YPD. Cells were harvested after 30 min, immediately put on ice and diluted to obtain equal cell number. Whole cell extracts were generated with 20% TCA as previously described (Kennedy, Daughdrill et al. 2013) and run on 10% SDS-PAGE for Western blot analysis. Phosphospecific Rad53 antibody, EL7, was a gift from A. Pellicoli (FIRC Institute of Molecular Oncology Foundation, Milan, Italy). Antibody sc-6680 (SCBT) was used for Mcm2, ab34680 (Abcam) for Adh1, ab46765 (Abcam) for histone H3, and RFA antibody AS07214 (Agrisera) for Rfa1.

Determination of dNTP levels

Cells grown to stationary phase were transferred to acidic media (pH 3.5) and grown to logarithmic phase. Cells were synchronized in G₁ phase over two hours with the addition of 2 μ g/ml alpha-factor (Genscript) every hour. Cells were washed twice with sterile water. 2.5×10^8 yeast cells were pelleted, resuspended in 1 ml 60% methanol, and disrupted by 5 consecutive freeze and thaw cycles using liquid nitrogen and warm water, followed by incubation at -20°C for 90 minutes, and boiling at 100°C for 3 minutes. The lysate was centrifuged at 19000 \times g for 15 minutes and the supernatant frozen in liquid nitrogen. Methanol was evaporated in a SpeedVac (Thermo Scientific) and the residue was rehydrated in 100 μ l Ultra-pure H₂O (Invitrogen, GIBCO). Determination of cellular dNTP concentration was performed as earlier described

(Desler, Munch-Petersen et al. 2007). Each extraction was performed at least in triplicate.

Yeast two-hybrid assay

For yeast-two hybrid yeast strain EGY48 with a reporter plasmid was transformed with the bait vector (pEG202) and a prey vector (pJG4-5*). Cells were plated on synthetic complete media lacking histidine and tryptophan (SC-Trp-His). Positive transformants were selected and re-suspended in liquid SC-Trp-His media supplemented with 2% galactose and 1% raffinose, and cultured overnight at 30°C. Cells were diluted to an $OD_{600} = 0.2$, cultured to a final $OD_{600} = 0.8$, and serially dilutions were spotted on SC-Trp-His-Leu supplemented with either 2% glucose or 2% galactose in the presence or absence of hydroxyurea (HU) or methyl methanesulfonate (MMS). Pictures of cell growth were taken after 72 hours.

Analysis of meiotic products

Diploids heterozygous for the desired mutant alleles (*rrm3::TRP1*, *mrc1::HIS3*) transformed with plasmid-borne alleles of *RRM3* (linked to *LEU2*) were sporulated by nitrogen starvation in 0.1% potassium acetate for 5 days at 30°C with vigorous shaking. Asci were incubated in the presence of 500 µg/ml of zymolase in 1M sorbitol for 20 min at 30°C, enriched for meiotic products as previously described (Rockmill, Lambie et al. 1991) and plated on nonselective media (YPD). After incubation for 2 days at 30°C, colonies were spotted on SC-Leu media and 100 leu⁺ colonies genotyped further by

spotting on SC-Leu-Trp, SC-Leu-His, and SC-Leu-Trp-His to identify *rrm3* Δ , *mrc1* Δ and *rrm3* Δ *mrc1* Δ mutants, respectively, all harboring various plasmid borne *RRM3* alleles.

FIGURES AND TABLES

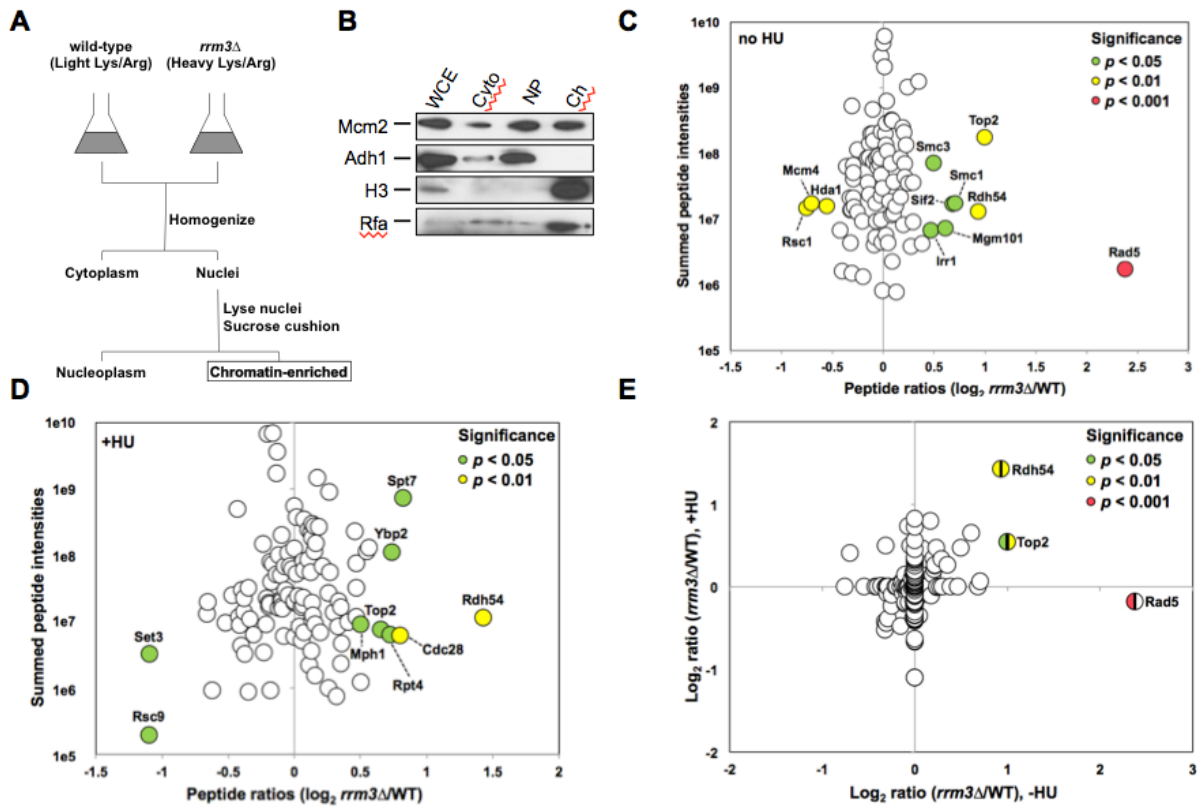


Figure 4.1. SILAC-based quantification of changes in chromatin association in cells lacking Rrm3. (A) Equal numbers of light-labeled (wildtype) and heavy-labeled (*rrm3* Δ) cells were mixed, nuclei isolated, and the chromatin fraction extracted and analyzed by tandem mass spectrometry using a hybrid linear ion trap-Orbitrap instrument. (B) Subcellular fractionation was verified by following the distribution of proteins in cytoplasmic (Cyto), nucleoplasm (NP), and chromatin (Ch) fractions during the enrichment procedure by Western blotting. Chromatin fractions were analyzed from three biological replicates in (C) the absence of hydroxyurea and (D) in the presence of hydroxyurea. (E) Merger of peptide quantification in the absence and presence of hydroxyurea.

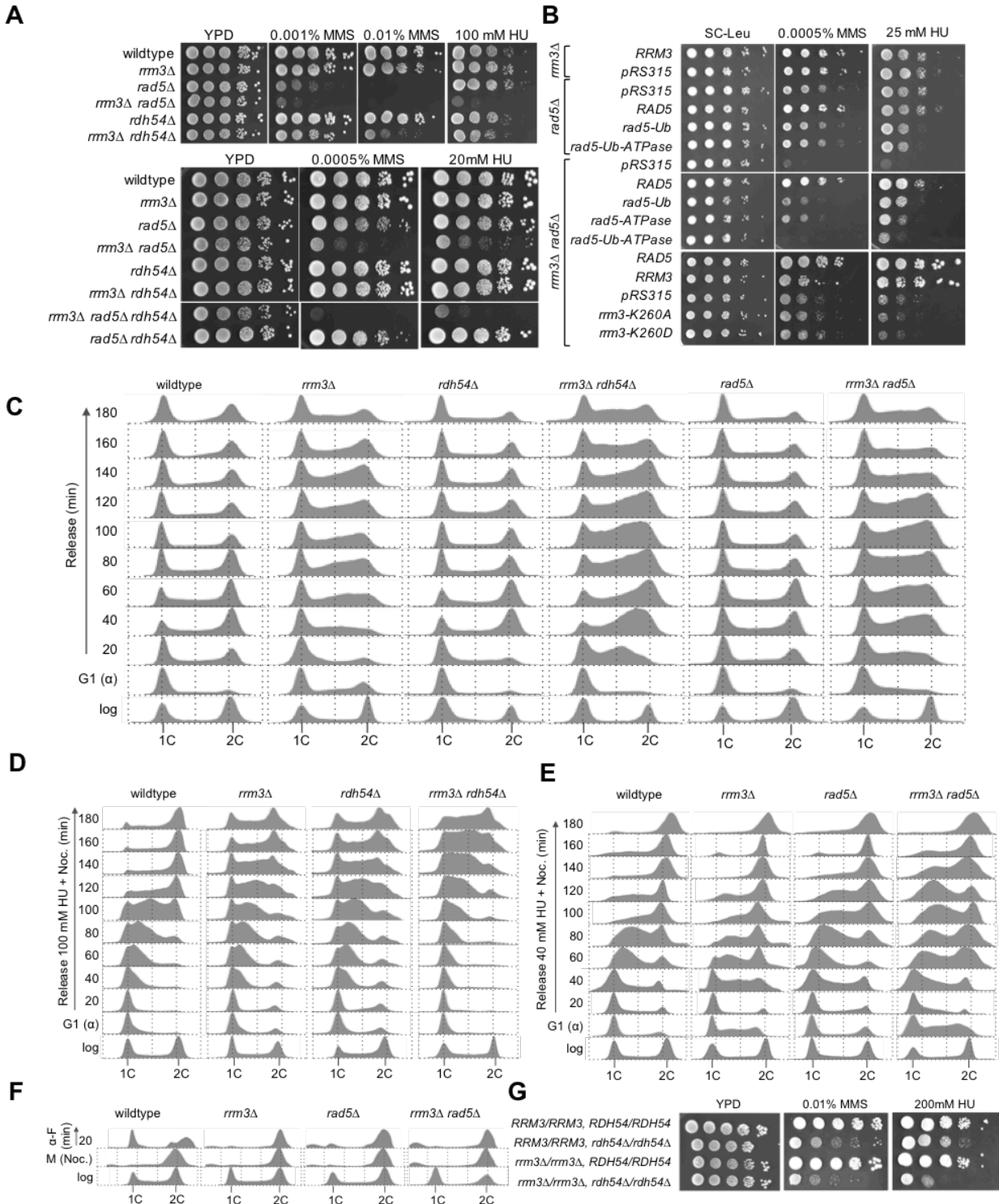


Figure 4.2. Rad5 and Rdh54 contribute independently to DNA lesion bypass/repair in cells lacking Rrm3. (A) Synergistic increases in DNA-damage sensitivity of *rrm3Δ* mutant lacking *RAD5* and/or *RDH54* were identified by spotting serial dilutions of exponentially growing cultures of the indicated mutants on MMS and HU. **(B)** Ubiquitin ligase and ATPase activities of Rad5 contribute independently to DNA damage

tolerance in the absence of Rrm3. The ATPase/helicase activity of Rrm3 is required for growth of the *rad5Δ* mutant under chronic exposure to HU or MMS. **(C)** Accumulation of *rrm3Δ* cells in S phase increases upon deletion of *RAD5* or *RDH54*. Cells were synchronized in G1 phase with α -factor, released in YPD to resume the cell cycle, and DNA content analyzed by fluorescence-activated cell sorting every 20 minutes for 3 hours. **(D-E)** Deletion of *RAD5* or *RDH54* slows progression of *rrm3Δ* cells through S phase in the presence of HU. Cells were synchronized in G1 with α -factor, released into media containing 100 mM HU (*rdh54Δ*) or 40 mM HU (*rad5Δ*) and nocodazole (to trap cells in G2/M). DNA content was analyzed by fluorescence activated cell sorting every 20 minutes for 3 hours. **(F)** *rrm3Δ* and *rad5Δ* mutations slow progression through mitosis to G1 phase. Cells were trapped in mitosis with nocodazole and released into media with α -factor. **(G)** Deletion of *RRM3* increases DNA damage sensitivity of the diploid *rdh54Δ* mutant. Serial dilutions of exponentially growing cultures of diploids heterozygous or homozygous for *rrm3Δ* or *rdh54Δ* mutations were spotted on HU and MMS.

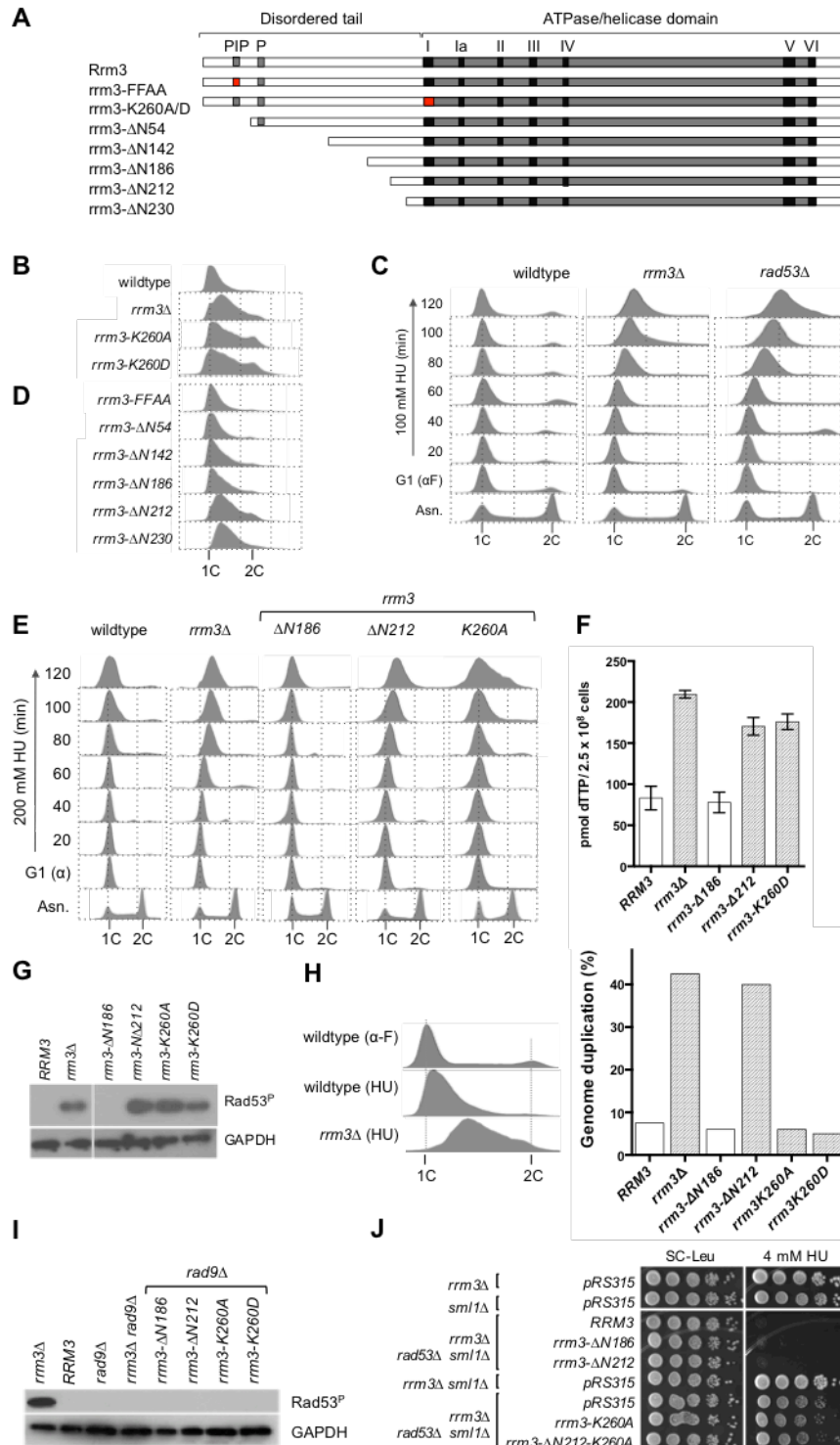


Figure 4.3. A 26-residue region in the N-terminal tail of Rrm3 is required for the control of DNA replication under replication stress independently of ATPase/helicase activity. (A) Rrm3 consist of a ~230-residue disordered N-terminal tail and a ~400 residue ordered C-terminal ATPase/helicase domain. A putative PCNA-interaction motif (PIP) between residues 35-42 (Schmidt, Derry et al. 2002) and a

cluster of phosphorylated residues (P) between residues 85-95 (Rossi, Ajazi et al. 2015) are indicated by gray boxes in the disordered tail. N-terminal tail truncations (*rrm3* Δ N54, *rrm3* Δ N142, *rrm3* Δ N186, *rrm3* Δ N212, *rrm3* Δ N230) and point mutations designed to inactivate the PIP box (*rrm3*-FFAA) and the Walker A motif of the helicase domain (*rrm3*-K260A, *rrm3*-K260D) were constructed. Point mutations are indicated by a red box. **(B)** DNA content analysis by fluorescence-activated cell sorting (FACS) of *rrm3* mutants shows continued DNA replication in *rrm3* Δ , *rrm3*- Δ N212 and *rrm3*- Δ N230 mutants during a 2-hour incubation in 200 mM hydroxyurea, but maintenance of a peak at 1C DNA content for wildtype cells and the other *rrm3* mutants. **(C)** Similar to checkpoint-deficient *rad53* Δ *sml1* Δ cells, *rrm3* Δ cells continue DNA replication in the presence of HU, but not MMS (Figure S2B). Cells were synchronized in G1 phase with α -factor and released into media containing 100 mM HU. DNA content was analyzed by FACS every 20 minutes for 2 hours after G1 release. **(D)** Cells expressing an N-terminal truncations of 212 residues continue DNA replication in the presence of 200 mM HU whereas those expressing a 186-residue truncation or the ATPase/helicase-dead mutant arrest with 1C DNA content like wildtype cells. Cells were synchronized in G1 with α -factor and released into 200 mM HU for 2 hours. Aliquots were removed prior to release from G1 and then every 20 minutes for 2 hours and DNA content analyzed by FACS. **(E)** Nucleotide pool, represented here by dTTP, is increased in *rrm3* Δ cells and in cells expressing the *rrm3*- Δ N212 truncation or the ATPase/helicase-dead *rrm3*-K260A mutant, but not in cells expressing the shorter *rrm3*- Δ N186 truncation. **(F)** Rad53 is constitutively activated in catalytically inactive *rrm3* Δ , *rrm3*-K260A and *rrm3*-K260D mutants, and in the *rrm3*- Δ N212 truncation mutant. Cells were arrested in G₁ with α -factor and Rad53 phosphorylation analyzed 30 min after release from arrest with a phospho-specific Rad53 antibody. Rad53 activation in *rrm3* mutants correlates with an increased dNTP pool, but not with continued DNA synthesis in the presence of hydroxyurea. **(G)** DNA content in wildtype cells and *rrm3* mutants in the presence of hydroxyurea was analyzed by FACS analysis and progression toward genome duplication (2n) estimated by setting the 1C peak of untreated wildtype cells to 0% and the 2C peak to 100%. **(H)** Rad53 phosphorylation in *rrm3* mutants, irrespective of continued DNA replication in HU or catalytic activity, is Rad9-dependent. **(I)** Rrm3 truncated by 212 N-terminal residues is an active ATPase/helicase. Deletion of *RRM3* or inactivation of its ATPase/helicase activity suppresses HU hypersensitivity of the *rad53* Δ *sml1* Δ mutant whereas the *rrm3*- Δ N212 allele does not, exhibiting wildtype ATPase/helicase activity.

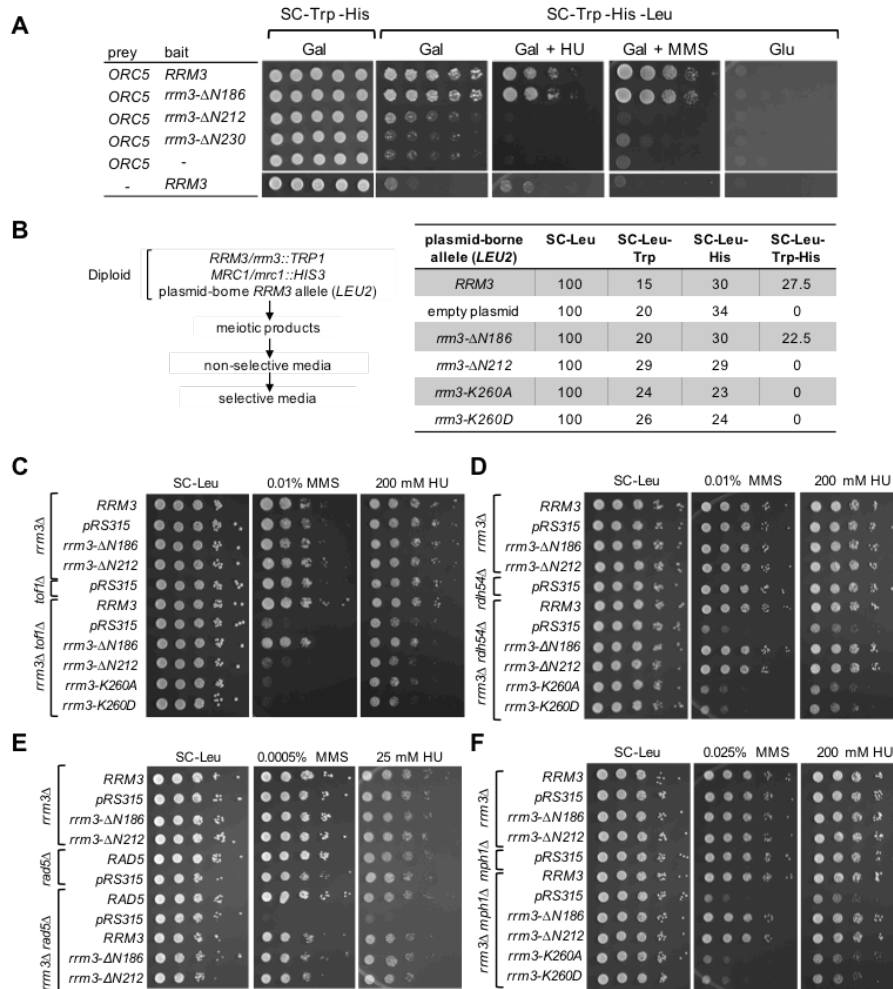


Figure 4.4. The N-terminal Rrm3 region that controls DNA replication is an Orc5-binding site that is required for cell viability and DNA lesion avoidance in the absence of Mrc1/Tof1 but not in the absence of Rad5, Rdh54 or Mph1. (A) Residues 186-212 of Rrm3 are critical for physical interaction with origin recognition complex (ORC) subunit Orc5. Orc5 binding to wildtype Rrm3 and *rrm3* mutants was assessed by yeast-two-hybrid analysis on media lacking leucine to identify cells expressing the *LEU2* reporter gene upon bait-prey binding. Rrm3 truncated by 186 residues binds Orc5, in the presence or absence of HU or MMS, whereas deletion of an additional 26 residues (*rrm3-ΔN212*) eliminates binding of Orc5. **(B)** Orc5-Rrm3 binding site is required for *mrc1Δ* viability. Diploids heterozygous for *mrc1Δ* and *rrm3Δ* mutations were transformed with plasmids expressing N-terminal truncations of Rrm3 and 100 meiotic products that grew on SC-Leu media, indicating the presence of the plasmid-borne *RRM3* alleles, were genotyped. Absence of meiotic products that grew on SC-Leu-Trp-His indicates synthetic lethality between the *rrm3* allele and *mrc1Δ*. **(C)** Deletion of the Orc5-Rrm3 binding site increases DNA-damage sensitivity of the *tof1Δ* mutant. **(D-F)** Requirement of the ATPase/helicase activity of Rrm3, but not the Orc5-binding site, for suppression of HU and MMS hypersensitivity of *rad5Δ*, *rdh54Δ*, and *mph1Δ* mutants.

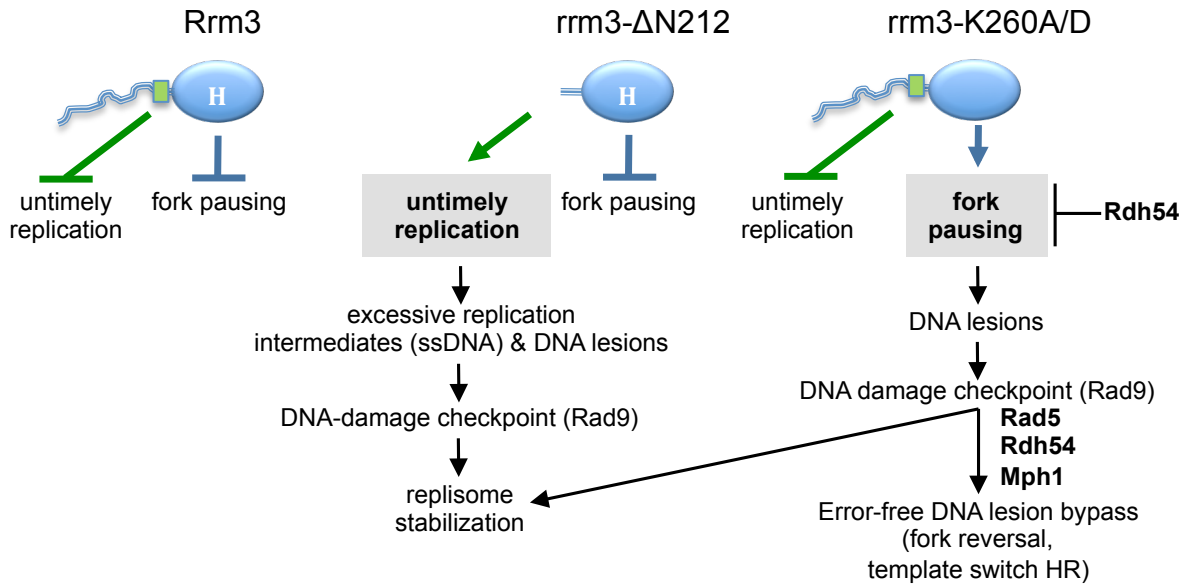


Figure 4.5. Rrm3 performs two genetically and physically separable functions during DNA replication. (A) Rrm3 controls DNA synthesis via residues 186-212 (green rectangle) in its disordered N-terminal tail (blue double line). The involvement of this region in Orc5 binding suggests that Rrm3 may control DNA synthesis by controlling origin activity to prevent untimely replication events during replication stress and during normal S phase, as indicated by constitutive checkpoint activation. Rrm3 assists in replication through nonhistone-protein-bound sites throughout the genome, including the rRNA coding region, and may also be needed in other highly transcribed regions and those with convergent transcription. Such regions often contain late-firing origins. Independently of its N-terminal tail, Rrm3 associates with the replisome and utilizes its ATPase/helicase activity (blue oval labeled H) to facilitate fork progression through replication blocks. **(B)** Deleting the Orc5-binding domain disrupts Rrm3's function in controlling DNA synthesis, leading to untimely DNA synthesis and accumulation of point mutations in normal S-phase and in HU. Excessive accumulation of replication intermediates and ensuing DNA lesions are the most probable cause of intra-S checkpoint activation in these cells. Despite loss of the N-terminal function, the ATPase/helicase-dependent function of Rrm3 in fork progression through blockages is intact, suggesting that Rrm3 can be recruited to replisomes independently of the N-terminal tail. **(C)** Disrupting the ATPase/helicase activity of Rrm3 maintains control over DNA synthesis timing, but forks are unable to progress through replication blocks, leading to DNA lesions that require Rad5, Rdh54, and Mph1 for bypass or repair and activate the intra-S checkpoint. In contrast to loss of the Orc5-binding site, GCRs form in addition to point mutations, indicating the formation of different types of DNA lesions in the ATPase/helicase mutant, most likely DNA breaks.

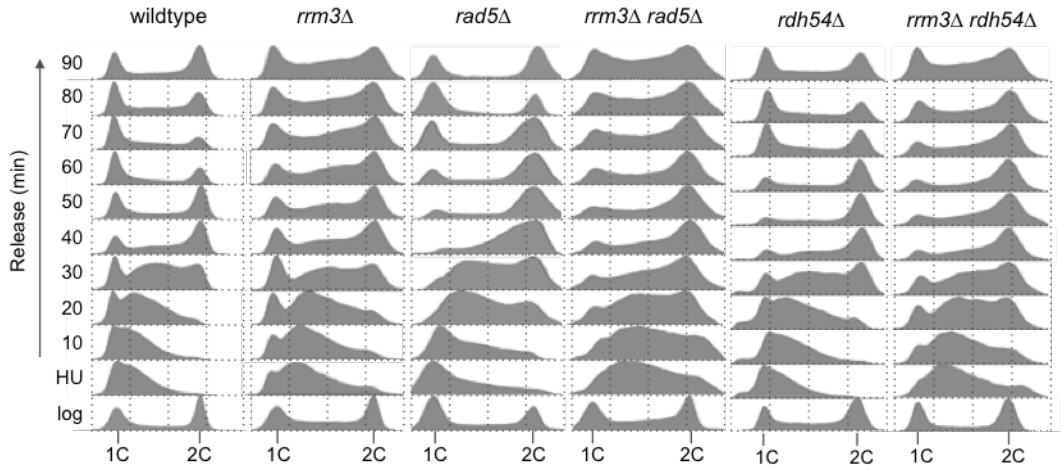


Figure 4.S1. Rad5 and Rdh54 are not required for S phase progression of *rrm3Δ* cells after release from 2 hour exposure to 100 mM HU.

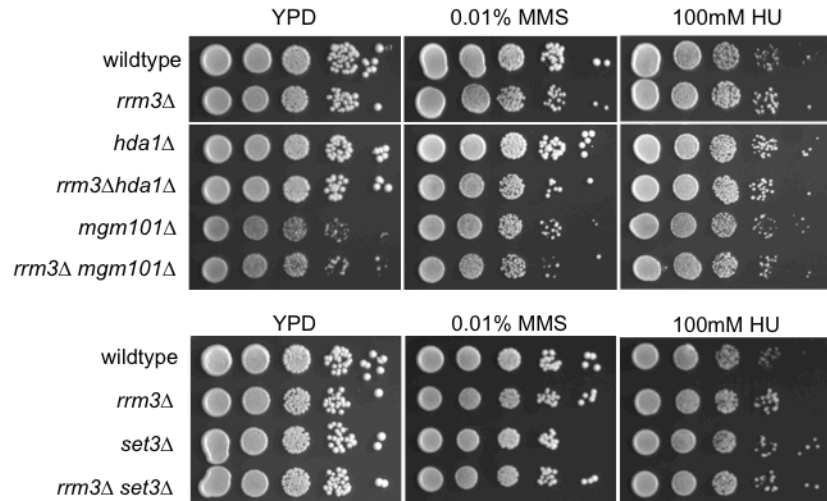


Figure 4.S2. Deletion of the nonessential *HDA1*, *SET3*, or *MGM101* genes does not affect the DNA damage sensitivity of the *rrm3Δ* mutant. Chromatin association of Hda1 and Set3 significantly decreased in the absence of Rrm3 whereas Mgm101 increased. Deletion of *MGM101* resulted in the 'petite' phenotype. Serial dilutions of exponentially growing cultures of the indicated mutants were spotted on rich media containing 0.01% MMS or 100 mM HU, or no drug (YPD), followed by incubation for 2-3 days at 30°C.

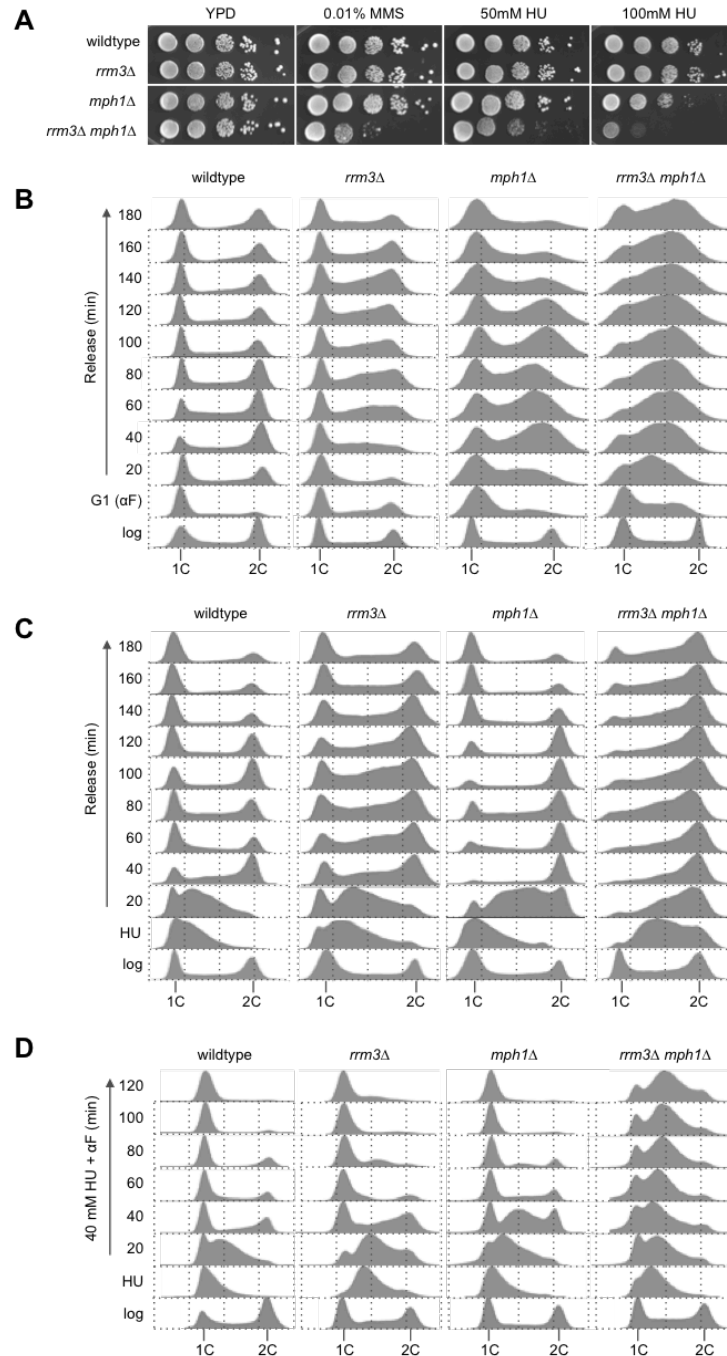


Figure 4.S3. Requirement of Mph1 for DNA repair and DNA replication in the absence of Rrm3. (A) Deletion of *RRM3* causes a synergistic increase in DNA damage sensitivity of cells lacking the DNA helicase Mph1. Absence of Mph1 causes delayed S phase progression of *rrm3Δ* cells in the absence of DNA damaging agents **(B)**, after release from HU into an undisturbed S phase **(C)**, and, most severely, during chronic exposure to HU **(D)**.

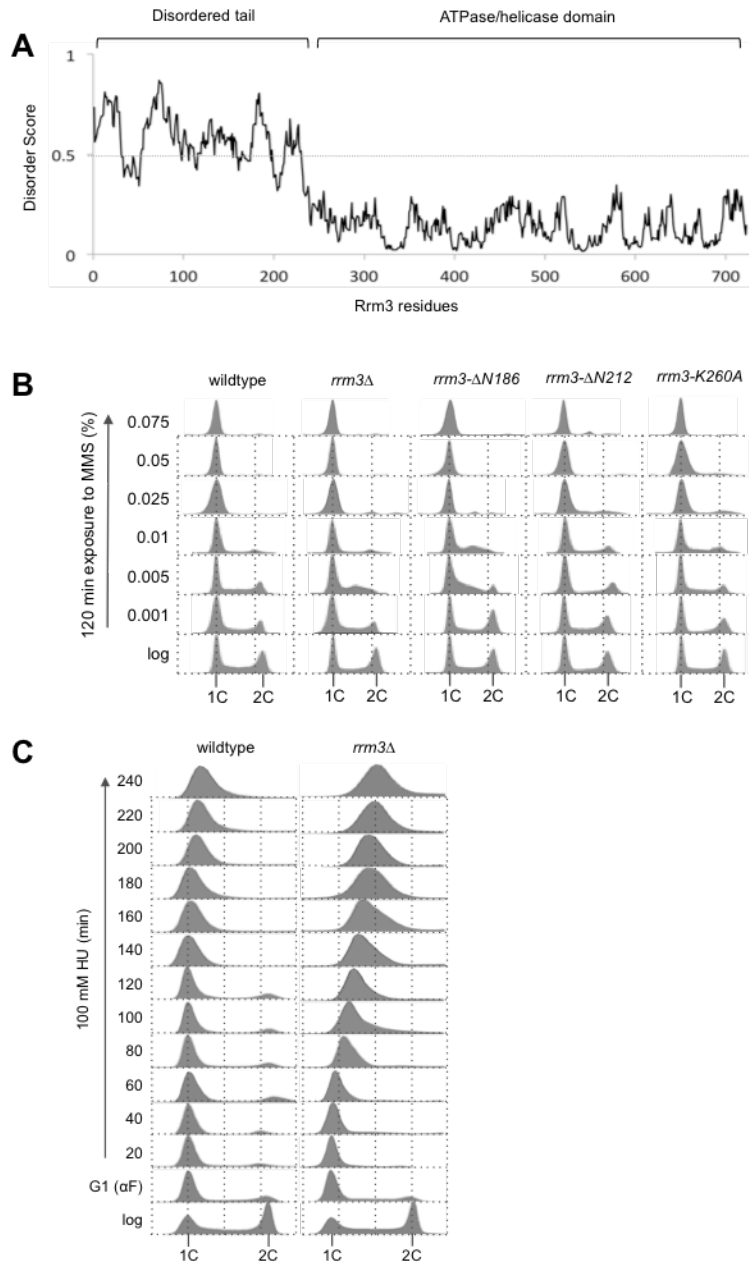


Figure 4.S4. The Rrm3 N-terminal tail controls DNA replication. (A) The N-terminal tail of Rrm3 is predicted to be unstructured. A disorder score of >0.5 indicates a disordered residue whereas a score <0.5 indicates a residue in a ordered region (Dosztanyi et al., 2005). (B) In contrast to HU, *rrm3*- Δ N212 and *rrm3* Δ mutants arrest with 1C DNA content when exposed to MMS. (C) 4 hour time course of *rrm3* Δ mutant released from G1 arrest into 100 mM HU.

Table 4.1. Effect of Deletions of *RRM3*, *RAD5*, *RDH54* on Accumulation of Gross-Chromosomal Rearrangements in the Presence or Absence of Genotoxic Agents

| Genotype | GCR rate (Can ^r 5-FOA ^r) (x 10 ⁻¹⁰) | GCR rate (Can ^r 5-FOA ^r) (x 10 ⁻¹⁰) +HU | GCR rate (Can ^r 5-FOA ^r) (x 10 ⁻¹⁰) +MMS |
|--|--|---|--|
| | GCR Rate | | |
| wildtype | 1.1 (<1-6.1) | 20 (9.6-35) | 65 (55-75) |
| <i>rrm3</i> Δ | 14 (11-27) | 139 (106-171) | 97 (90-114) |
| Δ <i>rad5</i> | 237 (220-271) | 1477 (1300-1590) | 928 (837-1020) |
| Δ <i>rrm3</i> Δ <i>rad5</i> | 260 (224-263) | 1600 (1390-1680) | 1040 (834-1220) |
| Δ <i>rdh54</i> | 17 (11-27) | 191 (144-212) | 108 (87-135) |
| Δ <i>rrm3</i> Δ <i>rdh54</i> | 25 (14-54) | 202 (194-224) | 120 (99-266) |
| Δ <i>rad5</i> Δ <i>rdh54</i> | 263 (244-272) | 1578 (1320-1710) | 991 (907-1160) |
| Δ <i>rrm3</i> Δ <i>rad5</i> Δ <i>rdh54</i> | 322 (278-419) | 2446 (2140-2670) | 1664 (1350-1810) |

Table 4.2. Accumulation of Forward Mutations at *CAN1* and Gross-chromosomal Rearrangements in Untreated *rrm3* Mutants and after Treatment with Genotoxic Agents

| Genotype | Can (x10 ⁻⁷) | Can (x10 ⁻⁷) +HU | Can (x10 ⁻⁶) +MMS | GCR rate (Can ^r 5-FOA ^r) (x 10 ⁻¹⁰) | GCR rate (Can ^r 5- FOA ^r) (x 10 ⁻¹⁰) +HU | GCR rate (Can ^r 5- FOA ^r) (x 10 ⁻¹⁰) +MMS |
|--------------------|-----------------------------|------------------------------------|-------------------------------------|--|---|--|
| | Mutation rate | | | GCR Rate | | |
| Wildtype | 1.6 (1.4- 1.9) | 2.3 (2.0- 2.8) | 1.9 (1.7- 2.3) | 1.1 (<1-6.1) | 20 (9.6- 35) | 65 (55-75) |
| <i>rrm3</i> Δ | 5.1 (4.3- 5.8) | 8.1 (7.4- 8.8) | 3.2 (2.8- 3.4) | 14 (11-27) | 139 (106- 171) | 97 (90- 114) |
| <i>rrm3</i> -ΔN186 | 1.9 (1.7- 2.3) | 2.5 (2.2- 2.9) | 2.3 (1.9- 2.4) | 4.4 (<1-8.8) | 43 (18- 47) | 56 (39-71) |
| <i>rrm3</i> -ΔN212 | 2.8 (2.6- 3.0) | 4.1 (4.0- 4.5) | 2.1 (2.0- 2.4) | 4.5 (<1-13) | 33 (17- 39) | 78 (63-92) |
| <i>rrm3</i> -K260A | 4.3 (4.0- 5.0) | 8.0 (7.9- 8.4) | 3.0 (2.7- 3.1) | 14 (10-23) | 158 (105- 201) | 93 (81- 117) |
| <i>rrm3</i> -K260D | 4.4 (4.3- 4.8) | 8.2 (7.6- 9.2) | 2.9 (2.7- 3.3) | 18 (10-25) | 132 (110- 170) | 97 (88- 113) |

TABLE 4.S1. Proteins that undergo significant changes in cells lacking Rrm3 in the presence and absence of HU

| Protein ID | Fold Change -HU | Description |
|------------|-----------------|---|
| Rad5 | 5.1 | RING domain-containing ubiquitin ligase involved in error free DDT |
| Top2 | 1.9 | Type II topoisomerase that catalyzes decatenation of DNA |
| Rdh54 | 1.8 | DNA-dependent ATPase activity, can supercoil and unwind DNA and promote D-loop formation and branch migration to promote HR |
| Smc1 | 1.5 | Subunit of the cohesin complex that associates with SMC3 and is required for sister chromatid cohesion |
| Sif2 | 1.5 | Subunit of Set3C histone deacetylase complex |
| Mgm101 | 1.4 | Role in mitochondrial DNA recombinational repair and interstrand cross-link repair |
| Smc3 | 1.3 | Subunit of the cohesin complex that associates with SMC1 and is required for sister chromatid cohesion |
| Irr1 | 1.3 | Subunit of the cohesin complex, thought to close the cohesion ring |
| Hda1 | -1.7 | Putative catalytic subunit of a class II histone deacetylase complex |
| Mcm4 | -1.9 | Essential helicase component of heterohexameric MCM2-7 complexes |
| Rsc1 | -2.0 | Component of the RSC chromatin remodeling complex |

| Protein ID | Fold Change +HU | Description |
|------------|-----------------|---|
| Rdh54 | 2.6 | DNA-dependent ATPase activity, can supercoil and unwind DNA and promote D-loop formation and branch migration to promote HR |
| Spt7 | 1.7 | SAGA core component which may regulate Spt20 and Ada1, components of the SAGA complex. |
| Ybp2 | 1.6 | Central kinetochore associated protein |
| Cdc28 | 1.6 | Associates with six B-type cyclins to direct mitotic spindle assembly in S-phase and spindle function during mitosis |
| Rpt4 | 1.6 | ATPase of the 19S regulatory particle of the 26S proteasome. One of six ATPases of the regulatory particle, involved in degradation of ubiquitinated substrates |
| Mgm101 | 1.5 | Role in mitochondrial DNA recombinational repair and interstrand cross-link repair |
| Mph1 | 1.4 | 3'-5' DNA helicase involved in error-free bypass of DNA lesions |

Table 4.S1 (continued)

| | | |
|-------|------|--|
| Top2 | 1.4 | Type II topoisomerase that catalyzes decatenation of DNA |
| Rsc9 | -1.9 | Component of the RSC chromatin remodeling complex which targets genes regulated by stress |
| Set3 | -2.7 | Component of the 7-subunit HDAC complex with a role in transcription |
| Vps72 | -2.7 | Part of the SWR1 complex, exchanges histone variant H2AZ (Htz1p) for chromatin-bound histone H2A |

Table 4.S2. Yeast Strains used in this study

| Strain | Genotype |
|----------------------|---|
| EGY48 ^[1] | <i>MATα ura3-52, trp1Δ63, his3Δ200, LexA_{op} (x6)-LEU2</i> |
| KHSY304 | <i>MATα ura3-52, trp1Δ63, his3Δ200, rrm3::TRP1</i> |
| KHSY745 | <i>ura3-52/ura3-52, trp1Δ63/trp1Δ63, his3Δ200/his3Δ200, RRM3/rrm3::TRP1, MRC1/mrc1::HIS3</i> |
| KHSY802 | <i>MATα ura3-52, leu2Δ1, trp1Δ63, his3Δ200, lys2ΔBgl, hom3-10, ade2Δ1, ade8, YEL069C::URA3</i> |
| KHSY1063 | <i>MATα ura3-52, leu2Δ1, trp1Δ63, his3Δ200, lys2ΔBgl, hom3-10, ade2Δ1, ade8, YEL069C::URA3, rrm3::TRP1</i> |
| KHSY1065 | <i>ura3-52/ura3-52, leu2Δ1/leu2Δ1, trp1Δ63/trp1Δ63, his3Δ200/his3Δ200, lys2ΔBgl/lys2ΔBgl, hom3-10/hom3-10, ade2Δ1/ade2Δ1, ade8/ade8. YEL069C::URA3/YEL069C::URA3, RAD53/rad53::his3, SML1/sml1::G418, RRM3/rrm3::TRP1</i> |
| KHSY1133 | <i>ura3-52, lys2-801 amber, ade2-101 ochre, trp1-Δ63, his3-Δ200, leu2-Δ1, rad9::G418, rrm3::URA3</i> |
| KHSY1157 | <i>ura3-52/ura3-52, leu2Δ1/leu2Δ1, trp1Δ63/trp1Δ63, his3Δ200/his3Δ200, lys2ΔBgl/lys2ΔBgl, hom3-10/hom3-10, ade2Δ1/ade2Δ1, ade8/ade8. YEL069C::URA3/YEL069C::URA3</i> |
| KHSY1557 | <i>MATα ura3-52, leu2Δ1, trp1Δ63, his3Δ200, lys2ΔBgl, hom3-10, ade2Δ1, ade8, YEL069C::URA3, mph1::HIS3</i> |
| KHSY1713 | <i>MATα ura3-52, leu2Δ1, trp1Δ63, his3Δ200, lys2ΔBgl, hom3-10, ade2Δ1, ade8, YEL069C::URA3, rrm3::TRP1, mph1::HIS3</i> |
| KHSY2331 | <i>MATα ura3-52, leu2Δ1, trp1Δ63, his3Δ200, lys2ΔBgl, hom3-10, ade2Δ1, ade8, YEL069C::URA3, lig4::loxP-G418-loxP</i> |
| KHSY4570 | <i>MATα ura3-52, trp1Δ63, his3Δ200</i> |
| KHSY4743 | <i>ura3-52/ura3-52, trp1Δ63/trp1Δ63, his3Δ200/his3Δ200, RRM3/rrm3::TRP1</i> |
| KHSY5143 | <i>MATα ura3-52, trp1Δ63, his3Δ200, arg4::G418, lys2::HIS3</i> |
| KHSY5144 | <i>MATα ura3-52, trp1Δ63, his3Δ200, arg4::G418, lys2::HIS3, rrm3::TRP1</i> |
| KHSY5145 | <i>MATα ura3-52, leu2Δ1, trp1Δ63, his3Δ200, lys2ΔBgl, hom3-10, ade2Δ1, ade8, YEL069C::URA3, rad5::HIS3</i> |
| KHSY5146 | <i>MATα ura3-52, leu2Δ1, trp1Δ63, his3Δ200, lys2ΔBgl, hom3-10, ade2Δ1, ade8, YEL069C::URA3, rrm3::TRP1, rad5::HIS3</i> |
| KHSY5147 | <i>MATα ura3-52, leu2Δ1, trp1Δ63, his3Δ200, lys2ΔBgl, hom3-10, ade2Δ1, ade8, YEL069C::URA3, rdh54::HIS3</i> |

Table 4.S2 (continued)

| | |
|----------|---|
| KHSY5148 | <i>MATa ura3-52, leu2Δ1, trp1Δ63, his3Δ200, lys2ΔBgl, hom3-10, ade2Δ1, ade8, YEL069C::URA3, rrm3::TRP1, rdh54::HIS3</i> |
| KHSY5149 | <i>MATa ura3-52, leu2Δ1, trp1Δ63, his3Δ200, lys2ΔBgl, hom3-10, ade2Δ1, ade8, YEL069C::URA3, rad5::HIS3 rdh54::G418</i> |
| KHSY5150 | <i>MATa ura3-52, leu2Δ1, trp1Δ63, his3Δ200, lys2ΔBgl, hom3-10, ade2Δ1, ade8, YEL069C::URA3, rrm3::TRP1, rdh54::HIS3, rad5::TRP1</i> |
| KHSY5151 | <i>MATa ura3-52, leu2Δ1, trp1Δ63, his3Δ200, lys2ΔBgl, hom3-10, ade2Δ1, ade8, YEL069C::URA3, set3::HIS3</i> |
| KHSY5152 | <i>MATa ura3-52, leu2Δ1, trp1Δ63, his3Δ200, lys2ΔBgl, hom3-10, ade2Δ1, ade8, YEL069C::URA3, rrm3::TRP1, set3::HIS3</i> |
| KHSY5153 | <i>MATa ura3-52, leu2Δ1, trp1Δ63, his3Δ200, lys2ΔBgl, hom3-10, ade2Δ1, ade8, YEL069C::URA3, tof1::HIS3</i> |
| KHSY5154 | <i>MATa ura3-52, leu2Δ1, trp1Δ63, his3Δ200, lys2ΔBgl, hom3-10, ade2Δ1, ade8, YEL069C::URA3, rrm3::TRP1, tof1::HIS3</i> |
| KHSY5155 | <i>MATa ura3-52, leu2Δ1, trp1Δ63, his3Δ200, lys2ΔBgl, hom3-10, ade2Δ1, ade8, YEL069C::URA3, ies4::HIS3</i> |
| KHSY5156 | <i>MATa ura3-52, leu2Δ1, trp1Δ63, his3Δ200, lys2ΔBgl, hom3-10, ade2Δ1, ade8, YEL069C::URA3, rrm3::TRP1, ies4::HIS3</i> |
| KHSY5157 | <i>MATa ura3-52, leu2Δ1, trp1Δ63, his3Δ200, lys2ΔBgl, hom3-10, ade2Δ1, ade8, YEL069C::URA3, had1::HIS3</i> |
| KHSY5158 | <i>MATa ura3-52, leu2Δ1, trp1Δ63, his3Δ200, lys2ΔBgl, hom3-10, ade2Δ1, ade8, YEL069C::URA3, rrm3::TRP1, had1::HIS3</i> |
| KHSY5159 | <i>MATa ura3-52, leu2Δ1, trp1Δ63, his3Δ200, lys2ΔBgl, hom3-10, ade2Δ1, ade8, YEL069C::URA3, mgm101::HIS3</i> |
| KHSY5160 | <i>MATa ura3-52, leu2Δ1, trp1Δ63, his3Δ200, lys2ΔBgl, hom3-10, ade2Δ1, ade8, YEL069C::URA3, rrm3::TRP1, mgm101::HIS3</i> |
| KHSY5161 | <i>MATa ura3-52, leu2Δ1, trp1Δ63, his3Δ200, lys2ΔBgl, hom3-10, ade2Δ1, ade8, YEL069C::URA3, sml1::G418</i> |
| KHSY5162 | <i>MATa ura3-52, leu2Δ1, trp1Δ63, his3Δ200, lys2ΔBgl, hom3-10, ade2Δ1, ade8, YEL069C::URA3, sml1::G418, rrm3::TRP1</i> |
| KHSY5163 | <i>MATa ura3-52, leu2Δ1, trp1Δ63, his3Δ200, lys2ΔBgl, hom3-10, ade2Δ1, ade8, YEL069C::URA3, sml1::G418, rrm3::TRP1, rad53::HIS3</i> |

Table 4.S2 (continued)

| | |
|----------|--|
| KHSY5164 | <i>ura3-52/ura3-52, leu2Δ1/leu2Δ1, trp1Δ63/trp1Δ63, his3Δ200/his3Δ200, lys2ΔBgl/lys2ΔBgl, hom3-10/hom3-10, ade2Δ1/ade2Δ1, ade8/ade8. YEL069C::URA3/YEL069C::URA3, rdh54::HIS3/rdh54::HIS3</i> |
| KHSY5165 | <i>ura3-52/ura3-52, leu2Δ1/leu2Δ1, trp1Δ63/trp1Δ63, his3Δ200/his3Δ200, lys2ΔBgl/lys2ΔBgl, hom3-10/hom3-10, ade2Δ1/ade2Δ1, ade8/ade8. YEL069C::URA3/YEL069C::URA3, rrm3::TRP1/rrm3::TRP1, rdh54::HIS3/rdh54::HIS3</i> |
| KHSY5166 | <i>ura3-52/ura3-52, leu2Δ1/leu2Δ1, trp1Δ63/trp1Δ63, his3Δ200/his3Δ200, lys2ΔBgl/lys2ΔBgl, hom3-10/hom3-10, ade2Δ1/ade2Δ1, ade8/ade8. YEL069C::URA3/YEL069C::URA3, rrm3::TRP1/rrm3::TRP1</i> |
| KHSY5167 | <i>ura3-52/ura3-52, leu2Δ1/leu2Δ1, trp1Δ63/trp1Δ63, his3Δ200/his3Δ200, lys2ΔBgl/lys2ΔBgl, hom3-10/hom3-10, ade2Δ1/ade2Δ1, ade8/ade8. YEL069C::URA3/YEL069C::URA3, RRM3/rrm3::TRP1, RDH54/rdh54::HIS3</i> |
| KHSY5168 | <i>ura3-52/ura3-52, leu2Δ1/leu2Δ1, trp1Δ63/trp1Δ63, his3Δ200/his3Δ200, lys2ΔBgl/lys2ΔBgl, hom3-10/hom3-10, ade2Δ1/ade2Δ1, ade8/ade8. YEL069C::URA3/YEL069C::URA3, RRM3/rrm3::TRP1</i> |
| KHSY5169 | <i>ura3-52/ura3-52, leu2Δ1/leu2Δ1, trp1Δ63/trp1Δ63, his3Δ200/his3Δ200, lys2ΔBgl/lys2ΔBgl, hom3-10/hom3-10, ade2Δ1/ade2Δ1, ade8/ade8. YEL069C::URA3/YEL069C::URA3, RDH54/rdh54::HIS3</i> |
| KHSY5170 | <i>ura3-52/ura3-52, leu2Δ1/leu2Δ1, trp1Δ63/trp1Δ63, his3Δ200/his3Δ200, lys2ΔBgl/lys2ΔBgl, hom3-10/hom3-10, ade2Δ1/ade2Δ1, ade8/ade8. YEL069C::URA3/YEL069C::URA3, RRM3/rrm3::TRP1, rdh54::HIS3/rdh54::HIS3</i> |
| KHSY5171 | <i>ura3-52/ura3-52, leu2Δ1/leu2Δ1, trp1Δ63/trp1Δ63, his3Δ200/his3Δ200, lys2ΔBgl/lys2ΔBgl, hom3-10/hom3-10, ade2Δ1/ade2Δ1, ade8/ade8. YEL069C::URA3/YEL069C::URA3, rrm3::TRP1/rrm3::TRP1, RDH54/rdh54::HIS3</i> |

1. Gyuris, J., et al., *Cdi1, a human G1 and S phase protein phosphatase that associates with Cdk2*. Cell, 1993. **75**(4): p. 791-803.

TABLE 4.S3. Plasmids used in this study

| Plasmid | Description | Reference |
|----------------|---|------------------------------|
| pRS315 | <i>CEN/ARS, LEU2</i> | (Sikorski and Hieter 1989) |
| pEG202 | LexA bait plasmid, <i>HIS3</i> , 2 μ m | (Estojak, Brent et al. 1995) |
| pR5-19 | <i>CEN/ARS, LEU2, rad5-C914A/C917A</i> | (Pages, Bresson et al. 2008) |
| pR5-28 | <i>CEN/ARS, LEU2, RAD5</i> | (Pages, Bresson et al. 2008) |
| pR5-30 | <i>CEN/ARS, LEU2, rad5-D681A/E682A</i> | (Pages, Bresson et al. 2008) |
| pJG4-5* | <i>GALI</i> promoter- <i>GAL4</i> _{AD} , <i>TRP1</i> , 2 μ m | (Schmidt, Derry et al. 2002) |
| pKHS124 | <i>pJG-4-5*-RRM3</i> | (Schmidt, Derry et al. 2002) |
| pKHS126 | <i>pEG202-RRM3</i> | (Schmidt, Derry et al. 2002) |
| pKHS133 | <i>pEG202-rrm3-ΔN54</i> | (Schmidt, Derry et al. 2002) |
| pKHS135 | <i>pEG202-rrm3ΔN230</i> | (Schmidt, Derry et al. 2002) |
| pKHS136 | <i>pRS315-rrm3-ΔN54</i> | this study |
| pKHS137 | <i>pRS315-rrm3-ΔN230</i> | this study |
| pKHS170 | <i>pRS315-RRM3</i> | this study |
| pKHS174 | <i>pRS315-rrm3-F41A/F42A</i> | this study |
| pKHS183 | <i>pEG202-rrm3-F41A/F42A</i> | (Schmidt, Derry et al. 2002) |
| pKHS644 | <i>pR5-30-rad5-D681A/E682A/C914A/C917A</i> | this study |
| pKHS645 | <i>pRS315-rrm3-NΔ142</i> | this study |
| pKHS646 | <i>pRS315-rrm3-ΔN186</i> | this study |
| pKHS647 | <i>pRS315-rrm3-Δ212</i> | this study |
| pKHS648 | <i>pRS315-rrm3-K260A</i> | this study |
| pKHS649 | <i>pRS315-rrm3-K260D</i> | this study |
| pKHS650 | <i>pRS315-rrm3-D102P</i> | this study |
| pKHS651 | <i>pRS315-rrm3-S605A</i> | this study |
| pKHS652 | <i>pRS315-rrm3-S605D</i> | this study |
| pKHS653 | <i>peg202-rrm3-ΔN186</i> | this study |
| pKHS654 | <i>peg202-rrm3-ΔN212</i> | this study |
| pKHS655 | <i>peg202-rrm3-ΔN230</i> | (Schmidt, Derry et al. 2002) |

Table 4.S3 (continued)

| | | |
|---------|---------------------|------------|
| pKHS656 | <i>pJG4-5*-ORC5</i> | this study |
|---------|---------------------|------------|

REFERENCES

- Alcasabas, A. A., A. J. Osborn, J. Bachant, F. Hu, P. J. Werler, K. Bousset, K. Furuya, J. F. Diffley, A. M. Carr and S. J. Elledge (2001). "Mrc1 transduces signals of DNA replication stress to activate Rad53." Nat Cell Biol **3**(11): 958-965.
- Azvolinsky, A., S. Dunaway, J. Z. Torres, J. B. Bessler and V. A. Zakian (2006). "The *S. cerevisiae* Rrm3p DNA helicase moves with the replication fork and affects replication of all yeast chromosomes." Genes Dev **20**(22): 3104-3116.
- Bell, S. P. and A. Dutta (2002). "DNA replication in eukaryotic cells." Annu Rev Biochem **71**: 333-374.
- Benjamini, Y., D. Drai, G. Elmer, N. Kafkafi and I. Golani (2001). "Controlling the false discovery rate in behavior genetics research." Behav Brain Res **125**(1-2): 279-284.
- Blastyak, A., I. Hajdu, I. Unk and L. Haracska (2010). "Role of double-stranded DNA translocase activity of human HLTF in replication of damaged DNA." Mol Cell Biol **30**(3): 684-693.
- Blastyak, A., L. Pinter, I. Unk, L. Prakash, S. Prakash and L. Haracska (2007). "Yeast Rad5 protein required for postreplication repair has a DNA helicase activity specific for replication fork regression." Mol Cell **28**(1): 167-175.
- Bowers, J. L., J. C. Randell, S. Chen and S. P. Bell (2004). "ATP hydrolysis by ORC catalyzes reiterative Mcm2-7 assembly at a defined origin of replication." Mol Cell **16**(6): 967-978.
- Branzei, D., J. Sollier, G. Liberi, X. Zhao, D. Maeda, M. Seki, T. Enomoto, K. Ohta and M. Foiani (2006). "Ubc9- and mms21-mediated sumoylation counteracts recombinogenic events at damaged replication forks." Cell **127**(3): 509-522.
- Chi, P., Y. Kwon, C. Seong, A. Epshtein, I. Lam, P. Sung and H. L. Klein (2006). "Yeast recombination factor Rdh54 functionally interacts with the Rad51 recombinase and catalyzes Rad51 removal from DNA." J Biol Chem **281**(36): 26268-26279.
- Cox, J. and M. Mann (2008). "MaxQuant enables high peptide identification rates, individualized p.p.b.-range mass accuracies and proteome-wide protein quantification." Nat Biotechnol **26**(12): 1367-1372.
- Crabbe, L., A. Thomas, V. Pantesco, J. De Vos, P. Pasero and A. Lengronne (2010). "Analysis of replication profiles reveals key role of RFC-Ctf18 in yeast replication stress response." Nat Struct Mol Biol **17**(11): 1391-1397.
- Desler, C., B. Munch-Petersen, T. Stevnsner, S. Matsui, M. Kulawiec, K. K. Singh and L. J. Rasmussen (2007). "Mitochondria as determinant of nucleotide pools and chromosomal stability." Mutat Res **625**(1-2): 112-124.

- Estojak, J., R. Brent and E. A. Golemis (1995). "Correlation of two-hybrid affinity data with in vitro measurements." Mol Cell Biol **15**(10): 5820-5829.
- Fachinetti, D., R. Bermejo, A. Cocito, S. Minardi, Y. Katou, Y. Kanoh, K. Shirahige, A. Azvolinsky, V. A. Zakian and M. Foiani (2010). "Replication termination at eukaryotic chromosomes is mediated by Top2 and occurs at genomic loci containing pausing elements." Mol Cell **39**(4): 595-605.
- Gangavarapu, V., L. Haracska, I. Unk, R. E. Johnson, S. Prakash and L. Prakash (2006). "Mms2-Ubc13-dependent and -independent roles of Rad5 ubiquitin ligase in postreplication repair and translesion DNA synthesis in *Saccharomyces cerevisiae*." Mol Cell Biol **26**(20): 7783-7790.
- Gietz, R. D. and R. A. Woods (2006). "Yeast transformation by the LiAc/SS Carrier DNA/PEG method." Methods Mol Biol **313**: 107-120.
- Gsponer, J. and M. M. Babu (2009). "The rules of disorder or why disorder rules." Prog Biophys Mol Biol **99**(2-3): 94-103.
- Haracska, L., C. A. Torres-Ramos, R. E. Johnson, S. Prakash and L. Prakash (2004). "Opposing effects of ubiquitin conjugation and SUMO modification of PCNA on replicational bypass of DNA lesions in *Saccharomyces cerevisiae*." Mol Cell Biol **24**(10): 4267-4274.
- Hochberg, Y. and Y. Benjamini (1990). "More powerful procedures for multiple significance testing." Stat Med **9**(7): 811-818.
- Hodgson, B., A. Calzada and K. Labib (2007). "Mrc1 and Tof1 regulate DNA replication forks in different ways during normal S phase." Mol Biol Cell **18**(10): 3894-3902.
- Hoege, C., B. Pfander, G. L. Moldovan, G. Pyrowolakis and S. Jentsch (2002). "RAD6-dependent DNA repair is linked to modification of PCNA by ubiquitin and SUMO." Nature **419**(6903): 135-141.
- Holzen, T. M., P. P. Shah, H. A. Olivares and D. K. Bishop (2006). "Tid1/Rdh54 promotes dissociation of Dmc1 from nonrecombinogenic sites on meiotic chromatin." Genes Dev **20**(18): 2593-2604.
- Huang, M. E., A. G. Rio, A. Nicolas and R. D. Kolodner (2003). "A genomewide screen in *Saccharomyces cerevisiae* for genes that suppress the accumulation of mutations." Proc Natl Acad Sci U S A **100**(20): 11529-11534.
- Ivessa, A. S., B. A. Lenzmeier, J. B. Bessler, L. K. Goudsouzian, S. L. Schnakenberg and V. A. Zakian (2003). "The *Saccharomyces cerevisiae* helicase Rrm3p facilitates replication past nonhistone protein-DNA complexes." Mol Cell **12**(6): 1525-1536.

- Ivessa, A. S., J. Q. Zhou, V. P. Schulz, E. K. Monson and V. A. Zakian (2002). "Saccharomyces Rrm3p, a 5' to 3' DNA helicase that promotes replication fork progression through telomeric and subtelomeric DNA." Genes Dev **16**(11): 1383-1396.
- Ivessa, A. S., J. Q. Zhou and V. A. Zakian (2000). "The Saccharomyces Pif1p DNA helicase and the highly related Rrm3p have opposite effects on replication fork progression in ribosomal DNA." Cell **100**(4): 479-489.
- Johnson, R. E., S. T. Henderson, T. D. Petes, S. Prakash, M. Bankmann and L. Prakash (1992). "Saccharomyces cerevisiae RAD5-encoded DNA repair protein contains DNA helicase and zinc-binding sequence motifs and affects the stability of simple repetitive sequences in the genome." Mol Cell Biol **12**(9): 3807-3818.
- Johnson, R. E., S. Prakash and L. Prakash (1994). "Yeast DNA repair protein RAD5 that promotes instability of simple repetitive sequences is a DNA-dependent ATPase." J Biol Chem **269**(45): 28259-28262.
- Johnson, R. E., S. Prakash and L. Prakash (1999). "Efficient bypass of a thymine-thymine dimer by yeast DNA polymerase, Poleta." Science **283**(5404): 1001-1004.
- Katou, Y., Y. Kanoh, M. Bando, H. Noguchi, H. Tanaka, T. Ashikari, K. Sugimoto and K. Shirahige (2003). "S-phase checkpoint proteins Tof1 and Mrc1 form a stable replication-pausing complex." Nature **424**(6952): 1078-1083.
- Keil, R. L. and A. D. McWilliams (1993). "A gene with specific and global effects on recombination of sequences from tandemly repeated genes in Saccharomyces cerevisiae." Genetics **135**(3): 711-718.
- Kennedy, J. A., G. W. Daughdrill and K. H. Schmidt (2013). "A transient alpha-helical molecular recognition element in the disordered N-terminus of the Sgs1 helicase is critical for chromosome stability and binding of Top3/Rmi1." Nucleic Acids Res **41**(22): 10215-10227.
- Klein, H. L. (1997). "RDH54, a RAD54 homologue in Saccharomyces cerevisiae, is required for mitotic diploid-specific recombination and repair and for meiosis." Genetics **147**(4): 1533-1543.
- Kobayashi, T. (2003). "The replication fork barrier site forms a unique structure with Fob1p and inhibits the replication fork." Mol Cell Biol **23**(24): 9178-9188.
- Kobayashi, T., M. Nomura and T. Horiuchi (2001). "Identification of DNA cis elements essential for expansion of ribosomal DNA repeats in Saccharomyces cerevisiae." Mol Cell Biol **21**(1): 136-147.
- Kubota, T., D. A. Stead, S. Hiraga, S. ten Have and A. D. Donaldson (2012). "Quantitative proteomic analysis of yeast DNA replication proteins." Methods **57**(2): 196-202.

- Kwon, Y., C. Seong, P. Chi, E. C. Greene, H. Klein and P. Sung (2008). "ATP-dependent chromatin remodeling by the *Saccharomyces cerevisiae* homologous recombination factor Rdh54." J Biol Chem **283**(16): 10445-10452.
- Labib, K. (2010). "How do Cdc7 and cyclin-dependent kinases trigger the initiation of chromosome replication in eukaryotic cells?" Genes Dev **24**(12): 1208-1219.
- Lea, D. E. and C. A. Coulson (1949). "The distribution of the numbers of mutants in bacterial populations." J Genet **49**(3): 264-285.
- Luke, B., G. Versini, M. Jaquenoud, I. W. Zaidi, T. Kurz, L. Pintard, P. Pasero and M. Peter (2006). "The cullin Rtt101p promotes replication fork progression through damaged DNA and natural pause sites." Curr Biol **16**(8): 786-792.
- Matsuda, K., M. Makise, Y. Sueyasu, M. Takehara, T. Asano and T. Mizushima (2007). "Yeast two-hybrid analysis of the origin recognition complex of *Saccharomyces cerevisiae*: interaction between subunits and identification of binding proteins." FEMS Yeast Res **7**(8): 1263-1269.
- Minca, E. C. and D. Kowalski (2010). "Multiple Rad5 activities mediate sister chromatid recombination to bypass DNA damage at stalled replication forks." Mol Cell **38**(5): 649-661.
- Mohanty, B. K., N. K. Bairwa and D. Bastia (2006). "The Tof1p-Csm3p protein complex counteracts the Rrm3p helicase to control replication termination of *Saccharomyces cerevisiae*." Proc Natl Acad Sci U S A **103**(4): 897-902.
- Mohanty, B. K., N. K. Bairwa and D. Bastia (2009). "Contrasting roles of checkpoint proteins as recombination modulators at Fob1-Ter complexes with or without fork arrest." Eukaryot Cell **8**(4): 487-495.
- Mohanty, B. K. and D. Bastia (2004). "Binding of the replication terminator protein Fob1p to the Ter sites of yeast causes polar fork arrest." J Biol Chem **279**(3): 1932-1941.
- Nair, K. R. (1940). "Table of confidence intervals for the median in samples from any continuous population." Sankhya(4): 551-558.
- Nash, R., G. Tokiwa, S. Anand, K. Erickson and A. B. Futcher (1988). "The WHI1+ gene of *Saccharomyces cerevisiae* tethers cell division to cell size and is a cyclin homolog." EMBO J **7**(13): 4335-4346.
- Naylor, M. L., J. M. Li, A. J. Osborn and S. J. Elledge (2009). "Mrc1 phosphorylation in response to DNA replication stress is required for Mec1 accumulation at the stalled fork." Proc Natl Acad Sci U S A **106**(31): 12765-12770.
- Nelson, J. R., C. W. Lawrence and D. C. Hinkle (1996). "Thymine-thymine dimer bypass by yeast DNA polymerase zeta." Science **272**(5268): 1646-1649.

Ong, S. E., B. Blagoev, I. Kratchmarova, D. B. Kristensen, H. Steen, A. Pandey and M. Mann (2002). "Stable isotope labeling by amino acids in cell culture, SILAC, as a simple and accurate approach to expression proteomics." Mol Cell Proteomics **1**(5): 376-386.

Ong, S. E. and M. Mann (2006). "A practical recipe for stable isotope labeling by amino acids in cell culture (SILAC)." Nat Protoc **1**(6): 2650-2660.

Ortiz-Bazan, M. A., M. Gallo-Fernandez, I. Saugar, A. Jimenez-Martin, M. V. Vazquez and J. A. Tercero (2014). "Rad5 plays a major role in the cellular response to DNA damage during chromosome replication." Cell Rep **9**(2): 460-468.

Osborn, A. J. and S. J. Elledge (2003). "Mrc1 is a replication fork component whose phosphorylation in response to DNA replication stress activates Rad53." Genes Dev **17**(14): 1755-1767.

Pages, V., A. Bresson, N. Acharya, S. Prakash, R. P. Fuchs and L. Prakash (2008). "Requirement of Rad5 for DNA polymerase zeta-dependent translesion synthesis in *Saccharomyces cerevisiae*." Genetics **180**(1): 73-82.

Petukhova, G., P. Sung and H. Klein (2000). "Promotion of Rad51-dependent D-loop formation by yeast recombination factor Rdh54/Tid1." Genes Dev **14**(17): 2206-2215.

Poli, J., O. Tsaponina, L. Crabbe, A. Keszthelyi, V. Pantesco, A. Chabes, A. Lengronne and P. Pasero (2012). "dNTP pools determine fork progression and origin usage under replication stress." EMBO J **31**(4): 883-894.

Prakash, S., R. E. Johnson and L. Prakash (2005). "Eukaryotic translesion synthesis DNA polymerases: specificity of structure and function." Annu Rev Biochem **74**: 317-353.

Randell, J. C., J. L. Bowers, H. K. Rodriguez and S. P. Bell (2006). "Sequential ATP hydrolysis by Cdc6 and ORC directs loading of the Mcm2-7 helicase." Mol Cell **21**(1): 29-39.

Reenan, R. A. and R. D. Kolodner (1992). "Characterization of insertion mutations in the *Saccharomyces cerevisiae* MSH1 and MSH2 genes: evidence for separate mitochondrial and nuclear functions." Genetics **132**(4): 975-985.

Rockmill, B., E. J. Lambie and G. S. Roeder (1991). "Spore enrichment." Methods Enzymol **194**: 146-149.

Rossi, S. E., A. Ajazi, W. Carotenuto, M. Foiani and M. Giannattasio (2015). "Rad53-Mediated Regulation of Rrm3 and Pif1 DNA Helicases Contributes to Prevention of Aberrant Fork Transitions under Replication Stress." Cell Rep.

San Filippo, J., P. Sung and H. Klein (2008). "Mechanism of eukaryotic homologous recombination." Annu Rev Biochem **77**: 229-257.

Santocanale, C. and J. F. Diffley (1998). "A Mec1- and Rad53-dependent checkpoint controls late-firing origins of DNA replication." Nature **395**(6702): 615-618.

Schmidt, K. H., K. L. Derry and R. D. Kolodner (2002). "Saccharomyces cerevisiae RRM3, a 5' to 3' DNA helicase, physically interacts with proliferating cell nuclear antigen." J Biol Chem **277**(47): 45331-45337.

Schmidt, K. H. and R. D. Kolodner (2004). "Requirement of Rrm3 helicase for repair of spontaneous DNA lesions in cells lacking Srs2 or Sgs1 helicase." Mol Cell Biol **24**(8): 3213-3226.

Schmidt, K. H. and R. D. Kolodner (2006). "Suppression of spontaneous genome rearrangements in yeast DNA helicase mutants." Proc Natl Acad Sci U S A **103**(48): 18196-18201.

Schmidt, K. H., V. Pennaneach, C. D. Putnam and R. D. Kolodner (2006). "Analysis of gross-chromosomal rearrangements in Saccharomyces cerevisiae." Methods Enzymol **409**: 462-476.

Schmidt, K. H., E. B. Viebranz, L. B. Harris, H. Mirzaei-Souderjani, S. Syed and R. Medicus (2010). "Defects in DNA lesion bypass lead to spontaneous chromosomal rearrangements and increased cell death." Eukaryot Cell **9**(2): 315-324.

Shah, P. P., X. Zheng, A. Epshtein, J. N. Carey, D. K. Bishop and H. L. Klein (2010). "Swi2/Snf2-related translocases prevent accumulation of toxic Rad51 complexes during mitotic growth." Mol Cell **39**(6): 862-872.

Shimada, K., P. Pasero and S. M. Gasser (2002). "ORC and the intra-S-phase checkpoint: a threshold regulates Rad53p activation in S phase." Genes Dev **16**(24): 3236-3252.

Shinohara, M., E. Shita-Yamaguchi, J. M. Buerstedde, H. Shinagawa, H. Ogawa and A. Shinohara (1997). "Characterization of the roles of the Saccharomyces cerevisiae RAD54 gene and a homologue of RAD54, RDH54/TID1, in mitosis and meiosis." Genetics **147**(4): 1545-1556.

Shirahige, K., Y. Hori, K. Shiraishi, M. Yamashita, K. Takahashi, C. Obuse, T. Tsurimoto and H. Yoshikawa (1998). "Regulation of DNA-replication origins during cell-cycle progression." Nature **395**(6702): 618-621.

Shor, E., C. L. Warren, J. Tietjen, Z. Hou, U. Muller, I. Alborelli, F. H. Gohard, A. I. Yemm, L. Borisov, J. R. Broach, M. Weinreich, C. A. Nieduszynski, A. Z. Ansari and C. A. Fox (2009). "The origin recognition complex interacts with a subset of metabolic genes tightly linked to origins of replication." PLoS Genet **5**(12): e1000755.

Sikorski, R. S. and P. Hieter (1989). "A system of shuttle vectors and yeast host strains designed for efficient manipulation of DNA in Saccharomyces cerevisiae." Genetics **122**(1): 19-27.

- Soriano, I., E. C. Morafraila, E. Vazquez, F. Antequera and M. Segurado (2014). "Different nucleosomal architectures at early and late replicating origins in *Saccharomyces cerevisiae*." BMC Genomics **15**: 791.
- Stamenova, R., P. H. Maxwell, A. E. Kenny and M. J. Curcio (2009). "Rrm3 protects the *Saccharomyces cerevisiae* genome from instability at nascent sites of retrotransposition." Genetics **182**(3): 711-723.
- Suter, B., A. Tong, M. Chang, L. Yu, G. W. Brown, C. Boone and J. Rine (2004). "The origin recognition complex links replication, sister chromatid cohesion and transcriptional silencing in *Saccharomyces cerevisiae*." Genetics **167**(2): 579-591.
- Szyjka, S. J., C. J. Viggiani and O. M. Aparicio (2005). "Mrc1 is required for normal progression of replication forks throughout chromatin in *S. cerevisiae*." Mol Cell **19**(5): 691-697.
- Torres, J. Z., S. L. Schnakenberg and V. A. Zakian (2004). "*Saccharomyces cerevisiae* Rrm3p DNA helicase promotes genome integrity by preventing replication fork stalling: viability of *rrm3* cells requires the intra-S-phase checkpoint and fork restart activities." Mol Cell Biol **24**(8): 3198-3212.
- Torres-Ramos, C. A., S. Prakash and L. Prakash (2002). "Requirement of RAD5 and MMS2 for postreplication repair of UV-damaged DNA in *Saccharomyces cerevisiae*." Mol Cell Biol **22**(7): 2419-2426.
- Tourriere, H., G. Versini, V. Cordon-Preciado, C. Alabert and P. Pasero (2005). "Mrc1 and Tof1 promote replication fork progression and recovery independently of Rad53." Mol Cell **19**(5): 699-706.
- Tsaponina, O. and J. E. Haber (2014). "Frequent Interchromosomal Template Switches during Gene Conversion in *S. cerevisiae*." Mol Cell **55**(4): 615-625.
- Ulrich, H. D. and S. Jentsch (2000). "Two RING finger proteins mediate cooperation between ubiquitin-conjugating enzymes in DNA repair." EMBO J **19**(13): 3388-3397.
- Xu, H., C. Boone and H. L. Klein (2004). "Mrc1 is required for sister chromatid cohesion to aid in recombination repair of spontaneous damage." Mol Cell Biol **24**(16): 7082-7090.
- Zhao, X. and R. Rothstein (2002). "The Dun1 checkpoint kinase phosphorylates and regulates the ribonucleotide reductase inhibitor Sml1." Proc Natl Acad Sci U S A **99**(6): 3746-3751.

CHAPTER FIVE: IMPLICATIONS AND FUTURE DIRECTIONS

IMPLICATIONS

DNA helicases are conserved amongst species and are enzymes that function to unwind DNA in several processes, including replication, DNA repair, and transcription. Defective helicases can lead to human genetic disorders with high incidence of genomic instability and predisposition to cancer. For example, mutations to *XPB* and *XPD*, can result in xeroderma pigmentosum, Cockayne syndrome, or trichothiodystrophy [1-3]. Mutations to these genes result in defects during nucleotide excision repair and transcription [3]. Mutations to the RecQ family members in humans, *BLM*, *WRN*, and *RECQL4* can result in Bloom syndrome, Werner syndrome, and Rothmund-Thomson syndrome [4-9] and these patients are characterized by having increased genomic instability and mutation rates [10-12]. If the integrity of the genome is not maintained from one generation to another, chromosomal defects may arise, which can result in cancer predisposition, developmental defects, and premature aging. Better understanding the role of these helicases in DNA repair may allow us to better develop therapeutic approaches to help individuals affected by these syndromes and allow for a better quality of life.

Here we investigated the role of RecQ-like helicases Sgs1, BLM and RecQL5 using yeast as a model system. We also looked at a non-RecQ-like helicase, Rrm3,

which is involved in maintaining genome stability by promoting fork progression.

FUTURE DIRECTIONS

Humanized yeast model for BLM characterization

In chapter two of this dissertation we were able to create a yeast model to study BLM function [13]. This humanized yeast model was used to study the functional impact of 27 variants in the C terminal region of BLM and with this approach we found nine new functionally defective BLM variants [13, 14]. Unlike the known Bloom syndrome, causing mutations that have been characterized biochemically, these new variants are uncharacterized and may be informative in better understanding BLM function [8]. Of the newly identified variants, three only partially impair BLM function, leading to a new class of *BLM* alleles that may have an impact on the risk for disease [14]. These new variants in BLM (R791C, P868L, G1120R) were evaluated in patient derived BLM deficient cells (GMO8505) to determine if they complement cellular defects [15]. These variants were tested for their ability to suppress sister chromatid exchanges, resistance to DNA damage, and ability to induce the DNA damage response [15]. Through these assays it was found that these variants produced defects similar to a Bloom syndrome cell, but these defects were less pronounced [15]. The implication for this study and discovery of these new variants is that individuals who possess these variants may have an increased risk for cancer or Bloom syndrome associated disorders. The next step is to biochemically characterize these variants and determine if they have defects in catalytic activity. For this, we will look at DNA binding, unwinding, and annealing activities of these variants.

RQC domain of Sgs1 is critical in maintaining genome stability, whereas the HRDC domain is dispensable

In chapter two of this dissertation we created systematic truncations to the C terminus of Sgs1 and found that impinging on the RQC domain was deleterious to the cell whereas removing the HRDC domain had no effect [13]. To further narrow down the requirement of the C terminus of Sgs1 we further truncated the region between Sgs1 1147-1247 and found that deleting C terminal 260 amino acids resulted in sensitivity to DNA damaging agents HU and MMS and there was an accumulation of gross chromosomal rearrangements [13]. We looked at the possibility that the inability of the *sgs1* Δ C260 mutant to resist DNA damaging agents was due to loss of protein-protein interaction. It has been shown previously that Rad51 interacts with the C terminus of Sgs1 but the precise location of this interaction has not been determined [16]. Using pull down experiments we have validated Sgs1-Rad51 interaction and isolated the interaction to regions 1187-1207 of Sgs1. We narrowed down the binding site to the flexible linker region between the winged helix and HRDC domains and have found important residues for binding. Generating a Sgs1F1197D mutant located within this region resulted in loss of interaction with Rad51. In contrast to the *sgs1* Δ C260 truncation, Sgs1F1197D was resistant to DNA damaging agents suggesting that loss of interaction with Rad51 is not important for conferring resistance but may be important for other functions of Sgs1, and that impinging on the RQC domain is deleterious to the cell. This interaction is being genetically characterized to see if this loss of interaction is important in combination with other DNA metabolic factors.

Novel RecQL5 interaction with Ube2I and Hlp2

In this dissertation we looked at the human RecQ like helicase, RecQL5 β , which has not been associated with a syndrome but defects in this helicase lead to increased levels of sister chromatid exchanges, broken chromosomes, and quadriradials [17, 18]. To better understand the molecular mechanism of this helicase we used yeast as a model system to investigate its ability to complement Sgs1 functions. We found that it is unable to perform functions of Sgs1 suggesting its role in the cell is different than its Sgs1 counterpart, BLM. We performed a yeast two-hybrid assay using the human testis cDNA library to gain better insight into functions of RecQL5 by determining proteins it interacts with. From this screen we found that Hlp2 and Ube2I showed strong interaction with RecQL5. Human Hlp2 is an ATP-dependent RNA helicase that belongs to the DEAD box family of helicases [19, 20]. Ube2I is a SUMO-conjugating enzyme that has several roles in regulating DNA repair [21]. To further investigate these interactions we will use two approaches.

Interaction will be tested first by performing co-immunoprecipitation of endogenous proteins or tagged protein. If interaction is verified then we will map the interaction domain of each protein by placing a stop codon using site-directed mutagenesis and evaluate this loss of interaction in cells. If the co-immunoprecipitation approach fails to work we will determine protein-protein interactions by mass spectrometry. For mass spectrometry, we will create a stable cell line expressing Flag-tagged RecQL5 and immunoprecipitate tagged RecQL5 and isolate polypeptides for analysis by mass spectrometry. This approach will help confirm interaction of our proteins and may elucidate new candidates for further study. We will then perform a

reciprocal IP using antibodies against Hlp2 and Ube2I to determine if we can identify RecQL5. We will look for interaction with Rad51, PCNA, and the MRN complex as positive controls.

In addition to the helicase domain and RQC domain, RecQL5 also possess a KIX domain and SRI domain [22, 23]. The KIX domain is located between amino acids 540-620 and the SRI domain is between 909-991 amino acids [23]. The KIX domain has been found in many Pol II transcriptional regulators and the SRI domain is found in the histone methyltransferase SetD2, which also has a role in transcription [22]. It is possible that RecQL5 interaction with Hlp2 may help regulate transcription and prevent head-on collisions between the replication and transcription machinery, resulting in fewer stalled forks [24].

To test if the interaction with Hlp2 is regulating transcription we can recreate mammalian RNAPII transcription using purified general transcription factors (GTFs), RNAPII, and template DNA with a adenovirus major late promoter. To determine if RecQL5 is inhibitory to transcription, we can add increasing concentration of RecQL5 and observe the production of the transcript. After determining the site of Hlp2 interaction we can create a point mutation abolishing this interaction and perform the same experiment to determine if interaction with Hlp2 is regulating transcription and should see more run-off transcripts if this interaction is important. Additionally, we can determine if this regulation is helicase dependent by generating point mutations inactivating the helicase activity of RecQL5 (D157A) and loss of protein-protein interaction. It will be interesting to see if RecQL5 has dual roles, one in maintaining genome stability by preventing head-on collisions between the replication and

transcription machineries and another in preventing chromosomal instability by using its helicase activity to reduce unwanted homologous recombination events through its ability to resolve D loops [25].

Unlike Hlp2, Ube2I is a SUMO-conjugating enzyme that can regulate DNA repair, the stress response, and cell cycle progression [21]. Since Ube2I has a more diverse role in cell compared to Hlp2, it is possible that RecQL5 may target Ube2I to sites of DNA damage so that it can regulate downstream proteins for repair. Determining the interaction site of this protein on RecQL5 will help determine if it interacts with any RecQL5 conserved domains. We can then create targeted point mutations to assess if loss of interaction with Ube2I contributes to some of the cellular defects in cells deficient for RecQL5. We can perform similar assays looking at the role of RecQL5-Ube2I interaction during transcription by assessing formation of run-off transcripts. It is more reasonable to assume that interaction with Ube2I is important for maintaining genome stability by regulating repair during replication, possibly by preventing sister chromatid exchanges. It has been shown previously in DT40 cells that deleting *RecQL5*^{-/-} / *BLM*^{-/-} resulted in higher SCE level than *BLM*^{-/-} cells [26]. Introducing RecQL5 into *RecQL5*^{-/-} / *BLM*^{-/-} resulted in a level similar to *BLM*^{-/-} cells [26]. Considering RecQL5 can suppress SCEs in this double mutant, we can look at the importance of interaction with Hlp2 and Ube2I in preventing SCEs. In addition to increased SCEs in the absence of *RecQL5*^{-/-}, these cells also have increased sensitivity to camptothecin, a topoisomerase I inhibitor that blocks replication [26]. *RecQL5*^{-/-} / *BLM*^{-/-} cells have a synergistic increase in sensitivity to CPT, so we can look at RecQL5 interactions to see if they are important in suppressing this sensitivity. Through these experiments it will be possible to determine

the importance of these protein-protein interactions and better determine the molecular mechanism of RecQL5 in DNA repair.

New role for Rrm3 in controlling replication

In addition to RecQ like helicases we also looked at a non-RecQ like helicase, Rrm3, which is involved in promoting fork progression through protein-DNA complexes. Using quantitative mass spectrometry we were able to find two significant mechanisms that act on DNA lesions created in the absence of Rrm3 catalytic activity. Rdh54, is a chromatin remodeler, and Rad5 is involved in error-free DNA damage bypass, and both were significantly increased in our screen [27, 28]. In addition to this, we found a novel function for Rrm3 in controlling replication through residues 186-212 that interact with Orc5. In the absence of this region we observe that cells replicate much faster, and this is independent of activation of Rad53, suggesting Rrm3 is physically controlling the activity of origins where Orc5 is located.

To test if Rrm3 is controlling origin activity, we can perform an experiment where we probe for origins in specific loci where Rrm3 is thought to function such as highly transcribed regions, rRNA and tRNA coding loci, and highly transcribed metabolic genes [29, 30]. Using 2D gel electrophoresis we can probe for origins in cells lacking Rrm3 under replication stress to see if they have fired. Alternatively, we can use a genomics approach and perform NextGen sequencing to look at origins. This approach will reveal more detail because we can look at all origins and determine precisely where Rrm3 may play a role. To determine mechanistically how it controls replication we will look at the interaction sites between Rrm3 and Orc5. Orc5 is the ATP-binding subunit of

the origin recognition complex (ORC) and is an essential gene. We hypothesize that Rrm3 has a role in controlling origin activity by inhibiting Orc5 activity, possibly by preventing it from binding ATP and initiating replication. To validate this, we can use two approaches. First we can generate truncations to Orc5 keeping in mind not to disturb the ATP-binding subunit and locate the interaction site for Rrm3. Alternatively, we can perform an experiment where we pull down Rrm3 in yeast and analyze the sample using mass spectrometry and analyze the results to see which peptides from Orc5 interact with Rrm3.

Through these approaches we can gain a better understanding of how the genome deals with stalled replication forks and replication stress. Determining where Rrm3 plays a role will help us better understand whether it has a global role in the cell or a more specific role in controlling replication.

REFERENCES

1. Coin, F., et al., *Mutations in XPB and XPD helicases found in xeroderma pigmentosum patients impair the transcription function of TFIIH*. EMBO J, 1999. **18**(5): p. 1357-66.
2. Cooper, P.K., et al., *Defective transcription-coupled repair of oxidative base damage in Cockayne syndrome patients from XP group G*. Science, 1997. **275**(5302): p. 990-3.
3. Cleaver, J.E., et al., *A summary of mutations in the UV-sensitive disorders: xeroderma pigmentosum, Cockayne syndrome, and trichothiodystrophy*. Hum Mutat, 1999. **14**(1): p. 9-22.
4. Ellis, N.A., et al., *The Bloom's syndrome gene product is homologous to RecQ helicases*. Cell, 1995. **83**(4): p. 655-66.
5. Yu, C.E., et al., *Positional cloning of the Werner's syndrome gene*. Science, 1996. **272**(5259): p. 258-62.
6. Kitao, S., et al., *Cloning of two new human helicase genes of the RecQ family: biological significance of multiple species in higher eukaryotes*. Genomics, 1998. **54**(3): p. 443-52.
7. Kitao, S., et al., *Mutations in RECQL4 cause a subset of cases of Rothmund-Thomson syndrome*. Nat Genet, 1999. **22**(1): p. 82-4.
8. German, J., et al., *Syndrome-causing mutations of the BLM gene in persons in the Bloom's Syndrome Registry*. Hum Mutat, 2007. **28**(8): p. 743-53.
9. Garcia-Rubio, M., et al., *Different physiological relevance of yeast THO/TREX subunits in gene expression and genome integrity*. Mol Genet Genomics, 2008. **279**(2): p. 123-32.
10. Chaganti, R.S., S. Schonberg, and J. German, *A manyfold increase in sister chromatid exchanges in Bloom's syndrome lymphocytes*. Proc Natl Acad Sci U S A, 1974. **71**(11): p. 4508-12.
11. Hojo, E.T., et al., *Spontaneous chromosomal aberrations in Fanconi anaemia, ataxia telangiectasia fibroblast and Bloom's syndrome lymphoblastoid cell lines as detected by conventional cytogenetic analysis and fluorescence in situ hybridisation (FISH) technique*. Mutat Res, 1995. **334**(1): p. 59-69.
12. Bachrati, C.Z. and I.D. Hickson, *RecQ helicases: suppressors of tumorigenesis and premature aging*. Biochem J, 2003. **374**(Pt 3): p. 577-606.

13. Mirzaei, H., et al., *Sgs1 truncations induce genome rearrangements but suppress detrimental effects of BLM overexpression in Saccharomyces cerevisiae*. J Mol Biol, 2011. **405**(4): p. 877-91.
14. Mirzaei, H. and K.H. Schmidt, *Non-Bloom syndrome-associated partial and total loss-of-function variants of BLM helicase*. Proc Natl Acad Sci U S A, 2012. **109**(47): p. 19357-62.
15. Shastri, V.M. and K.H. Schmidt, *Cellular defects caused by hypomorphic variants of the Bloom syndrome helicase gene BLM*. Mol Genet Genomic Med, 2016. **4**(1): p. 106-19.
16. Wu, L., et al., *Potential role for the BLM helicase in recombinational repair via a conserved interaction with RAD51*. J Biol Chem, 2001. **276**(22): p. 19375-81.
17. Shimamoto, A., et al., *Human RecQ5beta, a large isomer of RecQ5 DNA helicase, localizes in the nucleoplasm and interacts with topoisomerases 3alpha and 3beta*. Nucleic Acids Res, 2000. **28**(7): p. 1647-55.
18. Nakayama, M., et al., *The possible roles of the DNA helicase and C-terminal domains in RECQ5/QE: complementation study in yeast*. DNA Repair (Amst), 2004. **3**(4): p. 369-78.
19. Rocak, S. and P. Linder, *DEAD-box proteins: the driving forces behind RNA metabolism*. Nat Rev Mol Cell Biol, 2004. **5**(3): p. 232-41.
20. Cordin, O., et al., *The DEAD-box protein family of RNA helicases*. Gene, 2006. **367**: p. 17-37.
21. Scheffner, M., J.M. Huibregtse, and P.M. Howley, *Identification of a human ubiquitin-conjugating enzyme that mediates the E6-AP-dependent ubiquitination of p53*. Proc Natl Acad Sci U S A, 1994. **91**(19): p. 8797-801.
22. Kizer, K.O., et al., *A novel domain in Set2 mediates RNA polymerase II interaction and couples histone H3 K36 methylation with transcript elongation*. Mol Cell Biol, 2005. **25**(8): p. 3305-16.
23. Parker, D., et al., *Phosphorylation of CREB at Ser-133 induces complex formation with CREB-binding protein via a direct mechanism*. Mol Cell Biol, 1996. **16**(2): p. 694-703.
24. Islam, M.N., et al., *RecQL5 promotes genome stabilization through two parallel mechanisms--interacting with RNA polymerase II and acting as a helicase*. Mol Cell Biol, 2010. **30**(10): p. 2460-72.
25. Hu, Y., et al., *RECQL5/Recql5 helicase regulates homologous recombination and suppresses tumor formation via disruption of Rad51 presynaptic filaments*. Genes Dev, 2007. **21**(23): p. 3073-84.

26. Wang, W., et al., *Functional relation among RecQ family helicases RecQL1, RecQL5, and BLM in cell growth and sister chromatid exchange formation*. Mol Cell Biol, 2003. **23**(10): p. 3527-35.
27. Kwon, Y., et al., *ATP-dependent chromatin remodeling by the Saccharomyces cerevisiae homologous recombination factor Rdh54*. J Biol Chem, 2008. **283**(16): p. 10445-52.
28. Unk, I., et al., *Role of yeast Rad5 and its human orthologs, HLTF and SHPRH in DNA damage tolerance*. DNA Repair (Amst), 2010. **9**(3): p. 257-67.
29. Soriano, I., et al., *Different nucleosomal architectures at early and late replicating origins in Saccharomyces cerevisiae*. BMC Genomics, 2014. **15**: p. 791.
30. Shor, E., et al., *The origin recognition complex interacts with a subset of metabolic genes tightly linked to origins of replication*. PLoS Genet, 2009. **5**(12): p. e1000755.

APPENDIX A:

DEFECTS IN DNA LESION BYPASS LEAD TO SPONTANEOUS CHROMOSOMAL REARRANGEMENTS AND INCREASED CELL DEATH

Note to the reader: This chapter has been previously published with permission from the publisher as Schmidt, KH, Viebranz, EB, Harris, LB, Mirzaei, H, Syed, S, Medicus, R (2010). "Defects in DNA Lesion Bypass Lead to Spontaneous Chromosomal Rearrangements and Increased Cell Death." *Eukaryotic Cell*. 2010;9(2):315-324. Research was designed by K. Schmidt. Corresponding author: Kristina Schmidt, Department of Cell Biology, Microbiology and Molecular Biology, University of South Florida, 4202 E. Fowler Avenue, ISA2015, Tampa, FL 33620. Phone: (813) 974-1592. Fax: (813) 974- 1614.; E-mail: kschmidt@usf.edu

ABSTRACT

Rev3 polymerase and Mph1 DNA helicase participate in error-prone and error-free pathways, respectively, for the bypassing of template lesions during DNA replication. Here we have investigated the role of these pathways and their genetic interaction with recombination factors, other nonreplicative DNA helicases, and DNA damage checkpoint components in the maintenance of genome stability, viability, and sensitivity to the DNA-damaging agent methyl methanesulfonate (MMS). We find that cells lacking Rev3 and Mph1 exhibit a synergistic, Srs2-dependent increase in the rate of accumulating spontaneous, gross chromosomal rearrangements, suggesting that the

suppression of point mutations by deletion of *REV3* may lead to chromosomal rearrangements. While *mph1Δ* is epistatic to homologous recombination (HR) genes, both Rad51 and Rad52, but not Rad59, are required for normal growth of the *rev3Δ* mutant and are essential for survival of *rev3Δ* cells during exposure to MMS, indicating that Mph1 acts in a Rad51-dependent, Rad59-independent subpathway of HR-mediated lesion bypass. Deletion of *MPH1* helicase leads to synergistic DNA damage sensitivity increases in cells with *chl1Δ* or *rrm3Δ* helicase mutations, whereas *mph1Δ* is hypostatic to *sgs1Δ*. Previously reported slow growth of *mph1Δ srs2Δ* cells is accompanied by G2/M arrest and fully suppressed by disruption of the Mec3-dependent DNA damage checkpoint. We propose a model for replication fork rescue mediated by translesion DNA synthesis and homologous recombination that integrates the role of Mph1 in unwinding D loops and its genetic interaction with Rev3 and Srs2-regulated pathways in the suppression of spontaneous genome rearrangements and in mutation avoidance.

INTRODUCTION

Nonreplicative DNA helicases play an important role in the maintenance of genome stability from bacteria to humans, most likely by affecting the formation and/or resolution of recombination intermediates and by facilitating replication fork progression through chromosomal regions with a propensity to adopt unusual DNA structures or those bound by proteins. In *Saccharomyces cerevisiae*, this group of DNA helicases includes the 3'-to-5' helicases Sgs1 and Srs2 and the 5'-to-3' DNA helicase Rrm3. In the absence of any two of these three helicases, unresolved recombination intermediates accumulate and lead to extremely slow growth that is fully suppressed by deletion of

genes encoding early homologous recombination (HR) factors (Lee, Johnson et al. 1999, Gangloff, Soustelle et al. 2000, Klein 2001, Fabre, Chan et al. 2002, Schmidt and Kolodner 2004, Torres, Schnakenberg et al. 2004). In the absence of Sgs1, cells exhibit increased rates of mitotic recombination, frequent chromosome missegregation, accumulation of extrachromosomal ribosomal DNA (rDNA) circles, and increased rates of gross chromosomal rearrangements (GCRs) involving nonhomologous chromosomes (Gangloff, McDonald et al. 1994, Watt, Louis et al. 1995, Sinclair, Mills et al. 1997, Yamagata, Kato et al. 1998, Mullen, Kaliraman et al. 2000, Myung, Datta et al. 2001, Schmidt and Kolodner 2006, Schmidt, Wu et al. 2006). Based on the increased crossover frequency during HO endonuclease-induced double-strand breaks (DSBs) in cells lacking Sgs1, it has also been proposed that Sgs1 may function in decatenation of Holliday junctions (HJs) to yield noncrossovers (Ira, Malkova et al. 2003, Lo, Paffett et al. 2006). Like Sgs1, Srs2 acts to favor noncrossover outcomes during DSB repair but appears to act earlier than Sgs1 in regulating recombination outcomes through its ability to dislodge Rad51 from recombinogenic 3' overhangs, thereby promoting a noncrossover synthesis-dependent single-strand annealing (SDSA) pathway (Ira, Malkova et al. 2003, Robert, Dervins et al. 2006, Prakash, Satory et al. 2009). In contrast, Rrm3 has not been implicated in DNA repair but is thought to be important for avoidance of recombination substrate formation by removal of DNA protein complexes in certain chromosomal locations, such as chromosome ends and replication fork barriers at the rDNA locus, thus facilitating replication fork progression (Ivessa, Zhou et al. 2002, Ivessa, Lenzmeier et al. 2003).

In addition to Sgs1, Rrm3, and Srs2, the yeast genome encodes two other

nonreplicative DNA helicases with proposed functions in DNA repair, Mph1 and Chl1. Mph1 possesses 3'-to-5' helicase activity, and its ATPase activity requires a relatively long fragment of single-stranded DNA (ssDNA) (≥ 40 nucleotides [nt]) for full activity *in vitro* (Prakash, Krejci et al. 2005). Mph1 is also necessary for resistance to the DNA damaging agents methyl methanesulfonate (MMS) and 4-nitroquinoline-1-oxide (4-NQO) and suppresses spontaneous mutations toward canavanine resistance (Entian, Schuster et al. 1999, Schurer, Rudolph et al. 2004). The modest mutator phenotype of the *mph1 Δ* mutant is enhanced by additional mutations in base excision repair (*apn1 Δ* and *apn2 Δ*) and is suppressed by mutations in translesion DNA synthesis (TLS) (*rev3 Δ*) (Scheller, Schurer et al. 2000, Schurer, Rudolph et al. 2004). These findings, in combination with the observation of an epistatic relationship between *mph1 Δ* and homologous recombination mutations, have led to the proposal that Mph1 may act in Rad52-dependent, error-free bypassing of DNA lesions (Schurer, Rudolph et al. 2004). Like the 3'-to-5' DNA helicases Sgs1 and Srs2, Mph1 was recently shown to affect crossover frequency during repair of an HO endonuclease-induced DNA DSB, favoring noncrossovers as the outcome (Prakash, Satory et al. 2009). The authors showed that Mph1 can unwind intermediates of homologous recombination *in vitro*, specifically D loops that are thought to form early during homologous recombination when a homoduplex is invaded by a Rad51 filament. While Srs2 has been shown to be able to disassemble Rad51 filaments *in vitro*, it does not appear to possess Mph1's ability to dissociate D loops once they have formed (Krejci, Van Komen et al. 2003, Veaute, Jeusset et al. 2003).

Although Chl1 has been shown to be required for the establishment of sister

chromatid cohesion, a possible role in DNA repair by homologous recombination has also been proposed (Shiratori, Shibata et al. 1999, Holloway 2000, Petronczki, Chwalla et al. 2004, Ogiwara, Ui et al. 2007). While Chl1 possesses a conserved helicase domain, helicase activity has so far been shown only for its putative human homolog, hCHLR1 (Hirota and Lahti 2000).

To further elucidate the functional interaction between nonreplicative DNA helicases and DNA repair pathways, we generated a series of mutants with combinations of *mph1Δ*, *chl1Δ*, *rrm3Δ*, *srs2Δ*, and *sgs1Δ* mutations and mutations in translesion DNA synthesis (TLS), base excision repair (BER), homologous recombination (HR), and DNA damage checkpoints. In addition to synthetic fitness defects due to aberrant HR and checkpoint activation, we identified epistatic and synergistic relationships with regard to fitness, the accumulation of gross chromosomal rearrangements (GCRs), and sensitivity to DNA damage. We propose that Mph1 functions in a Rad51-dependent, Rad59-independent pathway of HR for DNA lesion bypass and interacts genetically with *REV3* in the suppression of gross chromosomal rearrangements.

RESULTS

Translesion DNA synthesis suppresses GCR accumulation in *mph1Δ* cells

Deletion of *MPH1* has been shown to cause an increase in spontaneous base substitutions at *CAN1*, which can be suppressed by disrupting error-prone translesion DNA synthesis (Schurer, Rudolph et al. 2004). To determine how spontaneous DNA lesions are processed if they cannot be bypassed by Mph1 or TLS, we deleted *MPH1*

and *REV3* in a yeast strain that has been modified to allow the detection of gross chromosomal rearrangements, such as translocations, large deletions, and de novo telomere additions (Kolodner, Putnam et al. 2002, Schmidt, Pennaneach et al. 2006). We found that the *rev3Δ mph1Δ* mutant showed a statistically significant increase in the GCR rate over that of the single mutants, as indicated by the nonoverlapping 95% confidence intervals ($\alpha < 0.05$) for the median GCR rates (Table 2). This may indicate that the avoidance of point mutations by deletion of the error-prone DNA polymerase Rev3 occurs at the expense of increased formation of chromosomal rearrangements, suggesting that as long as Rev3 is present, spontaneous DNA lesions in the *mph1Δ* mutant are preferentially taken care of by TLS, whereas an alternative repair pathway preferentially utilized in the *rev3Δ mph1Δ* mutant is prone to GCR formation. To test the possibility that Srs2, a DNA helicase that has been shown to regulate homologous recombination by disrupting recombinogenic Rad51-filaments (Krejci, Van Komen et al. 2003, Veaute, Jeusset et al. 2003), may channel DNA lesions into this alternative DNA repair pathway, we determined the effect of an *srs2Δ* mutation on GCR formation in the *rev3Δ mph1Δ* mutant and found that GCR formation was eliminated (Table 2). That the viability of the *rev3Δ mph1Δ* mutant was significantly reduced upon introduction of the *srs2Δ* mutation (Fig. 1A) is consistent with previous reports of reduced fitness for the *mph1Δ srs2Δ* mutant (Tong, Evangelista et al. 2001, Tong, Lesage et al. 2004, Prakash, Satory et al. 2009) and suggests that spontaneous DNA lesions in the *rev3Δ mph1Δ* mutant may become substrates for homologous recombination pathways that need to be regulated by Srs2 to prevent cell death. In contrast to the *mph1Δ* mutant, the *rev3Δ* mutant does not require Srs2 for normal growth (Fig. 1A).

To test whether slow growth of the *mph1Δ srs2Δ* and *rev3Δ mph1Δ srs2Δ* mutants was due to increased G2/M arrest or to slowed progression through S phase resulting from impaired DNA lesion bypass, cell cycle profiles were obtained (Fig. 2A) and the fraction of cells in each cell cycle phase from three independent cultures was quantified (Fig. 2B). We found that the *mph1Δ srs2Δ* and *rev3Δ mph1Δ srs2Δ* mutants showed increased arrest in G2/M compared to the corresponding single and double mutants, but the mutations lacked any discernible effect on S phase. That the fraction of cells in S phase was largely unaffected indicates that impairment of DNA lesion bypass does not hinder the timely completion of genome replication but may instead cause the formation of DNA structures that later in the cell cycle impair progress through mitosis.

Deletion of *RAD51*, which had previously been shown to improve colony growth of the *mph1Δ srs2Δ* mutant and other DNA helicase double mutants (Lee, Johnson et al. 1999, Gangloff, Soustelle et al. 2000, Klein 2001, Fabre, Chan et al. 2002, Schmidt and Kolodner 2004, Torres, Schnakenberg et al. 2004, Prakash, Satory et al. 2009), abolished the G2/M arrest of *mph1Δ srs2Δ* cells and allowed them to progress through the cell cycle as did the *srs2Δ* single mutant (Fig. 3A). In addition to disrupting homologous recombination, we found that disruption of the DNA damage checkpoint clamp by *MEC3* deletion also improved growth of the *mph1Δ srs2Δ* mutant (Fig. 1A) and had the same effect on viability and cell cycle progression as the deletion of *RAD51* (Fig. 3). In contrast, introduction of a *rev3Δ* mutation into the *mph1Δ srs2Δ* mutant did not affect growth (Fig. 1A) but led to a small increase in the fraction of G2/M-arrested cells (Fig. 2). Similarly, sensitivity of the *mph1Δ srs2Δ* mutant to MMS was aggravated further by a *rev3Δ* mutation but was alleviated by a *rad51Δ* mutation (Fig. 4). In the

presence of MMS, *rev3Δ mph1Δ srs2Δ* cells emerged only after incubation for >72 h. This strong synergistic increase in MMS sensitivity of the triple mutant compared to that of any of the double mutants suggests that all three genes mediate independent pathways for survival in the presence of DNA damage. Taken together, these findings suggest that deleting the error-prone DNA polymerase Rev3 in *mph1Δ* cells while effectively avoiding points mutations causes the appearance of a different mutation type, i.e., gross chromosomal rearrangements, which activates the DNA damage checkpoint in G2/M and causes cell death if Srs2 is not present to regulate HR-dependent DNA lesion bypass.

Suppression of genome rearrangements by *srs2Δ* depends on functional DNA damage checkpoint

Genome instability in cells lacking Sgs1 helicase is suppressed by the DNA damage checkpoint, as demonstrated by synergistic GCR rate increases upon introduction of the *mec3Δ*, *rad24Δ*, *mec1Δ*, *rad53Δ* or *rad9Δ* mutation into the *sgs1Δ* mutant (Schmidt, Wu et al. 2006). As demonstrated by overlapping 95% confidence intervals, no statistically significant changes in the GCR rate of the *mph1Δ* mutant were observed upon introduction of checkpoint mutations (*mec3Δ* and *mec1Δ*) (Table 2), suggesting that the DNA damage checkpoint is not required for the suppression of GCRs in the *mph1Δ* mutant. However, when we introduced the *mec3Δ* mutation into the *mph1Δ srs2Δ* mutant, which itself exhibited wild-type levels of GCRs, the GCR rate increased to that of the *mph1Δ mec3Δ* mutant (Table 2), thus suggesting that, in contrast to the case with the *rev3Δ mph1Δ* and *mph1Δ* mutants, GCR formation in

checkpoint-deficient mutants is not dependent on Srs2. Similarly, the GCR rate of the *mec3Δ* mutant did not change upon introduction of an *srs2Δ* mutation. This ability of the *srs2Δ* mutation to suppress GCR formation in checkpoint-proficient cells but not in checkpoint-deficient cells suggests that the Mec3 checkpoint detects the aberrant HR intermediates that form in the absence of Srs2, leading to G2/M arrest and avoidance of GCRs, whereas in the absence of the checkpoint, these aberrant HR intermediates go on to form GCRs.

Lack of Rev3 and Mph1 causes synergistic GCR rate increase in new GCR strain susceptible to duplication-mediated rearrangements

Putnam et al. (Putnam, Hayes et al. 2009) recently showed that the rate of GCR accumulation depends significantly on chromosomal features in the breakpoint region. For example, while GCRs in the standard GCR strain background (RDKY3615) are due largely to single-copy-sequence-mediated rearrangements, GCRs in a newly designed strain (RDKY6678) are duplication mediated due to the presence of imperfect homology between the *HXT13-DSF1* sequence in the breakpoint region on chromosome V and sequences on chromosomes IV, X, and XIV (Putnam, Hayes et al. 2009). This new GCR strain accumulates chromosomal rearrangements at an increased rate compared to that for the standard GCR strain, with wild-type cells having a 56-fold-higher GCR rate than the standard strain (Putnam, Hayes et al. 2009). To assess the effect of DNA lesion bypass defects on GCR formation in this new strain, *rev3Δ*, *mph1Δ*, *srs2Δ*, and *mec3Δ* mutations were introduced into RDKY6678 (Table 3). Consistent with our observations with the standard GCR strain background (Table 2), the *rev3Δ mph1Δ*

double mutant exhibited a synergistic GCR rate increase compared to results for the *mph1Δ* and *rev3Δ* single mutants. Interestingly, the significantly greater synergistic effect of combining the *rev3Δ* and *mph1Δ* mutations in the new GCR strain background (Table 3; 167-fold increase over rates for the RDKY6678 wild type) compared to results with the standard GCR strain background (Table 2, 16-fold increase over rates for the RDKY3615 wild type) indicates that alternative pathways utilized for DNA lesion bypass in the *rev3Δ mph1Δ* mutant may be more prone to duplication-mediated than to single-copy-sequence mediated genome rearrangements. As in the standard GCR strain (Table 2), deletion of *SRS2* in the new GCR strain led to a significant decrease in the GCR rate of the *rev3Δ mph1Δ* mutant to the level of the *srs2Δ* mutant, suggesting that viable GCR formation depends on the antirecombinase Srs2 despite the different breakpoint regions in the two GCR strain backgrounds and the different GCR types that are likely to arise from them. The fact that deletion of *SRS2* did not cause a GCR rate increase in the *mph1Δ mec3Δ* mutant in the standard GCR background (Table 2) but led to a significant GCR rate increase in the new GCR background (Table 3) is likely due to the greater requirement of Srs2 for GCR suppression in the new GCR strain background (Table 3, *srs2Δ*: 26-fold increase over wild-type level) than in the standard GCR strain (Table 2, *srs2Δ*: 0.6-fold increase over wild-type level).

Genetic interactions between *MPH1* and other DNA helicases

Negative genetic interactions between any two of the DNA helicases Sgs1, Srs2, and Rrm3 have previously been shown to be caused by the accumulation of aberrant intermediates of homologous recombination (Gangloff, Soustelle et al. 2000, Ooi,

Shoemaker et al. 2003, Schmidt and Kolodner 2004, Torres, Schnakenberg et al. 2004). Since such a negative, HR-dependent genetic interaction has now also been established between *mph1Δ* and *srs2Δ*, we tested *mph1Δ* mutants with deletions of other confirmed or putative DNA helicase genes (*sgs1Δ*, *rrm3Δ*, and *chl1Δ*) for growth defects, GCR accumulation, and sensitivity to MMS. We observed that unlike the case with the *mph1Δ srs2Δ* mutant, the meiotic products of diploids heterozygous for the *mph1Δ* mutation and either the *sgs1Δ*, *rrm3Δ*, or *chl1Δ* mutation grew normally. In addition to a synergistic increase in sensitivity to MMS for the *mph1Δ srs2Δ* mutant (Banerjee, Smith et al. 2008), we also identified synergistic increases in sensitivity for the *mph1Δ rrm3* and *mph1Δ chl1Δ* mutants but not for the *mph1Δ sgs1Δ* mutant, which appeared as sensitive as the *sgs1Δ* single mutant (Fig. 5). This indicates that Mph1, Chl1, Rrm3, and Srs2 contribute independently to survival during exposure to MMS, while Mph1 appears to be hypostatic to Sgs1. Since Schurer et al. (Schurer, Rudolph et al. 2004) reported a synergistic increase in mitotic homologous recombination at three markers for the *mph1Δ sgs1Δ* mutant and therefore suggested that Mph1 may play an antirecombinogenic role in the *sgs1Δ* mutant, we tested whether Mph1 also interacted with Sgs1 or other DNA helicases in the suppression of GCRs. However, we found that the *mph1Δ sgs1Δ* mutant accumulates GCRs at the same rate as the *sgs1Δ* mutant, indicating no genetic interaction between *MPH1* and *SGS1* in the suppression of chromosomal rearrangements (Table 2). Deletion of *MPH1* also failed to induce significant changes in the accumulation of GCRs in *srs2Δ*, *chl1Δ*, and *rrm3Δ* mutants, as indicated by the overlap between 95% confidence intervals (Table 2).

Rad52/Rad51, but not Rad59, are essential for DNA damage tolerance and normal growth in the absence of translesion DNA synthesis

Although the *rev3Δ mph1Δ* mutant exhibits a synergistic increase in the GCR rate and in sensitivity to MMS, it grows unimpaired in the absence of MMS, with a doubling time indistinguishable from that of the single mutants (Fig. 1B). However, sporulation of diploids heterozygous for the *rev3Δ* and *rad52Δ* mutations revealed slower growth for the *rev3Δ rad52Δ* mutant that was unaffected by deletion of *MPH1* (Fig. 1B). That the *rev3Δ rad52Δ* mutant does grow, albeit slowly, could mean that spontaneous DNA lesions needing to be bypassed during DNA replication are rare and/or that alternative, yet minor, pathways for lesion bypass exist in addition to HR and TLS. To distinguish between these possibilities, the ability of the HR-deficient *rev3Δ* mutant to grow in the presence of MMS was assessed (Fig. 4). While the *rev3Δ* mutant was no more sensitive than wild-type cells, consistent with previous findings (Schurer, Rudolph et al. 2004), the *rev3Δ rad52Δ* mutant was significantly more sensitive than the *rad52Δ* mutant. In fact, not a single colony emerged in repeated experiments, even after a >72-h incubation time on 0.001% MMS, for strains lacking both *REV3* and *RAD52*, lending support to the proposal that besides HR and TLS, no other pathways exist in yeast for the bypassing of induced DNA lesions. To determine whether Rad51- or Rad59-dependent branches of homologous recombination are essential for *rev3Δ* survival, the viability of spores obtained from diploids heterozygous for *rev3Δ* and either the *rad51Δ* or *rad59Δ* mutation was assessed, revealing normal growth for the *rev3Δ rad59Δ* mutant while the *rev3Δ rad51Δ* mutant grew slowly (Fig. 1B). Moreover, the *rev3Δ rad59Δ* mutant was no more sensitive than the single mutants, whereas the

rev3Δ rad51Δ mutant could not form any colonies in the presence of MMS (Fig. 4), similar to the case with the *rev3Δ rad52Δ* mutant. Thus, although *rev3Δ* exhibits synergistic increases in sensitivity to MMS when combined with *mph1Δ*, *mph1Δ srs2Δ*, *rad52Δ*, or *rad51Δ*, the normal growth of the *rev3Δ mph1Δ* mutant as opposed to the impaired growth of the *rev3Δ rad51Δ* and *rev3Δ rad52Δ* mutants suggests that in addition to Mph1-dependent HR, other, Mph1-independent, Rad51-dependent HR pathways exist for DNA lesion bypass.

DISCUSSION

We have investigated genetic interactions between genes involved in DNA lesion bypass (*MPH1* and *REV3*), homologous recombination (*RAD52*, *RAD51*, *RAD59*, and *SRS2*), and the DNA damage checkpoint (*MEC3* and *MEC1*) with regard to fitness, MMS sensitivity, and suppression of genome instability. We find that suppression of point mutations that arise in an *mph1Δ* mutant as a result of the error-prone Rev3 polymerase replicating across a template lesion results in the appearance of GCRs. This finding may suggest that mutations are not actually avoided but are simply shifted toward a different mutation type. Synergistic GCR rate increases in two strain backgrounds, each designed to accumulate different GCR spectra (Putnam, Hayes et al. 2009), demonstrate that *REV3* and *MPH1* interact genetically to suppress various types of spontaneous GCRs but are especially effective at suppressing GCRs in the newly designed GCR strain background. For this new GCR strain, Putnam et al. (Putnam, Hayes et al. 2009) determined that GCRs accumulate largely as a result of nonallelic homologous recombination (NAHR) between DNA sequences in the

breakpoint region on chromosome V and similar regions on chromosomes IV, X, and XIV. Hence, the greater synergistic GCR rate increase identified here in this new GCR background compared to that for the standard GCR strain suggests greater roles for *MPH1* and *REV3* in the suppression of such NAHR-mediated GCRs than in the suppression of single-copy-sequence-mediated rearrangements. The requirement of Srs2, which regulates the outcomes of HR by antagonizing strand invasion, for the formation of viable chromosomal rearrangements further supports a prominent role of HR in the formation of GCRs when Mph1 and Rev3 are absent for DNA lesion bypass. We further show that the negative genetic interaction between the *mph1Δ* and *srs2Δ* mutations, coupled with accumulation of cells in G2/M and further exacerbation of the G2/M arrest by disruption of *REV3*, is suppressed by disrupting the DNA damage checkpoint. Synergism in MMS sensitivity was observed for *mph1Δ* mutants lacking *CHL1*, *RRM3*, *SRS2*, or *REV3*, whereas epistasis was observed for *mph1Δ* mutants lacking *RAD52*, *RAD51*, or *SGS1*. Combined with our observation that the *rev3Δ* mutant required *RAD51* and *RAD52* but not *RAD59* or *MPH1* for normal growth, this suggests that Rev3 (TLS) and RAD51 (HR) are the two pathways for bypass of spontaneous DNA lesions, with Mph1 defining only one Rad51 subpathway. While the *rad51Δ* mutation appeared to suppress MMS sensitivity of the *mph1Δ srs2Δ* mutant to the level exhibited by a *rad51Δ* single mutant, the *rev3Δ* mutation led to a further synergistic increase, suggesting that Mph1, Srs2, and Rev3 contribute to bypass and/or repair of induced DNA lesions independently.

Our observation of suppression of the G2/M arrest of the *mph1Δ srs2Δ* mutant by *mec3Δ*, in addition to the recently reported suppression by *rad51Δ* (Prakash, Satory et

al. 2009), suggests that cells lacking Mph1 and Srs2 are overwhelmed with HR intermediates that do not impair S phase but activate the DNA damage checkpoint prior to mitosis. That Srs2 is essential for normal growth in the absence of Mph1 could mean that DNA lesions, normally bypassed by the Mph1 pathway, will enter another HR pathway that is potentially lethal if it is not regulated by Srs2. According to recent findings by Prakash et al. (Prakash, Satory et al. 2009), Srs2, Mph1, and Sgs1 independently promote noncrossover pathways during mitotic DSB repair. They suggest that Srs2 diverts DNA lesions away from crossover events that can result from double Holliday junction (dHJ) resolution into the noncrossover SDSA pathway by preventing second-strand invasion. Accumulation of dHJs due to the absence of Srs2 could overwhelm resolution pathways, especially when alternative pathways for DNA lesion bypass, such as TLS, are absent. In addition to its ability to inhibit crossover formation during repair of an HO-induced DSB, Mph1 has also been reported to unwind D loops *in vitro* (Prakash, Satory et al. 2009). It has therefore been proposed that Mph1 promotes SDSA and may reverse strand invasion events before they can form dHJs. Thus, the overall burden of lesions that are committed to HR pathways and could potentially go on to form dHJs would be expected to increase in the absence of Mph1 and even further when Rev3 is also absent.

Recent findings suggest how FANCM, a human homolog of Mph1, could perform a role in error-free bypass of DNA lesions. FANCM is part of the eight-component Fanconi anemia core complex, which is involved in the repair of intrastrand cross-links and is associated with Fanconi anemia (Joenje and Patel 2001, Niedzwiedz, Mosedale et al. 2004, Kennedy and D'Andrea 2005, Mathew 2006, Wang 2007). FANCM can

branch migrate three- and four-way junctions and, like Mph1, unwind D loops (Gari, Decaillet et al. 2008, Gari, Decaillet et al. 2008). Combining these two activities, it has been proposed that FANCM may stall and remodel replication forks to promote repair of an approaching DNA lesion, thus preventing the fork from encountering the lesion and collapsing (Gari, Decaillet et al. 2008). Without FANCM, forks would collapse, leading to broken chromatids and increased gross chromosomal rearrangements, both hallmarks of Fanconi cells (Thompson, Hinz et al. 2005).

The recruitment of Srs2 to the replisome when PCNA becomes sumoylated in the presence of DNA damage (Pfander, Moldovan et al. 2005) and the ability of the human Mph1 homolog FANCM to remodel replication forks *in vitro* lead us to propose a model in which Mph1 and Srs2 perform their roles in recombination directly at the fork to restart replication after encountering a DNA lesion (Fig. 6). Based on the slow growth of Rad52/Rad51-deficient *rev3Δ* cells and the inability of the *rev3Δ rad52Δ* and *rev3Δ rad51Δ* mutants to form any colonies in the presence of MMS, we propose that in wild-type cells, DNA lesions may be bypassed by either Rev3-mediated TLS or Rad51-dependent HR, with Mph1 being involved in only one subpathway of Rad51-dependent HR. Rev3-mediated TLS is prone to errors but not GCR formation, while properly regulated HR pathways, including the Mph1 pathway, are error free. Mph1 may act at a stalled replication fork by unwinding the leading strand from its template, a scenario which has been suggested to resemble unwinding of a D loop (Gari, Decaillet et al. 2008). Mediated by HR proteins, the leading strand may then anneal with the lagging strand, forming a chicken foot (Fig. 6, structure A), or invade the sister chromatid, forming a D loop (Fig. 6, structure B), followed by DNA synthesis at the 3' end. Based

on the ability of Mph1 to reverse D loops *in vitro*, it also seems possible that Mph1 acts to resolve these HR intermediates. For example, Mph1 could unwind the D loop formed by HR proteins after limited DNA synthesis or dissolve the chicken-foot structure by reverse branch migration. Reannealing of the daughter strands with their templates would then result in error-free bypass of the DNA lesion in the template strand and resumption of replication. While FANCM has been shown to migrate three- and four-way junctions *in vitro* (Gari, Decaillet et al. 2008, Gari, Decaillet et al. 2008), as proposed in this model, this remains to be determined for Mph1. The recent report of a physical interaction between Mph1 and RPA (Banerjee, Smith et al. 2008) could suggest that Mph1 is recruited to stalled replication forks via RPA-bound regions of ssDNA that are generated when the replication machinery stalls at a lesion in the template. While Mph1 can unwind 40 bp by itself, it requires RPA to unwind duplexes that are 100 bp and fails on those that are 500 bp (Prakash, Krejci et al. 2005). This rather modest helicase activity could ensure that Mph1 does not expose unnecessarily large regions of ssDNA at stalled forks while at the same time being sufficiently strong to unwind the leading strand from its template needed for D-loop/chicken-foot formation and/or to reverse HR-mediated invasion of the sister chromatid. Moreover, the ATPase activity of Mph1 requires a relatively long stretch of ssDNA (≥ 40 nt) for full activation *in vitro* (Prakash, Krejci et al. 2005), which could help to ensure that Mph1 is active only on replication forks that have stalled because they are likely to contain longer regions of ssDNA than unperturbed forks. In our model, Srs2 is recruited to damaged replication forks to suppress dHJ formation, thereby promoting Mph1-mediated fork rescue. Such a role for Srs2 at the replication fork is consistent with recent findings (Liberi, Chiolo et al.

2000, Pfander, Moldovan et al. 2005). Hence, in the absence of Srs2, an increasing number of forks would enter dHJ pathways for rescue, overwhelming dHJ resolution pathways and leading to aberrant and/or unresolved intermediates and eventually G2/M arrest. This accumulation of *srs2Δ* cells in G2/M accelerates as more DNA lesions become substrates for dHJ pathways upon elimination of Mph1 and Rev3. Unresolved or aberrant DNA structures may not be the only cause for Mec3-dependent cell cycle arrest of *mph1Δ srs2Δ* cells. According to findings by Prakash et al. (Prakash, Satory et al. 2009), HR intermediates during DSB repair are increasingly resolved as crossovers when Srs2 and Mph1 are absent, possibly due to increased HR and impairment of single-strand annealing pathways, such as SDSA. Thus, not only is increased dHJ formation likely to overwhelm dHJ resolution pathways, it is also likely to increase the number of crossovers, which could be dangerous for haploid mitotic cells and contribute to diminished cell proliferation. Although formation and unwinding of D-loop-like structures could be envisaged at replication forks and the recently proposed role of Mph1 in SDSA repair of DSBs could be likened to reversing chicken-foot/D-loop structures at stalled forks, it remains to be tested whether Mph1 can branch migrate three- or four-way junctions to reverse these HR intermediates and does indeed function at the replication fork.

MATERIALS AND METHODS

Yeast strains and media

All strains used in this study are derived from *Saccharomyces cerevisiae* strain S288C and are listed in Table 1. For GCR rate measurements, desired gene deletions

were introduced into KHSY802 (*MATa ura3-52 trp1Δ63 his3Δ200 leu2Δ1 lys2Bgl hom3-10 ade2Δ1 ade8 hxt13::URA3*), RDKY5027 (*MATα ura3-52 trp1Δ63 his3Δ200 leu2Δ1 lys2Bgl hom3-10 ade2Δ1 ade8 hxt13::URA3*), or RDKY6678 (*MATa ura3-52 leu2Δ1 trp1Δ63 his3Δ200 lys2ΔBgl hom3-10 ade2Δ1 ade8 can1::hisG yel072w::CAN1/URA3 iYEL072::hph*) by HR-mediated integration of PCR products by the lithium acetate method (Gietz and Woods 2006). All haploid strains, including single mutants, for GCR rate measurements, growth analysis, and fluorescence-activated cell sorting (FACS) were obtained by sporulating diploids heterozygous for the desired mutation(s). Spores were genotyped on selective media or by PCR. For tetrad dissection, desired mutations were introduced by HR-mediated integration of PCR fragments in the strain background RDKY2666 (*MATa ura3-52 trp1Δ63 his3Δ200*) or RDKY2664 (*MATα ura3-52 trp1Δ63 his3Δ200*). Media for propagating strains have been previously described (Chen, Umezu et al. 1998).

GCR analysis

GCR rates were determined exactly as previously described (Schmidt, Pennaneach et al. 2006). Initially, GCR rates were derived from 10-ml cultures of two or three independent strain isolates. For mutants with low GCR rates, up to 75 cultures, ranging from 10 to 50 ml in volume, were analyzed per mutant. To determine the statistical significance of differences between median GCR rates, 95% confidence intervals ($\alpha < 0.05$) for all median GCR rates were calculated according to the method of Nair (Nair 1940). GCR rates were measured in the standard GCR strain background RDKY3615 and a modified GCR strain background, RDKY6678 (both strains were

kindly provided by Richard Kolodner, University of California—San Diego). In RDKY3615, the *CAN1* gene is in its wild-type location on chromosome V and a *URA3* cassette was used to replace the *HXT13* gene on chromosome V (Schmidt, Pennaneach et al. 2006, Putnam, Hayes et al. 2009). In RDKY6678, the *CAN1* gene is deleted (*can1::hisG*) and a *URA3/CAN1* cassette is inserted into *YEL072W*, located telomeric of *HXT13* on chromosome V (Putnam, Hayes et al. 2009).

Tetrad analysis

Diploids were sporulated in 1% potassium acetate for 5 days at 30°C, washed, digested with zymolase (500 µg/ml in 1 M sorbitol), and dissected on yeast extract-peptone-dextrose (YPD) agar plates using a micromanipulator mounted on an Axioskop 40 microscope (Zeiss). The YPD plates were incubated for 2 days at 30°C and photographed.

Doubling time measurement

Overnight cultures of independent isolates were diluted in 5 ml of YPD to an optical density at 600 nm (OD₆₀₀) of 0.1 to 0.2, and the OD₆₀₀ was measured in 60-min or 120-min intervals for 6 to 8 h. Doubling times are reported in minutes and are presented as the average doubling time of two or three independent strains for each genotype, with error bars showing the standard deviations.

DNA content analysis

Cells were grown overnight at 30°C in YPD medium. Cultures were diluted in YPD to an OD600 of 0.2, and incubation was continued until cultures reached an OD600 of 0.6 to 0.8. Cells were then fixed in 70% ethanol for 1 h at room temperature and sonicated in 50 mM sodium citrate (pH 7). The cells were washed once in 50 mM sodium citrate (pH 7), and RNase A was added to a final concentration of 250 µg/ml. After overnight incubation at 37°C, the cells were washed twice in 50 mM sodium citrate. To stain the DNA, Sytox green (Molecular Probes) was added to a final concentration of 1 µM and the cells were incubated in the dark at room temperature for 1 h immediately prior to fluorescence-activated cell sorting (FACS) on a BD LSR II analyzer. The distribution of cells throughout the cell cycle phases was quantified with the FlowJo v8.3.3 software program. The mean obtained from measurements of at least three cultures and standard deviation are reported for every strain.

MMS sensitivity

Overnight cultures were diluted in YPD to an OD600 of 0.2 and grown at 30°C to an OD600 of 0.6. A series of 10-fold dilutions was prepared for every yeast culture, and 5 µl was spotted on YPD and on YPD containing the appropriate levels of MMS. Colony growth was recorded after 24 h, 48 h, and 72 h of incubation at 30°C. The 48-h time point is shown.

FIGURES AND TABLES

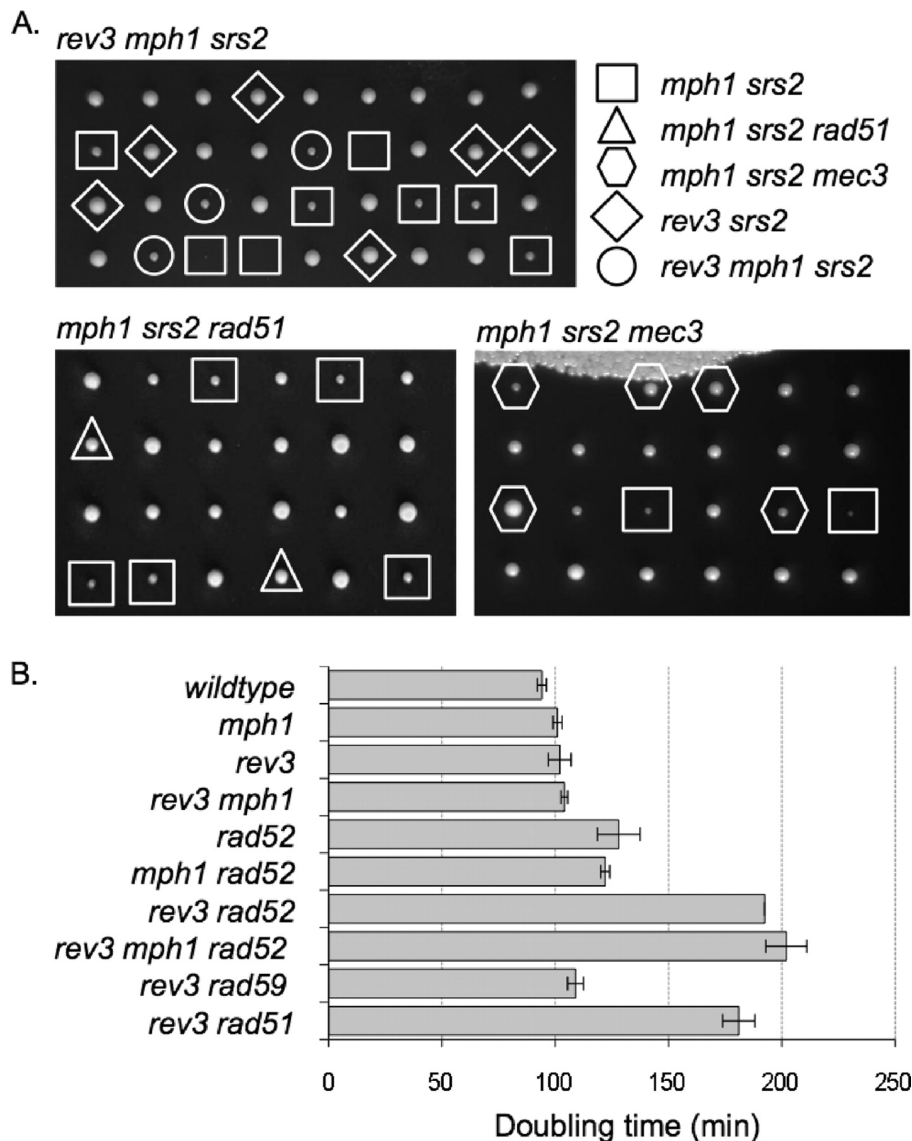


Figure A.1. Genetic interactions between *rev3Δ*, *mph1Δ*, *srs2Δ*, and HR mutations were assessed by testing the fitness of mutants. (A) Tetrads from diploids heterozygous for *rev3Δ*, *mph1Δ*, and *srs2Δ*; *mph1Δ*, *srs2Δ*, and *rad51Δ*; or *mph1Δ*, *srs2Δ*, and *mec3Δ* were dissected on rich medium and genotyped by spotting on selective medium or by PCR to determine the presence of gene deletions. In contrast to the *mph1Δ* mutant, the *rev3Δ* mutant does not require SRS2 for normal growth. Deletion of MEC3 or disruption of HR rescues the slow growth of the *mph1Δ srs2Δ* mutant. **(B)** Doubling times of mutant strains and appropriate controls in rich medium (YPD) are shown with standard deviations. Cells lacking Rev3 require Rad51 and Rad52 but not Rad59 for normal growth, and these growth defects are unaffected by Mph1.

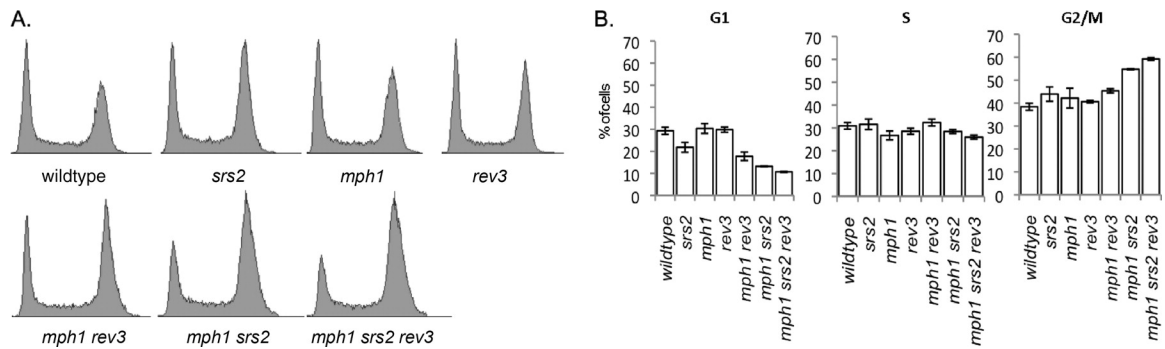


Figure A.2. Effect of *rev3Δ* and *srs2Δ* mutations on cell cycle progression of cells lacking *Mph1*. Asynchronous cultures were grown to mid-log phase, fixed, and stained with Sytox green to measure DNA content by FACS. **(A)** Cell cycle profiles reveal that *mph1Δ srs2Δ* cells accumulate in G2/M phase, which is enhanced further by a *rev3Δ* mutation. **(B)** Quantification of cell fractions in G1, S, and G2/M phases, determined by FACS analysis of three cell cultures for each strain, using FlowJo v8.3.3. Error bars indicate the standard deviations.

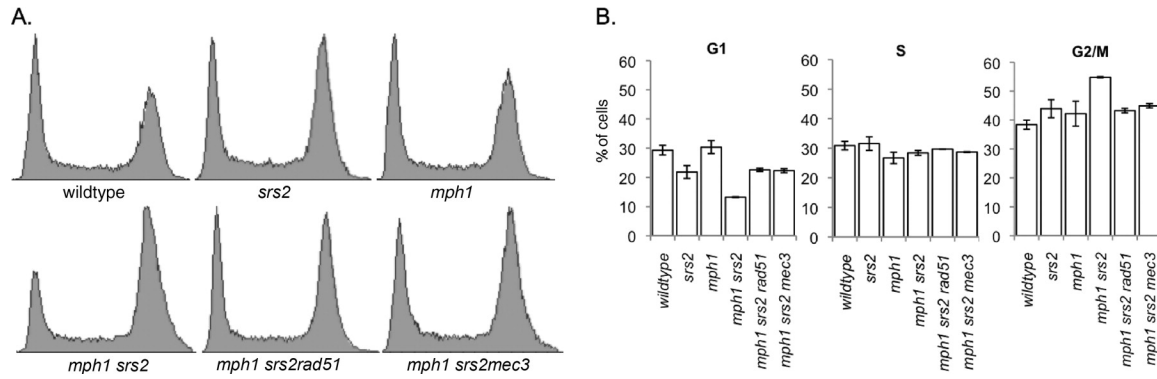


Figure A.3. The G2/M arrest of *mph1Δ srs2Δ* cells is suppressed by disrupting homologous recombination or the DNA damage checkpoint. Cell cycle profiles (**A**) and quantification (**B**) of the fractions of cells in G1, S, and G2/M phases show that the *rad51Δ* and *mec3Δ* mutations are equally effective at decreasing cell accumulation in G2/M, showing an increase in the fraction of cells in G1. Neither mutation affects the fraction of cells in S phase. The DNA content of Sytox green-stained cells from at least three mid-log-phase cultures of every strain was analyzed by FACS.

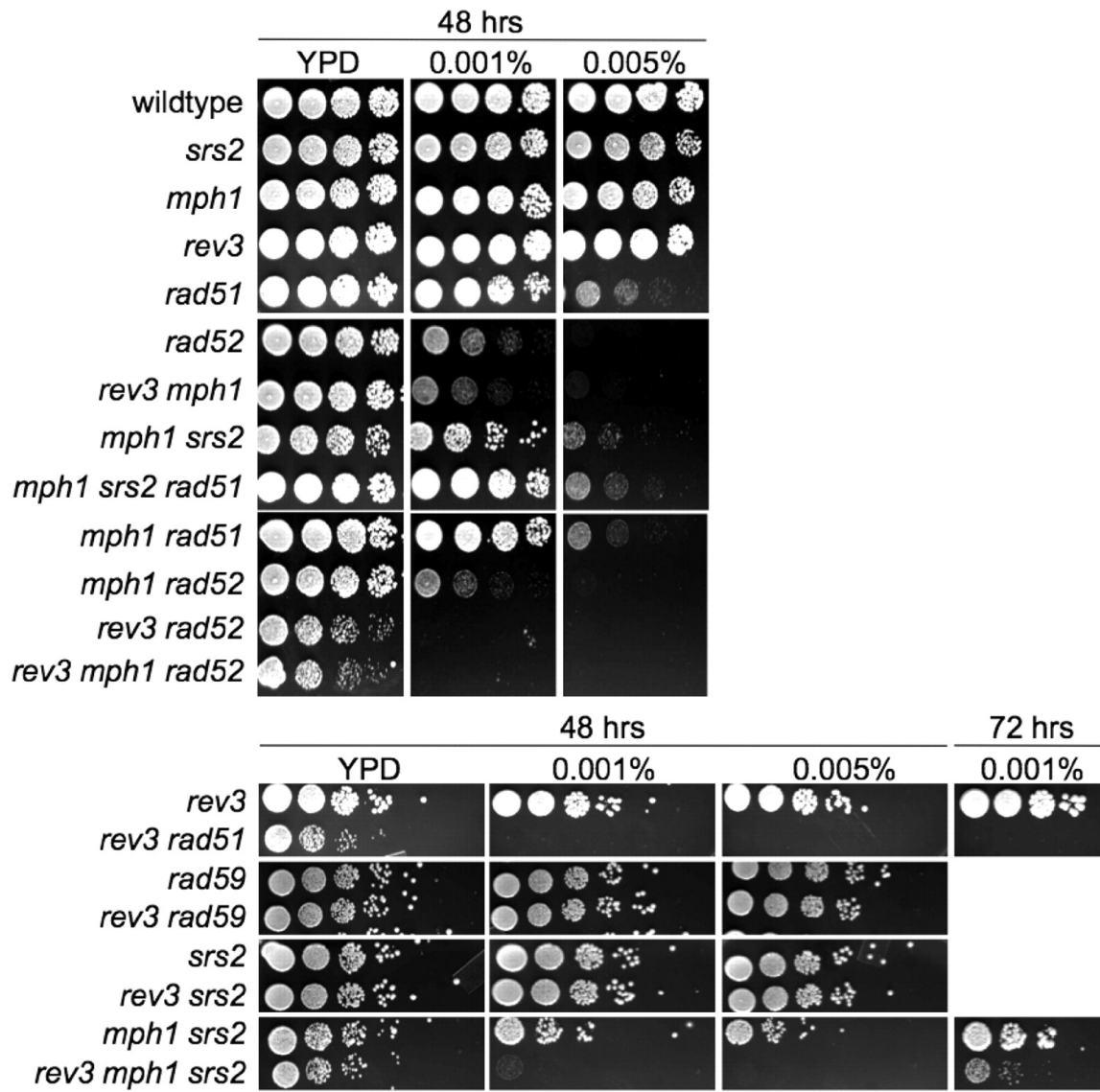


Figure A.4. Effect of mutations affecting translesion DNA synthesis and homologous recombination on sensitivity to MMS. Tenfold dilutions of exponentially growing cultures were spotted on YPD (viable cell count) or YPD containing 0.001% or 0.005% MMS. Colony growth after 48 h (and 72 h for selected mutants) of incubation at 30°C is shown.

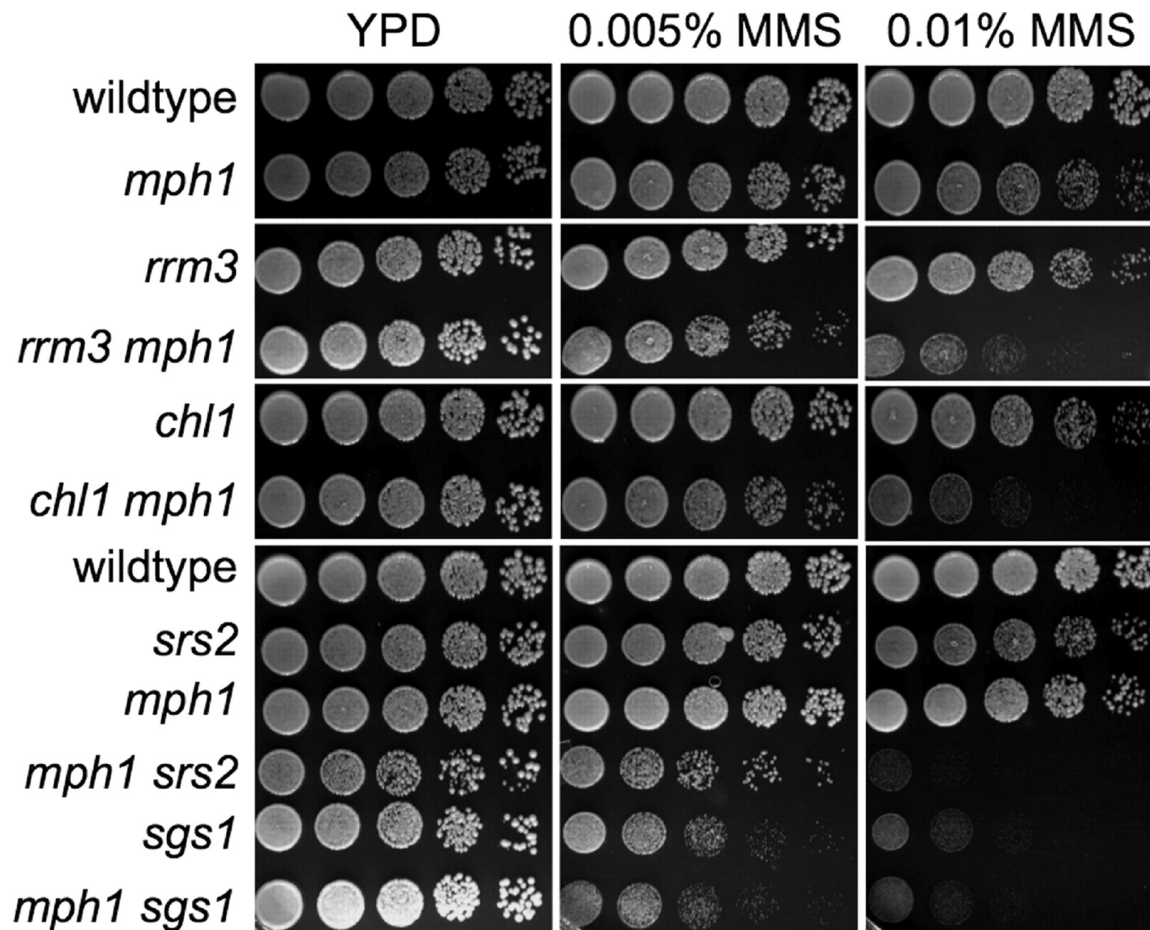


Figure A.5. Effect of an *mph1*Δ mutation on MMS sensitivity of mutants lacking various other confirmed (*Sgs1*, *Rrm3*, and *Srs2*) or putative (*Chl1*) DNA helicases. Tenfold dilutions of exponentially growing cultures were spotted on YPD or YPD containing 0.01% or 0.005% MMS. Colony growth after 48 h of incubation at 30°C is shown.

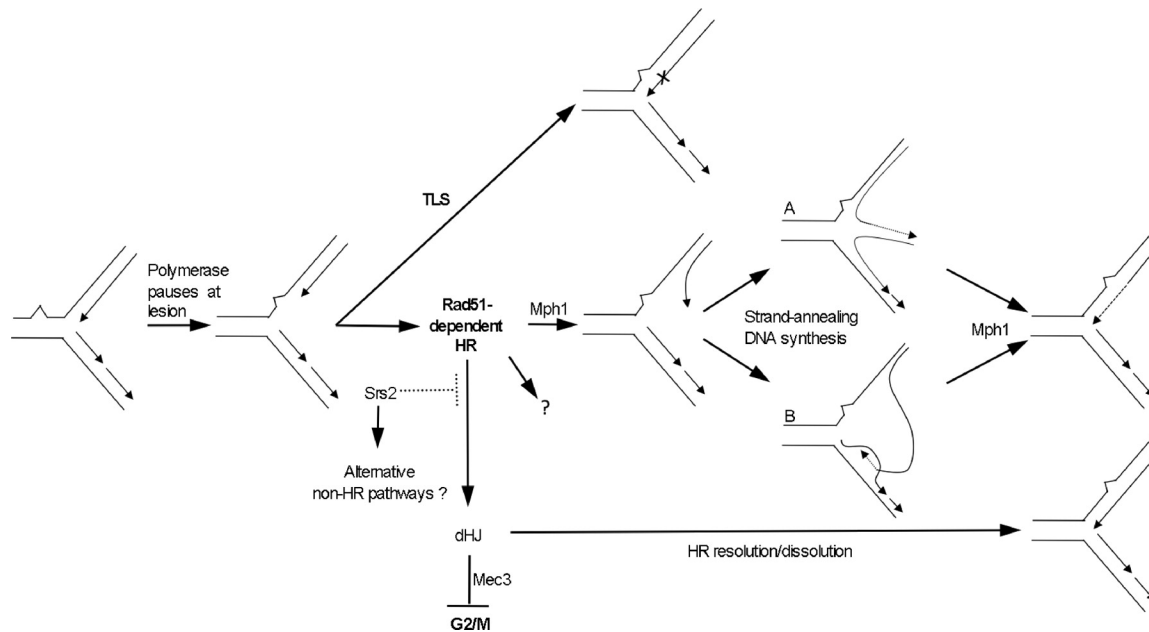


Figure A.6. Model for the role of Mph1 in the maintenance of genome stability. DNA lesions arise spontaneously during DNA replication and are bypassed by an error-free, Mph1-mediated, noncrossover pathway of homologous recombination (HR). Mph1 may unwind the leading strand from its template, suggested to resemble a D loop (Gari, Decaillet et al. 2008), followed by Rad51/52-mediated chicken-foot formation (**A**) and then resolution by reverse branch migration. A D-loop structure could also form when the leading strand switches template (**B**), and Mph1 could dissolve this D loop by reverse branch migration. In the absence of Mph1, lesions are bypassed by error-prone, Rev3-mediated TLS or they are channeled by Srs2 into alternative bypass pathways that can result in GCRs. If TLS is disrupted in the *mph1* Δ mutant, point mutations from TLS are avoided, but GCRs arise as a consequence of aberrant repair, most likely nonallelic HR. In the absence of both Mph1 and Srs2, cells accumulate at G2/M and lose viability due to Rad51-mediated accumulation of dHJs and Mec3-mediated checkpoint activation. In the absence of the checkpoint, cells continue through the cell cycle in the presence of DNA lesions. The dotted line emerging from Srs2 indicates that Srs2 tightly regulates the levels of dHJ formation at paused replication forks by inhibiting Rad51-mediated strand invasion.

TABLE A.1. *Saccharomyces cerevisiae* strains used in this study

| Strain | Genotype |
|-----------------------|--|
| RDKY3615 ^a | <i>MATa ura3-52 trp1Δ63 his3Δ200 leu2Δ1 lys2ΔBgl hom3-10 ade2Δ1 ade8 hxt13::URA3</i> |
| RDKY2666 ^a | <i>MATa ura3-52 trp1Δ63 his3Δ200</i> |
| RDKY2664 ^a | <i>MATα ura3-52 trp1Δ63 his3Δ200</i> |
| RDKY6678 ^a | <i>MATa ura3-52 leu2Δ1 trp1Δ63 his3Δ200 lys2ΔBgl hom3-10 ade2Δ1 ade8 can1::hisG yel072w::CAN1/URA3 iYEL072::hph</i> |
| RDKY6795 ^a | <i>MATa ura3-52 leu2Δ1 trp1Δ63 his3Δ200 lys2ΔBgl hom3-10 ade2Δ1 ade8 can1::hisG yel072w::CAN1/URA3 iYEL072::hph mph1::HIS3</i> |
| KHSY883 | <i>MATa ura3-52 trp1Δ63 his3Δ200 leu2Δ1 lys2ΔBgl hom3-10 ade2Δ1 ade8 hxt13::URA3 rad51::HIS3</i> |
| KHSY1258 | <i>MATa ura3-52 trp1Δ63 his3Δ200 leu2Δ1 lys2ΔBgl hom3-10 ade2Δ1 ade8 hxt13::URA3 rad52::HIS3</i> |
| KHSY1399 | <i>MATa ura3-52 trp1Δ63 his3Δ200 leu2Δ1 lys2ΔBgl hom3-10 ade2Δ1 ade8 hxt13::URA3 rrm3::kanMX6</i> |
| KHSY1557 | <i>MATa ura3-52 trp1Δ63 his3Δ200 leu2Δ1 lys2ΔBgl hom3-10 ade2Δ1 ade8 hxt13::URA3 mph1::HIS3</i> |
| KHSY1561 | <i>MATa ura3-52 trp1Δ63 his3Δ200 leu2Δ1 lys2ΔBgl hom3-10 ade2Δ1 ade8 hxt13::URA3 chl1::HIS3</i> |
| KHSY1598 | <i>MATa ura3-52 trp1Δ63 his3Δ200 leu2Δ1 lys2ΔBgl hom3-10 ade2Δ1 ade8 hxt13::URA3 rad52::HIS3 mph1::HIS3</i> |

TABLE A1.1 (continued)

| | |
|----------|---|
| KHSY1600 | <i>MATa ura3-52 trp1Δ63 his3Δ200 leu2Δ1 lys2ΔBgl hom3-10 ade2Δ1 ade8</i> <i>hxt13::URA3 sgs1::TRP1 mph1::HIS3</i> |
| KHSY1630 | <i>MATa ura3-52 trp1Δ63 his3Δ200 leu2Δ1 lys2ΔBgl hom3-10 ade2Δ1 ade8</i> <i>hxt13::URA3 sgs1::TRP1</i> |
| KHSY1702 | <i>MATa ura3-52 trp1Δ63 his3Δ200 leu2Δ1 lys2ΔBgl hom3-10 ade2Δ1 ade8</i> <i>hxt13::URA3 srs2::kanMX6 mph1::HIS3</i> |
| KHSY1713 | <i>MATa ura3-52 trp1Δ63 his3Δ200 leu2Δ1 lys2ΔBgl hom3-10 ade2Δ1 ade8</i> <i>hxt13::URA3 rrm3::TRP1 mph1::HIS3</i> |
| KHSY1725 | <i>MATa ura3-52 trp1Δ63 his3Δ200 leu2Δ1 lys2ΔBgl hom3-10 ade2Δ1 ade8</i> <i>hxt13::URA3 chl1::HIS3 mph1::HIS3</i> |
| KHSY1872 | <i>MATa/α ura3-52/ura3-52 trp1Δ63/trp1Δ63 his3Δ200/his3Δ200</i> <i>MPH1/mph1::HIS3 SRS2/srs2::TRP1</i> |
| KHSY1878 | <i>MATa ura3-52 trp1Δ63 his3Δ200 leu2Δ1 lys2ΔBgl hom3-10 ade2Δ1 ade8</i> <i>hxt13::URA3 mec3::kanMX6 mph1::HIS3</i> |
| KHSY1889 | <i>MATa/α ura3-52/ura3-52 trp1Δ63/trp1Δ63 his3Δ200/his3Δ200</i> <i>MPH1/mph1::HIS3 MRE11/mre11::URA3</i> |
| KHSY1894 | <i>MATa ura3-52 trp1Δ63 his3Δ200 leu2Δ1 lys2ΔBgl hom3-10 ade2Δ1 ade8</i> <i>hxt13::URA3 mph1::HIS3 mec1::HIS3 sml1::TRP1</i> |
| KHSY1932 | <i>MATa/α ura3-52/ura3-52 trp1Δ63/trp1Δ63 his3Δ200/his3Δ200</i> <i>MPH1/mph1::URA3 SRS2/srs2::HIS3 MEC3/mec3::TRP1</i> |

TABLE A1.1 (continued)

| | | | | | | | |
|----------|---------------|------------------------|------------------------|--------------------------|------------------------|------------------------|--|
| KHSY1935 | <i>MATa/α</i> | <i>ura3-52/ura3-52</i> | <i>trp1Δ63/trp1Δ63</i> | <i>his3Δ200/his3Δ200</i> | <i>MPH1/mph1::HIS3</i> | <i>SRS2/srs2::TRP1</i> | <i>RAD51/rad51::kanMX6</i> |
| KHSY1954 | <i>MATa</i> | <i>ura3-52</i> | <i>trp1Δ63</i> | <i>his3Δ200</i> | <i>leu2Δ1</i> | <i>lys2ΔBgl</i> | <i>hom3-10 ade2Δ1 ade8</i> <i>hxt13::URA3 rev3::TRP1</i> |
| KHSY1957 | <i>MATa</i> | <i>ura3-52</i> | <i>trp1Δ63</i> | <i>his3Δ200</i> | <i>leu2Δ1</i> | <i>lys2ΔBgl</i> | <i>hom3-10 ade2Δ1 ade8</i> <i>hxt13::URA3 apn1::TRP1</i> |
| KHSY1970 | <i>MATa</i> | <i>ura3-52</i> | <i>trp1Δ63</i> | <i>his3Δ200</i> | <i>leu2Δ1</i> | <i>lys2ΔBgl</i> | <i>hom3-10 ade2Δ1 ade8</i> <i>hxt13::URA3 apn1::TRP1 mph1::HIS3</i> |
| KHSY1976 | <i>MATa</i> | <i>ura3-52</i> | <i>trp1Δ63</i> | <i>his3Δ200</i> | <i>leu2Δ1</i> | <i>lys2ΔBgl</i> | <i>hom3-10 ade2Δ1 ade8</i> <i>hxt13::URA3 rev3::TRP1 mph1::HIS3</i> |
| KHSY2020 | <i>MATa</i> | <i>ura3-52</i> | <i>trp1Δ63</i> | <i>his3Δ200</i> | <i>leu2Δ1</i> | <i>lys2ΔBgl</i> | <i>hom3-10 ade2Δ1 ade8</i> <i>hxt13::URA3 rad51::HIS3 srs2::kanMX6 mph1::HIS3</i> |
| KHSY2038 | <i>MATa</i> | <i>ura3-52</i> | <i>trp1Δ63</i> | <i>his3Δ200</i> | <i>leu2Δ1</i> | <i>lys2ΔBgl</i> | <i>hom3-10 ade2Δ1 ade8</i> <i>hxt13::URA3 mec3::HIS3 srs2::kanMX6 mph1::TRP1</i> |
| KHSY2226 | <i>MATa</i> | <i>ura3-52</i> | <i>trp1Δ63</i> | <i>his3Δ200</i> | <i>leu2Δ1</i> | <i>lys2ΔBgl</i> | <i>hom3-10 ade2Δ1 ade8</i> <i>hxt13::URA3 rev3::TRP1 srs2::kanMX6 mph1::HIS3</i> |
| KHSY2416 | <i>MATa</i> | <i>ura3-52</i> | <i>trp1Δ63</i> | <i>his3Δ200</i> | <i>leu2Δ1</i> | <i>lys2ΔBgl</i> | <i>hom3-10 ade2Δ1 ade8</i> <i>hxt13::URA3 rev3::TRP1 rad52::HIS3 mph1::HIS3</i> |
| KHSY2420 | <i>MATa</i> | <i>ura3-52</i> | <i>trp1Δ63</i> | <i>his3Δ200</i> | <i>leu2Δ1</i> | <i>lys2ΔBgl</i> | <i>hom3-10 ade2Δ1 ade8</i> <i>hxt13::URA3 rev3::TRP1 rad52::HIS3</i> |

TABLE A1.1 (continued)

| | |
|----------|--|
| KHSY2492 | <i>MATa ura3-52 trp1Δ63 his3Δ200 leu2Δ1 lys2ΔBgl hom3-10 ade2Δ1 ade8 hxt13::URA3 mph1::HIS3 rad51::HIS3</i> |
| KHSY3042 | <i>MATa ura3-52 leu2Δ1 trp1Δ63 his3Δ200 lys2ΔBgl hom3-10 ade2Δ1 ade8 can1::hisG yel072w::CAN1/URA3 iYEL072::hph mec3::TRP1 mph1::HIS3</i> |
| KHSY3056 | <i>MATa ura3-52 leu2Δ1 trp1Δ63 his3Δ200 lys2ΔBgl hom3-10 ade2Δ1 ade8 can1::hisG yel072w::CAN1/URA3 iYEL072::hph rev3::TRP1 mph1::HIS3</i> |
| KHSY3065 | <i>MATa ura3-52 leu2Δ1 trp1Δ63 his3Δ200 lys2ΔBgl hom3-10 ade2Δ1 ade8 can1::hisG yel072w::CAN1/URA3 iYEL072::hph mec3::TRP1</i> |
| KHSY3067 | <i>MATa ura3-52 leu2Δ1 trp1Δ63 his3Δ200 lys2ΔBgl hom3-10 ade2Δ1 ade8 can1::hisG yel072w::CAN1/URA3 iYEL072::hph srs2::HIS3</i> |
| KHSY3101 | <i>MATa ura3-52 leu2Δ1 trp1Δ63 his3Δ200 lys2ΔBgl hom3-10 ade2Δ1 ade8 can1::hisG yel072w::CAN1/URA3 iYEL072::hph srs2::HIS3 mph1::HIS3</i> |
| KHSY3123 | <i>MATa ura3-52 leu2Δ1 trp1Δ63 his3Δ200 lys2ΔBgl hom3-10 ade2Δ1 ade8 can1::hisG yel072w::CAN1/URA3 iYEL072::hph srs2::HIS3 mph1::HIS3 rev3::TRP1</i> |
| KHSY3126 | <i>MATa ura3-52 leu2Δ1 trp1Δ63 his3Δ200 lys2ΔBgl hom3-10 ade2Δ1 ade8 can1::hisG yel072w::CAN1/URA3 iYEL072::hph srs2::HIS3 mph1::HIS3 mec3::TRP1</i> |

^a Obtained from Richard Kolodner (University of California—San Diego).

TABLE A.2. Effect of defects in DNA lesion bypass, homologous recombination, DNA helicases, and the DNA damage checkpoint on accumulation of gross chromosomal rearrangements in the standard GCR strain background RDKY3615

| Relevant genotype | Strain | GCR rate (Can ^r 5-FOA ^r) ($\times 10^{-10}$) ^a | 95% CI ^b (Can ^r 5-FOA ^r) ($\times 10^{-10}$) | Fold increase over wild-type level |
|---|----------|--|--|------------------------------------|
| Wild type | RDKY3615 | 3.5 ^c | | 1 |
| <i>mph1</i> | KHSY1557 | 20 | 5–34 | 6 |
| <i>rev3</i> | KHSY1954 | 10 | 5–21 | 3 |
| <i>rev3</i> <i>mph1</i> | KHSY1976 | 56 | 44–71 | 16 |
| <i>rev3</i> <i>mph1</i> <i>srs2</i> | KHSY2226 | <14 | <11–18 | <4 |
| <i>srs2</i> | RDKY5557 | 2 ^d | <2–11 | 0.6 |
| <i>mph1</i> <i>srs2</i> | KHSY1702 | 1.2 | <2–6 | 0.3 |
| <i>mph1</i> <i>mec3</i> | KHSY1878 | 55 | 24–73 | 16 |
| <i>mph1</i> <i>mec3</i> <i>srs2</i> | KHSY2038 | 56 | 30–68 | 16 |
| <i>mec1</i> <i>sml1</i> | KHSY895 | 471 | 209–859 | 135 |

Table A.2 (continued)

| | | | | |
|--------------|----------|-----------------|---------|-----|
| <i>mec1</i> | KHSY1894 | 290 | 154–467 | 83 |
| <i>sml1</i> | | | | |
| <i>mph1</i> | | | | |
| <i>apn1</i> | KHSY1957 | 19 | 14–41 | 5 |
| <i>apn1</i> | KHSY1970 | 15 | <15–51 | 4 |
| <i>mph1</i> | | | | |
| <i>rad52</i> | KHSY1258 | 435 | 317–520 | 124 |
| <i>rad52</i> | KHSY1598 | 275 | 131–467 | 79 |
| <i>mph1</i> | | | | |
| <i>sgs1</i> | KHSY1630 | 220 | 144–276 | 64 |
| <i>sgs1</i> | KHSY1600 | 239 | 162–528 | 68 |
| <i>mph1</i> | | | | |
| <i>chl1</i> | KHSY1561 | 14 | <14–94 | 4 |
| <i>chl1</i> | KHSY1725 | 40 | <10–202 | 11 |
| <i>mph1</i> | | | | |
| <i>rrm3</i> | KHSY1399 | 14 ^d | 5–28 | 4 |
| <i>rrm3</i> | KHSY1713 | 21 | <17–48 | 6 |
| <i>mph1</i> | | | | |

^a 5-FOA, 5-fluoroorotic acid.

^b Ninety-five percent confidence intervals (CIs) were calculated according to the method of Nair (Nair 1940), with nonoverlapping confidence intervals indicating statistically significant differences ($\alpha < 0.05$) between median GCR rates.

^c GCR rate from reference (Chen, Umezu et al. 1998).

^d GCR rate from reference (Schmidt and Kolodner 2006).

REFERENCES

Banerjee, S., S. Smith, J. H. Oum, H. J. Liaw, J. Y. Hwang, N. Sikdar, A. Motegi, S. E. Lee and K. Myung (2008). "Mph1p promotes gross chromosomal rearrangement through partial inhibition of homologous recombination." J Cell Biol **181**(7): 1083-1093.

Chen, C., K. Umezu and R. D. Kolodner (1998). "Chromosomal rearrangements occur in *S. cerevisiae* rfa1 mutator mutants due to mutagenic lesions processed by double-strand-break repair." Mol Cell **2**(1): 9-22.

Entian, K. D., T. Schuster, J. H. Hegemann, D. Becher, H. Feldmann, U. Guldener, R. Gotz, M. Hansen, C. P. Hollenberg, G. Jansen, W. Kramer, S. Klein, P. Kotter, J. Kricke, H. Launhardt, G. Mannhaupt, A. Maierl, P. Meyer, W. Mewes, T. Munder, R. K. Niedenthal, M. Ramezani Rad, A. Rohmer, A. Romer, A. Hinnen and et al. (1999). "Functional analysis of 150 deletion mutants in *Saccharomyces cerevisiae* by a systematic approach." Mol Gen Genet **262**(4-5): 683-702.

Fabre, F., A. Chan, W. D. Heyer and S. Gangloff (2002). "Alternate pathways involving Sgs1/Top3, Mus81/ Mms4, and Srs2 prevent formation of toxic recombination intermediates from single-stranded gaps created by DNA replication." Proc Natl Acad Sci U S A **99**(26): 16887-16892.

Gangloff, S., J. P. McDonald, C. Bendixen, L. Arthur and R. Rothstein (1994). "The yeast type I topoisomerase Top3 interacts with Sgs1, a DNA helicase homolog: a potential eukaryotic reverse gyrase." Mol Cell Biol **14**(12): 8391-8398.

Gangloff, S., C. Soustelle and F. Fabre (2000). "Homologous recombination is responsible for cell death in the absence of the Sgs1 and Srs2 helicases." Nat Genet **25**(2): 192-194.

Gari, K., C. Decaillet, M. Delannoy, L. Wu and A. Constantinou (2008). "Remodeling of DNA replication structures by the branch point translocase FANCM." Proc Natl Acad Sci U S A **105**(42): 16107-16112.

Gari, K., C. Decaillet, A. Z. Stasiak, A. Stasiak and A. Constantinou (2008). "The Fanconi anemia protein FANCM can promote branch migration of Holliday junctions and replication forks." Mol Cell **29**(1): 141-148.

Gietz, R. D. and R. A. Woods (2006). "Yeast transformation by the LiAc/SS Carrier DNA/PEG method." Methods Mol Biol **313**: 107-120.

Hirota, Y. and J. M. Lahti (2000). "Characterization of the enzymatic activity of hChIR1, a novel human DNA helicase." Nucleic Acids Res **28**(4): 917-924.

Holloway, S. (2000). "CHL1 is a nuclear protein with an essential ATP binding site that exhibits a size-dependent effect on chromosome segregation." Nucleic Acids Res **28**(16): 3056-3064.

- Ira, G., A. Malkova, G. Liberi, M. Foiani and J. E. Haber (2003). "Srs2 and Sgs1-Top3 suppress crossovers during double-strand break repair in yeast." Cell **115**(4): 401-411.
- Ivessa, A. S., B. A. Lenzmeier, J. B. Bessler, L. K. Goudsouzian, S. L. Schnakenberg and V. A. Zakian (2003). "The *Saccharomyces cerevisiae* helicase Rrm3p facilitates replication past nonhistone protein-DNA complexes." Mol Cell **12**(6): 1525-1536.
- Ivessa, A. S., J. Q. Zhou, V. P. Schulz, E. K. Monson and V. A. Zakian (2002). "Saccharomyces Rrm3p, a 5' to 3' DNA helicase that promotes replication fork progression through telomeric and subtelomeric DNA." Genes Dev **16**(11): 1383-1396.
- Joenje, H. and K. J. Patel (2001). "The emerging genetic and molecular basis of Fanconi anaemia." Nat Rev Genet **2**(6): 446-457.
- Kennedy, R. D. and A. D. D'Andrea (2005). "The Fanconi Anemia/BRCA pathway: new faces in the crowd." Genes Dev **19**(24): 2925-2940.
- Klein, H. L. (2001). "Mutations in recombinational repair and in checkpoint control genes suppress the lethal combination of srs2Delta with other DNA repair genes in *Saccharomyces cerevisiae*." Genetics **157**(2): 557-565.
- Kolodner, R. D., C. D. Putnam and K. Myung (2002). "Maintenance of genome stability in *Saccharomyces cerevisiae*." Science **297**(5581): 552-557.
- Krejci, L., S. Van Komen, Y. Li, J. Villemain, M. S. Reddy, H. Klein, T. Ellenberger and P. Sung (2003). "DNA helicase Srs2 disrupts the Rad51 presynaptic filament." Nature **423**(6937): 305-309.
- Lee, S. K., R. E. Johnson, S. L. Yu, L. Prakash and S. Prakash (1999). "Requirement of yeast SGS1 and SRS2 genes for replication and transcription." Science **286**(5448): 2339-2342.
- Liberi, G., I. Chiolo, A. Pellicoli, M. Lopes, P. Plevani, M. Muzi-Falconi and M. Foiani (2000). "Srs2 DNA helicase is involved in checkpoint response and its regulation requires a functional Mec1-dependent pathway and Cdk1 activity." Embo J **19**(18): 5027-5038.
- Lo, Y. C., K. S. Paffett, O. Amit, J. A. Clikeman, R. Sterk, M. A. Brenneman and J. A. Nickoloff (2006). "Sgs1 regulates gene conversion tract lengths and crossovers independently of its helicase activity." Mol Cell Biol **26**(11): 4086-4094.
- Mathew, C. G. (2006). "Fanconi anaemia genes and susceptibility to cancer." Oncogene **25**(43): 5875-5884.
- Mullen, J. R., V. Kaliraman and S. J. Brill (2000). "Bipartite structure of the SGS1 DNA helicase in *Saccharomyces cerevisiae*." Genetics **154**(3): 1101-1114.

Myung, K., A. Datta, C. Chen and R. D. Kolodner (2001). "SGS1, the *Saccharomyces cerevisiae* homologue of BLM and WRN, suppresses genome instability and homeologous recombination." Nat Genet **27**(1): 113-116.

Nair, K. R. (1940). "Table of confidence intervals for the median in samples from any continuous population." Sankhya(4): 551-558.

Niedzwiedz, W., G. Mosedale, M. Johnson, C. Y. Ong, P. Pace and K. J. Patel (2004). "The Fanconi anaemia gene FANCC promotes homologous recombination and error-prone DNA repair." Mol Cell **15**(4): 607-620.

Ogiwara, H., A. Ui, M. S. Lai, T. Enomoto and M. Seki (2007). "Chl1 and Ctf4 are required for damage-induced recombinations." Biochem Biophys Res Commun **354**(1): 222-226.

Ooi, S. L., D. D. Shoemaker and J. D. Boeke (2003). "DNA helicase gene interaction network defined using synthetic lethality analyzed by microarray." Nat Genet **35**(3): 277-286.

Petronczki, M., B. Chwalla, M. F. Siomos, S. Yokobayashi, W. Helmhart, A. M. Deutschbauer, R. W. Davis, Y. Watanabe and K. Nasmyth (2004). "Sister-chromatid cohesion mediated by the alternative RF-CCtf18/Dcc1/Ctf8, the helicase Chl1 and the polymerase-alpha-associated protein Ctf4 is essential for chromatid disjunction during meiosis II." J Cell Sci **117**(Pt 16): 3547-3559.

Pfander, B., G. L. Moldovan, M. Sacher, C. Hoege and S. Jentsch (2005). "SUMO-modified PCNA recruits Srs2 to prevent recombination during S phase." Nature **436**(7049): 428-433.

Prakash, R., L. Krejci, S. Van Komen, K. Anke Schurer, W. Kramer and P. Sung (2005). "*Saccharomyces cerevisiae* MPH1 gene, required for homologous recombination-mediated mutation avoidance, encodes a 3' to 5' DNA helicase." J Biol Chem **280**(9): 7854-7860.

Prakash, R., D. Satory, E. Dray, A. Papusha, J. Scheller, W. Kramer, L. Krejci, H. Klein, J. E. Haber, P. Sung and G. Ira (2009). "Yeast Mph1 helicase dissociates Rad51-made D-loops: implications for crossover control in mitotic recombination." Genes Dev **23**(1): 67-79.

Putnam, C. D., T. K. Hayes and R. D. Kolodner (2009). "Specific pathways prevent duplication-mediated genome rearrangements." Nature **460**(7258): 984-989.

Robert, T., D. Dervins, F. Fabre and S. Gangloff (2006). "Mrc1 and Srs2 are major actors in the regulation of spontaneous crossover." Embo J **25**(12): 2837-2846.

Scheller, J., A. Schurer, C. Rudolph, S. Hettwer and W. Kramer (2000). "MPH1, a yeast gene encoding a DEAH protein, plays a role in protection of the genome from spontaneous and chemically induced damage." Genetics **155**(3): 1069-1081.

Schmidt, K. H. and R. D. Kolodner (2004). "Requirement of Rrm3 helicase for repair of spontaneous DNA lesions in cells lacking Srs2 or Sgs1 helicase." Mol Cell Biol **24**(8): 3213-3226.

Schmidt, K. H. and R. D. Kolodner (2006). "Suppression of spontaneous genome rearrangements in yeast DNA helicase mutants." Proc Natl Acad Sci U S A **103**(48): 18196-18201.

Schmidt, K. H., V. Pennaneach, C. D. Putnam and R. D. Kolodner (2006). "Analysis of gross-chromosomal rearrangements in *Saccharomyces cerevisiae*." Methods Enzymol **409**: 462-476.

Schmidt, K. H., J. Wu and R. D. Kolodner (2006). "Control of translocations between highly diverged genes by Sgs1, the *Saccharomyces cerevisiae* homolog of the Bloom's syndrome protein." Mol Cell Biol **26**(14): 5406-5420.

Schurer, K. A., C. Rudolph, H. D. Ulrich and W. Kramer (2004). "Yeast MPH1 gene functions in an error-free DNA damage bypass pathway that requires genes from Homologous recombination, but not from postreplicative repair." Genetics **166**(4): 1673-1686.

Shiratori, A., T. Shibata, M. Arisawa, F. Hanaoka, Y. Murakami and T. Eki (1999). "Systematic identification, classification, and characterization of the open reading frames which encode novel helicase-related proteins in *Saccharomyces cerevisiae* by gene disruption and Northern analysis." Yeast **15**(3): 219-253.

Sinclair, D. A., K. Mills and L. Guarente (1997). "Accelerated aging and nucleolar fragmentation in yeast *sgs1* mutants." Science **277**(5330): 1313-1316.

Thompson, L. H., J. M. Hinz, N. A. Yamada and N. J. Jones (2005). "How Fanconi anemia proteins promote the four Rs: replication, recombination, repair, and recovery." Environ Mol Mutagen **45**(2-3): 128-142.

Tong, A. H., M. Evangelista, A. B. Parsons, H. Xu, G. D. Bader, N. Page, M. Robinson, S. Raghbizadeh, C. W. Hogue, H. Bussey, B. Andrews, M. Tyers and C. Boone (2001). "Systematic genetic analysis with ordered arrays of yeast deletion mutants." Science **294**(5550): 2364-2368.

Tong, A. H., G. Lesage, G. D. Bader, H. Ding, H. Xu, X. Xin, J. Young, G. F. Berriz, R. L. Brost, M. Chang, Y. Chen, X. Cheng, G. Chua, H. Friesen, D. S. Goldberg, J. Haynes, C. Humphries, G. He, S. Hussein, L. Ke, N. Krogan, Z. Li, J. N. Levinson, H. Lu, P. Menard, C. Munyana, A. B. Parsons, O. Ryan, R. Tonikian, T. Roberts, A. M. Sdicu, J. Shapiro, B. Sheikh, B. Suter, S. L. Wong, L. V. Zhang, H. Zhu, C. G. Burd, S. Munro, C. Sander, J. Rine, J. Greenblatt, M. Peter, A. Bretscher, G. Bell, F. P. Roth, G. W. Brown, B. Andrews, H. Bussey and C. Boone (2004). "Global mapping of the yeast genetic interaction network." Science **303**(5659): 808-813.

Torres, J. Z., S. L. Schnakenberg and V. A. Zakian (2004). "Saccharomyces cerevisiae Rrm3p DNA helicase promotes genome integrity by preventing replication fork stalling: viability of rrm3 cells requires the intra-S-phase checkpoint and fork restart activities." Mol Cell Biol **24**(8): 3198-3212.

Veaute, X., J. Jeusset, C. Soustelle, S. C. Kowalczykowski, E. Le Cam and F. Fabre (2003). "The Srs2 helicase prevents recombination by disrupting Rad51 nucleoprotein filaments." Nature **423**(6937): 309-312.

Wang, W. (2007). "Emergence of a DNA-damage response network consisting of Fanconi anaemia and BRCA proteins." Nat Rev Genet **8**(10): 735-748.

Watt, P. M., E. J. Louis, R. H. Borts and I. D. Hickson (1995). "Sgs1: a eukaryotic homolog of E. coli RecQ that interacts with topoisomerase II in vivo and is required for faithful chromosome segregation." Cell **81**(2): 253-260.

Yamagata, K., J. Kato, A. Shimamoto, M. Goto, Y. Furuichi and H. Ikeda (1998). "Bloom's and Werner's syndrome genes suppress hyperrecombination in yeast sgs1 mutant: implication for genomic instability in human diseases." Proc Natl Acad Sci U S A **95**(15): 8733-8738.

APPENDIX B:

STRUCTURAL MOTIFS CRITICAL FOR *IN VIVO* FUNCTION AND STABILITY OF THE RECQ-MEDIATED GENOME INSTABILITY PROTEIN RMI1

Note to the reader: This chapter was previously published with permission from the publisher as Kennedy, JA, Syed, S, and Schmidt, KH (2015). "Structural Motifs Critical for *In Vivo* Function and Stability of the RecQ-Mediated Genome Instability Protein Rmi1." PLoS One, 2015. 10(12): p.e0145466. Research was designed by K. Schmidt and J. Kennedy. Experiments were performed by J. Kennedy and S. Syed. Data was analyzed by K. Schmidt, J. Kennedy, and S. Syed. Reagents/materials/analysis tools were provided by K. Schmidt and J. Kennedy. Paper was written by K. Schmidt and J. Kennedy. Corresponding author: Kristina Schmidt, Department of Cell Biology, Microbiology and Molecular Biology, University of South Florida, 4202 E. Fowler Avenue, ISA2015, Tampa, FL 33620. Phone: (813) 974-1592. Fax: (813) 974- 1614.; E-mail: kschmidt@usf.edu

ABSTRACT

Rmi1 is a member of the Sgs1/Top3/Rmi1 (STR) complex of *Saccharomyces cerevisiae* and has been implicated in binding and catalytic enhancement of Top3 in the dissolution of double Holliday junctions. Deletion of *RMI1* results in a severe growth defect resembling that of *top3Δ*. Despite the importance of Rmi1 for cell viability, little is

known about its functional domains, particularly in Rmi1 of *S. cerevisiae*, which does not have a resolved crystal structure and the primary sequence is poorly conserved. Here, we rationally designed point mutations based on bioinformatics analysis of order/disorder and helical propensity to define three functionally important motifs in yeast Rmi1 outside of the proposed OB-fold core. Replacing residues F63, Y218 and E220 with proline, designed to break predicted N-terminal and C-terminal α -helices, or with lysine, designed to eliminate hydrophobic residues at positions 63 and 218, while maintaining α -helical structure, caused hypersensitivity to hydroxyurea. Further, Y218P and E220P mutations, but not F63P and F63K mutations, led to reduced Rmi1 levels compared to wild type Rmi1, suggesting a role of the C-terminal α -helix in Rmi1 stabilization, most likely by protecting the integrity of the OB-fold core. Our bioinformatics analysis also suggests the presence of a disordered linker between the N-terminal α -helix and the OB fold core; a P88A mutation, designed to increase helicity in this linker, also impaired Rmi1 function in vivo. In conclusion, we propose a model that maps all functionally important structural features for yeast Rmi1 based on biological findings in yeast and structure-prediction-based alignment with the recently established crystal structure of the N-terminus of human Rmi1.

INTRODUCTION

The RecQ-like DNA helicase family is evolutionarily conserved and necessary for genomic stability from bacteria to humans. In yeast the RecQ-like Sgs1 helicase forms a complex with the topoisomerase Top3 and the recQ-mediated genome instability 1 protein Rmi1 (STR) and facilitates both early and late steps of DNA double-strand break

(DSB) repair (Chang, Bellaoui et al. 2005, Mullen, Nallaseth et al. 2005, Chu and Hickson 2009). Early in the repair of a two-ended DSB, STR contributes to DSB end resection to facilitate the formation of a single-strand 3' overhang on which the homologous recombination (HR) factor Rad51 filament assembles (Bennett, Keck et al. 1999, Mimitou and Symington 2008, Zhu, Chung et al. 2008, Daley, Chiba et al. 2014). This Rad51 filament is then able to initiate a genome-wide search for sequence homology, eventually leading to the formation of double Holliday Junctions (dHJs) that need to be resolved prior to cell division. Resolution can be achieved by the HJ-specific endonuclease Yen1, randomly leading to crossover and noncrossover products, or dHJs can be dissolved by STR in a process involving dHJ migration and decatenation of the single strands, yielding exclusively noncrossover products (Mitchel, Lehner et al. 2013). STR has also been implicated in the unwinding of strand invasion after extension of the invading 3' end by DNA synthesis to promote DSB repair by synthesis-dependent strand annealing, as well as reversal of strand invasion prior to 3' end extension (Fasching, Cejka et al. 2015). Through these functions, STR promotes noncrossover outcomes of HR and regulates HR levels. Hence, yeast cells that lack the helicase activity of the STR complex (*sgs1Δ*) are prone to hyper-recombination, accumulate gross chromosomal rearrangements, and are hypersensitive to DNA-damaging agents, with cells lacking Top3 or Rmi1 additionally exhibiting a severe growth defect not seen in cells lacking Sgs1 (Gangloff, McDonald et al. 1994, Myung, Datta et al. 2001, Chang, Bellaoui et al. 2005, Mullen, Nallaseth et al. 2005). Similarly, in mice inactivation of RMI1 or Topo III α leads to embryonic lethality earlier (no blastocysts) than inactivation of BLM (day 13.5), the human RecQ-like helicase most closely related Sgs1 (Chen, You

et al. 2011).

Despite the growth defect of the *rmi1Δ* mutant, the contribution of Rmi1 to the function of the STR complex and the regions of Rmi1 that are critical for these functional contributions are still poorly understood. Rmi1, was first discovered in *S. cerevisiae* in a screen for components of the Sgs1/Top3 pathway (Mullen, Nallaseth et al. 2005). Yeast cells lacking Rmi1 are hypersensitive to hydroxyurea (HU) and several other genotoxic agents, have an increased rate of spontaneous DNA damage as indicated by an increase in Rad52 foci, an increase in chromosomal rearrangements, and deficiency in activation of the DNA-damage checkpoint kinase Rad53 (Chang, Bellaoui et al. 2005, Mullen, Nallaseth et al. 2005). Diploids lacking Rmi1 are defective in meiosis, and deletion of genes with roles in the checkpoint response to replication stress, such as Mrc1, Tof1, Csm3, cause synthetic lethality, implying a diverse role for Rmi1 in several chromatin processes (Chang, Bellaoui et al. 2005, Mullen, Nallaseth et al. 2005). Despite the severity of *rmi1Δ* phenotypes, Rmi1 has no known catalytic function. It has been shown to stimulate the final decatenation step of dHJ dissolution by Sgs1/Top3, while inhibiting the relaxation activity of the topoisomerase on negatively supercoiled DNA, possibly by affecting the conformation of the topoisomerase gate (Chen and Brill 2007, Cejka, Plank et al. 2010, Yang, O'Donnell et al. 2012). This function is conserved in the BLM/Topo III α /Rmi1/Rmi2 (BTR) complex, the human variant of STR, and studies in human cell lines also imply a role for Rmi1 in Topo III α stability (Wu, Bachrati et al. 2006, Yang, O'Donnell et al. 2012, Guiraldelli, Eyster et al. 2013).

The N-terminal 219 residues of the 625-residue long human Rmi1 have been crystallized, providing some clues to its role in catalytic enhancement and stability of the

BTR complex (Wang, Yang et al. 2010, Bocquet, Bizard et al. 2014). The N-terminus of human Rmi1 is most closely related to *S. cerevisiae* Rmi1, is capable of binding BLM and Topo III α , and contains an oligonucleotide-binding (OB) fold that is similar in structure to that of the replication protein A subunit RPA70, though it is suggested that it is incapable of binding DNA like RPA (Raynard, Bussen et al. 2006, Wang, Yang et al. 2010). Human Rmi1 contains a disordered loop needed for dHJ dissolution enhancement of Topo III α (Bocquet, Bizard et al. 2014). Co-crystallization of the Rmi1 N-terminal lobe peptide with Topo III α reveals that the OB-fold of Rmi1 lies opposite of the ssDNA-binding domain of Topo III α , and a mostly disordered loop that protrudes from the OB fold of Rmi1 physically interacts with the topoisomerase by inserting itself into the central topoisomerase gate (Ira, Malkova et al. 2003). It has been hypothesized that this loop may be what facilitates the catalytic enhancement of Topo III α by regulating opening and closing of the gate (Wang, Yang et al. 2010, Bocquet, Bizard et al. 2014).

Because of the severe growth retardation, low viability and rapid accumulation of suppressor mutations, the identification and functional analysis of deleterious *rmi1* mutations through genetic screens has proved difficult; one *rmi1* mutant, the temperature-sensitive E69K, was identified through this conventional approach (Ashton, Mankouri et al. 2011). In an effort to better understand the molecular basis of Rmi1 function, we have combined structure prediction tools with an *in vivo* mutational analysis of *RM11* function in yeast. This approach has identified structural motifs that are essential for Rmi1 function and stability and we propose hypotheses for how these motifs contribute to Rmi1's role in maintaining the functional integrity of the STR

complex. As an alternative to primary sequence alignments, which have been only minimally informative because of the poor sequence conservation among Rmi1 homologues, we present a structure-based alignment between yeast and human Rmi1 that maps the location of conserved motifs and suggests differences in the size and structure of the DUF1767 domain.

MATERIALS AND METHODS

Bioinformatics analysis

The 241 residues of *S. cerevisiae* Rmi1 and the N-terminal 240 residues of the 625-residue human Rmi1 were analyzed with algorithms for helical propensity (Munoz and Serrano 1995, Munoz and Serrano 1997), structural disorder using a combination of three predictors in VL-XT (Li, Romero et al. 1999, Romero, Obradovic et al. 2001), and amino acid sequence alignments based on phylogenetic analysis in PhylomeDB v4 (Huerta-Cepas, Capella-Gutierrez et al. 2014).

Plasmids

The open reading frame of *RMI1* plus 500 bp up- and downstream was amplified by PCR from the endogenous *RMI1* locus of KHSY1338 (*ura3-52, leu2Δ1, trp1Δ63, his3Δ200, lys2-Bgl, hom3-10, ade2Δ1, ade8, sgs1::HIS3, YEL069C::URA3*). The fragment was inserted into *Xba*I-digested pRS415 by gap-repair cloning using the non-homologous-endjoining deficient yeast strain KHSY2331 (*ura3-52, leu2Δ1, trp1Δ63, his3Δ200, lys2ΔBgl, hom3-10, ade2Δ1, ade8, YEL069C::URA3, lig4::loxP-G418-loxP*) and standard lithium-acetate transformation (Gietz and Woods 2006). The integrity of

RMI1 and the promoter region in the resulting plasmid pKHS621 was verified by sequencing. Point mutations were introduced into the *RMI1* ORF in pKHS621 by QuikChange site-directed mutagenesis (Agilent Technologies). To construct pKHS621 derivatives that express myc-epitope-tagged Rmi1 and *rmi1* mutant proteins, pKHS621 was linearized with *BoxI* and the *HIS3*-linked myc-epitope-coding sequence from pFA6a-13MYC-HIS3MX6 (Longtine, McKenzie et al. 1998) was inserted by gap-repair cloning. Point mutations were introduced into the resulting plasmid (pKHS630, S1 Table Plasmids used in this study) using the QuikChange protocol (Agilent Technologies).

Hydroxyurea hypersensitivity assay

Derivatives of pKHS621 were transformed into KHSY4695 (*MAT α* , *ura3 Δ 0*, *leu2 Δ 0*, *his3 Δ 1*, *lys2 Δ 0*, *rmi1::HIS3*, *TOP3.V5.VSV.KANMX6*), grown to OD₆₀₀ = 0.5 in synthetic complete media lacking leucine (SC-Leu), and spotted in 10-fold dilutions on yeast extract/peptone/dextrose (YPD) and on YPD supplemented with 150 mM hydroxyurea. Growth was documented after 3 to 5 days of incubation at 30°C.

Viability assay

Yeast strain KHSY4695 (*rmi1 Δ*) was transformed with plasmids pKHS621, pKHS624, and pKHS626. Independent cultures were set up from 9 to 12 transformants for each plasmid and grown to approximately 2 x 10⁷ cells/ml. Actual cell counts were determined using a hemocytometer and cultures were diluted to plate ~ 400 cells. Plates were incubated for 3 days at 30°C and colonies counted. Viability was calculated by dividing the number of colony forming units by the number of cells plated based on

the hemocytometer count.

Protein extraction and western blotting

A BY4741 derivative (*MATa*, *ura3Δ0*, *leu2Δ0*, *his3Δ1*, *lys2Δ0*, *RAD51-V5-6xHIS.KANMX6*) from the Yeast Cross and Capture Collection (GE Dharmacon) was transformed with pKHS630 or its derivatives (S1 Table Plasmids used in this study) expressing myc-tagged Rmi1 or *rmi1* mutants and grown in synthetic complete media lacking histidine overnight. Cultures were then diluted to OD600 = 0.2 and grown to OD600 = 0.4. Cultures were synchronized in G1 phase with 2 μg/ml of α-factor for one hour, followed by addition of 1 μg/ml of α-factor for a second hour. Cells were released for 30 min and cells equivalent to 2 ODs were harvested and washed twice in distilled water. Whole cell extract was prepared with 20% trichloroacetic acid as previously described (Kennedy, Daughdrill et al. 2013), separated by SDS-PAGE, and myc-tagged Rmi1 and *rmi1* mutants detected by Western blotting on PVDF and hybridization with c-myc (9E10) monoclonal antibody (Covance).

RESULTS

Computational analysis of yeast Rmi1 structure

Determining functionally important residues in *S. cerevisiae* Rmi1 has been challenging as it lacks catalytic activity and a crystal structure has not been resolved. The primary sequence is only minimally conserved (~35% identical residues between yeast genera, 18% between *S. cerevisiae* and human Rmi1) and lengths range from 241 residues in *S. cerevisiae* to 625 residues in humans. The crystal structure of the N-

terminal 219 residues of human Rmi1 was recently resolved (Wang, Yang et al. 2010). It revealed an N-terminal three-helix bundle of unknown function (DUF1767) followed by an OB-fold with a largely unstructured loop inserted between strands $\beta 1$ and $\beta 2$ by which Rmi1 binds to Topo III α . In the absence of catalytic activity/domains and very limited sequence identity, we reasoned that structure prediction tools (Munoz and Serrano 1997, Lacroix, Viguera et al. 1998, Peng, Vucetic et al. 2005) could reveal functionally important motifs in yeast Rmi1. Analyzing the distribution of ordered and disordered residues, we noticed disordered N- and C-termini as well as two internal regions of increased disorder (Fig 1A). Further, we identified two regions of increased helical propensity, spanning residues 58–74 and residues 212–228 near the N- and C-terminal disordered regions, as well as two regions of lesser helical propensity between residues 125–132 and 137–145 (Fig 1B). Alignment of these two predictors would be consistent with the putative OB-fold core mapping to the central, ordered region, and the topoisomerase-binding loop to the disordered insertion with two segments of weak helical propensity. The DUF1767 domain, predicted to be present in Rmi1 of all species, is typically located N-terminally of the OB-fold core, and appears to be connected to it in yeast Rmi1 by a disordered linker (Fig 1A).

Mutational analysis of predicted structural elements of yeast Rmi1

We had previously determined that disruption of an α -helix was most effective when a residue with high helical propensity near the peak or in the N-terminal half of the helix was replaced with the helix breaker proline (Kennedy, Daughdrill et al. 2013). Therefore, to determine the importance of the four regions of increased helicity for Rmi1

function, we constructed F63P, A128P, A139P and E220P mutations. The proline substitutions led to marked decreases in predicted helical propensity in these regions (Fig 1C–1F). We also noticed that the proline at position 88 seemed to disrupt what might otherwise be a region with high helical propensity, and hypothesized that this native break was helping to maintain a degree of flexibility in what would otherwise be a persistent, structured region. We considered that replacing P88 with a residue with high helical propensity that was otherwise benign, such as alanine, would restore helicity to this region. Indeed, the P88A mutation is predicted to lead to an extraordinary increase in helical propensity not seen in any region of the wildtype forms of yeast or human Rmi1 (Fig 1G). We exploited the HU hypersensitivity of yeast cells lacking Rmi1 (Chang, Bellaoui et al. 2005) to assess the functional impact of these proline substitutions *in vivo*. We found that *rmi1*Δ cells expressing *rmi1*-A128P and *rmi1*-A139P exhibited the same HU sensitivity as the *rmi1*Δ mutant complemented with wildtype *RMI1*, whereas the *rmi1*-P88A allele was only able to partially suppress the HU hypersensitivity of *rmi1*Δ (Fig 1H). This mild, 5- to 10-fold, increase in HU sensitivity of the *rmi1*-P88A mutant compared to wildtype or the *rmi1*-A128P mutant was not due to decreased viability of the *rmi1*-P88A mutant as the viability of all three strains was similar (33–36%).

The *rmi1*-F63P allele caused the same degree of HU hypersensitivity as a deletion of *RMI1*, indicating that it was a null allele (Fig 1H). We also considered the possibility that the phenotype of the F63P mutation could be due to the loss of a strong hydrophobic interaction via the aromatic residue. Thus, we chose to replace F63 with a hydrophilic residue with high helical propensity, such as lysine, that would be predicted

to maintain the structural integrity of the motif, but change its chemical properties. We found that the F63K mutation caused the same hypersensitivity to HU as the F63P mutation (Fig 1H), implicating that this residue maps to an α -helical structure that must conserve both its shape and hydrophobic character in order to maintain wildtype function of Rmi1. Similar to F63, proline substitution of E220 in the predicted C-terminal helix abolished Rmi1 function *in vivo* (Fig 1F and 1H).

The function of the putative helices defined by F63 and E220 may arise from stabilizing the putative OB-fold core of Rmi1 as seen in other proteins containing this fold type (Theobald, Mitton-Fry et al. 2003) or by otherwise contributing to Rmi1 stability. To test this possibility, we inserted a myc-epitope-coding sequence at the 3' end of *RM11* in pRS415 and introduced the deleterious F63P, F63K and E220P mutations, as well as the benign A128P mutation as a control. Equal numbers of cells were harvested from synchronized cultures for protein extraction and Western blotting, which revealed that mutations in the C-terminal helix, but neither in the N-terminal helix nor the helical elements in the insertion loop led to reduced Rmi1 levels (Fig 2).

Structure predictions and *in vivo* mutagenesis suggest differences in the N-termini of yeast and human Rmi1

Structural prediction analysis indicated a single α -helical region in the N-terminus of yeast Rmi1, centered on F63 (Fig 3A). When we extended this analysis to the N-terminus of human Rmi1, we identified three segments of increased helical propensity (Fig 3B), which form a three-helix bundle in the crystal structure (Wang, Yang et al. 2010, Bocquet, Bizard et al. 2014). The lack of helical propensity in the first 57 residues

of yeast Rmi1 suggests that this region may not adopt helical structures in the apo form as human Rmi1 does. To identify conserved residues and regions of conserved chemical character that could be indicative of a functional role, we analyzed primary sequence alignments of Rmi1. We found that *S.c.* Rmi1 is ~85% identical to Rmi1 of other *Saccharomyces* species, but identity markedly decreased to ~30% when compared to yeast species outside of the genus (e.g., *K. lactis*, *C. glabrata*), and to ~18% when compared to the N-terminal 241 residues of human Rmi1. Because of the low level of sequence identity between human and yeast Rmi1 we decided to analyze the alignment of the N-termini of twelve closely related Rmi1 sequences from fully sequenced *Saccharomyces* and non-*Saccharomyces* yeast species in PhylomeDB v4 (Huerta-Cepas, Capella-Gutierrez et al. 2014). We noticed two discrete regions (Fig 3C, residues S2-I15 and R27-L41 of *S.c.* Rmi1) that contain hydrophobic residues in the $i,i+4$ pattern typical of an α -helix and are separated from each other by residues with the lowest helical propensity, proline and glycine. To test the possibility that these two regions could become helical upon binding to another protein, possibly Sgs1, or could be analogous to $\alpha 1$ and $\alpha 2$ in human Rmi1, we replaced L7 and Y35 with proline (Fig 3C). Expression of either mutant, however, was sufficient to fully restore wildtype growth to the *rmi1* Δ mutant on HU (Fig 3D), suggesting either that, unlike in human Rmi1, this region in yeast Rmi1 does not adopt α -helical structures or that any helical structure or binding-induced folding in this region is not required for Rmi1's role in tolerating HU-induced DNA-damage. Based on comparisons of helical propensity and primary sequences of yeast Rmi1 and the N-terminus of human Rmi1 (Fig 3A–3C), we propose

structural equivalence between the sole predicted α -helix in yeast and α 3 in human Rmi1, with a potential equivalent of F63 at residue F53 in human Rmi1.

A conserved alpha helix in the C-terminus contributes to yeast Rmi1 stability

When we extended the analysis of sequence alignments to the C-terminus of Rmi1 it revealed that the chemical characteristics of the predicted α -helical region centered on residue E220 were conserved, with a short stretch of hydrophobic residues surrounded by charged residues (Fig 4C). Whereas neither E220 nor the acidic or hydrophilic character of the residue was conserved outside of the *Saccharomyces* genus, the hydrophobic residues were, including a tyrosine at position 218. We hypothesized that this residue was not only part of the functional α -helical structure we had inferred from the E220P mutant, but was also a key residue for binding in an otherwise fairly charged α -helix. Indeed, we found that either breaking the helix (rmi1-Y218P) or increasing its hydrophilicity (rmi1-Y218K) abolished Rmi1 function (Fig 4D). Although yeast and human Rmi1 are only 18% identical, we found that they share regions of similar helical propensity, including the region that surrounds Y218 in yeast and Y201 in an amphipathic α -helix in human Rmi1 (Fig 4A–4C). Similar to the disruption of the C-terminal helix by the E220P mutation, the Y218P mutation led to reduced Rmi1 levels (Fig 2).

Taken together, the bioinformatics analysis and corresponding mutagenesis of Rmi1 *in vivo* indicates the presence of two functionally critical N-terminal and C-terminal α -helices, with the latter contributing to Rmi1 stability. It further indicates a disordered

linker, defined by the P88A mutation, that appears to connect the N-terminal α -helix to the putative OB-fold core. The function of a disordered loop in the OB fold whose equivalent in human Rmi1 binds Topo III α , was not disrupted by mutagenesis of two predicted, albeit very weak, helical motifs.

DISCUSSION

In this study, we have combined three bioinformatics tools—order/disorder prediction, helical propensity and phylomes (Munoz and Serrano 1994, Munoz and Serrano 1997, Lacroix, Viguera et al. 1998, Li, Romero et al. 1999, Peng, Vucetic et al. 2005, Huerta-Cepas, Capella-Gutierrez et al. 2014)—with *in vivo* mutagenesis to elucidate structure/function relationships in yeast Rmi1. We focused on the regions that surround a putative OB-fold core previously identified in human Rmi1 that is involved in binding BLM and Topo III α (Munoz and Serrano 1997, Ira, Malkova et al. 2003). The regions surrounding the central OB-fold core are predicted to contain two short regions of increased helical propensity (residues 58–74, 212–228) and a highly disordered linker (residues 82–97) connecting the N-terminal helix to the OB-fold core. We determined that the structural and chemical integrity of the N-terminal α -helix defined by F63P/K, and the C-terminal α -helix defined by E220P and Y218P/K, are critical for Rmi1 function *in vivo*, and that the disorder of the linker, defined by P88A, contributes to normal Rmi1 function.

Performing the same structural prediction analysis for human Rmi1 suggests that the two N- and C-terminal α -helices and the spacing between them, where the core of an OB-fold has been confirmed in human Rmi1, are conserved (Fig 5). In human Rmi1,

a loop that maps to residues 98–134 emerges from the OB-fold between strands $\beta 1$ and $\beta 2$ and inserts itself into the Topo III α gate; its deletion eliminates complex formation of Rmi1 with BLM and Topo III α (Wang, Yang et al. 2010). Based on a sequence alignment Bocquet and colleagues (Bocquet, Bizard et al. 2014) suggested that the equivalent loop for Top3 binding in yeast Rmi1 maps to residues 87–146 and showed that replacement of this region with a scrambled version of equal chemistry still mediated binding to Sgs1 and Top3, but failed to stimulate Top3 catalytic activity and dHJ dissolution. The structural alignment in our study, however, which we explored because of the poor sequence conservation of only 18% between yeast and human Rmi1, suggests that residues 87–116 of yeast Rmi1 contain the $\beta 1$ strand of the OB-fold and the disordered linker that connects $\beta 1$ to the N-terminal helical region (Fig 5). The insertion loop in yeast Rmi1, therefore, may be significantly shorter, mapping to residues 116–145. As in human Rmi1, this insertion loop contains two segments of increased helical propensity (Figs 1B and 6E), but proline mutagenesis of these segments (A128P, A139P) suggests that the adoption of helical structure is not required for Rmi1's function. Since both regions adopt short helices, if any, and the prolines replaced alanines that are likely to be in the first turn, it is also possible that proline substitution is not structurally disruptive in this disordered loop.

The N-terminal region flanking the OB-fold in the crystal structure of human Rmi1 forms a three-helix bundle that has been designated a DUF1767 domain (Ira, Malkova et al. 2003). The three α -helices are also indicated in our structural analysis, whereas the corresponding region in yeast Rmi1 contains only one predicted α -helix (residues 58–74). Our structural alignment (Fig 5) suggests that it corresponds to $\alpha 3$ of human

Rmi1 (Fig 6C); this is also supported by our manual alignment of the N-terminus of human Rmi1 with the N-terminal sequences of the yeast Rmi1 phylome (Fig 3C). How this α -helix contributes to yeast Rmi1 function is unclear. Genetic analysis of Rmi1 from *Arabidopsis thaliana* showed that the OB-fold core and the N-terminal helical region DUF1767 can function independently of each other (Bonnet, Knoll et al. 2013). In human Rmi1, the three-helix bundle in the corresponding DUF1767 region makes contacts with the top region of the OB-fold core and was shown to be indispensable for its folding and solubility (Ira, Malkova et al. 2003). The F63P mutation, which we designed to disrupt the N-terminal α -helix in yeast Rmi1, caused a null phenotype; however, it had no noticeable effect on Rmi1 levels in the cell. This is in contrast to the C-terminal α -helix whose amphipathic properties and importance for Rmi1 stability strongly suggest that it protects the OB-fold core. Instead, the N-terminal α -helix—and the region N-terminal of the OB-fold in general—could also mediate association with another protein, possibly Sgs1, whose binding site on Top3/Rmi1 is unknown. This type of small binding motif paired with disorder has been seen in other proteins, including yeast Adr1, which contains two small zinc finger motifs in a disordered domain (Hyre and Klevit 1998); interestingly, the disordered components of this domain undergo extensive folding when contact is made between the zinc fingers and DNA. The structural alignment between yeast and human Rmi1 put forth in this study also suggests that the N-terminus of yeast Rmi1 is extended by approximately 18 residues. Since residues 1–16 are arranged in the typical $i, i+4$ pattern of an α -helix (residues F3, L7, I11, I15) and the yeast phylome indicates two regions of similarity in the N-terminal 57 residues, we tested if binding-induced helix formation could also be a function of the

extended unstructured N-terminus of yeast Rmi1, but found that introducing proline residues where prospective helices might form (L7, Y35), did not impair Rmi1 function. This limited analysis, however, cannot exclude the possibility that shorter helices fully capable of supporting Rmi1 function *in vivo* can still be induced with the L7P and Y35P mutations present.

In contrast to the N-terminal α -helix, our findings suggest that the C-terminal α -helix defined by the Y218P/K and E220P mutations plays a major role in stabilizing Rmi1 as seen in other proteins containing an OB-fold (Theobald, Mitton-Fry et al. 2003). Our structural prediction suggests that the C-terminal α -helix extends from residues 212 to 228 and is equivalent to the α -helix between residues 194–211 in human Rmi1, with Y201 corresponding to Y218 in yeast Rmi1 (Figs 4A–4C and 5). In contrast to mutations that disrupt the N-terminal helix, the Y218P and E220P mutations cause substantially reduced Rmi1 levels, which is the most likely cause of their null phenotype. Indeed, in the crystal structure of human Rmi1 the hydrophobic face of the corresponding amphipathic α -helix packs against the bottom of the OB-fold core, which is likely to stabilize it by shielding it from the solvent (Fig 6D) (Bocquet, Bizard et al. 2014). Binding of human Rmi1 to Rmi2 involves extensive interactions between the α -helices C-terminal of the second OB-fold of Rmi1 and the OB-fold of Rmi2 (Ira, Malkova et al. 2003, Hoadley, Xu et al. 2010); however, a similar function in mediating interaction with another protein has not been identified for the α -helix C-terminal of the N-terminal OB-folds of human or yeast Rmi1.

Finally, our bioinformatics analysis suggests a disordered loop in yeast Rmi1 linking the OB-fold core to an N-terminal α -helix. The structural disorder in this linker

appears to depend largely on a single proline, whereas multiple prolines are present in human Rmi1, suggesting a more flexible linkage of the three-helix bundle to the OB-fold core (Fig 6F). A mutation predicted to increase helicity of this flexible linker partially impaired Rmi1 function. This mutant grows normally, but exhibits increased DNA-damage sensitivity, most likely by reducing the overall conformational elasticity of Rmi1.

FIGURES

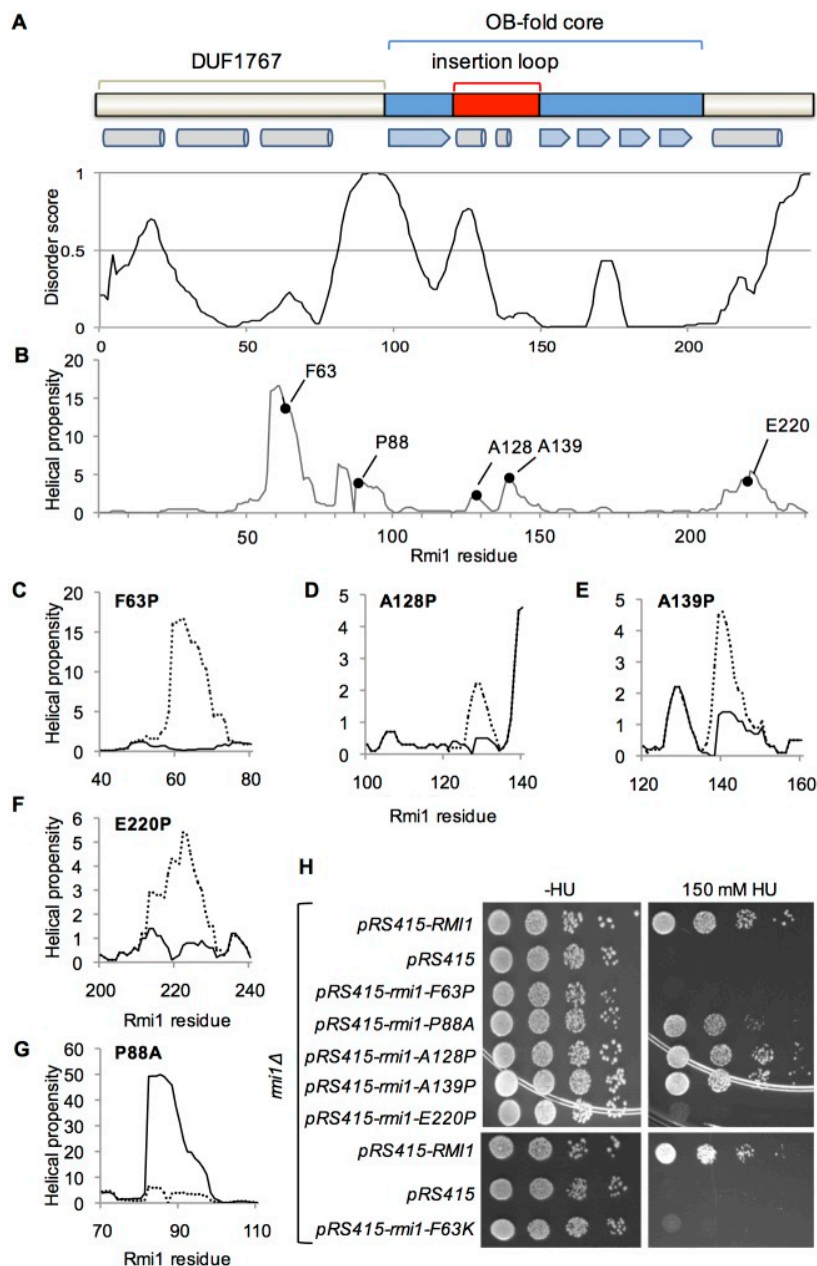


Figure B.1. Structure-prediction-guided mutagenesis of *S.c.* Rmi1.

A, prediction of order/disorder in Rmi1 by the VLXT algorithm (Li, Romero et al. 1999, Romero, Obradovic et al. 2001). A score of 1 denotes an ideal prediction of disorder and a score of 0 an ideal prediction of order with the order/disorder threshold at a score of 0.5. A domain of unknown function (DUF1767), and an OB-fold with an insertion loop are conserved in all Rmi1 species (Xu, Guo et al. 2008). The position of DUF1767, the OB-fold, the insertion loop and a predicted flexible linker between DUF1767 and the OB-fold shown above the disorder plot are based on the VLXT order/disorder prediction. α -helices (cylinders) and β -strands (arrows) in this region of human Rmi1 are indicated

below the domain map. B, prediction of four regions of increased helical in Rmi1 with residues F63, A128,A139, E220 having some of the highest helical propensity in the DUF1767 domain, the insertion loop, and the C-terminus, respectively. We predict that P88 is responsible for the sudden loss in helical propensity in the linker that connects N-terminal domain and the OB-fold. C–G, substitution of F63, A128, A139 and E220 with proline, which has the lowest helical propensity of all amino acids, is predicted to disrupt the increased helical propensity in these regions, whereas substitution of P88 with alanine, which has excellent helical propensity, is predicted to lead to a strong increase in continuous helical propensity of the linker. H, plasmid pRS415 expressing *RMI1* and *rmi1* mutants under control of the endogenous *RMI1* promoter were transformed into $\Delta rmi1$ mutant KHSY4695 and tested for the ability to suppress the hypersensitivity of the *rmi1* Δ strain to hydroxyurea.

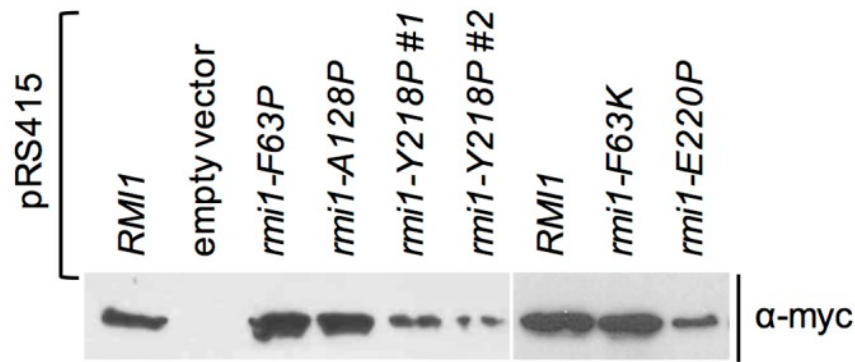


Figure B.2. Effect on expression levels of mutations designed to disrupt structural motifs of yeast Rmi1.

Mutants of Rmi1 with point mutations that disrupt the function of the putative N-terminal α -helix (F63P, F63K) are expressed at similar levels as wildtype Rmi1 and the benign rmi1-A128P mutant, whereas mutations that disrupt the function of the putative C-terminal α -helix (Y218P, E220P) are expressed at reduced levels. Whole cells extracts from equal numbers of cells from synchronized cultures expressing myc-epitope-tagged Rmi1 or rmi1 mutants were analyzed by Western blotting. Expression levels of two independently constructed plasmids expressing rmi1-Y218P are shown.

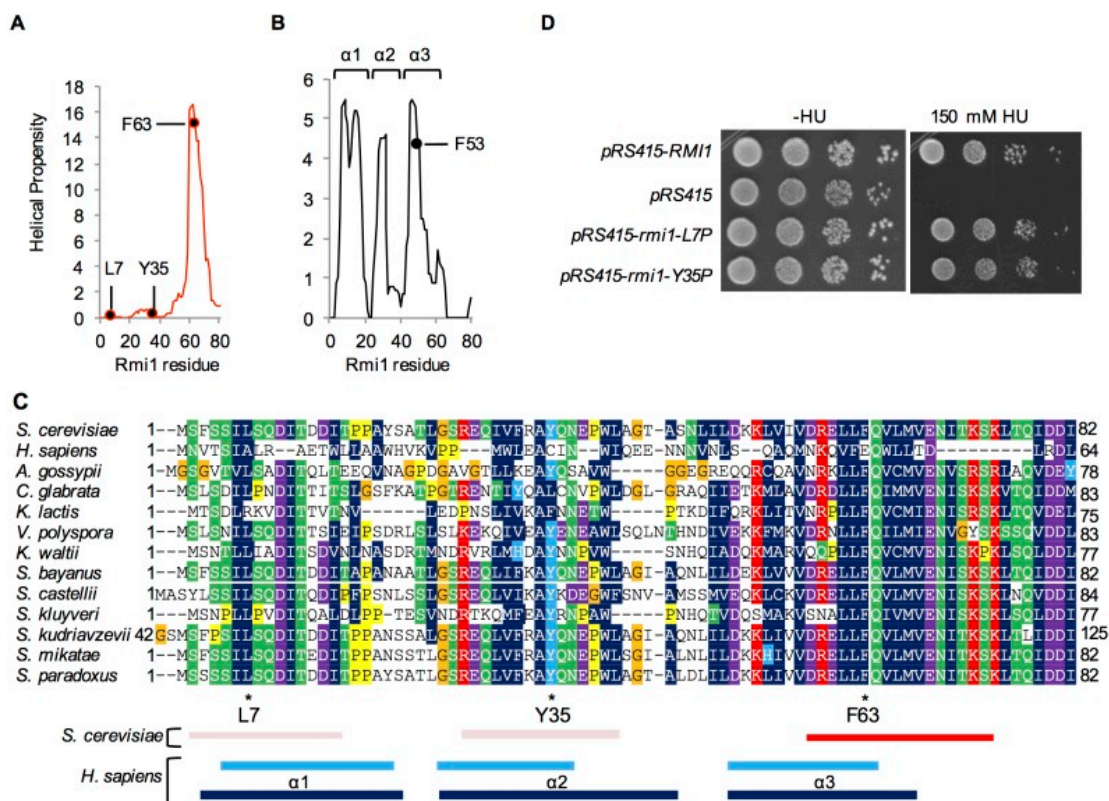


Figure B.3. Structural prediction and *in vivo* functional analysis suggest differences between the N-termini of yeast and human Rmi1.

A and B, one segment of increased helical propensity (residues 58–74) is predicted for the N-terminus of yeast Rmi1, whereas three such segments (residues 5–18, 23–32, 44–55) are predicted for human Rmi1, corresponding to the three-helix bundle confirmed in the Rmi1 crystal structure [4CGY (Bocquet, Bizard et al. 2014)]. The estimated equivalent to yeast F63, F53 in $\alpha 3$ of human Rmi1, is indicated. C, alignment of Rmi1 N-termini from twelve yeast species in PhylomeDB (Huerta-Cepas, Capella-Gutierrez et al. 2014) suggests two segments of conserved residue chemistry between residues 2–15 and residues 27–41 (indicated below the alignment by light red rectangles), in addition to the highly conserved segment predicted to have high helical propensity (indicated by a red rectangle). The N-terminus of human Rmi1 was aligned to *S.c.* Rmi1 by ClustalW and manually adjusted. The three segments of increased helical propensity predicted in the DUF1767 region of human Rmi1 are shown as light blue rectangles (residues 5–18, 23–32, 44–55) and dark blue rectangles (residues 3–19, 23–38, 44–58) indicate the confirmed location of α -helices that make up the three-helix bundle in the DUF1767 domain in the crystal structure of the N-terminus of Rmi1 with Topo III α (4CGY) (Bocquet, Bizard et al. 2014). D, substitution of L7 and Y35 with proline, aimed at preventing the two segments from adopting α -helical structure induced by intra- or intermolecular binding events, does not impair Rmi1 function *in vivo*.

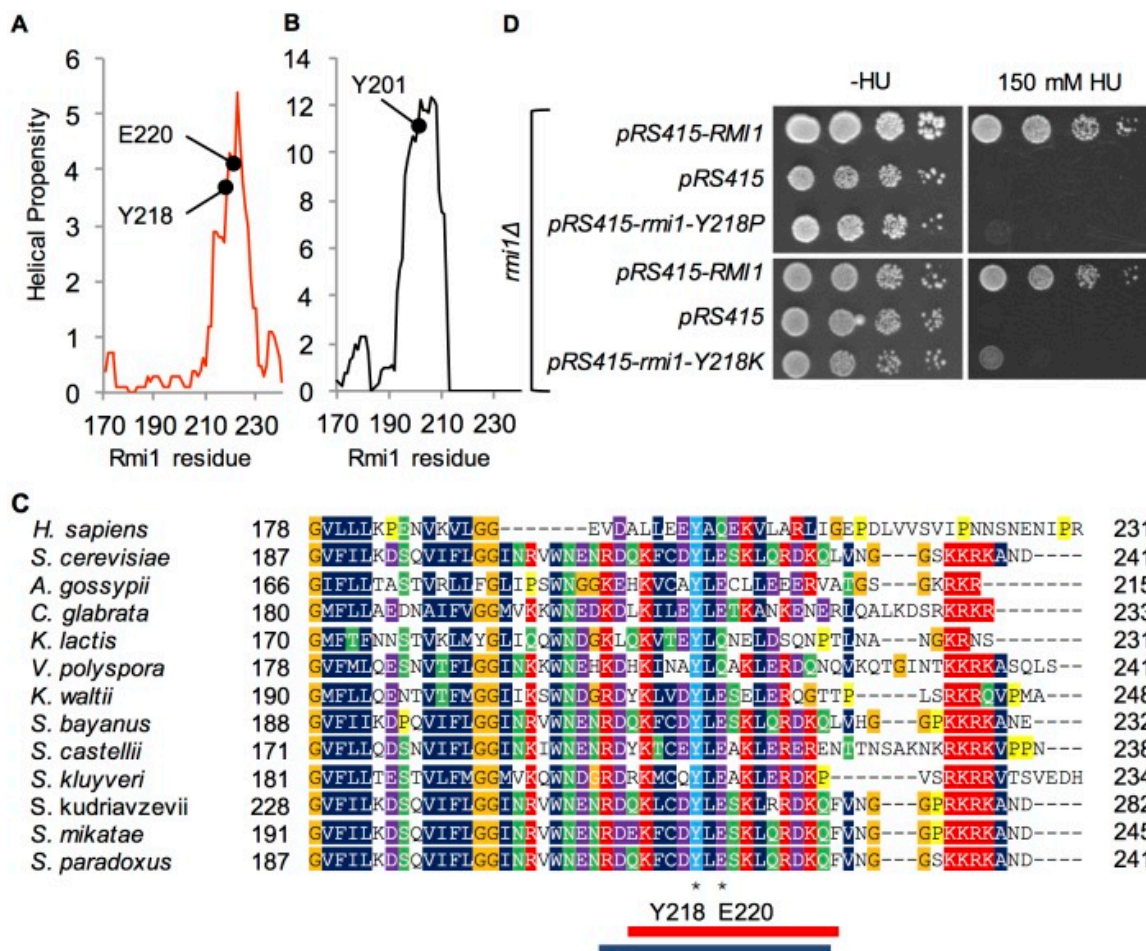


Figure B.4. Mutational analysis of the C-terminal region of increased helical propensity.

A and B, Yeast Rmi1 and human Rmi1-N, the N-terminal 240-residue region of human Rmi1 that is most similar to yeast Rmi1, have comparable predicted structure in the far C-terminus. Y218 is in the same predicted helix as E220 and has a potential equivalent in Y201 in human Rmi1. C, PhylomeDB alignment of Rmi1 C-termini from different yeast species reveals a highly conserved tyrosine at position 218. The corresponding region of human Rmi1 (residues 178–231) was manually aligned to the yeast Rmi1 phylome. The position of the predicted α -helix in yeast Rmi1 is indicated by a red rectangle below the alignment. The corresponding α -helix defined by Y201 in the crystal structure of human Rmi1 (PDB: 4CGY) is indicated by a blue rectangle. D, like *rmi1-E220P*, *rmi1-Y218P* and *rmi1-Y218K* mutants fail to complement the hydroxyurea hypersensitivity of an $\Delta rmi1$ mutant.

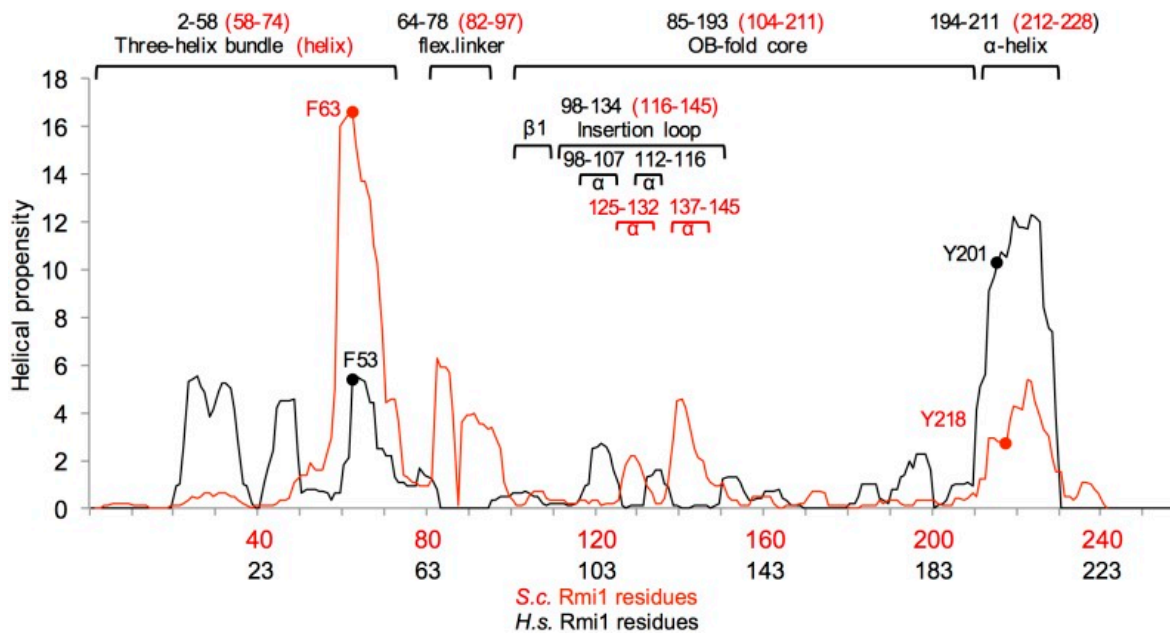


Figure B.5. Proposed structure-prediction-based alignment of yeast and human Rmi1.

Residues to which confirmed domains in the human Rmi1 crystal structure (4CGY) map are indicated above the alignment in black. Proposed location of conserved domains and motifs in yeast Rmi1 are indicated in red. Conserved residues whose mutation to proline abolished Rmi1 function *in vivo* are indicated in the alignment with the proposed corresponding residue in human Rmi1 (F63/F53; Y281/Y201). Compared to human Rmi1, the N-terminus (DUF1767) of yeast Rmi1 appears to be extended by approximately 18 residues. The predicted size and location of the topoisomerase-binding loop (residues 116–145) differs from that previously proposed (residues 87–145) for yeast Rmi1 (Bocquet, Bizard et al. 2014).

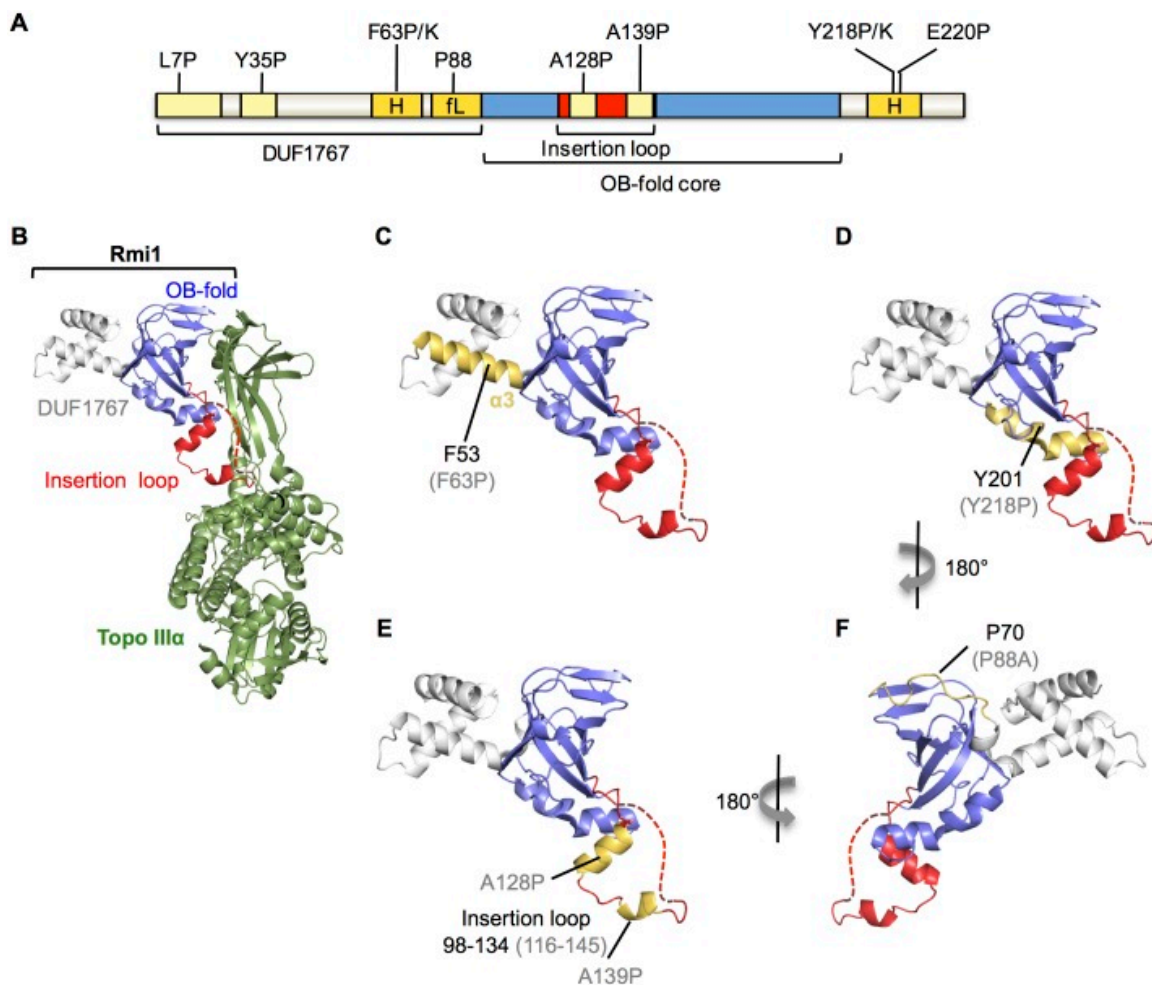


Figure B.6. Conserved domains, and putative differences between yeast Rmi1 and the N-terminus of human Rmi1.

A, functional importance of seven structural motifs predicted in yeast Rmi1 was tested by analyzing point mutations *in vivo*. Mutation of putative motifs highlighted in light yellow did not impair Rmi1 function *in vivo*, including L7P and Y35P mutations in the putative DUF1767 domain, and A128P and A139P in the topoisomerase-binding loop. Mutations in motifs highlighted in dark yellow impaired Rmi1 function *in vivo*; F63P and F63K mutations in an N-terminal α -helix (H), Y218P, Y218K, and E220P mutations in a C-terminal α -helix (H) caused null phenotypes, and the P88A mutation in the flexible linker (fL) between the DUF1767 domain and the OB-fold caused intermediate functional impairment. B, the crystal structure of the N-terminus of human Rmi1 bound to Topo III α (4CGY (Bocquet, Bizard et al. 2014)) was rendered in PyMol. The DUF1767 domain, the OB-fold core and the insertion loop extending between strands β 1 and β 2 are shown in grey, blue, and red, respectively. A part of the disordered insertion loop missing from the crystal structure is indicated by a red dashed line. Topo III α is shown in green. C, the domain structure of Rmi1 is shown as in (B) with α 3, corresponding to the functionally important, putative α -helix in yeast Rmi1, highlighted in yellow. Residue F53

of human Rmi1 and the corresponding F63P null mutation in yeast Rmi1 (in brackets) are indicated. D, the C-terminal α -helix interacting with the bottom of the OB-fold core is shown in yellow. Y201 and the corresponding Y218P null mutation in yeast Rmi1 (in parentheses) are indicated. Disruption of this α -helix leads to lower Rmi1 expression levels and total loss of Rmi1 function (Fig 3E). E, human Rmi1 contains two helical segments in the insertion loop, shown in yellow. A128P and A139P mutations were designed to disrupt helical propensity in the corresponding insertion loop in yeast Rmi1, but did not interrupt Rmi1 function. F, a flexible linker connects the DUF1767 domain to the OB-fold in human Rmi1, indicated in yellow. A single proline at position 88 is predicted to disrupt the strong helical propensity of this linker in yeast Rmi1 whereas this linker is more proline-rich in human Rmi1. The location of P70 in human Rmi1, corresponding to P88 in yeast Rmi1, is indicated.

SUPPORTING INFORMATION

Table B.S1. Plasmids used in this study

| Plasmid | Description |
|---------|--------------------------------------|
| pKHS621 | <i>pRS415-RMI1</i> |
| pKHS622 | <i>pRS415-rmi1-F63P</i> |
| pKHS635 | <i>pRS415-rmi1-F63K</i> |
| pKHS623 | <i>pRS415-rmi1-E220P</i> |
| pKHS624 | <i>pRS415-rmi1-A128P</i> |
| pKHS625 | <i>pRS415-rmi1-A139P</i> |
| pKHS626 | <i>pRS415-rmi1-P88A</i> |
| pKHS627 | <i>pRS415-rmi1-Y218P</i> |
| pKHS634 | <i>pRS415-rmi1-Y218K</i> |
| pKHS628 | <i>pRS415-rmi1-L7P</i> |
| pKHS629 | <i>pRS415-rmi1-Y35P</i> |
| pKHS630 | <i>pRS415-RMI1-myc.HIS3MX6</i> |
| pKHS631 | <i>pRS415-rmi1-F63P-myc.HIS3MX6</i> |
| pKHS632 | <i>pRS415-rmi1-A128P-myc.HIS3MX6</i> |
| pKHS633 | <i>pRS415-rmi1-Y218P-myc.HIS3MX6</i> |
| pKHS642 | <i>pRS415-rmi1-F63K-myc.HIS3MX6</i> |
| pKHS643 | <i>pRS415-rmi1-E220P-myc.HIS3MX6</i> |

REFERENCES

- Ashton, T. M., H. W. Mankouri, A. Heidenblut, P. J. McHugh and I. D. Hickson (2011). "Pathways for Holliday junction processing during homologous recombination in *Saccharomyces cerevisiae*." Mol Cell Biol **31**(9): 1921-1933.
- Bennett, R. J., J. L. Keck and J. C. Wang (1999). "Binding specificity determines polarity of DNA unwinding by the Sgs1 protein of *S. cerevisiae*." J Mol Biol **289**(2): 235-248.
- Bocquet, N., A. H. Bizard, W. Abdulrahman, N. B. Larsen, M. Faty, S. Cavadini, R. D. Bunker, S. C. Kowalczykowski, P. Cejka, I. D. Hickson and N. H. Thoma (2014). "Structural and mechanistic insight into Holliday-junction dissolution by topoisomerase IIIalpha and RMI1." Nat Struct Mol Biol **21**(3): 261-268.
- Bonnet, S., A. Knoll, F. Hartung and H. Puchta (2013). "Different functions for the domains of the *Arabidopsis thaliana* RMI1 protein in DNA cross-link repair, somatic and meiotic recombination." Nucleic Acids Res **41**(20): 9349-9360.
- Cejka, P., J. L. Plank, C. Z. Bachrati, I. D. Hickson and S. C. Kowalczykowski (2010). "Rmi1 stimulates decatenation of double Holliday junctions during dissolution by Sgs1-Top3." Nat Struct Mol Biol **17**(11): 1377-1382.
- Chang, M., M. Bellaoui, C. Zhang, R. Desai, P. Morozov, L. Delgado-Cruzata, R. Rothstein, G. A. Freyer, C. Boone and G. W. Brown (2005). "RMI1/NCE4, a suppressor of genome instability, encodes a member of the RecQ helicase/Topo III complex." EMBO J **24**(11): 2024-2033.
- Chen, C. F. and S. J. Brill (2007). "Binding and activation of DNA topoisomerase III by the Rmi1 subunit." J Biol Chem **282**(39): 28971-28979.
- Chen, H., M. J. You, Y. Jiang, W. Wang and L. Li (2011). "RMI1 attenuates tumor development and is essential for early embryonic survival." Mol Carcinog **50**(2): 80-88.
- Chu, W. K. and I. D. Hickson (2009). "RecQ helicases: multifunctional genome caretakers." Nat Rev Cancer **9**(9): 644-654.
- Daley, J. M., T. Chiba, X. Xue, H. Niu and P. Sung (2014). "Multifaceted role of the Topo IIIalpha-RMI1-RMI2 complex and DNA2 in the BLM-dependent pathway of DNA break end resection." Nucleic Acids Res **42**(17): 11083-11091.
- Fasching, C. L., P. Cejka, S. C. Kowalczykowski and W. D. Heyer (2015). "Top3-Rmi1 dissolve Rad51-mediated D loops by a topoisomerase-based mechanism." Mol Cell **57**(4): 595-606.
- Gangloff, S., J. P. McDonald, C. Bendixen, L. Arthur and R. Rothstein (1994). "The yeast type I topoisomerase Top3 interacts with Sgs1, a DNA helicase homolog: a potential eukaryotic reverse gyrase." Mol Cell Biol **14**(12): 8391-8398.

- Gietz, R. D. and R. A. Woods (2006). "Yeast transformation by the LiAc/SS Carrier DNA/PEG method." Methods Mol Biol **313**: 107-120.
- Guiraldelli, M. F., C. Eyster and R. J. Pezza (2013). "Genome instability and embryonic developmental defects in RMI1 deficient mice." DNA Repair (Amst) **12**(10): 835-843.
- Hoadley, K. A., D. Xu, Y. Xue, K. A. Satyshur, W. Wang and J. L. Keck (2010). "Structure and cellular roles of the RMI core complex from the bloom syndrome dissolvosome." Structure **18**(9): 1149-1158.
- Huerta-Cepas, J., S. Capella-Gutierrez, L. P. Pryszcz, M. Marcet-Houben and T. Gabaldon (2014). "PhylomeDB v4: zooming into the plurality of evolutionary histories of a genome." Nucleic Acids Res **42**(Database issue): D897-902.
- Hyre, D. E. and R. E. Klevit (1998). "A disorder-to-order transition coupled to DNA binding in the essential zinc-finger DNA-binding domain of yeast ADR1." J Mol Biol **279**(4): 929-943.
- Ira, G., A. Malkova, G. Liberi, M. Foiani and J. E. Haber (2003). "Srs2 and Sgs1-Top3 suppress crossovers during double-strand break repair in yeast." Cell **115**(4): 401-411.
- Kennedy, J. A., G. W. Daughdrill and K. H. Schmidt (2013). "A transient alpha-helical molecular recognition element in the disordered N-terminus of the Sgs1 helicase is critical for chromosome stability and binding of Top3/Rmi1." Nucleic Acids Res **41**(22): 10215-10227.
- Lacroix, E., A. R. Viguera and L. Serrano (1998). "Elucidating the folding problem of alpha-helices: local motifs, long-range electrostatics, ionic-strength dependence and prediction of NMR parameters." J Mol Biol **284**(1): 173-191.
- Li, X., P. Romero, M. Rani, A. K. Dunker and Z. Obradovic (1999). "Predicting Protein Disorder for N-, C-, and Internal Regions." Genome Inform Ser Workshop Genome Inform **10**: 30-40.
- Longtine, M. S., A. McKenzie, 3rd, D. J. Demarini, N. G. Shah, A. Wach, A. Brachat, P. Philippsen and J. R. Pringle (1998). "Additional modules for versatile and economical PCR-based gene deletion and modification in *Saccharomyces cerevisiae*." Yeast **14**(10): 953-961.
- Mimitou, E. P. and L. S. Symington (2008). "Sae2, Exo1 and Sgs1 collaborate in DNA double-strand break processing." Nature **455**(7214): 770-774.
- Mitchel, K., K. Lehner and S. Jinks-Robertson (2013). "Heteroduplex DNA position defines the roles of the Sgs1, Srs2, and Mph1 helicases in promoting distinct recombination outcomes." PLoS Genet **9**(3): e1003340.

- Mullen, J. R., F. S. Nallaseth, Y. Q. Lan, C. E. Slagle and S. J. Brill (2005). "Yeast Rmi1/Nce4 controls genome stability as a subunit of the Sgs1-Top3 complex." Mol Cell Biol **25**(11): 4476-4487.
- Munoz, V. and L. Serrano (1994). "Elucidating the folding problem of helical peptides using empirical parameters." Nat Struct Biol **1**(6): 399-409.
- Munoz, V. and L. Serrano (1995). "Elucidating the folding problem of helical peptides using empirical parameters. II. Helix macrodipole effects and rational modification of the helical content of natural peptides." J Mol Biol **245**(3): 275-296.
- Munoz, V. and L. Serrano (1997). "Development of the multiple sequence approximation within the AGADIR model of alpha-helix formation: comparison with Zimm-Bragg and Lifson-Roig formalisms." Biopolymers **41**(5): 495-509.
- Myung, K., A. Datta, C. Chen and R. D. Kolodner (2001). "SGS1, the *Saccharomyces cerevisiae* homologue of BLM and WRN, suppresses genome instability and homeologous recombination." Nat Genet **27**(1): 113-116.
- Peng, K., S. Vucetic, P. Radivojac, C. J. Brown, A. K. Dunker and Z. Obradovic (2005). "Optimizing long intrinsic disorder predictors with protein evolutionary information." J Bioinform Comput Biol **3**(1): 35-60.
- Raynard, S., W. Bussen and P. Sung (2006). "A double Holliday junction dissolvasome comprising BLM, topoisomerase IIIalpha, and BLAP75." J Biol Chem **281**(20): 13861-13864.
- Romero, P., Z. Obradovic, X. Li, E. C. Garner, C. J. Brown and A. K. Dunker (2001). "Sequence complexity of disordered protein." Proteins **42**(1): 38-48.
- Theobald, D. L., R. M. Mitton-Fry and D. S. Wuttke (2003). "Nucleic acid recognition by OB-fold proteins." Annu Rev Biophys Biomol Struct **32**: 115-133.
- Wang, F., Y. Yang, T. R. Singh, V. Busygina, R. Guo, K. Wan, W. Wang, P. Sung, A. R. Meetei and M. Lei (2010). "Crystal structures of RMI1 and RMI2, two OB-fold regulatory subunits of the BLM complex." Structure **18**(9): 1159-1170.
- Wu, L., C. Z. Bachrati, J. Ou, C. Xu, J. Yin, M. Chang, W. Wang, L. Li, G. W. Brown and I. D. Hickson (2006). "BLAP75/RMI1 promotes the BLM-dependent dissolution of homologous recombination intermediates." Proc Natl Acad Sci U S A **103**(11): 4068-4073.
- Xu, D., R. Guo, A. Sobeck, C. Z. Bachrati, J. Yang, T. Enomoto, G. W. Brown, M. E. Hoatlin, I. D. Hickson and W. Wang (2008). "RMI, a new OB-fold complex essential for Bloom syndrome protein to maintain genome stability." Genes Dev **22**(20): 2843-2855.

Yang, J., L. O'Donnell, D. Durocher and G. W. Brown (2012). "RMI1 promotes DNA replication fork progression and recovery from replication fork stress." Mol Cell Biol **32**(15): 3054-3064.

Zhu, Z., W. H. Chung, E. Y. Shim, S. E. Lee and G. Ira (2008). "Sgs1 helicase and two nucleases Dna2 and Exo1 resect DNA double-strand break ends." Cell **134**(6): 981-994.

APPENDIX C:
YEAST STRAINS

| Strains (KHSY) | Genotype |
|---------------------------|---|
| 304 | <i>his3Δ200, trp1Δ63, ura3-52, rrm3::TRP1</i> |
| 421 | <i>ura3-52, trp1Δ63, his3Δ200, leu2Δ1</i> |
| 802 | <i>ura3-52, leu2Δ1, trp1Δ63, his3Δ200, lys2ΔBgl, hom3-10, ade2Δ1, ade8. YEL069C::URA3</i> |
| 1062 | <i>ura3-52, leu2Δ1, trp1Δ63, his3Δ200, lys2ΔBgl, hom3-10, ade2Δ1, ade8. YEL069C::URA3, rrm3::TRP1</i> |
| 1063 | <i>ura3-52, leu2Δ1, trp1Δ63, his3Δ200, lys2ΔBgl, hom3-10, ade2Δ1, ade8. YEL069C::URA3, rrm3::TRP1</i> |
| 1064 | <i>ura3-52, leu2Δ1, trp1Δ63, his3Δ200, lys2ΔBgl, hom3-10, ade2Δ1, ade8. YEL069C::URA3, rrm3::TRP1</i> |
| 1338 | <i>ura3-52, leu2Δ1, trp1Δ63, his3Δ200, lys2ΔBgl, hom3-10, ade2Δ1, ade8. YEL069C::URA3, sgs1::HIS3</i> |
| 1866 | <i>ura3-52, leu2Δ1, trp1Δ63, his3Δ200, lys2ΔBgl, hom3-10, ade2Δ1, ade8. YEL069C::URA3, sgs1::sgs1-hd. TRP1</i> |
| 1867 | <i>ura3-52, leu2Δ1, trp1Δ63, his3Δ200, lys2ΔBgl, hom3-10, ade2Δ1, ade8. YEL069C::URA3, sgs1::sgs1-hd. TRP1</i> |
| 1868 | <i>ura3-52, leu2Δ1, trp1Δ63, his3Δ200, lys2ΔBgl, hom3-10, ade2Δ1, ade8. YEL069C::URA3, sgs1::sgs1-hd. TRP1</i> |
| 1869 | <i>ura3-52, leu2Δ1, trp1Δ63, his3Δ200, lys2ΔBgl, hom3-10, ade2Δ1, ade8. YEL069C::URA3, sgs1::sgs1.ΔC795. TRP1</i> |
| 1870 | <i>ura3-52, leu2Δ1, trp1Δ63, his3Δ200, lys2ΔBgl, hom3-10, ade2Δ1, ade8. YEL069C::URA3, sgs1::sgs1ΔC795. TRP1</i> |
| 1871 | <i>ura3-52, leu2Δ1, trp1Δ63, his3Δ200, lys2ΔBgl, hom3-10, ade2Δ1, ade8. YEL069C::URA3, sgs1::sgs1ΔC795. TRP1</i> |
| 1875 | <i>ura3-52, leu2Δ1, trp1Δ63, his3Δ200, lys2ΔBgl, hom3-10, ade2Δ1, ade8. YEL069C::URA3, sgs1::sgs1ΔC200. TRP1</i> |
| 1876 | <i>ura3-52, leu2Δ1, trp1Δ63, his3Δ200, lys2ΔBgl, hom3-10, ade2Δ1, ade8. YEL069C::URA3, sgs1::sgs1ΔC200. TRP1</i> |
| 1877 | <i>ura3-52, leu2Δ1, trp1Δ63, his3Δ200, lys2ΔBgl, hom3-10, ade2Δ1, ade8. YEL069C::URA3, sgs1::sgs1ΔC200. TRP1</i> |
| 1999 | <i>ura3-52, leu2Δ1, trp1Δ63, his3Δ200, lys2ΔBgl, hom3-10, ade2Δ1, ade8. YEL069C::URA3, sgs1::sgs1-hd.myc. HIS</i> |
| 2000 | <i>ura3-52, leu2Δ1, trp1Δ63, his3Δ200, lys2ΔBgl, hom3-10, ade2Δ1, ade8. YEL069C::URA3, sgs1::sgs1-hd.myc. HIS</i> |

Yeast Strains (continued)

- 2001 *ura3-52, leu2Δ1, trp1Δ63, his3Δ200, lys2ΔBgl, hom3-10, ade2Δ1, ade8. YEL069C::URA3, sgs1::sgs1-hd.myc.HIS*
- 2017 *ura3-52, leu2Δ1, trp1Δ63, his3Δ200, lys2ΔBgl, hom3-10, ade2Δ1, ade8. YEL069C::URA3, sgs1::HIS3*
- 2018 *ura3-52, leu2Δ1, trp1Δ63, his3Δ200, lys2ΔBgl, hom3-10, ade2Δ1, ade8. YEL069C::URA3, sgs1::HIS3*
- 2019 *ura3-52, leu2Δ1, trp1Δ63, his3Δ200, lys2ΔBgl, hom3-10, ade2Δ1, ade8. YEL069C::URA3, sgs1::HIS3*
- 2341 *ura3-52, leu2Δ1, trp1Δ63, his3Δ200, lys2ΔBgl, hom3-10, ade2Δ1, ade8. YEL069C::URA3, mec3::G418, sgs1C200.myc.HIS3*
- 2342 *ura3-52, leu2Δ1, trp1Δ63, his3Δ200, lys2ΔBgl, hom3-10, ade2Δ1, ade8. YEL069C::URA3, mec3::G418, sgs1C200.myc.HIS3*
- 2343 *ura3-52, leu2Δ1, trp1Δ63, his3Δ200, lys2ΔBgl, hom3-10, ade2Δ1, ade8. YEL069C::URA3, mec3::G418, sgs1C200.myc.HIS3*
- 2344 *ura3-52, leu2Δ1, trp1Δ63, his3Δ200, lys2ΔBgl, hom3-10, ade2Δ1, ade8. YEL069C::URA3, mec3::G418, sgs1C200.myc.HIS3*
- 2345 *ura3-52, leu2Δ1, trp1Δ63, his3Δ200, lys2ΔBgl, hom3-10, ade2Δ1, ade8. YEL069C::URA3, sgs1C200.myc.HIS3*
- 2346 *ura3-52, leu2Δ1, trp1Δ63, his3Δ200, lys2ΔBgl, hom3-10, ade2Δ1, ade8. YEL069C::URA3, sgs1C200.myc.HIS3*
- 2347 *ura3-52, leu2Δ1, trp1Δ63, his3Δ200, lys2ΔBgl, hom3-10, ade2Δ1, ade8. YEL069C::URA3, mec3::G418, sgs1C300.myc.HIS3*
- 2348 *ura3-52, leu2Δ1, trp1Δ63, his3Δ200, lys2ΔBgl, hom3-10, ade2Δ1, ade8. YEL069C::URA3, mec3::G418, sgs1C300.myc.HIS3*
- 2349 *ura3-52, leu2Δ1, trp1Δ63, his3Δ200, lys2ΔBgl, hom3-10, ade2Δ1, ade8. YEL069C::URA3, mec3::G418, sgs1C300.myc.HIS3*
- 2350 *ura3-52, leu2Δ1, trp1Δ63, his3Δ200, lys2ΔBgl, hom3-10, ade2Δ1, ade8. YEL069C::URA3, mec3::G418, sgs1C300.myc.HIS3*
- 2351 *ura3-52, leu2Δ1, trp1Δ63, his3Δ200, lys2ΔBgl, hom3-10, ade2Δ1, ade8. YEL069C::URA3, sgs1C300.myc.HIS3*
- 2352 *ura3-52, leu2Δ1, trp1Δ63, his3Δ200, lys2ΔBgl, hom3-10, ade2Δ1, ade8. YEL069C::URA3, sgs1C300.myc.HIS3*
- 2353 *ura3-52/ura3-52, leu2Δ1/leu2Δ1, trp1Δ63/trp1Δ63, his3Δ200/his3Δ200, lys2ΔBgl/lys2ΔBgl, hom3-10/hom3-10, ade2Δ1/ade2Δ1, ade8/ade8. YEL069C::URA3/YEL069C::URA3, SGS1/sgs1C400.myc.HIS3, MEC3/mec3::G418*
- 2354 *ura3-52/ura3-52, leu2Δ1/leu2Δ1, trp1Δ63/trp1Δ63, his3Δ200/his3Δ200, lys2ΔBgl/lys2ΔBgl, hom3-10/hom3-10, ade2Δ1/ade2Δ1, ade8/ade8. YEL069C::URA3/YEL069C::URA3, SGS1/sgs1C400.myc.HIS3, MEC3/mec3::G418*
- 2355 *ura3-52/ura3-52, leu2Δ1/leu2Δ1, trp1Δ63/trp1Δ63, his3Δ200/his3Δ200, lys2ΔBgl/lys2ΔBgl, hom3-10/hom3-10, ade2Δ1/ade2Δ1, ade8/ade8. YEL069C::URA3/YEL069C::URA3, SGS1/sgs1C400.myc.HIS3, MEC3/mec3::G418*

Yeast Strains (continued)

- 2356 *ura3-52/ura3-52, leu2Δ1/leu2Δ1, trp1Δ63/trp1Δ63, his3Δ200/his3Δ200, lys2ΔBgl/lys2ΔBgl, hom3-10/hom3-10, ade2Δ1/ade2Δ1, ade8/ade8. YEL069C::URA3/YEL069C::URA3, SGS1/sgs1C500.myc.HIS3, MEC3/mec3::G418*
- 2357 *ura3-52/ura3-52, leu2Δ1/leu2Δ1, trp1Δ63/trp1Δ63, his3Δ200/his3Δ200, lys2ΔBgl/lys2ΔBgl, hom3-10/hom3-10, ade2Δ1/ade2Δ1, ade8/ade8. YEL069C::URA3/YEL069C::URA3, SGS1/sgs1C500.myc.HIS3, MEC3/mec3::G418*
- 2358 *ura3-52/ura3-52, leu2Δ1/leu2Δ1, trp1Δ63/trp1Δ63, his3Δ200/his3Δ200, lys2ΔBgl/lys2ΔBgl, hom3-10/hom3-10, ade2Δ1/ade2Δ1, ade8/ade8. YEL069C::URA3/YEL069C::URA3, SGS1/sgs1C500.myc.HIS3, MEC3/mec3::G418*
- 2383 *(ura3Δ0, leu2Δ0, his3Δ1, met15Δ0), SGS1.V5.6xHIS*
- 2385 *(ura3Δ0, leu2Δ0, his3Δ1, lys2Δ0), RAD51.V5.VSV*
- 2473 *(ura3Δ0/ura3Δ0, leu2Δ0/leu2Δ0, his3Δ1/his3Δ1, met15Δ0/met15, lys2Δ0/lys2), SGS1/SGS1.V5.6xHIS, RAD51/RAD51.V5.3xVSV*
- 2474 *(ura3Δ0/ura3Δ0, leu2Δ0/leu2Δ0, his3Δ1/his3Δ1, met15Δ0/met15, lys2Δ0/lys2), SGS1/SGS1.V5.6xHIS, RAD51/RAD51.V5.3xVSV*
- 2475 *(ura3Δ0/ura3Δ0, leu2Δ0/leu2Δ0, his3Δ1/his3Δ1, met15Δ0/met15, lys2Δ0/lys2), SGS1/SGS1.V5.6xHIS, RAD51/RAD51.V5.3xVSV*
- 2494 *(ura3Δ0, leu2Δ0, his3Δ1, met15Δ0), RAD51.V5.6xHIS*
- 2495 *(ura3Δ0, leu2Δ0, his3Δ1, met15Δ0), TOP3.V5.6xHIS*
- 2496 *(ura3Δ0, leu2Δ0, his3Δ1, met15Δ0), MLH1.V5.6xHIS*
- 2497 *(ura3Δ0, leu2Δ0, his3Δ1, lys2Δ0), TOP3.V5.3xVSV.G418*
- 2498 *(ura3Δ0, leu2Δ0, his3Δ1, lys2Δ0), SGS1.V5.3xVSV*
- 2499 *(ura3Δ0, leu2Δ0, his3Δ1, lys2Δ0), MLH1.V5.3xVSV*
- 2529 *(ura3Δ0/ura3Δ0, leu2Δ0/leu2Δ0, his3Δ1/his3Δ1, met15Δ0/met15, lys2Δ0/lys2), Rad51/Rad51.V5.6xHIS, Sgs1/Sgs1.V5.3xVSV*
- 2530 *(ura3Δ0/ura3Δ0, leu2Δ0/leu2Δ0, his3Δ1/his3Δ1, met15Δ0/met15, lys2Δ0/lys2), Rad51/Rad51.V5.6xHIS, Sgs1/Sgs1.V5.3xVSV*
- 2531 *(ura3Δ0/ura3Δ0, leu2Δ0/leu2Δ0, his3Δ1/his3Δ1, met15Δ0/met15, lys2Δ0/lys2), Rad51/Rad51.V5.6xHIS, Sgs1/Sgs1.V5.3xVSV*
- 2532 *(ura3Δ0/ura3Δ0, leu2Δ0/leu2Δ0, his3Δ1/his3Δ1, met15Δ0/met15, lys2Δ0/lys2), Sgs1/Sgs1.V5.6xHIS, Top3/Top3.V5.3xVSV*
- 2533 *(ura3Δ0/ura3Δ0, leu2Δ0/leu2Δ0, his3Δ1/his3Δ1, met15Δ0/met15, lys2Δ0/lys2), Sgs1/Sgs1.V5.6xHIS, Top3/Top3.V5.3xVSV*
- 2534 *(ura3Δ0/ura3Δ0, leu2Δ0/leu2Δ0, his3Δ1/his3Δ1, met15Δ0/met15, lys2Δ0/lys2), Sgs1/Sgs1.V5.6xHIS, Top3/Top3.V5.3xVSV*
- 2535 *(ura3Δ0/ura3Δ0, leu2Δ0/leu2Δ0, his3Δ1/his3Δ1, met15Δ0/met15, lys2Δ0/lys2), Sgs1/Sgs1.V5.6xHIS, Mlh1/Mlh1.V5.3xVSV*
- 2536 *(ura3Δ0/ura3Δ0, leu2Δ0/leu2Δ0, his3Δ1/his3Δ1, met15Δ0/met15, lys2Δ0/lys2), Sgs1/Sgs1.V5.6xHIS, Mlh1/Mlh1.V5.3xVSV*
- 2537 *(ura3Δ0/ura3Δ0, leu2Δ0/leu2Δ0, his3Δ1/his3Δ1, met15Δ0/met15, lys2Δ0/lys2), Sgs1/Sgs1.V5.6xHIS, Mlh1/Mlh1.V5.3xVSV*

Yeast Strains (continued)

- 2538 *(ura3Δ0/ura3Δ0, leu2Δ0/leu2Δ0, his3Δ1/his3Δ1, met15Δ0/met15, lys2Δ0/lys2), Top3/Top3.V5.6xHIS, Sgs1/Sgs1.V5.3xVSV*
- 2539 *(ura3Δ0/ura3Δ0, leu2Δ0/leu2Δ0, his3Δ1/his3Δ1, met15Δ0/met15, lys2Δ0/lys2), Top3/Top3.V5.6xHIS, Sgs1/Sgs1.V5.3xVSV*
- 2540 *(ura3Δ0/ura3Δ0, leu2Δ0/leu2Δ0, his3Δ1/his3Δ1, met15Δ0/met15, lys2Δ0/lys2), Top3/Top3.V5.6xHIS, Sgs1/Sgs1.V5.3xVSV*
- 2541 *(ura3Δ0/ura3Δ0, leu2Δ0/leu2Δ0, his3Δ1/his3Δ1, met15Δ0/met15, lys2Δ0/lys2), Mlh1/Mlh1.V5.6xHIS, Sgs1/Sgs1.V5.3xVSV*
- 2542 *(ura3Δ0/ura3Δ0, leu2Δ0/leu2Δ0, his3Δ1/his3Δ1, met15Δ0/met15, lys2Δ0/lys2), Mlh1/Mlh1.V5.6xHIS, Sgs1/Sgs1.V5.3xVSV*
- 2543 *(ura3Δ0/ura3Δ0, leu2Δ0/leu2Δ0, his3Δ1/his3Δ1, met15Δ0/met15, lys2Δ0/lys2), Mlh1/Mlh1.V5.6xHIS, Sgs1/Sgs1.V5.3xVSV*
- 2651 *can1Δ::STE2pr-Sp_his5 lyp1Δ; his3Δ1 leu2Δ0 ura3Δ0 met15Δ0*
- 2681 *ura3-52, leu2Δ1, trp1Δ63, his3Δ200, lys2ΔBgl, hom3-10, ade2Δ1, ade8. YEL069C::URA3, SGS1.myc.HIS3*
- 2682 *ura3-52/ura3Δ0, leu2Δ1/leu2Δ0, trp1Δ63/trp1, his3Δ200/his3Δ1, lys2ΔBgl/lys2Δ0, hom3-10/hom3, ade2Δ1/ade2, ade8/ade8. YEL069C::URA3/YEL069C, sgs1C200.myc.his3/sgs1, top3.v5.6xHIS/top3*
- 2683 *ura3-52/ura3Δ0, leu2Δ1/leu2Δ0, trp1Δ63/trp1, his3Δ200/his3Δ1, lys2ΔBgl/lys2Δ0, hom3-10/hom3, ade2Δ1/ade2, ade8/ade8. YEL069C::URA3/YEL069C, sgs1C200.myc.his3/sgs1, top3.v5.6xHIS/top3*
- 2684 *ura3-52/ura3Δ0, leu2Δ1/leu2Δ0, trp1Δ63/trp1, his3Δ200/his3Δ1, lys2ΔBgl/lys2Δ0, hom3-10/hom3, ade2Δ1/ade2, ade8/ade8. YEL069C::URA3/YEL069C, sgs1C200.myc.his3/sgs1, mlh1.v5.6xHIS/mlh1*
- 2685 *ura3-52/ura3Δ0, leu2Δ1/leu2Δ0, trp1Δ63/trp1, his3Δ200/his3Δ1, lys2ΔBgl/lys2Δ0, hom3-10/hom3, ade2Δ1/ade2, ade8/ade8. YEL069C::URA3/YEL069C, sgs1C200.myc.his3/sgs1, mlh1.v5.6xHIS/mlh1*
- 2686 *ura3-52/ura3Δ0, leu2Δ1/leu2Δ0, trp1Δ63/trp1, his3Δ200/his3Δ1, lys2ΔBgl/lys2Δ0, hom3-10/hom3, ade2Δ1/ade2, ade8/ade8. YEL069C::URA3/YEL069C, sgs1C200.myc.his3/sgs1, rad51.v5.6xHIS/rad51*
- 2687 *ura3-52/ura3Δ0, leu2Δ1/leu2Δ0, trp1Δ63/trp1, his3Δ200/his3Δ1, lys2ΔBgl/lys2Δ0, hom3-10/hom3, ade2Δ1/ade2, ade8/ade8. YEL069C::URA3/YEL069C, sgs1C200.myc.his3/sgs1, rad51.v5.6xHIS/rad51*
- 2946 *ura3Δ0, leu2Δ0, his3Δ1, met15Δ0, RAD16.V5.6xHIS*
- 2947 *ura3Δ0, leu2Δ0, his3Δ1, met15Δ0, SRS2.V5.6xHIS*
- 2948 *ura3-52/ura3Δ0, leu2Δ1/leu2Δ0, trp1Δ63/trp1, his3Δ200/his3Δ1, lys2ΔBgl/lys2Δ0, hom3-10/hom3, ade2Δ1/ade2, ade8/ade8. YEL069C::URA3/YEL069C, sgs1C300.myc.his3/sgs1, mlh1.v5.6xHIS/mlh1*
- 2949 *ura3-52/ura3Δ0, leu2Δ1/leu2Δ0, trp1Δ63/trp1, his3Δ200/his3Δ1, lys2ΔBgl/lys2Δ0, hom3-10/hom3, ade2Δ1/ade2, ade8/ade8. YEL069C::URA3/YEL069C, sgs1C300.myc.his3/sgs1, mlh1.v5.6xHIS/mlh1*
- 2950 *ura3-52/ura3Δ0, leu2Δ1/leu2Δ0, trp1Δ63/trp1, his3Δ200/his3Δ1, lys2ΔBgl/lys2Δ0, hom3-10/hom3, ade2Δ1/ade2, ade8/ade8. YEL069C::URA3/YEL069C, sgs1C300.myc.his3/sgs1, top3.v5.6xHIS/top3*

Yeast Strains (continued)

- 2952 *ura3-52/ura3Δ0, leu2Δ1/leu2Δ0, trp1Δ63/trp1, his3Δ200/his3Δ1, lys2ΔBgl/lys2Δ0, hom3-10/hom3, ade2Δ1/ade2, ade8/ade8. YEL069C::URA3/YEL069C, sgs1C300.myc.his3/sgs1, top3.v5.6xHIS/top3*
- 2953 *ura3-52/ura3Δ0, leu2Δ1/leu2Δ0, trp1Δ63/trp1, his3Δ200/his3Δ1, lys2ΔBgl/lys2Δ0, hom3-10/hom3, ade2Δ1/ade2, ade8/ade8. YEL069C::URA3/YEL069C, sgs1C300.myc.his3/sgs1, rad51.v5.6xHIS/rad51*
- 2954 *ura3-52/ura3Δ0, leu2Δ1/leu2Δ0, trp1Δ63/trp1, his3Δ200/his3Δ1, lys2ΔBgl/lys2Δ0, hom3-10/hom3, ade2Δ1/ade2, ade8/ade8. YEL069C::URA3/YEL069C, sgs1C300.myc.his3/sgs1, rad51.v5.6xHIS/rad51*
- 2955 *ura3-52/ura3-52, leu2Δ1/leu2Δ1, trp1Δ63/trp1Δ63, his3Δ200/his3Δ200, lys2ΔBgl/lys2ΔBgl, hom3-10/hom3-10, ade2Δ1/ade2Δ1, ade8/ade8. YEL069C::URA3/YEL069C::URA3, SGS1/sgs1C200.myc.HIS3*
- 2956 *ura3-52/ura3-52, leu2Δ1/leu2Δ1, trp1Δ63/trp1Δ63, his3Δ200/his3Δ200, lys2ΔBgl/lys2ΔBgl, hom3-10/hom3-10, ade2Δ1/ade2Δ1, ade8/ade8. YEL069C::URA3/YEL069C::URA3, SGS1/sgs1C200.myc.HIS3*
- 2957 *ura3-52/ura3-52, leu2Δ1/leu2Δ1, trp1Δ63/trp1Δ63, his3Δ200/his3Δ200, lys2ΔBgl/lys2ΔBgl, hom3-10/hom3-10, ade2Δ1/ade2Δ1, ade8/ade8. YEL069C::URA3/YEL069C::URA3, SGS1/sgs1C300.myc.HIS3*
- 2958 *ura3-52/ura3-52, leu2Δ1/leu2Δ1, trp1Δ63/trp1Δ63, his3Δ200/his3Δ200, lys2ΔBgl/lys2ΔBgl, hom3-10/hom3-10, ade2Δ1/ade2Δ1, ade8/ade8. YEL069C::URA3/YEL069C::URA3, SGS1/sgs1C300.myc.HIS3*
- 2959 *ura3-52/ura3-52, leu2Δ1/leu2Δ1, trp1Δ63/trp1Δ63, his3Δ200/his3Δ200, lys2ΔBgl/lys2ΔBgl, hom3-10/hom3-10, ade2Δ1/ade2Δ1, ade8/ade8. YEL069C::URA3/YEL069C::URA3, SGS1/sgs1.myc.HIS3, MEC3/mec3::G418*
- 2960 *ura3-52/ura3-52, leu2Δ1/leu2Δ1, trp1Δ63/trp1Δ63, his3Δ200/his3Δ200, lys2ΔBgl/lys2ΔBgl, hom3-10/hom3-10, ade2Δ1/ade2Δ1, ade8/ade8. YEL069C::URA3/YEL069C::URA3, SGS1/sgs1.myc.HIS3, MEC3/mec3::G418*
- 2970 *ura3-52, leu2Δ1, trp1Δ63, his3Δ200, lys2ΔBgl, hom3-10, ade2Δ1, ade8. YEL069C::URA3, sgs1.myc.His3*
- 2971 *ura3-52, leu2Δ1, trp1Δ63, his3Δ200, lys2ΔBgl, hom3-10, ade2Δ1, ade8. YEL069C::URA3, sgs1.myc.His3*
- 2972 *ura3-52, leu2Δ1, trp1Δ63, his3Δ200, lys2ΔBgl, hom3-10, ade2Δ1, ade8. YEL069C::URA3, sgs1C200.myc.HIS3*
- 2973 *ura3-52, leu2Δ1, trp1Δ63, his3Δ200, lys2ΔBgl, hom3-10, ade2Δ1, ade8. YEL069C::URA3, sgs1C300.myc.HIS3*
- 2974 *ura3-52, leu2Δ1, trp1Δ63, his3Δ200, lys2ΔBgl, hom3-10, ade2Δ1, ade8. YEL069C::URA3, sgs1C400.myc.HIS3*
- 2975 *ura3-52, leu2Δ1, trp1Δ63, his3Δ200, lys2ΔBgl, hom3-10, ade2Δ1, ade8. YEL069C::URA3, sgs1C500.myc.HIS3*
- 2976 *ura3-52, leu2Δ1, trp1Δ63, his3Δ200, lys2ΔBgl, hom3-10, ade2Δ1, ade8. YEL069C::URA3, sgs1C600.myc.HIS3*

Yeast Strains (continued)

- 2977 *ura3-52, leu2Δ1, trp1Δ63, his3Δ200, lys2ΔBgl, hom3-10, ade2Δ1, ade8. YEL069C::URA3, sgs1C700.myc.HIS3*
- 2978 *ura3-52, leu2Δ1, trp1Δ63, his3Δ200, lys2ΔBgl, hom3-10, ade2Δ1, ade8. YEL069C::URA3, sgs1C800.myc.HIS3*
- 2979 *ura3-52, leu2Δ1, trp1Δ63, his3Δ200, lys2ΔBgl, hom3-10, ade2Δ1, ade8. YEL069C::URA3, sgs1C1428.myc.HIS3*
- 2980 *ura3-52, leu2Δ1, trp1Δ63, his3Δ200, lys2ΔBgl, hom3-10, ade2Δ1, ade8. YEL069C::URA3, SGS1.myc.HIS3*
- 2981 *ura3-52, leu2Δ1, trp1Δ63, his3Δ200, lys2ΔBgl, hom3-10, ade2Δ1, ade8. YEL069C::URA3, SGS1.myc.HIS3*
- 2982 *ura3-52, leu2Δ1, trp1Δ63, his3Δ200, lys2ΔBgl, hom3-10, ade2Δ1, ade8. YEL069C::URA3, SGS1.myc.HIS3*
- 2983 *ura3-52/ura3-52, leu2Δ1/leu2Δ1, trp1Δ63/trp1Δ63, his3Δ200/his3Δ200, lys2ΔBgl/lys2ΔBgl, hom3-10/hom3-10, ade2Δ1/ade2Δ1, ade8/ade8. YEL069C::URA3/YEL069C::URA3, SGS1/sgs1.myc.HIS3*
- 2984 *ura3-52/ura3-52, leu2Δ1/leu2Δ1, trp1Δ63/trp1Δ63, his3Δ200/his3Δ200, lys2ΔBgl/lys2ΔBgl, hom3-10/hom3-10, ade2Δ1/ade2Δ1, ade8/ade8. YEL069C::URA3/YEL069C::URA3, SGS1/sgs1.myc.HIS3*
- 2985 *ura3-52/ura3-52, leu2Δ1/leu2Δ1, trp1Δ63/trp1Δ63, his3Δ200/his3Δ200, lys2ΔBgl/lys2ΔBgl, hom3-10/hom3-10, ade2Δ1/ade2Δ1, ade8/ade8. YEL069C::URA3/YEL069C::URA3, SGS1/sgs1.myc.HIS3*
- 2986 *ura3-52/ura3-52, leu2Δ1/leu2Δ1, trp1Δ63/trp1Δ63, his3Δ200/his3Δ200, lys2ΔBgl/lys2ΔBgl, hom3-10/hom3-10, ade2Δ1/ade2Δ1, ade8/ade8. YEL069C::URA3/YEL069C::URA3, SGS1/sgs1.myc.HIS3*
- 2987 *ura3-52/ura3Δ0, leu2Δ1/leu2Δ0, trp1Δ63/trp1, his3Δ200/his3Δ1, lys2ΔBgl/lys2Δ0, hom3-10/hom3, ade2Δ1/ade2, ade8/ade8. YEL069C::URA3/YEL069C, sgs1.myc.his3/sgs1, rad51.v5.6xHIS/rad51*
- 2988 *ura3-52/ura3Δ0, leu2Δ1/leu2Δ0, trp1Δ63/trp1, his3Δ200/his3Δ1, lys2ΔBgl/lys2Δ0, hom3-10/hom3, ade2Δ1/ade2, ade8/ade8. YEL069C::URA3/YEL069C, sgs1.myc.his3/sgs1, rad51.v5.6xHIS/rad51*
- 2989 *ura3-52/ura3Δ0, leu2Δ1/leu2Δ0, trp1Δ63/trp1, his3Δ200/his3Δ1, lys2ΔBgl/lys2Δ0, hom3-10/hom3, ade2Δ1/ade2, ade8/ade8. YEL069C::URA3/YEL069C, sgs1.myc.his3/sgs1, mlh1.v5.6xHIS/mlh1*
- 2990 *ura3-52/ura3Δ0, leu2Δ1/leu2Δ0, trp1Δ63/trp1, his3Δ200/his3Δ1, lys2ΔBgl/lys2Δ0, hom3-10/hom3, ade2Δ1/ade2, ade8/ade8. YEL069C::URA3/YEL069C, sgs1.myc.his3/sgs1, mlh1.v5.6xHIS/mlh1*
- 2991 *ura3-52/ura3Δ0, leu2Δ1/leu2Δ0, trp1Δ63/trp1, his3Δ200/his3Δ1, lys2ΔBgl/lys2Δ0, hom3-10/hom3, ade2Δ1/ade2, ade8/ade8. YEL069C::URA3/YEL069C, sgs1.myc.his3/sgs1, top3.v5.6xHIS/top3*
- 2992 *ura3-52/ura3Δ0, leu2Δ1/leu2Δ0, trp1Δ63/trp1, his3Δ200/his3Δ1, lys2ΔBgl/lys2Δ0, hom3-10/hom3, ade2Δ1/ade2, ade8/ade8. YEL069C::URA3/YEL069C, sgs1.myc.his3/sgs1, top3.v5.6xHIS/top3*

Yeast Strains (continued)

- 2993 *ura3-52/ura3Δ0, leu2Δ1/leu2Δ0, trp1Δ63/trp1, his3Δ200/his3Δ1, lys2ΔBgl/lys2Δ0, hom3-10/hom3, ade2Δ1/ade2, ade8/ade8. YEL069C::URA3/YEL069C, sgs1.myc.his3/sgs1, srs2.v5.6xHIS/srs2*
- 2994 *ura3-52/ura3Δ0, leu2Δ1/leu2Δ0, trp1Δ63/trp1, his3Δ200/his3Δ1, lys2ΔBgl/lys2Δ0, hom3-10/hom3, ade2Δ1/ade2, ade8/ade8. YEL069C::URA3/YEL069C, sgs1.myc.his3/sgs1, srs2.v5.6xHIS/srs2*
- 2995 *ura3-52/ura3Δ0, leu2Δ1/leu2Δ0, trp1Δ63/trp1, his3Δ200/his3Δ1, lys2ΔBgl/lys2Δ0, hom3-10/hom3, ade2Δ1/ade2, ade8/ade8. YEL069C::URA3/YEL069C, sgs1.myc.his3/sgs1, rad16.v5.6xHIS/rad16*
- 2996 *ura3-52/ura3Δ0, leu2Δ1/leu2Δ0, trp1Δ63/trp1, his3Δ200/his3Δ1, lys2ΔBgl/lys2Δ0, hom3-10/hom3, ade2Δ1/ade2, ade8/ade8. YEL069C::URA3/YEL069C, sgs1.myc.his3/sgs1, rad16.v5.6xHIS/rad16*
- 2997 *ura3-52/ura3Δ0, leu2Δ1/leu2Δ0, trp1Δ63/trp1, his3Δ200/his3Δ1, lys2ΔBgl/lys2Δ0, hom3-10/hom3, ade2Δ1/ade2, ade8/ade8. YEL069C::URA3/YEL069C, sgs1C200.myc.his3/sgs1, srs2.v5.6xHIS/srs2*
- 2998 *ura3-52/ura3Δ0, leu2Δ1/leu2Δ0, trp1Δ63/trp1, his3Δ200/his3Δ1, lys2ΔBgl/lys2Δ0, hom3-10/hom3, ade2Δ1/ade2, ade8/ade8. YEL069C::URA3/YEL069C, sgs1C200.myc.his3/sgs1, srs2.v5.6xHIS/srs2*
- 2999 *ura3-52/ura3Δ0, leu2Δ1/leu2Δ0, trp1Δ63/trp1, his3Δ200/his3Δ1, lys2ΔBgl/lys2Δ0, hom3-10/hom3, ade2Δ1/ade2, ade8/ade8. YEL069C::URA3/YEL069C, sgs1C200.myc.his3/sgs1, rad16.v5.6xHIS/rad16*
- 3000 *ura3-52/ura3Δ0, leu2Δ1/leu2Δ0, trp1Δ63/trp1, his3Δ200/his3Δ1, lys2ΔBgl/lys2Δ0, hom3-10/hom3, ade2Δ1/ade2, ade8/ade8. YEL069C::URA3/YEL069C, sgs1C200.myc.his3/sgs1, rad16.v5.6xHIS/rad16*
- 3001 *ura3-52/ura3Δ0, leu2Δ1/leu2Δ0, trp1Δ63/trp1, his3Δ200/his3Δ1, lys2ΔBgl/lys2Δ0, hom3-10/hom3, ade2Δ1/ade2, ade8/ade8. YEL069C::URA3/YEL069C, sgs1C300.myc.his3/sgs1, srs2.v5.6xHIS/srs2*
- 3002 *ura3-52/ura3Δ0, leu2Δ1/leu2Δ0, trp1Δ63/trp1, his3Δ200/his3Δ1, lys2ΔBgl/lys2Δ0, hom3-10/hom3, ade2Δ1/ade2, ade8/ade8. YEL069C::URA3/YEL069C, sgs1C300.myc.his3/sgs1, srs2.v5.6xHIS/srs2*
- 3003 *ura3-52/ura3Δ0, leu2Δ1/leu2Δ0, trp1Δ63/trp1, his3Δ200/his3Δ1, lys2ΔBgl/lys2Δ0, hom3-10/hom3, ade2Δ1/ade2, ade8/ade8. YEL069C::URA3/YEL069C, sgs1C300.myc.his3/sgs1, rad16.v5.6xHIS/rad16*
- 3004 *ura3-52/ura3Δ0, leu2Δ1/leu2Δ0, trp1Δ63/trp1, his3Δ200/his3Δ1, lys2ΔBgl/lys2Δ0, hom3-10/hom3, ade2Δ1/ade2, ade8/ade8. YEL069C::URA3/YEL069C, sgs1C300.myc.his3/sgs1, rad16.v5.6xHIS/rad16*
- 3130 *MATa, trp1-901, leu2-3, 112, ura3-52, his3-200, gal4Δ, gal80Δ, lys2::Gal1uas-Gal1tata-HIS3, GAL2uas-GAL2tata-ADE2, URA3::MEL1uas-MEL1tata-lacZ*
- 3467 *ura3-52, leu2Δ1, trp1Δ63, his3Δ200, lys2ΔBgl, hom3-10, ade2Δ1, ade8. YEL069C::URA3, sgs1C200.myc.HIS3*
- 3468 *ura3-52, leu2Δ1, trp1Δ63, his3Δ200, lys2ΔBgl, hom3-10, ade2Δ1, ade8. YEL069C::URA3, sgs1C200.myc.HIS3*

Yeast Strains (continued)

- 3469 *ura3-52, leu2Δ1, trp1Δ63, his3Δ200, lys2ΔBgl, hom3-10, ade2Δ1, ade8. YEL069C::URA3, sgs1C200.myc.HIS3*
- 3470 *ura3-52, leu2Δ1, trp1Δ63, his3Δ200, lys2ΔBgl, hom3-10, ade2Δ1, ade8. YEL069C::URA3, sgs1C220.myc.HIS3*
- 3471 *ura3-52, leu2Δ1, trp1Δ63, his3Δ200, lys2ΔBgl, hom3-10, ade2Δ1, ade8. YEL069C::URA3, sgs1C220.myc.HIS3*
- 3472 *ura3-52, leu2Δ1, trp1Δ63, his3Δ200, lys2ΔBgl, hom3-10, ade2Δ1, ade8. YEL069C::URA3, sgs1C220.myc.HIS3*
- 3473 *ura3-52, leu2Δ1, trp1Δ63, his3Δ200, lys2ΔBgl, hom3-10, ade2Δ1, ade8. YEL069C::URA3, sgs1C240.myc.HIS3*
- 3474 *ura3-52, leu2Δ1, trp1Δ63, his3Δ200, lys2ΔBgl, hom3-10, ade2Δ1, ade8. YEL069C::URA3, sgs1C240.myc.HIS3*
- 3475 *ura3-52, leu2Δ1, trp1Δ63, his3Δ200, lys2ΔBgl, hom3-10, ade2Δ1, ade8. YEL069C::URA3, sgs1C240.myc.HIS3*
- 3476 *ura3-52, leu2Δ1, trp1Δ63, his3Δ200, lys2ΔBgl, hom3-10, ade2Δ1, ade8. YEL069C::URA3, sgs1C260.myc.HIS3*
- 3477 *ura3-52, leu2Δ1, trp1Δ63, his3Δ200, lys2ΔBgl, hom3-10, ade2Δ1, ade8. YEL069C::URA3, sgs1C260.myc.HIS3*
- 3478 *ura3-52, leu2Δ1, trp1Δ63, his3Δ200, lys2ΔBgl, hom3-10, ade2Δ1, ade8. YEL069C::URA3, sgs1C260.myc.HIS3*
- 3479 *ura3-52, leu2Δ1, trp1Δ63, his3Δ200, lys2ΔBgl, hom3-10, ade2Δ1, ade8. YEL069C::URA3, sgs1C280.myc.HIS3*
- 3480 *ura3-52, leu2Δ1, trp1Δ63, his3Δ200, lys2ΔBgl, hom3-10, ade2Δ1, ade8. YEL069C::URA3, sgs1C280.myc.HIS3*
- 3481 *ura3-52, leu2Δ1, trp1Δ63, his3Δ200, lys2ΔBgl, hom3-10, ade2Δ1, ade8. YEL069C::URA3, sgs1C280.myc.HIS3*
- 3482 *ura3-52, leu2Δ1, trp1Δ63, his3Δ200, lys2ΔBgl, hom3-10, ade2Δ1, ade8. YEL069C::URA3, sgs1C300.myc.HIS3*
- 3483 *ura3-52, leu2Δ1, trp1Δ63, his3Δ200, lys2ΔBgl, hom3-10, ade2Δ1, ade8. YEL069C::URA3, sgs1C300.myc.HIS3*
- 3484 *ura3-52, leu2Δ1, trp1Δ63, his3Δ200, lys2ΔBgl, hom3-10, ade2Δ1, ade8. YEL069C::URA3, sgs1C300.myc.HIS3*
- 3485 *ura3-52, leu2Δ1, trp1Δ63, his3Δ200, lys2ΔBgl, hom3-10, ade2Δ1, ade8. YEL069C::URA3, sgs1C400.myc.HIS3*
- 3486 *ura3-52, leu2Δ1, trp1Δ63, his3Δ200, lys2ΔBgl, hom3-10, ade2Δ1, ade8. YEL069C::URA3, sgs1C400.myc.HIS3*
- 3487 *ura3-52, leu2Δ1, trp1Δ63, his3Δ200, lys2ΔBgl, hom3-10, ade2Δ1, ade8. YEL069C::URA3, sgs1C400.myc.HIS3*
- 3488 *ura3-52, leu2Δ1, trp1Δ63, his3Δ200, lys2ΔBgl, hom3-10, ade2Δ1, ade8. YEL069C::URA3, sgs1C500.myc.HIS3*
- 3489 *ura3-52, leu2Δ1, trp1Δ63, his3Δ200, lys2ΔBgl, hom3-10, ade2Δ1, ade8. YEL069C::URA3, sgs1C500.myc.HIS3*
- 3490 *ura3-52, leu2Δ1, trp1Δ63, his3Δ200, lys2ΔBgl, hom3-10, ade2Δ1, ade8. YEL069C::URA3, sgs1C500.myc.HIS3*

Yeast Strains (continued)

- 3491 *ura3-52, leu2Δ1, trp1Δ63, his3Δ200, lys2ΔBgl, hom3-10, ade2Δ1, ade8. YEL069C::URA3, sgs1C600.myc.HIS3*
- 3492 *ura3-52, leu2Δ1, trp1Δ63, his3Δ200, lys2ΔBgl, hom3-10, ade2Δ1, ade8. YEL069C::URA3, sgs1C600.myc.HIS3*
- 3493 *ura3-52, leu2Δ1, trp1Δ63, his3Δ200, lys2ΔBgl, hom3-10, ade2Δ1, ade8. YEL069C::URA3, sgs1C600.myc.HIS3*
- 3494 *ura3-52, leu2Δ1, trp1Δ63, his3Δ200, lys2ΔBgl, hom3-10, ade2Δ1, ade8. YEL069C::URA3, sgs1C700.myc.HIS3*
- 3495 *ura3-52, leu2Δ1, trp1Δ63, his3Δ200, lys2ΔBgl, hom3-10, ade2Δ1, ade8. YEL069C::URA3, sgs1C700.myc.HIS3*
- 3496 *ura3-52, leu2Δ1, trp1Δ63, his3Δ200, lys2ΔBgl, hom3-10, ade2Δ1, ade8. YEL069C::URA3, sgs1C700.myc.HIS3*
- 3497 *ura3-52, leu2Δ1, trp1Δ63, his3Δ200, lys2ΔBgl, hom3-10, ade2Δ1, ade8. YEL069C::URA3, sgs1C800.myc.HIS3*
- 3498 *ura3-52, leu2Δ1, trp1Δ63, his3Δ200, lys2ΔBgl, hom3-10, ade2Δ1, ade8. YEL069C::URA3, sgs1C800.myc.HIS3*
- 3499 *ura3-52, leu2Δ1, trp1Δ63, his3Δ200, lys2ΔBgl, hom3-10, ade2Δ1, ade8. YEL069C::URA3, sgs1C800.myc.HIS3*
- 3500 *ura3-52, leu2Δ1, trp1Δ63, his3Δ200, lys2ΔBgl, hom3-10, ade2Δ1, ade8. YEL069C::URA3, sgs1C900.myc.HIS3*
- 3501 *ura3-52, leu2Δ1, trp1Δ63, his3Δ200, lys2ΔBgl, hom3-10, ade2Δ1, ade8. YEL069C::URA3, sgs1C900.myc.HIS3*
- 3502 *ura3-52, leu2Δ1, trp1Δ63, his3Δ200, lys2ΔBgl, hom3-10, ade2Δ1, ade8. YEL069C::URA3, sgs1C1000.myc.HIS3*
- 3503 *ura3-52, leu2Δ1, trp1Δ63, his3Δ200, lys2ΔBgl, hom3-10, ade2Δ1, ade8. YEL069C::URA3, sgs1C1000.myc.HIS3*
- 3504 *ura3-52, leu2Δ1, trp1Δ63, his3Δ200, lys2ΔBgl, hom3-10, ade2Δ1, ade8. YEL069C::URA3, sgs1C1100.myc.HIS3*
- 3505 *ura3-52, leu2Δ1, trp1Δ63, his3Δ200, lys2ΔBgl, hom3-10, ade2Δ1, ade8. YEL069C::URA3, sgs1C1100.myc.HIS3*
- 3506 *ura3-52, leu2Δ1, trp1Δ63, his3Δ200, lys2ΔBgl, hom3-10, ade2Δ1, ade8. YEL069C::URA3, sgs1C1100.myc.HIS3*
- 3507 *ura3-52, leu2Δ1, trp1Δ63, his3Δ200, lys2ΔBgl, hom3-10, ade2Δ1, ade8. YEL069C::URA3, sgs1C1428.myc.HIS3*
- 3508 *ura3-52, leu2Δ1, trp1Δ63, his3Δ200, lys2ΔBgl, hom3-10, ade2Δ1, ade8. YEL069C::URA3, sgs1C1428.myc.HIS3*
- 3509 *ura3-52, leu2Δ1, trp1Δ63, his3Δ200, lys2ΔBgl, hom3-10, ade2Δ1, ade8. YEL069C::URA3, sgs1C1428.myc.HIS3*
- 3510 *ura3-52, leu2Δ1, trp1Δ63, his3Δ200, lys2ΔBgl, hom3-10, ade2Δ1, ade8. YEL069C::URA3, Pgal.TRP1.SGS1.myc.HIS3*
- 3511 *ura3-52, leu2Δ1, trp1Δ63, his3Δ200, lys2ΔBgl, hom3-10, ade2Δ1, ade8. YEL069C::URA3, Pgal.TRP1.SGS1.myc.HIS3*
- 3512 *ura3-52, leu2Δ1, trp1Δ63, his3Δ200, lys2ΔBgl, hom3-10, ade2Δ1, ade8. YEL069C::URA3, Pgal.TRP1.SGS1.myc.HIS3*

Yeast Strains (continued)

- 3513 *ura3-52, leu2Δ1, trp1Δ63, his3Δ200, lys2ΔBgl, hom3-10, ade2Δ1, ade8. YEL069C::URA3, sgs1C1047F. TRP1*
- 3514 *ura3-52, leu2Δ1, trp1Δ63, his3Δ200, lys2ΔBgl, hom3-10, ade2Δ1, ade8. YEL069C::URA3, sgs1C1047F. TRP1*
- 3515 *ura3-52, leu2Δ1, trp1Δ63, his3Δ200, lys2ΔBgl, hom3-10, ade2Δ1, ade8. YEL069C::URA3, sgs1C1047F. TRP1*
- 3516 *ura3-52, leu2Δ1, trp1Δ63, his3Δ200, lys2ΔBgl, hom3-10, ade2Δ1, ade8. YEL069C::URA3, sgs1F1056A. TRP1*
- 3517 *ura3-52, leu2Δ1, trp1Δ63, his3Δ200, lys2ΔBgl, hom3-10, ade2Δ1, ade8. YEL069C::URA3, sgs1C1047F.myc.HIS3*
- 3518 *ura3-52, leu2Δ1, trp1Δ63, his3Δ200, lys2ΔBgl, hom3-10, ade2Δ1, ade8. YEL069C::URA3, sgs1C1047F.myc.HIS3*
- 3519 *ura3-52, leu2Δ1, trp1Δ63, his3Δ200, lys2ΔBgl, hom3-10, ade2Δ1, ade8. YEL069C::URA3, sgs1C1047F.myc.HIS3*
- 3520 *ura3-52, leu2Δ1, trp1Δ63, his3Δ200, lys2ΔBgl, hom3-10, ade2Δ1, ade8. YEL069C::URA3, sgs1F1056A.myc.HIS3*
- 3521 *ura3-52, leu2Δ1, trp1Δ63, his3Δ200, lys2ΔBgl, hom3-10, ade2Δ1, ade8. YEL069C::URA3, sgs1F1056A.myc.HIS3*
- 3522 *ura3-52, leu2Δ1, trp1Δ63, his3Δ200, lys2ΔBgl, hom3-10, ade2Δ1, ade8. YEL069C::URA3, sgs1F1056A.myc.HIS3*
- 3543 *ura3-52, leu2Δ1, trp1Δ63, his3Δ200, lys2ΔBgl, hom3-10, ade2Δ1, ade8. YEL069C::URA3, sgs1ΔC800-blmΔN647.MYC. TRP1*
- 3544 *ura3-52, leu2Δ1, trp1Δ63, his3Δ200, lys2ΔBgl, hom3-10, ade2Δ1, ade8. YEL069C::URA3, sgs1ΔC800-blmΔN647.MYC. TRP1*
- 3545 *ura3-52, leu2Δ1, trp1Δ63, his3Δ200, lys2ΔBgl, hom3-10, ade2Δ1, ade8. YEL069C::URA3, Pgal.G418.BLM.MYC. TRP1*
- 3546 *ura3-52, leu2Δ1, trp1Δ63, his3Δ200, lys2ΔBgl, hom3-10, ade2Δ1, ade8. YEL069C::URA3, Pgal.G418.BLM.MYC. TRP1*
- 3547 *ura3-52, leu2Δ1, trp1Δ63, his3Δ200, lys2ΔBgl, hom3-10, ade2Δ1, ade8. YEL069C::URA3, Pgal.G418.BLM.MYC. TRP1*
- 3558 *MATa trp1-901 leu2-3,112 ura3-52 his3-200 gal4Δ gal80Δ LYS2::GAL1-HIS3 GAL2-ADE2 met2::GAL7-lacZ*
- 3559 *trp1-901 leu2-3,112 ura3-52 his3-200 gal4Δ gal80Δ LYS2::GAL1-HIS3 GAL2-ADE2 met2::GAL7-lacZ*
- 3560 *MATalpha trp1-901 leu2-3,112 ura3-52 his3-200 gal4Δ gal80Δ LYS2::GAL1-HIS3 GAL2-ADE2 met2::GAL7-lacZ, pBDC*
- 3777 *MATa ura3-52, leu2Δ1, trp1Δ63, his3Δ200, lys2ΔBgl, hom3-10, ade2Δ1, ade8. YEL069C::URA3, sgs1::RECQL5.HIS3*
- 3778 *MATa ura3-52, leu2Δ1, trp1Δ63, his3Δ200, lys2ΔBgl, hom3-10, ade2Δ1, ade8. YEL069C::URA3, sgs1::RECQL5.HIS3*
- 3779 *MATa ura3-52, leu2Δ1, trp1Δ63, his3Δ200, lys2ΔBgl, hom3-10, ade2Δ1, ade8. YEL069C::URA3, sgs1::RECQL5.HIS3*
- 3827 *MATa ura3-52, leu2Δ1, trp1Δ63, his3Δ200, lys2ΔBgl, hom3-10, ade2Δ1, ade8. YEL069C::URA3, sgs1::TRP1.PGAL1.RECQL5.HIS3*

Yeast Strains (continued)

- 3828 *MATa ura3-52, leu2Δ1, trp1Δ63, his3Δ200, lys2ΔBgl, hom3-10, ade2Δ1, ade8. YEL069C::URA3, sgs1::TRP1.PGAL1.RECQL5.HIS3*
- 3829 *MATa ura3-52, leu2Δ1, trp1Δ63, his3Δ200, lys2ΔBgl, hom3-10, ade2Δ1, ade8. YEL069C::URA3, sgs1::TRP1.PGAL1.RECQL5.HIS3*
- 3925 *Y258 pep4-3, his4-580, ura3-53, leu2-3, 112*
- 3926 *Y258 is MATa pep4-3, his4-580, ura3-53, leu2-3, 112*
- 3927 *Y258 is MATa pep4-3, his4-580, ura3-53, leu2-3, 112 Mgs1*
- 3928 *Y258 is MATa pep4-3, his4-580, ura3-53, leu2-3, 112 Exo1*
- 3929 *Y258 is MATa pep4-3, his4-580, ura3-53, leu2-3, 112 Sgs1*
- 3930 *Empty pOAD vector in 3558*
- 3983 *trp1-901 leu2-3,112 ura3-52 his3-200 gal4Δ gal80Δ LYS2::GAL1-HIS3 GAL2-ADE2 met2::GAL7-lacZ pOAD (empty) vector is in this strain*
- 3984 *trp1-901 leu2-3,112 ura3-52 his3-200 gal4Δ gal80Δ LYS2::GAL1-HIS3 GAL2-ADE2 met2::GAL7-lacZ Mec3 in pOAD*
- 3985 *trp1-901 leu2-3,112 ura3-52 his3-200 gal4Δ gal80Δ LYS2::GAL1-HIS3 GAL2-ADE2 met2::GAL7-lacZ*
- 3986 *trp1-901 leu2-3,112 ura3-52 his3-200 gal4Δ gal80Δ LYS2::GAL1-HIS3 GAL2-ADE2 met2::GAL7-lacZ pOBD vector in this strain*
- 3987 *trp1-901 leu2-3,112 ura3-52 his3-200 gal4Δ gal80Δ LYS2::GAL1-HIS3 GAL2-ADE2 met2::GAL7-lacZ Rad17 in pOBD*
- 3988 *trp1-901 leu2-3,112 ura3-52 his3-200 gal4Δ gal80Δ LYS2::GAL1-HIS3 GAL2-ADE2 met2::GAL7-lacZ*
- 4062 *his3, trp1, ura3-52, lex(leu2)3a*
- 4107 *MATa, trp1-901, leu2-3, 112, ura3-52, his3-200, gal4Δ, gal80Δ, lys2::Gal1uas-Gal1tata-HIS3, GAL2uas-GAL2tata-ADE2, URA3::MEL1uas-MEL1tata-lacZ SGS1 647-1447 in pBDC*
- 4108 *MATa, trp1-901, leu2-3, 112, ura3-52, his3-200, gal4Δ, gal80Δ, lys2::Gal1uas-Gal1tata-HIS3, GAL2uas-GAL2tata-ADE2, URA3::MEL1uas-MEL1tata-lacZ SGS1 647-1447 in pBDC*
- 4109 *MATa, trp1-901, leu2-3, 112, ura3-52, his3-200, gal4Δ, gal80Δ, lys2::Gal1uas-Gal1tata-HIS3, GAL2uas-GAL2tata-ADE2, URA3::MEL1uas-MEL1tata-lacZ SGS1 1-347 in pBDC*
- 4110 *MATa, trp1-901, leu2-3, 112, ura3-52, his3-200, gal4Δ, gal80Δ, lys2::Gal1uas-Gal1tata-HIS3, GAL2uas-GAL2tata-ADE2, URA3::MEL1uas-MEL1tata-lacZ SGS1 1-347 in pBDC*
- 4111 *MATa, trp1-901, leu2-3, 112, ura3-52, his3-200, gal4Δ, gal80Δ, lys2::Gal1uas-Gal1tata-HIS3, GAL2uas-GAL2tata-ADE2, URA3::MEL1uas-MEL1tata-lacZ SGS1 1-265 in pBDC*
- 4112 *MATa, trp1-901, leu2-3, 112, ura3-52, his3-200, gal4Δ, gal80Δ, lys2::Gal1uas-Gal1tata-HIS3, GAL2uas-GAL2tata-ADE2, URA3::MEL1uas-MEL1tata-lacZ SGS1 1-265 in pBDC*

Yeast Strains (continued)

- 4113 *MATa, trp1-901, leu2-3, 112, ura3-52, his3-200, gal4Δ, gal80Δ, lys2::Gal1uas-Gal1tata-HIS3, GAL2uas-GAL2tata-ADE2, URA3::MEL1uas-MEL1tata-lacZ SGS1 1-265 in pBDC*
- 4114 *MATa, trp1-901, leu2-3, 112, ura3-52, his3-200, gal4Δ, gal80Δ, lys2::Gal1uas-Gal1tata-HIS3, GAL2uas-GAL2tata-ADE2, URA3::MEL1uas-MEL1tata-lacZ SGS1 1-265 in pBDC*
- 4115 *MATa, trp1-901, leu2-3, 112, ura3-52, his3-200, gal4Δ, gal80Δ, lys2::Gal1uas-Gal1tata-HIS3, GAL2uas-GAL2tata-ADE2, URA3::MEL1uas-MEL1tata-lacZ SGS1 1-187 in pBDC*
- 4116 *MATa, trp1-901, leu2-3, 112, ura3-52, his3-200, gal4Δ, gal80Δ, lys2::Gal1uas-Gal1tata-HIS3, GAL2uas-GAL2tata-ADE2, URA3::MEL1uas-MEL1tata-lacZ SGS1 1-187 in pBDC*
- 4117 *MATa, trp1-901, leu2-3, 112, ura3-52, his3-200, gal4Δ, gal80Δ, lys2::Gal1uas-Gal1tata-HIS3, GAL2uas-GAL2tata-ADE2, URA3::MEL1uas-MEL1tata-lacZ SGS1 1-187 in pBDC*
- 4118 *MATa, trp1-901, leu2-3, 112, ura3-52, his3-200, gal4Δ, gal80Δ, lys2::Gal1uas-Gal1tata-HIS3, GAL2uas-GAL2tata-ADE2, URA3::MEL1uas-MEL1tata-lacZ SGS1 1-187 in pBDC*
- 4119 *MATa, trp1-901, leu2-3, 112, ura3-52, his3-200, gal4Δ, gal80Δ, lys2::Gal1uas-Gal1tata-HIS3, GAL2uas-GAL2tata-ADE2, URA3::MEL1uas-MEL1tata-lacZ SGS1 1-100 in pBDC*
- 4120 *MATa, trp1-901, leu2-3, 112, ura3-52, his3-200, gal4Δ, gal80Δ, lys2::Gal1uas-Gal1tata-HIS3, GAL2uas-GAL2tata-ADE2, URA3::MEL1uas-MEL1tata-lacZ SGS1 1-100 in pBDC*
- 4121 *MATa, trp1-901, leu2-3, 112, ura3-52, his3-200, gal4Δ, gal80Δ, lys2::Gal1uas-Gal1tata-HIS3, GAL2uas-GAL2tata-ADE2, URA3::MEL1uas-MEL1tata-lacZ SGS1 1-100 in pBDC*
- 4122 *MATa, trp1-901, leu2-3, 112, ura3-52, his3-200, gal4Δ, gal80Δ, lys2::Gal1uas-Gal1tata-HIS3, GAL2uas-GAL2tata-ADE2, URA3::MEL1uas-MEL1tata-lacZ SGS1 1-100 in pBDC*
- 4123 *MATa, trp1-901, leu2-3, 112, ura3-52, his3-200, gal4Δ, gal80Δ, lys2::Gal1uas-Gal1tata-HIS3, GAL2uas-GAL2tata-ADE2, URA3::MEL1uas-MEL1tata-lacZ SGS1 1-100 in pBDC*
- 4124 *MATa, trp1-901, leu2-3, 112, ura3-52, his3-200, gal4Δ, gal80Δ, lys2::Gal1uas-Gal1tata-HIS3, GAL2uas-GAL2tata-ADE2, URA3::MEL1uas-MEL1tata-lacZ SGS1 1-100 in pBDC*
- 4125 *MATa, trp1-901, leu2-3, 112, ura3-52, his3-200, gal4Δ, gal80Δ, lys2::Gal1uas-Gal1tata-HIS3, GAL2uas-GAL2tata-ADE2, URA3::MEL1uas-MEL1tata-lacZ SGS1 1-100 in pBDC*
- 4126 *MATa, trp1-901, leu2-3, 112, ura3-52, his3-200, gal4Δ, gal80Δ, lys2::Gal1uas-Gal1tata-HIS3, GAL2uas-GAL2tata-ADE2, URA3::MEL1uas-MEL1tata-lacZ SGS1 1-100 in pBDC*
- 4156 *trp1-901 leu2-3, 112 ura3-52 his3-200 gal4Δ gal80Δ LYS2::GAL1-HIS3 GAL2-ADE2 met2::GAL7-lacZ SGS1 647-1447 in pBDC*

Yeast Strains (continued)

- 4157 *trp1-901 leu2-3,112 ura3-52 his3-200 gal4Δ gal80Δ LYS2::GAL1-HIS3 GAL2-ADE2 met2::GAL7-lacZ SGS1 647-1447 in pBDC*
- 4158 *trp1-901 leu2-3,112 ura3-52 his3-200 gal4Δ gal80Δ LYS2::GAL1-HIS3 GAL2-ADE2 met2::GAL7-lacZ SGS1 1-265 in pBDC*
- 4159 *trp1-901 leu2-3,112 ura3-52 his3-200 gal4Δ gal80Δ LYS2::GAL1-HIS3 GAL2-ADE2 met2::GAL7-lacZ SGS1 1-265 in pBDC*
- 4160 *trp1-901 leu2-3,112 ura3-52 his3-200 gal4Δ gal80Δ LYS2::GAL1-HIS3 GAL2-ADE2 met2::GAL7-lacZ SGS1 1-265 in pBDC*
- 4161 *trp1-901 leu2-3,112 ura3-52 his3-200 gal4Δ gal80Δ LYS2::GAL1-HIS3 GAL2-ADE2 met2::GAL7-lacZ SGS1 1-265 in pBDC*
- 4162 *trp1-901 leu2-3,112 ura3-52 his3-200 gal4Δ gal80Δ LYS2::GAL1-HIS3 GAL2-ADE2 met2::GAL7-lacZ SGS1 1-187 in pBDC*
- 4163 *trp1-901 leu2-3,112 ura3-52 his3-200 gal4Δ gal80Δ LYS2::GAL1-HIS3 GAL2-ADE2 met2::GAL7-lacZ SGS1 1-187 in pBDC*
- 4164 *trp1-901 leu2-3,112 ura3-52 his3-200 gal4Δ gal80Δ LYS2::GAL1-HIS3 GAL2-ADE2 met2::GAL7-lacZ SGS1 1-187 in pBDC*
- 4165 *trp1-901 leu2-3,112 ura3-52 his3-200 gal4Δ gal80Δ LYS2::GAL1-HIS3 GAL2-ADE2 met2::GAL7-lacZ SGS1 1-187 in pBDC*
- 4166 *trp1-901 leu2-3,112 ura3-52 his3-200 gal4Δ gal80Δ LYS2::GAL1-HIS3 GAL2-ADE2 met2::GAL7-lacZ SGS1 1-100 in pBDC*
- 4167 *trp1-901 leu2-3,112 ura3-52 his3-200 gal4Δ gal80Δ LYS2::GAL1-HIS3 GAL2-ADE2 met2::GAL7-lacZ SGS1 1-100 in pBDC*
- 4168 *trp1-901 leu2-3,112 ura3-52 his3-200 gal4Δ gal80Δ LYS2::GAL1-HIS3 GAL2-ADE2 met2::GAL7-lacZ SGS1 1-100 in pBDC*
- 4169 *trp1-901 leu2-3,112 ura3-52 his3-200 gal4Δ gal80Δ LYS2::GAL1-HIS3 GAL2-ADE2 met2::GAL7-lacZ SGS1 1-100 in pBDC*
- 4170 *trp1-901 leu2-3,112 ura3-52 his3-200 gal4Δ gal80Δ LYS2::GAL1-HIS3 GAL2-ADE2 met2::GAL7-lacZ SGS1 1-100 in pBDC*
- 4171 *trp1-901 leu2-3,112 ura3-52 his3-200 gal4Δ gal80Δ LYS2::GAL1-HIS3 GAL2-ADE2 met2::GAL7-lacZ SGS1 1-100 in pBDC*
- 4172 *trp1-901 leu2-3,112 ura3-52 his3-200 gal4Δ gal80Δ LYS2::GAL1-HIS3 GAL2-ADE2 met2::GAL7-lacZ SGS1 1-100 in pBDC*
- 4173 *trp1-901 leu2-3,112 ura3-52 his3-200 gal4Δ gal80Δ LYS2::GAL1-HIS3 GAL2-ADE2 met2::GAL7-lacZ SGS1 1-100 in pBDC*
- 4174 *trp1-901 leu2-3,112 ura3-52 his3-200 gal4Δ gal80Δ LYS2::GAL1-HIS3 GAL2-ADE2 met2::GAL7-lacZ SGS1 1-187 in pBDC*
- 4175 *trp1-901 leu2-3,112 ura3-52 his3-200 gal4Δ gal80Δ LYS2::GAL1-HIS3 GAL2-ADE2 met2::GAL7-lacZ SGS1 1-187 in pBDC*
- 4176 *trp1-901 leu2-3,112 ura3-52 his3-200 gal4Δ gal80Δ LYS2::GAL1-HIS3 GAL2-ADE2 met2::GAL7-lacZ SGS1 1-100 in pBDC*
- 4177 *trp1-901 leu2-3,112 ura3-52 his3-200 gal4Δ gal80Δ LYS2::GAL1-HIS3 GAL2-ADE2 met2::GAL7-lacZ SGS1 1-100 in pBDC*
- 4178 *trp1-901 leu2-3,112 ura3-52 his3-200 gal4Δ gal80Δ LYS2::GAL1-HIS3 GAL2-ADE2 met2::GAL7-lacZ SGS1 1-100 in pBDC*

Yeast Strains (continued)

- 4179 *MATa, trp1-901, leu2-3, 112, ura3-52, his3-200, gal4Δ, gal80Δ, lys2::Gal1uas-Gal1tata-HIS3, GAL2uas-GAL2tata-ADE2, URA3::MEL1uas-MEL1tata-lacZ SGS1 647-1447 in pBDC*
- 4180 *MATa, trp1-901, leu2-3, 112, ura3-52, his3-200, gal4Δ, gal80Δ, lys2::Gal1uas-Gal1tata-HIS3, GAL2uas-GAL2tata-ADE2, URA3::MEL1uas-MEL1tata-lacZ SGS1 1-347 in pBDC*
- 4181 *MATa, trp1-901, leu2-3, 112, ura3-52, his3-200, gal4Δ, gal80Δ, lys2::Gal1uas-Gal1tata-HIS3, GAL2uas-GAL2tata-ADE2, URA3::MEL1uas-MEL1tata-lacZ SGS1 1-265 in pBDC*
- 4182 *MATa, trp1-901, leu2-3, 112, ura3-52, his3-200, gal4Δ, gal80Δ, lys2::Gal1uas-Gal1tata-HIS3, GAL2uas-GAL2tata-ADE2, URA3::MEL1uas-MEL1tata-lacZ SGS1 1-187 in pBDC*
- 4183 *MATa, trp1-901, leu2-3, 112, ura3-52, his3-200, gal4Δ, gal80Δ, lys2::Gal1uas-Gal1tata-HIS3, GAL2uas-GAL2tata-ADE2, URA3::MEL1uas-MEL1tata-lacZ SGS1 1-187 in pBDC*
- 4184 *MATa, trp1-901, leu2-3, 112, ura3-52, his3-200, gal4Δ, gal80Δ, lys2::Gal1uas-Gal1tata-HIS3, GAL2uas-GAL2tata-ADE2, URA3::MEL1uas-MEL1tata-lacZ SGS1 1-100 in pBDC*
- 4185 *MATa, trp1-901, leu2-3, 112, ura3-52, his3-200, gal4Δ, gal80Δ, lys2::Gal1uas-Gal1tata-HIS3, GAL2uas-GAL2tata-ADE2, URA3::MEL1uas-MEL1tata-lacZ SGS1 1-100 in pBDC*
- 4186 *MATa, trp1-901, leu2-3, 112, ura3-52, his3-200, gal4Δ, gal80Δ, lys2::Gal1uas-Gal1tata-HIS3, GAL2uas-GAL2tata-ADE2, URA3::MEL1uas-MEL1tata-lacZ SGS1 1-100 in pBDC*
- 4187 *MATa, trp1-901, leu2-3, 112, ura3-52, his3-200, gal4Δ, gal80Δ, lys2::Gal1uas-Gal1tata-HIS3, GAL2uas-GAL2tata-ADE2, URA3::MEL1uas-MEL1tata-lacZ SGS1 1-100 in pBDC*
- 4188 *MATa, trp1-901, leu2-3, 112, ura3-52, his3-200, gal4Δ, gal80Δ, lys2::Gal1uas-Gal1tata-HIS3, GAL2uas-GAL2tata-ADE2, URA3::MEL1uas-MEL1tata-lacZ SGS1 647-1447 in pBDC and empty pOAD*
- 4189 *MATa, trp1-901, leu2-3, 112, ura3-52, his3-200, gal4Δ, gal80Δ, lys2::Gal1uas-Gal1tata-HIS3, GAL2uas-GAL2tata-ADE2, URA3::MEL1uas-MEL1tata-lacZ SGS1 647-1447 in pBDC and empty pOAD*
- 4190 *MATa, trp1-901, leu2-3, 112, ura3-52, his3-200, gal4Δ, gal80Δ, lys2::Gal1uas-Gal1tata-HIS3, GAL2uas-GAL2tata-ADE2, URA3::MEL1uas-MEL1tata-lacZ SGS1 1-347 in pBDC and empty pOAD*
- 4191 *MATa, trp1-901, leu2-3, 112, ura3-52, his3-200, gal4Δ, gal80Δ, lys2::Gal1uas-Gal1tata-HIS3, GAL2uas-GAL2tata-ADE2, URA3::MEL1uas-MEL1tata-lacZ SGS1 1-347 in pBDC and empty pOAD*
- 4192 *MATa, trp1-901, leu2-3, 112, ura3-52, his3-200, gal4Δ, gal80Δ, lys2::Gal1uas-Gal1tata-HIS3, GAL2uas-GAL2tata-ADE2, URA3::MEL1uas-MEL1tata-lacZ SGS1 1-265 in pBDC and empty pOAD*

Yeast Strains (continued)

- 4193 *MATa, trp1-901, leu2-3, 112, ura3-52, his3-200, gal4Δ, gal80Δ, lys2::Gal1uas-Gal1tata-HIS3, GAL2uas-GAL2tata-ADE2, URA3::MEL1uas-MEL1tata-lacZ SGS1 1-265 in pBDC and empty pOAD*
- 4194 *MATa, trp1-901, leu2-3, 112, ura3-52, his3-200, gal4Δ, gal80Δ, lys2::Gal1uas-Gal1tata-HIS3, GAL2uas-GAL2tata-ADE2, URA3::MEL1uas-MEL1tata-lacZ SGS1 1-265 in pBDC and empty pOAD*
- 4195 *MATa, trp1-901, leu2-3, 112, ura3-52, his3-200, gal4Δ, gal80Δ, lys2::Gal1uas-Gal1tata-HIS3, GAL2uas-GAL2tata-ADE2, URA3::MEL1uas-MEL1tata-lacZ SGS1 1-265 in pBDC and empty pOAD*
- 4196 *MATa, trp1-901, leu2-3, 112, ura3-52, his3-200, gal4Δ, gal80Δ, lys2::Gal1uas-Gal1tata-HIS3, GAL2uas-GAL2tata-ADE2, URA3::MEL1uas-MEL1tata-lacZ SGS1 1-187 in pBDC and empty pOAD*
- 4197 *MATa, trp1-901, leu2-3, 112, ura3-52, his3-200, gal4Δ, gal80Δ, lys2::Gal1uas-Gal1tata-HIS3, GAL2uas-GAL2tata-ADE2, URA3::MEL1uas-MEL1tata-lacZ SGS1 1-187 in pBDC and empty pOAD*
- 4198 *MATa, trp1-901, leu2-3, 112, ura3-52, his3-200, gal4Δ, gal80Δ, lys2::Gal1uas-Gal1tata-HIS3, GAL2uas-GAL2tata-ADE2, URA3::MEL1uas-MEL1tata-lacZ SGS1 1-187 in pBDC and empty pOAD*
- 4199 *MATa, trp1-901, leu2-3, 112, ura3-52, his3-200, gal4Δ, gal80Δ, lys2::Gal1uas-Gal1tata-HIS3, GAL2uas-GAL2tata-ADE2, URA3::MEL1uas-MEL1tata-lacZ SGS1 1-187 in pBDC and empty pOAD*
- 4200 *MATa, trp1-901, leu2-3, 112, ura3-52, his3-200, gal4Δ, gal80Δ, lys2::Gal1uas-Gal1tata-HIS3, GAL2uas-GAL2tata-ADE2, URA3::MEL1uas-MEL1tata-lacZ SGS1 1-100 in pBDC and empty pOAD*
- 4201 *MATa, trp1-901, leu2-3, 112, ura3-52, his3-200, gal4Δ, gal80Δ, lys2::Gal1uas-Gal1tata-HIS3, GAL2uas-GAL2tata-ADE2, URA3::MEL1uas-MEL1tata-lacZ SGS1 1-100 in pBDC and empty pOAD*
- 4202 *MATa, trp1-901, leu2-3, 112, ura3-52, his3-200, gal4Δ, gal80Δ, lys2::Gal1uas-Gal1tata-HIS3, GAL2uas-GAL2tata-ADE2, URA3::MEL1uas-MEL1tata-lacZ SGS1 1-100 in pBDC and empty pOAD*
- 4203 *MATa, trp1-901, leu2-3, 112, ura3-52, his3-200, gal4Δ, gal80Δ, lys2::Gal1uas-Gal1tata-HIS3, GAL2uas-GAL2tata-ADE2, URA3::MEL1uas-MEL1tata-lacZ SGS1 1-100 in pBDC and empty pOAD*
- 4204 *MATa, trp1-901, leu2-3, 112, ura3-52, his3-200, gal4Δ, gal80Δ, lys2::Gal1uas-Gal1tata-HIS3, GAL2uas-GAL2tata-ADE2, URA3::MEL1uas-MEL1tata-lacZ SGS1 1-100 in pBDC and empty pOAD*
- 4205 *MATa, trp1-901, leu2-3, 112, ura3-52, his3-200, gal4Δ, gal80Δ, lys2::Gal1uas-Gal1tata-HIS3, GAL2uas-GAL2tata-ADE2, URA3::MEL1uas-MEL1tata-lacZ SGS1 1-100 in pBDC and empty pOAD*
- 4206 *MATa, trp1-901, leu2-3, 112, ura3-52, his3-200, gal4Δ, gal80Δ, lys2::Gal1uas-Gal1tata-HIS3, GAL2uas-GAL2tata-ADE2, URA3::MEL1uas-MEL1tata-lacZ SGS1 1-100 in pBDC and empty pOAD*

Yeast Strains (continued)

- 4207 *MATa, trp1-901, leu2-3, 112, ura3-52, his3-200, gal4Δ, gal80Δ, lys2::Gal1uas-Gal1tata-HIS3, GAL2uas-GAL2tata-ADE2, URA3::MEL1uas-MEL1tata-lacZ SGS1 1-100 in pBDC and empty pOAD*
- 4208 *MATa, trp1-901, leu2-3, 112, ura3-52, his3-200, gal4Δ, gal80Δ, lys2::Gal1uas-Gal1tata-HIS3, GAL2uas-GAL2tata-ADE2, URA3::MEL1uas-MEL1tata-lacZ empty pBDC and empty pOAD vectors*
- 4209 *MATa, trp1-901, leu2-3, 112, ura3-52, his3-200, gal4Δ, gal80Δ, lys2::Gal1uas-Gal1tata-HIS3, GAL2uas-GAL2tata-ADE2, URA3::MEL1uas-MEL1tata-lacZ empty pBDC and empty pOAD vectors*
- 4210 *MATa, trp1-901, leu2-3, 112, ura3-52, his3-200, gal4Δ, gal80Δ, lys2::Gal1uas-Gal1tata-HIS3, GAL2uas-GAL2tata-ADE2, URA3::MEL1uas-MEL1tata-lacZ empty pBDC and empty pOAD vectors*
- 4211 *MATa, trp1-901, leu2-3, 112, ura3-52, his3-200, gal4Δ, gal80Δ, lys2::Gal1uas-Gal1tata-HIS3, GAL2uas-GAL2tata-ADE2, URA3::MEL1uas-MEL1tata-lacZ empty pBDC and empty pOAD vectors*
- 4743 *his3Δ200/his3Δ200, trp1Δ63/trp1Δ63, ura3-52/ura3-52, rrm3::TRP1/RRM3*
- 4744 *his3Δ200/his3Δ200, trp1Δ63/trp1Δ63, ura3-52/ura3-52, rrm3::TRP1/RRM3*
- 4745 *his3Δ200/his3Δ200, trp1Δ63/trp1Δ63, ura3-52/ura3-52, sgs1::HIS3/SGS1*
- 4746 *his3Δ200/his3Δ200, trp1Δ63/trp1Δ63, ura3-52/ura3-52, sgs1::HIS3/SGS1*
- 4747 *his3Δ200/his3Δ200, trp1Δ63/trp1Δ63, ura3-52/ura3-52, sgs1::HIS3/SGS1*
- 4748 *his3Δ200/his3Δ200, trp1Δ63/trp1Δ63, ura3-52/ura3-52, sgs1::HIS3/SGS1*
- 4749 *his3Δ200/his3Δ200, trp1Δ63/trp1Δ63, ura3-52/ura3-52, srs2::HIS3/SRS2*
- 4750 *his3Δ200/his3Δ200, trp1Δ63/trp1Δ63, ura3-52/ura3-52, srs2::HIS3/SRS2*
- 4751 *his3Δ200/his3Δ200, trp1Δ63/trp1Δ63, ura3-52/ura3-52, srs2::HIS3/SRS2*
- 4752 *his3Δ200/his3Δ200, trp1Δ63/trp1Δ63, ura3-52/ura3-52, srs2::HIS3/SRS2*
- 4753 *ura3-52, trp1Δ63, hisΔ200*
- 4754 *ura3-52, trp1Δ63, hisΔ200*
- 4755 *ura3-52, trp1Δ63, hisΔ200*
- 4756 *ura3-52, trp1Δ63, hisΔ200*
- 4757 *ura3-52, trp1Δ63, hisΔ200*
- 4758 *ura3-52, trp1Δ63, hisΔ200, rrm3::TRP1*
- 4759 *ura3-52, trp1Δ63, hisΔ200, rrm3::TRP1*
- 4760 *his3Δ200, trp1Δ63, Δura3-52, Δrrm3::TRP1, Δlys2::HIS3, Δarg4::G418*
- 4761 *his3Δ200, trp1Δ63, Δura3-52, Δrrm3::TRP1, Δlys2::HIS3, Δarg4::G418*
- 4762 *his3Δ200, trp1Δ63, Δura3-52, Δrrm3::TRP1, Δlys2::HIS3, Δarg4::G418*
- 4763 *his3Δ200, trp1Δ63, Δura3-52, Δrrm3::TRP1, Δlys2::HIS3, Δarg4::G418*
- 4764 *his3Δ200/his3Δ200, trp1Δ63/trp1Δ63, Δura3-52/Δura3-52, RRM3/Δrrm3::TRP1, LYS2/Δlys2::HIS3, ARG4/Δarg4::G418*
- 4765 *his3Δ200/his3Δ200, trp1Δ63/trp1Δ63, Δura3-52/Δura3-52, RRM3/Δrrm3::TRP1, LYS2/Δlys2::HIS3, ARG4/Δarg4::G418*
- 4766 *his3Δ200/his3Δ200, trp1Δ63/trp1Δ63, Δura3-52/Δura3-52, RRM3/Δrrm3::TRP1, LYS2/Δlys2::HIS3, ARG4/Δarg4::G418*

Yeast Strains (continued)

- 4767 *his3Δ200/his3Δ200, trp1Δ63/trp1Δ63, Δura3-52/Δura3-52, RRM3/Δrrm3::TRP1, LYS2/Δlys2::HIS3, ARG4/Δarg4::G418*
- 4768 *his3Δ200/his3Δ200, trp1Δ63/trp1Δ63, Δura3-52/Δura3-52, RRM3/Δrrm3::TRP1, LYS2/Δlys2::HIS3, ARG4/Δarg4::G418*
- 4769 *his3Δ200/his3Δ200, trp1Δ63/trp1Δ63, Δura3-52/Δura3-52, RRM3/Δrrm3::TRP1, LYS2/Δlys2::HIS3, ARG4/Δarg4::G418*
- 4770 *his3Δ200/his3Δ200, trp1Δ63/trp1Δ63, Δura3-52/Δura3-52, RRM3/Δrrm3::TRP1, LYS2/Δlys2::HIS3, ARG4/Δarg4::G418*
- 4771 *his3Δ200/his3Δ200, trp1Δ63/trp1Δ63, Δura3-52/Δura3-52, RRM3/Δrrm3::TRP1, LYS2/Δlys2::HIS3, ARG4/Δarg4::G418*
- 4772 *his3Δ200, trp1Δ63, Δura3-52, Δtof1::His3*
- 4773 *his3Δ200, trp1Δ63, Δura3-52, Δtof1::His3*
- 4774 *his3Δ200, trp1Δ63, Δura3-52, Δtof1::His3*
- 4775 *his3Δ200, trp1Δ63, Δura3-52, Δtof1::His3*
- 4776 *his3Δ200, trp1Δ63, Δura3-52, Δrrm3::TRP1, Δtof1::His3*
- 4777 *his3Δ200, trp1Δ63, Δura3-52, Δrrm3::TRP1, Δtof1::His3*
- 4778 *his3Δ200, trp1Δ63, Δura3-52, Δrrm3::TRP1, Δtof1::His3*
- 4779 *his3Δ200, trp1Δ63, Δura3-52, Δume1::His3*
- 4780 *his3Δ200, trp1Δ63, Δura3-52, Δume1::His3*
- 4781 *his3Δ200, trp1Δ63, Δura3-52, Δume1::His3*
- 4782 *his3Δ200, trp1Δ63, Δura3-52, Δume1::His3*
- 4783 *his3Δ200, trp1Δ63, Δura3-52, Δrrm3::TRP1, Δume1::His3*
- 4784 *his3Δ200, trp1Δ63, Δura3-52, Δrrm3::TRP1, Δume1::His3*
- 4785 *his3Δ200, trp1Δ63, Δura3-52, Δrrm3::TRP1, Δume1::His3*
- 4786 *his3Δ200, trp1Δ63, Δura3-52, Δrrm3::TRP1, Δume1::His3*
- 4787 *his3Δ200, trp1Δ63, Δura3-52, Δdpb4::His3*
- 4788 *his3Δ200, trp1Δ63, Δura3-52, Δdpb4::His3*
- 4789 *his3Δ200, trp1Δ63, Δura3-52, Δrrm3::TRP1, Δdpb4::His3*
- 4790 *his3Δ200, trp1Δ63, Δura3-52, Δrrm3::TRP1, Δdpb4::His3*
- 4791 *his3Δ200, trp1Δ63, Δura3-52, Δrrm3::TRP1, Δdpb4::His3*
- 4792 *his3Δ200, trp1Δ63, Δura3-52, Δrrm3::TRP1, Δdpb4::His3*
- 5036 *ura3-52, trp1Δ63, hisΔ200*
- 5143 *MATα ura3-52, trp1Δ63, his3Δ200, arg4::G418, lys2::HIS3*
- 5144 *MATα ura3-52, trp1Δ63, his3Δ200, arg4::G418, lys2::HIS3, rrm3::TRP1*
- 5145 *MATα ura3-52, leu2Δ1, trp1Δ63, his3Δ200, lys2ΔBgl, hom3-10, ade2Δ1, ade8, YEL069C::URA3, rad5::HIS3*
- 5146 *MATα ura3-52, leu2Δ1, trp1Δ63, his3Δ200, lys2ΔBgl, hom3-10, ade2Δ1, ade8, YEL069C::URA3, rrm3::TRP1, rad5::HIS3*
- 5147 *MATα ura3-52, leu2Δ1, trp1Δ63, his3Δ200, lys2ΔBgl, hom3-10, ade2Δ1, ade8, YEL069C::URA3, rdh54::HIS3*
- 5148 *MATα ura3-52, leu2Δ1, trp1Δ63, his3Δ200, lys2ΔBgl, hom3-10, ade2Δ1, ade8, YEL069C::URA3, rrm3::TRP1, rdh54::HIS3*

Yeast Strains (continued)

- 5149 *MATa ura3-52, leu2Δ1, trp1Δ63, his3Δ200, lys2ΔBgl, hom3-10, ade2Δ1, ade8, YEL069C::URA3, rad5::HIS3 rdh54::G418*
- 5150 *MATa ura3-52, leu2Δ1, trp1Δ63, his3Δ200, lys2ΔBgl, hom3-10, ade2Δ1, ade8, YEL069C::URA3, rrm3::TRP1, rdh54::HIS3, rad5::TRP1*
- 5151 *MATa ura3-52, leu2Δ1, trp1Δ63, his3Δ200, lys2ΔBgl, hom3-10, ade2Δ1, ade8, YEL069C::URA3, set3::HIS3*
- 5152 *MATa ura3-52, leu2Δ1, trp1Δ63, his3Δ200, lys2ΔBgl, hom3-10, ade2Δ1, ade8, YEL069C::URA3, rrm3::TRP1, set3::HIS3*
- 5153 *MATa ura3-52, leu2Δ1, trp1Δ63, his3Δ200, lys2ΔBgl, hom3-10, ade2Δ1, ade8, YEL069C::URA3, tof1::HIS3*
- 5154 *MATa ura3-52, leu2Δ1, trp1Δ63, his3Δ200, lys2ΔBgl, hom3-10, ade2Δ1, ade8, YEL069C::URA3, rrm3::TRP1, tof1::HIS3*
- 5155 *MATa ura3-52, leu2Δ1, trp1Δ63, his3Δ200, lys2ΔBgl, hom3-10, ade2Δ1, ade8, YEL069C::URA3, ies4::HIS3*
- 5156 *MATa ura3-52, leu2Δ1, trp1Δ63, his3Δ200, lys2ΔBgl, hom3-10, ade2Δ1, ade8, YEL069C::URA3, rrm3::TRP1, ies4::HIS3*
- 5157 *MATa ura3-52, leu2Δ1, trp1Δ63, his3Δ200, lys2ΔBgl, hom3-10, ade2Δ1, ade8, YEL069C::URA3, had1::HIS3*
- 5158 *MATa ura3-52, leu2Δ1, trp1Δ63, his3Δ200, lys2ΔBgl, hom3-10, ade2Δ1, ade8, YEL069C::URA3, rrm3::TRP1, had1::HIS3*
- 5159 *MATa ura3-52, leu2Δ1, trp1Δ63, his3Δ200, lys2ΔBgl, hom3-10, ade2Δ1, ade8, YEL069C::URA3, mgm101::HIS3*
- 5160 *MATa ura3-52, leu2Δ1, trp1Δ63, his3Δ200, lys2ΔBgl, hom3-10, ade2Δ1, ade8, YEL069C::URA3, rrm3::TRP1, mgm101::HIS3*
- 5161 *MATa ura3-52, leu2Δ1, trp1Δ63, his3Δ200, lys2ΔBgl, hom3-10, ade2Δ1, ade8, YEL069C::URA3, sml1::G418*
- 5162 *MATa ura3-52, leu2Δ1, trp1Δ63, his3Δ200, lys2ΔBgl, hom3-10, ade2Δ1, ade8, YEL069C::URA3, sml1::G418, rrm3::TRP1*
- 5163 *MATa ura3-52, leu2Δ1, trp1Δ63, his3Δ200, lys2ΔBgl, hom3-10, ade2Δ1, ade8, YEL069C::URA3, sml1::G418, rrm3::TRP1, rad53::HIS3*
- 5164 *ura3-52/ura3-52, leu2Δ1/leu2Δ1, trp1Δ63/trp1Δ63, his3Δ200/his3Δ200, lys2ΔBgl/lys2ΔBgl, hom3-10/hom3-10, ade2Δ1/ade2Δ1, ade8/ade8. YEL069C::URA3/YEL069C::URA3, rdh54::HIS3/rdh54::HIS3*
- 5165 *ura3-52/ura3-52, leu2Δ1/leu2Δ1, trp1Δ63/trp1Δ63, his3Δ200/his3Δ200, lys2ΔBgl/lys2ΔBgl, hom3-10/hom3-10, ade2Δ1/ade2Δ1, ade8/ade8. YEL069C::URA3/YEL069C::URA3, rrm3::TRP1/rrm3::TRP1, rdh54::HIS3/rdh54::HIS3*
- 5166 *ura3-52/ura3-52, leu2Δ1/leu2Δ1, trp1Δ63/trp1Δ63, his3Δ200/his3Δ200, lys2ΔBgl/lys2ΔBgl, hom3-10/hom3-10, ade2Δ1/ade2Δ1, ade8/ade8. YEL069C::URA3/YEL069C::URA3, rrm3::TRP1/rrm3::TRP1*
- 5167 *ura3-52/ura3-52, leu2Δ1/leu2Δ1, trp1Δ63/trp1Δ63, his3Δ200/his3Δ200, lys2ΔBgl/lys2ΔBgl, hom3-10/hom3-10, ade2Δ1/ade2Δ1, ade8/ade8. YEL069C::URA3/YEL069C::URA3, RRM3/rrm3::TRP1, RDH54/rdh54::HIS3*

Yeast Strains (continued)

- 5168 *ura3-52/ura3-52, leu2Δ1/leu2Δ1, trp1Δ63/trp1Δ63, his3Δ200/his3Δ200, lys2ΔBgl/lys2ΔBgl, hom3-10/hom3-10, ade2Δ1/ade2Δ1, ade8/ade8. YEL069C::URA3/YEL069C::URA3, RRM3/rrm3::TRP1*
- 5169 *ura3-52/ura3-52, leu2Δ1/leu2Δ1, trp1Δ63/trp1Δ63, his3Δ200/his3Δ200, lys2ΔBgl/lys2ΔBgl, hom3-10/hom3-10, ade2Δ1/ade2Δ1, ade8/ade8. YEL069C::URA3/YEL069C::URA3, RDH54/rdh54::HIS3*
- 5170 *ura3-52/ura3-52, leu2Δ1/leu2Δ1, trp1Δ63/trp1Δ63, his3Δ200/his3Δ200, lys2ΔBgl/lys2ΔBgl, hom3-10/hom3-10, ade2Δ1/ade2Δ1, ade8/ade8. YEL069C::URA3/YEL069C::URA3, RRM3/rrm3::TRP1, rdh54::HIS3/rdh54::HIS3*
- 5171 *ura3-52/ura3-52, leu2Δ1/leu2Δ1, trp1Δ63/trp1Δ63, his3Δ200/his3Δ200, lys2ΔBgl/lys2ΔBgl, hom3-10/hom3-10, ade2Δ1/ade2Δ1, ade8/ade8. YEL069C::URA3/YEL069C::URA3, rrm3::TRP1/rrm3::TRP1, RDH54/rdh54::HIS3*
- 5172 *MATa ura3-52, leu2Δ1, trp1Δ63, his3Δ200, lys2ΔBgl, hom3-10, ade2Δ1, ade8. YEL069C::URA3, sgs1::RECQL5.13MYC.TRP1*
- 5173 *MATa ura3-52, leu2Δ1, trp1Δ63, his3Δ200, lys2ΔBgl, hom3-10, ade2Δ1, ade8. YEL069C::URA3, sgs1::RECQL5.13MYC.TRP1*
- 5174 *MATa ura3-52, leu2Δ1, trp1Δ63, his3Δ200, lys2ΔBgl, hom3-10, ade2Δ1, ade8. YEL069C::URA3, sgs1::RECQL5.13MYC.TRP1*
- 5175 *MATa ura3-52, leu2Δ1, trp1Δ63, his3Δ200, lys2ΔBgl, hom3-10, ade2Δ1, ade8. YEL069C::URA3, sgs1::TRP1.PGAL1.RECQL5.13MYC.kanMX6*
- 5176 *MATa ura3-52, leu2Δ1, trp1Δ63, his3Δ200, lys2ΔBgl, hom3-10, ade2Δ1, ade8. YEL069C::URA3, sgs1::TRP1.PGAL1.RECQL5.13MYC.kanMX6*
- 5177 *MATa ura3-52, leu2Δ1, trp1Δ63, his3Δ200, lys2ΔBgl, hom3-10, ade2Δ1, ade8. YEL069C::URA3, sgs1::TRP1.PGAL1.RECQL5.13MYC.kanMX6*
- 5178 *MATa ura3-52, leu2Δ1, trp1Δ63, his3Δ200, lys2ΔBgl, hom3-10, ade2Δ1, ade8. YEL069C::URA3, sgs1ΔC800-RECQL5.HIS3*
- 5179 *MATa ura3-52, leu2Δ1, trp1Δ63, his3Δ200, lys2ΔBgl, hom3-10, ade2Δ1, ade8. YEL069C::URA3, sgs1ΔC800-RECQL5.HIS3*
- 5180 *MATa ura3-52, leu2Δ1, trp1Δ63, his3Δ200, lys2ΔBgl, hom3-10, ade2Δ1, ade8. YEL069C::URA3, sgs1ΔC800-RECQL5.HIS3*
- 5181 *MATa ura3-52, leu2Δ1, trp1Δ63, his3Δ200, lys2ΔBgl, hom3-10, ade2Δ1, ade8. YEL069C::URA3, sgs1ΔC800-RECQL5.13MYC.TRP1*
- 5182 *MATa ura3-52, leu2Δ1, trp1Δ63, his3Δ200, lys2ΔBgl, hom3-10, ade2Δ1, ade8. YEL069C::URA3, sgs1ΔC800-RECQL5.13MYC.TRP1*
- 5183 *MATa ura3-52, leu2Δ1, trp1Δ63, his3Δ200, lys2ΔBgl, hom3-10, ade2Δ1, ade8. YEL069C::URA3, sgs1ΔC800-RECQL5.13MYC.TRP1*
- 5184 *MATa, trp1-901, leu2-3, 112, ura3-52, his3-200, gal4Δ, gal80Δ, lys2::Gal1uas-Gal1tata-HIS3, GAL2uas-GAL2tata-ADE2, URA3::MEL1uas-MEL1tata-lacZ RECQL5 in pBDC*
- 5185 *MATa, trp1-901, leu2-3, 112, ura3-52, his3-200, gal4Δ, gal80Δ, lys2::Gal1uas-Gal1tata-HIS3, GAL2uas-GAL2tata-ADE2, URA3::MEL1uas-MEL1tata-lacZ RECQL5 in pBDC*

Yeast Strains (continued)

- 5186 *MATa, trp1-901, leu2-3, 112, ura3-52, his3-200, gal4Δ, gal80Δ, lys2::Gal1uas-Gal1tata-HIS3, GAL2uas-GAL2tata-ADE2, URA3::MEL1uas-MEL1tata-lacZ RECQL5 in pBDC*
- 5187 *MATa, trp1-901, leu2-3, 112, ura3-52, his3-200, gal4Δ, gal80Δ, lys2::Gal1uas-Gal1tata-HIS3, GAL2uas-GAL2tata-ADE2, URA3::MEL1uas-MEL1tata-lacZ RECQL5 in pBDC and empty pOAD*
- 5188 *MATa, trp1-901, leu2-3, 112, ura3-52, his3-200, gal4Δ, gal80Δ, lys2::Gal1uas-Gal1tata-HIS3, GAL2uas-GAL2tata-ADE2, URA3::MEL1uas-MEL1tata-lacZ RECQL5 in pBDC and empty pOAD*
- 5189 *MATa, trp1-901, leu2-3, 112, ura3-52, his3-200, gal4Δ, gal80Δ, lys2::Gal1uas-Gal1tata-HIS3, GAL2uas-GAL2tata-ADE2, URA3::MEL1uas-MEL1tata-lacZ RECQL5 in pBDC and empty pOAD*
-

APPENDIX D:
PLASMIDS

| Strain (pKHS) | Description | Source |
|--------------------------|----------------------------|----------------------------------|
| pRS303 | <i>HIS3</i> | (Sikorski and Hieter 1989) |
| pRS304 | <i>TRP1</i> | (Sikorski and Hieter 1989) |
| pRS306 | <i>URA3</i> | (Sikorski and Hieter 1989) |
| pRS415 | <i>CEN/ARS, LEU2</i> | (Sikorski and Hieter 1989) |
| 124 | <i>pKHS619-RRM3</i> | (Schmidt, Derry et al. 2002) |
| 125 | <i>pKHS619-POL30</i> | (Schmidt, Derry et al. 2002) |
| 126 | <i>pKHS620-RRM3</i> | (Schmidt, Derry et al. 2002) |
| 127 | <i>pKHS620-POL30</i> | (Schmidt, Derry et al. 2002) |
| 133 | <i>pKHS620-rrm3ΔN54</i> | This study |
| 135 | <i>pKHS620-rrm3ΔN230</i> | This study |
| 136 | <i>pRS315-rrm3ΔN54</i> | This study |
| 137 | <i>pRS315-rrm3ΔN230</i> | This study |
| 220 | <i>pFA6a-kanMX6</i> | (Longtine, McKenzie et al. 1998) |
| 221 | <i>pFA6a-TRP1</i> | (Longtine, McKenzie et al. 1998) |
| 222 | <i>pFA6a-His3MX6</i> | (Longtine, McKenzie et al. 1998) |
| 226 | <i>pFA6a-3HA-kanMX6</i> | (Longtine, McKenzie et al. 1998) |
| 227 | <i>pFA6a-3HA-TRP1</i> | (Longtine, McKenzie et al. 1998) |
| 228 | <i>pFA6a-3HA-His3MX6</i> | (Longtine, McKenzie et al. 1998) |
| 229 | <i>pFA6a-13Myc-kanMX6</i> | (Longtine, McKenzie et al. 1998) |
| 230 | <i>pFA6a-13Myc-TRP1</i> | (Longtine, McKenzie et al. 1998) |
| 231 | <i>pFA6a-13Myc-His3MX6</i> | (Longtine, McKenzie et al. 1998) |
| 232 | <i>pFA6a-GST-kanMX6</i> | (Longtine, McKenzie et al. 1998) |
| 233 | <i>pFA6a-GST-TRP1</i> | (Longtine, McKenzie et al. 1998) |
| 234 | <i>pFA6a-GST-His3MX6</i> | (Longtine, McKenzie et al. 1998) |
| 235 | <i>pFA6a-kanMX6-PGAL1</i> | (Longtine, McKenzie et al. 1998) |
| 236 | <i>pFA6a-TRP1-PGAL1</i> | (Longtine, McKenzie et al. 1998) |
| 237 | <i>pFA6a-His3MX6-PGAL1</i> | (Longtine, McKenzie et al. 1998) |
| 257 | <i>pFA-kanMX</i> | (Goldstein and McCusker 1999) |
| 265 | <i>pCMV-SPORT6-RECQL5</i> | Open Biosystems |
| 273 | <i>sgs1ΔC795</i> | (Mullen, Kaliraman et al. 2000) |
| 274 | <i>sgs1-hd</i> | (Mullen, Kaliraman et al. 2000) |

Plasmids (continued)

| | | |
|-----|---|---------------------------------|
| 275 | <i>sgs1</i> ΔC200 | (Mullen, Kaliraman et al. 2000) |
| 276 | <i>SGS1</i> | (Mullen, Kaliraman et al. 2000) |
| 277 | <i>sgs1</i> ΔN158 | (Mullen, Kaliraman et al. 2000) |
| 278 | <i>sgs1</i> ΔN644 | (Mullen, Kaliraman et al. 2000) |
| 301 | <i>sgs1-hd.TRP1</i> | This study |
| 334 | <i>sgs1</i> ΔC200. <i>TRP1</i> | This study |
| 335 | <i>sgs1</i> ΔC200. <i>TRP1</i> | This study |
| 336 | <i>sgs1</i> ΔN158. <i>TRP1</i> | This study |
| 360 | <i>pKHS276-SGS1.TRP1</i> | This study |
| 392 | <i>pBDC</i> | (Uetz, Giot et al. 2000) |
| 481 | <i>pRS415-SGS1</i> | (Mullen, Kaliraman et al. 2000) |
| 487 | <i>pOAD</i> | (Uetz, Giot et al. 2000) |
| 503 | <i>pKHS360-sgs1-F30P</i> | This study |
| 504 | <i>pKHS360-sgs1-I33P</i> | This study |
| 505 | <i>pKHS360-sgs1-V29P</i> | This study |
| 506 | <i>pKHS392-sgs1-1-347</i> | This study |
| 507 | <i>pKHS392-sgs1-1-265</i> | This study |
| 508 | <i>pKHS392-sgs1-1-265</i> | This study |
| 509 | <i>pKHS392-sgs1-1-187</i> | This study |
| 510 | <i>pKHS392-sgs1-1-187</i> | This study |
| 511 | <i>pKHS392-sgs1-1-100</i> | This study |
| 512 | <i>pKHS392-sgs1-1-100</i> | This study |
| 513 | <i>pKHS392-sgs1-1-100</i> | This study |
| 514 | <i>pKHS392-sgs1-1-100</i> | This study |
| 515 | <i>pKHS392-sgs1-647-1447</i> | This study |
| 516 | <i>pKHS392-sgs1-647-1447</i> | This study |
| 517 | <i>pKHS392-sgs1-647-1447</i> | This study |
| 520 | <i>pJG-4-5*-MLH1</i> | This study |
| 521 | <i>pBC6, pJH1074</i> | This study |
| 522 | <i>pJM100-SGS1</i> | (Mullen, Kaliraman et al. 2000) |
| 523 | <i>pJM100-SGS1</i> | (Mullen, Kaliraman et al. 2000) |
| 524 | <i>pJM100-SGS1</i> | (Mullen, Kaliraman et al. 2000) |
| 525 | <i>pKHS392-RECQL5</i> | This study |
| 526 | <i>pKHS392-RECQL5</i> | This study |
| 527 | <i>pKHS392-RECQL5</i> | This study |
| 615 | <i>rad5 (C914,C917→AA) Ub ligase mutant</i> | (Blastyak, Pinter et al. 2007) |
| 616 | <i>Wt Rad5</i> | (Blastyak, Pinter et al. 2007) |
| 617 | <i>rad5 (D681, E682 →AA) ATPase mutant</i> | (Blastyak, Pinter et al. 2007) |
| 619 | <i>2-Hyb. Prey pJG4-5* vector</i> | (Schmidt, Derry et al. 2002) |

Plasmids (continued)

| | | |
|-----|---|------------------------------|
| 620 | <i>2-Hyb. Bait. pEG202 Vector</i> | (Schmidt, Derry et al. 2002) |
| 644 | <i>pR5-30-rad5- D681A/E682A/C914A/C917A</i> | This study |
| 645 | <i>pRS315-rrm3-NΔ142</i> | This study |
| 646 | <i>pRS315-rrm3-ΔN186</i> | This study |
| 647 | <i>pRS315-rrm3-Δ212</i> | This study |
| 648 | <i>pRS315-rrm3-K260A</i> | This study |
| 649 | <i>pRS315-rrm3-K260D</i> | This study |
| 650 | <i>pRS315-rrm3-D102P</i> | This study |
| 651 | <i>pRS315-rrm3-S605A</i> | This study |
| 652 | <i>pRS315-rrm3-S605D</i> | This study |
| 653 | <i>pKHS620-rrm3-ΔN186</i> | This study |
| 654 | <i>pKHS620-rrm3-ΔN212</i> | This study |
| 655 | <i>pKHS620-rrm3-ΔN230</i> | This study |
| 656 | <i>pKHS619-ORC5</i> | This study |
| 671 | <i>pKHS265-RECQL5.HIS3MX6</i> | This study |

REFERENCES

- Blastyak, A., L. Pinter, I. Unk, L. Prakash, S. Prakash and L. Haracska (2007). "Yeast Rad5 protein required for postreplication repair has a DNA helicase activity specific for replication fork regression." Mol Cell **28**(1): 167-175.
- Goldstein, A. L. and J. H. McCusker (1999). "Three new dominant drug resistance cassettes for gene disruption in *Saccharomyces cerevisiae*." Yeast **15**(14): 1541-1553.
- Longtine, M. S., A. McKenzie, 3rd, D. J. Demarini, N. G. Shah, A. Wach, A. Brachat, P. Philippsen and J. R. Pringle (1998). "Additional modules for versatile and economical PCR-based gene deletion and modification in *Saccharomyces cerevisiae*." Yeast **14**(10): 953-961.
- Mullen, J. R., V. Kaliraman and S. J. Brill (2000). "Bipartite structure of the SGS1 DNA helicase in *Saccharomyces cerevisiae*." Genetics **154**(3): 1101-1114.
- Schmidt, K. H., K. L. Derry and R. D. Kolodner (2002). "*Saccharomyces cerevisiae* RRM3, a 5' to 3' DNA helicase, physically interacts with proliferating cell nuclear antigen." J Biol Chem **277**(47): 45331-45337.
- Sikorski, R. S. and P. Hieter (1989). "A system of shuttle vectors and yeast host strains designed for efficient manipulation of DNA in *Saccharomyces cerevisiae*." Genetics **122**(1): 19-27.
- Uetz, P., L. Giot, G. Cagney, T. A. Mansfield, R. S. Judson, J. R. Knight, D. Lockshon, V. Narayan, M. Srinivasan, P. Pochart, A. Qureshi-Emili, Y. Li, B. Godwin, D. Conover, T. Kalbfleisch, G. Vijayadamar, M. Yang, M. Johnston, S. Fields and J. M. Rothberg (2000). "A comprehensive analysis of protein-protein interactions in *Saccharomyces cerevisiae*." Nature **403**(6770): 623-627.

APPENDIX E:
PERMISSIONS

| | |
|--|---|
| License Number | 3815530273800 |
| License date | Feb 24, 2016 |
| Licensed content publisher | Elsevier |
| Licensed content publication | Journal of Molecular Biology |
| Licensed content title | Sgs1 Truncations Induce Genome Rearrangements but Suppress Detrimental Effects of BLM Overexpression in <i>Saccharomyces cerevisiae</i> |
| Licensed content author | Hamed Mirzaei, Salahuddin Syed, Jessica Kennedy, Kristina H. Schmidt |
| Licensed content date | 28 January 2011 |
| Licensed content volume number | 405 |
| Licensed content issue number | 4 |
| Number of pages | 15 |
| Type of Use | reuse in a thesis/dissertation |
| Portion | full article |
| Format | both print and electronic |
| Are you the author of this Elsevier article? | Yes |
| Will you be translating? | No |
| Title of your thesis/dissertation | DNA Helicases Involved in Maintaining Genome Stability |
| Expected completion date | Mar 2016 |
| Estimated size (number of pages) | 300 |
| Elsevier VAT number | GB 494 6272 12 |
| Permissions price | 0.00 USD |
| VAT/Local Sales Tax | 0.00 USD / 0.00 GBP |
| Total | 0.00 USD |

Figure E.1: Permissions for content in Chapter Two provided by the Journal of Molecular Biology and Elsevier.



AMERICAN
SOCIETY FOR
MICROBIOLOGY

Title: Defects in DNA Lesion Bypass
Lead to Spontaneous
Chromosomal Rearrangements
and Increased Cell Death

Author: Kristina H. Schmidt, Emilie B.
Viebranz, Lorena B. Harris et al.

Publication: Eukaryotic Cell

Publisher: American Society for
Microbiology

Date: Feb 1, 2010

Copyright © 2010, American Society for Microbiology

Permissions Request

Authors in ASM journals retain the right to republish discrete portions of his/her article in any other publication (including print, CD-ROM, and other electronic formats) of which he or she is author or editor, provided that proper credit is given to the original ASM publication. ASM authors also retain the right to reuse the full article in his/her dissertation or thesis. For a full list of author rights, please see: http://journals.asm.org/site/misc/ASM_Author_Statement.xhtml

Figure E.2: Permissions for content in Appendix A provided by Eukaryotic Cell and the American Society for Microbiology.

Content License

The following policy applies to all of PLOS journals, unless otherwise noted.

PLOS applies the Creative Commons Attribution (CC BY) license to works we publish. This license was developed to facilitate open access – namely, free immediate access to, and unrestricted reuse of, original works of all types.

Under this license, authors agree to make articles legally available for reuse, without permission or fees, for virtually any purpose. Anyone may copy, distribute or reuse these articles, as long as the author and original source are properly cited.

Using PLOS Content

No permission is required from the authors or the publishers to reuse or repurpose PLOS content provided the original article is cited. In most cases, appropriate attribution can be provided by simply citing the original article.

Example citation:

Kaltenbach LS et al. (2007) Huntingtin Interacting Proteins Are Genetic Modifiers of Neurodegeneration. *PLOS Genet* 3(5): e82. doi:10.1371/journal.pgen.0030082.

If the item you plan to reuse is not part of a published article (e.g., a featured issue image), then indicate the originator of the work, and the volume, issue, and date of the journal in which the item appeared.

For any reuse or redistribution of a work, you must also make clear the license terms under which the work was published.

Figures, Tables, and Images

Figures, tables, and images are published under the Creative Commons Attribution (CC BY) license.

Data

If any relevant accompanying data is submitted to repositories with stated licensing policies, the policies should not be more restrictive than CC BY.

Submitting Copyrighted or Proprietary Content

Do not submit any figures, photos, tables, or other works that have been previously copyrighted or that contain proprietary data unless you have and can supply written permission from the copyright holder to use that content. This includes:

- maps and satellite images
- slogans and logos
- social media content.

Figure E.3: Permissions for content in Appendix B provided by PLOS ONE.